



**Assessment of antiretroviral drugs uptake by vegetables from  
contaminated soil and their adsorption by exfoliated graphite in  
river and wastewater**

**PHILISIWE NGANAKI KUNENE**



**Assessment of antiretroviral drugs uptake by vegetables from  
contaminated soil and their adsorption by exfoliated graphite in  
river and wastewater**

BY

**PHILISIWE NGANAKI KUNENE**

SUPERVISOR: DR P. MAHLAMBI

A thesis submitted to

The School of Chemistry and Physics

College of Agriculture, Engineering and Science

University of KwaZulu-Natal Pietermaritzburg, in fulfillment of the requirements for the  
degree of Doctor of Philosophy in Chemistry

## **Dedication**

---

To my superb mother Ntombikayise Bahlalile Kunene, my father Bhekumqondo Elijah Kunene, and the rest of the Kunene Family.

## **Declaration 1 - Plagiarism**

---

I, Philisiwe Nganaki Kunene, hereby declare that apart from the help from my supervisor and all the acknowledged sources, the research reported in this dissertation is my own work. It has never been submitted for examination in any university and degree apart from where it is being submitted at the University of KwaZulu-Natal for the degree of Doctor of Philosophy.

  
----- (Signature of the candidate)

  
----- (Supervisor)

School of Chemistry and Physics, University of KwaZulu-Natal, Pietermaritzburg, 2022

## Declaration 2 - Publications

---

DETAILS OF CONTRIBUTION TO PUBLICATIONS that form part and/or include research presented in this thesis (include publications in preparation, submitted, *in press* and published and give details of the contributions of each author to the experimental work and writing of each publication)

Publication 1: Philisiwe Naganaki Kunene, Precious Nokwethemba Mahlambi. Determination of selected antiretroviral drugs in vegetables: ultrasonic extraction and ultrasonic-assisted dispersive liquid-liquid microextraction methods comparison. *Submitted to Journal of Separation Science and Technology*.

Publication 2: Philisiwe Naganaki Kunene, Precious Nokwethemba Mahlambi. Assessment of antiretroviral drugs in vegetables: evaluation of microwave-assisted extraction performance with and without solid-phase extraction cleanup. *Journal of Separation Science Plus*; 1-10. <https://doi.org/10.1002/sscp.202200059>

Publication 3: Philisiwe Naganaki Kunene, Precious Nokwethemba Mahlambi. Case study on antiretroviral drugs uptake from soil irrigated with contaminated water: bio-accumulation and bio-translocation to roots, stem, leaves, and fruits. *Accepted by Journal of Environmental Pollution*.

Publication 2: Philisiwe Naganaki Kunene, Precious Nokwethemba Mahlambi. Adsorption of antiretroviral drugs, abacavir, nevirapine, and efavirenz from river water and wastewater using exfoliated graphite: isotherm and kinetic studies. *Submitted to Journal of Environmental Chemical Engineering*.

## Acknowledgments

---

I would like to express my sincere gratitude to my supervisor Dr. PN Mahlambi for her professional supervision, endless patience, generosity, guidance, support, and encouragement. I will always be grateful to work under your supervision.

I would also like to thank Dr. T Ndlovu for her help synthesizing exfoliated graphite. I would also like to thank Miss Zimbini Ngcingwana for her assistance during my laboratory work.

Thank you for your endless support to my lovely mother, my father, my sisters (Thandazile and Kwandile), my brothers (Mthembeni and Mphumzeni), and the rest of the Kunene family, my family friend Thamisanqa Nxumalo, and my friend Khulekani Mkhize.

My colleagues' especially the Analytical Chemistry group, thank you for your encouraging words and for being there for me whenever I needed you. Your encouragement helped me to put more effort into my work.

Thank you to the University of KwaZulu-Natal (UKZN, PMB), School of Chemistry and Physics, for allowing me to do my doctor of philosophy degree.

Thank you to the National Research Foundation (NRF) of South Africa under the Thuthuka grant (Grant number: 121869) for financial support.

*I want to thank Almighty God.*

*Psalms 107:1 "Give thanks to the LORD, for he is good; his love endures forever."*

*Thank You for strengthening me and for your endless love. I would have not accomplished anything in life without your mercy. Thank you, Lord, for guiding me through my difficulties to emerge strong. You have been so good to me.*

## Abstract

---

This study was directed toward vegetable uptake of the commonly used antiretroviral drugs (ARVDs), abacavir, nevirapine, and efavirenz. Antiretroviral drugs are used to treat the human immune-deficiency virus (HIV). South Africa (SA) is one of the countries with a high number of infected people on ARV therapy, therefore, the ARVDs are anticipated to be existing at high concentrations in the South African environment than in other countries worldwide. In recent years, the presence of ARVDs in the environment has drawn attention; hence studies have reported their presence in aquatic environments while very few studies have been conducted on their uptake using vegetables. This work was therefore based on the optimization and application of sensitive, simple, cost-effective, and robust techniques for quantifying ARVDs in vegetables. Based on this information, ultrasonic extraction (UE) and microwave-assisted extraction (MAE) were used to isolate target compounds from vegetable samples to the aqueous phase. Dispersive liquid-liquid microextraction (DLLME) and solid-phase extraction (SPE) were utilized to preconcentration and clean up the extracts from UE and MAE, respectively. A liquid chromatography photodiode array detector (LC-PDA) was utilized to detect and quantify the extracted compounds. The UE with and without DLLME cleanup were compared with each other, also, MAE with and without SPE cleanup were compared with each other. The methods comparison was done in terms of their detection (LOD) and quantification limits (LOQ), extraction efficiencies (%Recovery), relative standard deviations (%RSD), and concentrations of ARVDs found in vegetable samples.

In comparison of UE and ultrasonic-assisted dispersive liquid-liquid microextraction (UADLLME), the LOD and LOQ obtained ranged between 0.0081 - 0.015  $\mu\text{g/kg}$  and 0.027 - 0.049  $\mu\text{g/kg}$  for UE and 0.0028 - 0.0051  $\mu\text{g/kg}$  and 0.0094 - 0.017  $\mu\text{g/kg}$  for UADLLME respectively. High recoveries ranging from 93 to 113% in UE and 85 to 103% in UADLLME with less than 10% RSD in both procedures were obtained. These results indicated that UADLLME is more sensitive than the UE method, although they are both accurate and precise. The UE can be recommended for routine analysis as UADLLME showed the inability to extract analytes from root vegetables. The optimized UE and UADLLME methods were applied to extract ARVDs from vegetables bought from local fruit and veggie supermarket. Vegetables were categorized as root (carrot, potato, and sweet potatoes), leaf (cabbage and lettuce), and fruit (green paper, butternut, and tomato). The target ARVDs were quantified in most samples with concentrations up to 8.18  $\mu\text{g/kg}$ . The concentrations obtained were slightly high in

UADLLME than in UE as a result of its high sensitivity. Efavirenz was the most dominant drug, while the potato was the most contaminated vegetable.

In the comparison of MAE and MAESPE, the obtained LOD and LOQ ranged from 0.020 to 0.032  $\mu\text{g/kg}$  and 0.068 to 0.109  $\mu\text{g/kg}$  for MAE and 0.019 to 0.066  $\mu\text{g/L}$  and 0.065 to 0.22  $\mu\text{g/L}$  for MAE-SPE. The obtained recoveries ranged from 85 to 103% for MAE and from 82 to 98 % for MAE-SPE, respectively, and the RSDs were all less than 6%. These results showed that both methods have comparable sensitivity; however, the recoveries values for MAE were slightly higher than those obtained in MAE-SPE, which signals MAE's high accuracy. The optimized MAE and MAE-SPE methods were applied to remove ARVDs in the root (potatoes, onions, and beetroot), leaf (lettuce, and spinach), and fruit (green paper, cucumber, and eggplant) vegetables bought from local fruit and veggie supermarket. The obtained ARVDs concentration range was  $1.48 \pm 0.5 - 27.9 \pm 1.2 \mu\text{g/kg}$ . The MAE-SPE resulted in low concentration compared to MAE without cleanup. Beetroot exhibited high concentrations of the target ARVDs, while nevirapine was found to have high concentration and as a dominant compound. The results obtained revealed that the vegetables from the studied area are contaminated with ARVDs, which could indicate their possible irrigation with wastewater effluent or the use of sludge as biosolids in the agricultural areas. This is a concern as it leads to unintentional consumption by consumers which could lead to drug resistance by the human body or have human health effects.

The study was then expanded by conducting the phytoremediation approach to investigate the uptake of abacavir, nevirapine, and efavirenz by beetroot, spinach, and tomato from the contaminated soil. The three selected vegetable plants were planted and irrigated with ARVDs spiked (at 2000 and 5000  $\mu\text{g/L}$ ) water over a period of three months. The optimized UE and LC-PDA methods were used to extract and quantify the selected ARVDs from the target vegetables and soil. The obtained results showed that the studied vegetables have the potential to take up abacavir, nevirapine, and efavirenz from contaminated soil, be absorbed by the root, and translocate to the aerial part of the plants. Abacavir was found at high concentrations to a maximum of 40.21  $\mu\text{g/kg}$  in the root, 18.43  $\mu\text{g/kg}$  in the stem, and 6.77  $\mu\text{g/kg}$  in the soil, while efavirenz was the highest concentrations, up to 35.44  $\mu\text{g/kg}$  in leaves and 8.86  $\mu\text{g/kg}$  in fruits. Spinach root accumulated more ARVDs than beetroot and tomato. The bio-accumulation factor ranged from 2.0-14  $\mu\text{g/kg}$  in beetroot, 3.6 - 15  $\mu\text{g/kg}$  in spinach, and 6 – 10  $\mu\text{g/kg}$  in tomato. The root concentration factor range was 0.047 – 17.6  $\mu\text{g/kg}$ ; 0.34-5.9  $\mu\text{g/kg}$ , and 0.14-2.82  $\mu\text{g/kg}$  in beetroot, spinach, and tomato, respectively. The translocation factor range obtained



was 0.40 – 38  $\mu\text{g/kg}$ , 0.08 – 19  $\mu\text{g/kg}$ , and 0.14 – 49  $\mu\text{g/kg}$  in beetroot, spinach, and tomato, respectively. However, the accumulation of ARVDs in all studied plants showed that they could be used in phytoremediation.

The results obtained in the phytoremediation approach revealed that the utilization of the contaminated water has an influence on the presence ARVDs in vegetables; hence this work also focused on evaluating the exfoliated graphite adsorption of ARVDs in water. Natural graphite was intercalated with acids and exfoliated with thermal shock to obtain the exfoliated graphite. The scanning electron microscopy images showed that the exfoliated graphite had increased c-axis distance between the layers with accordion-like structure which were confirmed by the lower density of exfoliated graphite material ( $0.0068 \text{ g mL}^{-1}$ ) compared to the natural graphite ( $0.54 \text{ g mL}^{-1}$ ). Fourier Transformed Infrared Spectroscopy results showed the C=C in natural and exfoliated graphite at  $1635 \text{ cm}^{-1}$  stretching. The phenolic, alcoholic, and carboxylic groups were observed from 1000 to  $1700 \text{ cm}^{-1}$  for the intercalated and exfoliated graphite. The Energy-dispersive X-ray results further confirmed these results, which showed carbon and oxygen peaks in the intercalated and exfoliated graphite spectrum, whereas natural graphite showed only a carbon peak. Raman spectroscopy results showed that the material's crystallinity was not affected by the intercalation and exfoliation processes as observed from the ratios of the G and D peaks and the G' and D'. Natural, intercalated and exfoliated graphite contained the D, G, D', and G' peaks at about  $1350 \text{ cm}^{-1}$ ,  $1570 \text{ cm}^{-1}$ ,  $2440 \text{ cm}^{-1}$ , and  $2720 \text{ cm}^{-1}$ , respectively. The exfoliated graphite material showed the characteristic of a hexagonal phase graphitic structure by (002) and (110) reflections in the X-ray diffraction results. The exfoliated graphite adsorption method was optimized based on the pH of a solution, adsorbent dosage, and adsorption time prior to application to water samples. The optimum pH solution, adsorbent dosage, and adsorption time were 7, 30 mg,  $0.01 \mu\text{g/L}$ , and 30 minutes respectively. The kinetics and isotherm studies were conducted to assess the model that best fit and explain the experimental data obtained. The kinetic model and adsorption isotherm studies showed that the experimental data fit well pseudo-second-order kinetics and is well explained by Freundlich's adsorption isotherm. The maximum adsorption capacity of the exfoliated graphite (EG) for ARVDs ranges between 1.660-197.0, 1.660-232.5, and 1.650-237.7 mg/g for abacavir, nevirapine, and efavirenz, respectively. These results showed that under proper operating conditions, the EG adsorbent could potentially be applied as a water purifying tool for the removal of ARVDs pollutants.

## List of Publications

---

**Philisiwe Kunene**, Precious Mahlambi. Determination of selected antiretroviral drugs in vegetables: ultrasonic extraction and ultrasonic-assisted dispersive liquid-liquid microextraction methods comparison. *Submitted to Journal of Separation Science and Technology*.

**Philisiwe Kunene**, Precious Mahlambi. Assessment of antiretroviral drugs in vegetables: evaluation of microwave-assisted extraction performance with and without solid-phase extraction cleanup. *Journal of Separation Science Plus* (2022); 1-10. <https://doi.org/10.1002/sscp.202200059>

**Philisiwe Kunene**, Precious Mahlambi. Case study on antiretroviral drugs uptake from soil irrigated with contaminated water: bio-accumulation and bio-translocation to roots, stem, leaves, and fruits. *Submitted to Journal of Environmental Pollution*.

**Philisiwe Kunene**, Precious Mahlambi. Absorption of antiretroviral drugs, abacavir, nevirapine, and efavirenz from river water and wastewater using exfoliated graphite: isotherm and kinetic studies. *Submitted to Journal of Science of the Total Environment*.

## Table of Contents

Dedication .....	i
Declaration 1 - Plagiarism .....	ii
Declaration 2 - Publications.....	iii
Acknowledgments.....	iv
Abstract .....	v
List of Publications .....	viii
Table of Contents.....	ix
List of Tables .....	xiii
List of Figures .....	xiv
List of Supplementary Information (Tables) .....	xvi
List of Supplementary Information (Figures) .....	xvii
Abbreviations.....	xviii
Chapter one .....	1
1. Background .....	1
1.1. Introduction .....	1
1.2. Research questions .....	2
1.3. Problem statement.....	3
1.4. The novelty of this project .....	3
1.5. Aims .....	4
1.6. Objectives.....	4
Chapter two.....	5
2. Literature Review .....	5
2.1. What are antiretroviral drugs?.....	5
2.2. Physicochemical properties of the selected ARVDs understudy .....	6
2.3. Sources of ARVDs in the environment.....	9
2.4. Effects of ARVDs .....	10
2.5. Occurrence of ARVDs in the environment .....	11
2.6. Occurrence of pharmaceuticals .....	16
2.7. Phytoremediation .....	21
2.7.1. Accumulation of ARVDs .....	21
2.8. Extraction Techniques.....	22
2.8.1. Ultrasonic Extraction (UE).....	23
2.8.2. Ultrasonic assisted dispersive liquid-liquid microextraction (UADLLMAE) .....	24
2.8.3. Microwave-assisted extraction (MAE).....	25

2.8.4. Solid-phase extraction (SPE).....	26
2.9. Removal of pharmaceuticals .....	28
2.9.1. Removal of ARVDs during treatment processes of wastewater in WWTPs .....	28
2.9.2. Strategies for removal of ARVDs and other related organic drugs in water.....	28
2.10. Characterization techniques .....	29
2.10.1. Fourier Transform Infrared Spectroscopy .....	30
2.10.2. Scanning Electron Microscopy .....	30
2.10.3. Energy-dispersive X-ray spectroscopy .....	31
2.10.4. Ultraviolet-Visible .....	32
2.10.5. Transmission electron microscopy .....	32
2.10.6. Thermogravimetric analysis .....	32
2.10.7. Brunauer -Emmet Teller .....	33
2.10.8. X-Ray diffraction.....	33
2.10.9. Raman Spectroscopy .....	34
2.11. Quantification Techniques .....	35
2.11.1. High-performance liquid chromatography .....	35
2.11.2. Gas Chromatography .....	36
2.12. References .....	37
Chapter three .....	53
It is worth noting that this work is submitted in a form of papers, therefore, the details of procedures used are given in each paper. ....	53
3. Determination of selected antiretroviral drugs in vegetables: ultrasonic extraction and ultrasonic-assisted dispersive liquid-liquid microextraction methods comparison.....	54
Abstract .....	54
3.1. Introduction .....	54
3.2. Experimental .....	56
3.2.1 Materials and chemicals .....	56
3.2.2 Instrumentation .....	56
3.2.3 Preparation of stock solution .....	57
3.2.4 Sample collection and pre-treatment .....	57
3.3. Sample extraction and preconcentration methods.....	58
3.3.1 Ultrasonic extraction method.....	58
3.3.2 Ultrasonic-assisted dispersive liquid-liquid micro-extraction method.....	58
3.3.3 Method validation.....	58
3.4 Results and discussion.....	59

3.4.1 Optimization of ultrasonic extraction .....	59
3.4.2 Optimization of ultrasonic-assisted dispersive liquid-liquid extraction UADLLME .....	64
3.4.3 Method validation.....	67
3.4.4 Application of the optimized method in vegetables .....	68
3.5. Conclusion.....	71
References .....	71
Supplementary information.....	75
Chapter four .....	82
4. Assessment of antiretroviral drugs in vegetables: evaluation of microwave-assisted extraction performance with and without solid-phase extraction cleanup .....	82
Abstract .....	82
4.1. Introduction .....	82
4.2. Experimental .....	84
4.2.1. Standards and chemicals.....	84
4.2.2. Sample collection and pretreatment .....	84
4.2.3. Instrumentation.....	84
4.2.4. Microwave-assisted extraction procedure .....	85
4.2.5. SPE Cleanup method.....	85
4.2.6. Analytical method validation.....	86
4.3. Result and discussion .....	86
4.3.1. Optimization of Liquid Chromatograph-Photodiode array (LC-PDA) .....	86
4.3.2. Optimization of MAE.....	87
4.3.3. Optimization of SPE.....	91
4.3.4. Method validation .....	93
4.3.5. Application of MAE and MAE-SPE .....	96
4.4. Conclusion.....	99
References .....	99
Supplementary information.....	103
Chapter five.....	109
5. Case study on antiretroviral drugs uptake from soil irrigated with contaminated water: bio-accumulation and bio-translocation to roots, stem, leaves, and fruits .....	109
Abstract .....	109
5.1. Introduction .....	109
5.2. Experimental .....	114
5.2.1. Materials and chemicals .....	114

5.2.2. Liquid chromatography-photodiode array condition.....	114
5.2.3. Stock solution preparation .....	114
5.2.4. Field experiment .....	114
5.2.5. Sample collection and pre-treatment .....	115
5.2.6. Extraction and preconcentration of the selected compounds .....	116
5.2.7. Method validation.....	116
5.3. Results and discussion.....	118
5.3.1. Phytoremediation of ARVDs by vegetables from the contaminated soil.....	118
5.3.2. ARVDs bioaccumulation in roots and bio-translocation to stem, leaf and fruit ..	120
5.4. Conclusion.....	130
References .....	130
Supporting documents.....	134
Chapter six .....	135
Abstract .....	135
6.1. Introduction .....	135
6.2. Experimental .....	138
6.2.1. Chemical and reagents.....	138
6.2.2. Preparation of exfoliated graphite .....	138
6.2.3. Stock solution preparation .....	138
6.2.4. Instrumentation and liquid chromatography conditions.....	138
6.2.5. Batch adsorption .....	139
6.2.6. Sample collection .....	139
6.3. Result and discussion .....	140
6.3.1. Preparation of exfoliated graphite .....	140
6.3.2. Characterisation of exfoliated graphite.....	140
6.3.3. Adsorption studies .....	146
6.3.4. Adsorption isotherms.....	151
6.3.5. Absorption kinetics.....	153
6.4. Conclusion.....	159
References .....	159
Supporting documents.....	165
Chapter seven.....	169
7.1. Conclusion.....	169
7.2. Recommendations .....	170

## List of Tables

Table 2.1: Physicochemical properties of the ARVDs of interest .....	8
Table 2.2: ARVDs detected in South Africa, other African countries, and overseas countries .....	13
Table 2.3: Summarised studies of pharmaceutical uptake from soil and water by vegetables	19
Table 3.1: Effect of extraction solvent and sample mass on the recoveries (%) RSD% of ultrasonic extraction (n=3).....	62
Table 3.2: Effect of sonication time and spike concentration on the ARVDs recoveries % and RSD% of ultrasonic extraction (n=3) .....	63
Table 3.3: Effect of extraction solvent, dispersive solvent, and their ratios in a UDALLE recoveries .....	66
Table 3.4: Performance of ultrasonic extraction and ultrasonic-assisted dispersive liquid-liquid extraction in vegetables (n=3).....	67
Table 3.5: Average concentrations of selected ARVDs, RSD% traced in vegetables (n = 3).	70
Table 4.1: Optimal performance of analytical techniques in vegetables (n=3) .....	95
Table 4.2: Average concentrations of target ARVDs obtained in the selected vegetables (n=3) .....	98
Table 5.1: Abacavir, nevirapine, and efavirenz structures, molecular masses, Log K <sub>ow</sub> , and pKa values (Akenga et al., 2021) .....	113
Table 5.2: The linearity, lod (µg/kg), loq (µg/kg), % recoveries of the analytical method, (n=3) .....	117
Table 5.3: Summary of the detected average concentrations (µg/kg) of selected ARVDs in vegetables and soil (n=3) .....	123
Table 5.4: Average bio-accumulation and bio-translocation factors of the antiretroviral drugs found in different segments of vegetable plants (n=3). .....	125
Table 6.1: Parameters of Freundlich, and Langmuir isotherm for the adsorption of abacavir, nevirapine and efavirenz .....	153
Table 6.2: Kinetics constants for adsorption of ARVDs .....	156
Table 6.3: Average concentrations of ARVDs obtained in river water and wastewater .....	158

## List of Figures

Figure 2.1: Pharmaceutical sources and routes in the water and food chain (Patel et al., 2019)	10
Figure 2.2: Typical setup of ultrasonic extraction (William AndrewToshiro K et al., 2012)	23
Figure 2.3: A schematic diagram illustrating a basic DLLME using light extraction solvent (Shiri et al., 2020)	25
Figure 2.4: General process of Solid-phase extraction (Aries et al., 2019)	28
Figure 4.1: Effect of extraction solvent on the recoveries of antiretroviral drugs (n=3)	88
Figure 4.2: Effect of spike concentration on the recoveries of antiretroviral drugs (n=3)	89
Figure 4.3: Effect of extraction time on the recoveries of antiretroviral drugs (n=3)	90
Figure 4.4: Effect of conditioning solvent on the recoveries of antiretroviral drugs (n=3)	92
Figure 4.5: Effect of spike concentration on the recoveries of SPE (n=3)	93
Figure 5.1: The concentrations of the combined ARVDs in each vegetable (beetroot, spinach, and tomato)	127
Figure 5.2: The individual ARVDs concentration percentage (%) in each vegetable (beetroot, spinach, and tomato)	127
Figure 5.3: Assessment of a relationship between log Dow and BCF (a), RCF (b), and TF (c) in spinach.	128
Figure 5.4: Assessment of a relationship between log Dow and BCF (a), RCF (b), and TF (c) in tomato.	129
Figure 5.5: Assessment of a relationship between log Dow and BCF (a), RCF (b), and TF (c) in beetroot.	129
Figure 6.1: SEM images for NG (a), GIC (b), EG worm-like structure (c), EDX spectrum for NG (d) and EG (e).	142
Figure 6.2: The FTIR spectrum of NG, GIC, and EG	143
Figure 6.3: Raman spectrum of the different graphite material	144
Figure 6.4: XRD pattern for NG, GIC, and EG	145
Figure 6.5: Initial adsorbate dosage effect on the removal percentage removal values of ARVDs onto EG	148
Figure 6.6: Effect of pH variation on ARVDs percentage removal onto EG	149
Figure 6.7: Effect of adsorbent mass variation on ARVDs removal percentage	150



Figure 6.8: Effect of agitation time on the percentage removal of ARVDs onto EG..... 151

## **List of Supplementary Information (Tables)**

---

Table S3.1: t-Test result for the effect of extraction solvent on the recoveries (%) .....	75
Table S3.2: The t-test results for the effect of sample mass on the recoveries (%).....	76
Table S3. 3: The t-test results for the effect of extraction time on the recoveries (%) .....	77
Table S3.4: The t-test results for the effect of spike concentration on the recoveries (%).....	78
Table S3.5: The t-test results for the effect of extracting solvent on the recoveries (%).....	78
Table S3.6: The t-test results for the effect of dispersive solvent and dispersive and extracting solvent volume on the recoveries (%).....	79
Table S3.7: Average recoveries % obtained for selected ARVDs in different matrices .....	80
Table S3.8: The t-test results for the average LOD and LOQ for UE and UADLLME .....	80
Table S3.9: The t-test results for the average LOD and LOQ for UE and UADLLME .....	81
Table S4. 1: The t-Test result for the effect of extraction solvent on the recoveries of ARVDs in MAE.....	105
Table S4. 2: The t-Test result for the effect of spike concentration and extraction time on the recoveries ARVDs in MAE .....	106
Table S4. 3: The t-Test result for the effect of extraction solvent volume on the recoveries ARVDs in MAE.....	106
Table S4. 4: The t-Test result for the effect of conditioning solvent on the recoveries ARVDs in SPE.....	107
Table S4. 5: The t-Test result for the effect of concentration on the recoveries ARVDs in SPE .....	107
Table S4. 6: The t-Test result for MAE and MAE-SPE concentration limit and concentrations (µg/kg) obtained in vegetables.....	108
Table S5. 1: Soil parameters before plantation an after harvesting .....	134
Table S5. 2: The t-test results for overall concentration of ARVDs in each vegetable plant. ....	134
Table S5. 3: The t-test result for accumulation of ARVDs in each vegetable plant.....	134
Table S6. 1: Physicochemical parameter and sampling points coordinates .....	165

## List of Supplementary Information (Figures)

---

Figure S4. 1: A UV chromatogram of the selected ARVDs achieved at 254 nm, flow rate at 0.4 mL/min, column temperature 30 °C and gradient program of 50 % acetonitrile: 50 % water from 0-5 min and 70 % acetonitrile: 30 % water from 6-12 min. ....	103
Figure S4. 2: A UV chromatogram of the selected ARVDs achieved at 225 nm, flow rate at 0.4 mL/min, column temperature 30 °C and gradient program of 50 % acetonitrile: 50 % water from 0-5 min and 70 % acetonitrile: 30 % water from 6-12 min. ....	103
Figure S4.3: A UV chromatogram of the selected ARVDs achieved at 274 nm, flow rate at 0.4 mL/min, column temperature 30 °C and gradient program of 50 % acetonitrile: 50 % water from 0-5 min and 70 % acetonitrile: 30 % water from 6-12 min. ....	104
Figure S4. 4: Typical calibration curves for analytes obtained using LC-UV-PDA. ....	104
Figure S4. 5: A MAE chromatogram of the spiked green pepper sample obtained at 274 nm, the flow rate at 0.4 mL/min, column temperature 30 °C, and gradient program of 50 % acetonitrile: 50 % water from 0-5 min and 70 % acetonitrile: 30 % water from 6-12 min. ..	105
Figure S6.1: <b>a</b> Langmuir adsorption isotherm of abacavir, <b>b</b> Freundlich adsorption isotherm of abacavir, <b>c</b> Langmuir adsorption isotherm of nevirapine, <b>d</b> Freundlich adsorption isotherm of nevirapine, <b>e</b> Langmuir adsorption isotherm of efavirenz, and <b>f</b> Freundlich adsorption isotherm of efavirenz on EG at optimum conditions. ....	166
Figure S6.2: <b>a</b> pseudo-first-order adsorption kinetics of abacavir, <b>b</b> pseudo-second-order adsorption kinetics of abacavir, <b>c</b> pseudo-first-order adsorption kinetics of nevirapine, <b>d</b> pseudo-second-order adsorption kinetics of nevirapine, <b>e</b> pseudo-first-order adsorption kinetics of efavirenz, <b>f</b> pseudo-second-order adsorption kinetics of efavirenz on EG at optimum condition. ....	167
Figure S6.3: <b>a</b> Intra-particle diffusion model for the adsorption of abacavir, <b>b</b> Intra-particle diffusion model for the adsorption of nevirapine, <b>c</b> Intra-particle diffusion model for the adsorption of efavirenz on EG at optimum condition. ....	168

## Abbreviations

---

ARVDs	-	Antiretroviral drugs
BCF	-	Bio-concentration factor
BET	-	Brunauer -Emmet Teller
EDX	-	Energy-dispersive X-ray spectroscopy
EG	-	Exfoliated graphite
GIC	-	Graphite intercalated
FTIR	-	Fourier Transform Infrared spectroscopy
LC	-	Liquid chromatography
MAE	-	Microwave assisted extraction
MRL	-	Maximum Residue Limits
MS	-	Mass spectrometry
NG	-	Natural graphite
PDA	-	Photodiode array
RCF	-	Root concentration factor
SA	-	South Africa
SEM	-	Scanning electron microscopy
SPE	-	Solid phase extraction
TEM	-	Transmission electron microscopy
TF	-	Translocation factor
TGA	-	Thermogravimetric analysis
UADLLME	-	Ultrasonic assisted-dispersive liquid liquid-microextraction
UE	-	Ultrasonic extraction
UV-VIS	-	Visible-Ultraviolet spectroscopy
WWTP	-	Wastewater treatment plant
XRD	-	X-Ray diffraction

# Chapter one

---

## 1. Background

### 1.1. Introduction

A drastic increase in the number of people affected by various diseases has led to the development of new pharmaceutical drugs. Pharmaceuticals are natural or synthetic chemicals used in veterinary or human drugs as they consist of active ingredients designed to positively impact animals and human health. They are one of the emerging pollutants with a variety of groups, including antibiotics, non-steroidal anti-inflammatory drugs,  $\beta$ -blockers, contraceptives, sedatives, antidepressants, and antiretroviral drugs (ARVDs). Due to increasing production and wide usage of pharmaceuticals, most compartments of the environment are now overfilled with them. The presence of ARVDs in the environment raises concern due to their potential deleterious impact on human health if unintentionally consumed from contaminated water and food and in the aquatic organisms exposed to polluted water (Madikizela et al., 2017). After the consumption of any pharmaceuticals by patients, they are incompletely digested in the digestive system. About 90% of the consumed drugs are excreted in their original form or as metabolites from the human body through faecal or urine, thus introduced into the wastewater system and eventually reaching wastewater treatment plants (WWTPs) (Madikizela and Chimuka, 2017a). The WWTPs are mostly designed to remove nutrients effectively, dissolved organic matter, and solids (Kebede et al., 2020); therefore, they do not completely remove organic compounds. Hence, some organic compounds, including pharmaceuticals, are discharged with the effluent due to their high polarity. Some pollutants are partitioned with the sludge due to their high octanol-water partition coefficient (Mtollo et al., 2019). In addition, it was reported that during wastewater treatment processes, the de-conjugation occurs; hence some metabolites return to their biologically active form resulting in their presence in the effluent (Amdany et al., 2014). This results in high loads of active drugs discharged with effluents from WWTPs and received by the rivers (Madikizela and Chimuka, 2017a).

It has been reported that African countries have the highest number of people living with human immune deficiency virus (HIV), and in 2019, World Health Organization statistics reported about 5231809 people receiving ARVDs and about 6900 000 to 8 million people living with HIV (Adeola and Forbes, 2021). Therefore, there is a developing scientific monitoring and public concern since ARVDs have been detected in surface water. Many researchers reported

ARVDs occurrence in the aquatic samples (Kairigo et al., 2020, Ngumba et al., 2020, Mlunguza et al., 2020, Mosekiemang et al., 2019, Mtolo et al., 2019, Abafe et al., 2018, Rimayi et al., 2018, Schoeman et al., 2017, Wooding et al., 2017, K'oreje et al., 2016). On the other hand, the scarcity of water has led to extensive use of effluent wastewater for horticulture crop irrigation, and this activity introduces pharmaceuticals in agricultural areas. Furthermore, the application of biosolids, fertilizer, contaminated animal manure, and soil amendment could also contribute to the concentration of pharmaceuticals in agricultural areas (García et al., 2018). The introduced pharmaceuticals accumulate in the soil, be absorbed by vegetable plant's roots, and translocate to the edible aerial part of plant tissues via diffusion and transpiration. As a consequence, they are unintentionally consumed by human beings, which poses a potential health risk (Madikizela et al., 2018). This could lead to poor quality of food produced due to the potential risk of introducing traces of pharmaceuticals into the food chain. Therefore, it is important to monitor their occurrence in vegetables, study their uptake by vegetables, and evaluate some effective methods for their removal in water sources.

The uptake of pharmaceuticals by plants has been shown as one of the green approaches to eradication of persisting pollutants found in soil and water. In this regard, the phytoremediation aptitudes of various plant species regarding pharmaceuticals in the environment have been reported in the literature (Bartha et al., 2010, Iori et al., 2012, Hurtado et al., 2016, Madikizela et al., 2018, Mlunguza et al., 2019, Prabakaran et al., 2019). Other explored approaches for the removal of pharmaceuticals in water are the application of the adsorption methods (Akpomie et al., 2019, Tella et al., 2018). The adsorption methods are versatile, inexpensive, reliable, simple, have a high capacity, great efficiency, and require less energy (Rosli et al., 2021). As a result, in recent years, there has been a development of new different sorbents explored in the removal of ARVDs (Adeola et al., 2021, Kebede et al., 2020, Qwane et al., 2020). The EG sorbents have been used in the adsorption methods due to graphite's high hydrophobic nature, large-specific surface area, multi-porosity, low density, and high thermal and mechanical stability (Hoang et al., 2019).

## **1.2. Research questions**

1. Are the target ARVDs residues present in the vegetables understudy?
2. Can the selected vegetables for the plantation bioaccumulate and translocate the selected ARVDs?
3. Do the studied vegetables have the potential to be used in phytoremediation?

4. Which vegetable plant takes up highest concentration of ARVDs?
5. Which plant tissue retains highest concentration of ARVDs?
6. Do the selected ARVDs affect the growth of the vegetables selected?
7. Which analytical technique is most suitable for the extraction of ARVDs from vegetables?
8. Can exfoliated graphite (EG) be used as an adsorbent to remove ARVDs from water?

### **1.3. Problem statement**

South Africa is one of the countries with a large number of people living with HIV; therefore, tons of ARVDs are consumed every day. In 2021, the statistics reported about 8.2 million people living with HIV in South Africa, and each year, the number of patients on ARVDs therapy increases (Adeola and Forbes, 2021). The ARVDs are partially digested in the digestive system, and hence they are excreted from the human body in their original form or as metabolites via urine and feces. The excreted ARVDs reach the sewage system and are transported to WWTPS through sewage pipes where they are not completely removed. Therefore, they are discharged with the wastewater effluent into the environmental water, where they can affect aquatic organisms and be consumed by people through drinking water (Sharro et al., 2018). Some ARVDs bind in the solid waste (sludge) removed during wastewater cleaning processes. The sludge from wastewater is used as fertilizer, and wastewater effluent is used for irrigation in the agricultural area; therefore, ARVDs can be transferred to soil and be taken up by plants, and eventually be consumed by humans. This could result in extensive unintentional consumption of ARVDs, which could lead to drug resistance. The effect of ARVDs on crops is not yet known, also, there are no maximum residue limits documented for ARVDs in water, soil, and vegetables. Furthermore, there is little information on the investigation of ARVDs in vegetables and a full structured experimental approach done to evaluate the uptake of ARVDs by plants. In this regard, the novelty of this study was formulated.

### **1.4. The novelty of this project**

In this work, a full structured phytoremediation study was conducted to assess for the first time the uptake and translocation of ARVDs (efavirenz, abacavir, and nevirapine) by vegetables such as beetroot, tomato, and spinach and investigate their presence in vegetables (such carrot, potato, cabbage, lettuce, green pepper, butternut, tomato, beetroot, onions, spinach, cucumber,

and eggplant) purchased from the local supermarket in Scottville ( Kwazulu-Natal, South Africa). Also, the adsorption of ARVDs by exfoliated graphite was evaluated for the first time, according to the best of our knowledge. In addition, not much research has been published on the analysis of these ARVDs in KwaZulu-Natal, which was the study area in this project. This led to the following aim of this study.

### **1.5. Aims**

1. To assess the occurrence of ARVDs in vegetables.
2. To conduct a phytoremediation approach to evaluate the potential uptake of the commonly used ARVDs (abacavir, nevirapine, and efavirenz) by vegetable plants (beetroot, spinach, and tomato) in soil culture.
3. To conduct adsorption studies of ARVDs onto exfoliated graphite.

### **1.6. Objectives**

The aims of this study were achieved through the following objectives

1. To optimize the LC-PDA method for analysis of ARVDs concentration.
2. To optimize the UE, UADLLE, MAE, and MAE-SPE methods for removing ARVDs in vegetables.
3. To apply the optimized extraction, detection, and quantification methods in the bought and harvested vegetables for qualitative and quantitative analysis of ARVDs.
4. To compare the efficiency of UE and UADLLE methods for the removal of ARVDs in vegetables.
5. To compare the effectiveness of MAE and MAE-SPE methods for the removal of ARVDs in vegetables.
6. To conduct phytoremediation experiments approach by planting vegetables and irrigating them with ARVDs spiked water to assess ARVDs uptake and translocation by different vegetables (root, leaf, and fruit).
7. To compare the vegetable plant uptake of ARVDs to determine the plant with high potential for use in phytoremediation of ARVDs loads in the contaminated soil.
8. To monitor the effect of irrigating with ARVDs contaminated water on the plant growth.
9. To prepare and apply the exfoliated graphite to study its ability to adsorb ARVDs from river water and wastewater.



## Chapter two

---

This chapter presents detailed information about ARVDs including their physicochemical, their sources in the environment, their possible health, and environmental effects, and the finding reported by researchers worldwide. The ARVDs uptake by plants and their removal strategies on from water are discussed.

### 2. Literature Review

#### 2.1. What are antiretroviral drugs?

Antiretroviral drugs (ARVDs) are drugs used to prevent the multiplication of retroviral diseases, mainly human immunodeficiency virus type 1 (HIV-1). HIV-1 is a disease that primarily outbreaks the immune system cells called CD4-T cells. The ARVDs do not exterminate or cure HIV-1; instead, they inhibit the growth and formation of new HIV cells. After reducing the HIV level in the blood as a result of consuming ARVDs, there is no further harm done to the immune system (Ncube et al., 2018, Swanepoel et al., 2015). This results in improving many people's healthy lives, minimizing transmittance from one another, fewer opportunistic infections, and long-life expectancy. There are millions of people living with HIV whose lives were improved after the ARVDs were introduced in 1983 (Cihlar and Fordyce, 2016, Ngumba et al., 2016). The ARVDs fight HIV-1 in four categories include epidemiological, therapeutic, immunological, and virological purposes. The incompetence of ARVDs to entirely exterminate the HIV-1 in the body indicates that latent reservoirs of HIV-1 continue to persist in the infected T-cells. Therefore, when the infected T-cells reactivate and form new cells to substitute the old CD4 cells, they replicate the latent reservoir of HIV, reproducing HIV again. In this regard, the infected person requires to take ARVDs for the entire life to suppress the latent HIV reservoir (Cihlar and Fordyce, 2016). The ARVDs have been helpful to humans infected with HIV-1 and to protect unborn babies from infection (Schoeman et al., 2015).

The ARVDs are categorised into six classes depending on the resistance aspect of functional change and molecular mechanism. These classes include nucleoside reverse transcriptase inhibitors (NRTIs), non-nucleoside reverse transcriptase inhibitors (NNRTIs), protease inhibitors (PI), entry and fusion inhibitors (EFI), integrase inhibitors, and P450-3A inhibitors. This project only looked at NNRTIs (nevirapine and efavirenz) and NRTIs (abacavir). The NNRTIs are inhibitors that are used to inhibit the enzyme reverse transcriptase to prevent or

stop the replication of the viral. The NRTIs involve two mechanisms which are acting as a chain terminator and also as a competitor. When the inhibitors are acting as a chain terminator, it is where they prevent the extension of the DNA chain via hindrance for more nucleoside. The viral RNA reverse transcription is prevented from copying itself into DNA. Whereas the second mechanism is where the active drug is competing for binding into enzyme template primer complex to prevent the replication. NNRTIs are only able to do the second mechanism, which is a binding/competition (Bernardino and Arribas, 2017). For a long-lasting virological suppression, the combination of ARV therapy is required to ideally consist of three active drugs from two or more ARVDs classes (Cihlar and Fordyce, 2016). A combination of one drug from NNRTIs and two from NRTIs is commonly endorsed for first line treatment (Kanters et al., 2016).

## **2.2. Physicochemical properties of the selected ARVDs understudy**

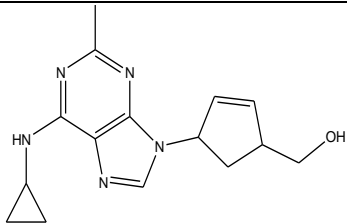
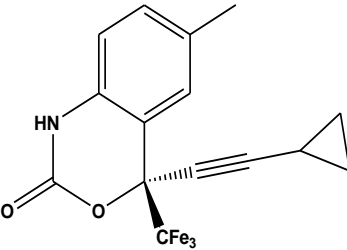
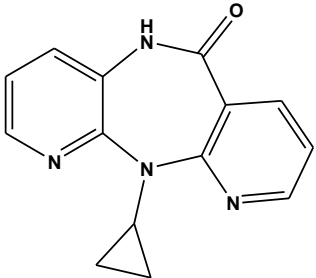
Abacavir (general name ziagen) belong to NRTIs class of ARVDs. It is chemically described as ((1S,4R)-4-[2-amino-6-(cyclopropylamino)-9H-purin-9-yl]cyclopent-2-en-1-yl)methanol with a chemical formula  $C_{14}H_{18}N_6O$  (Qwane et al., 2020). Abacavir consists of polar functional groups that make it soluble in water with a solubility value of 77 mg/L. Therefore, a high concentration of abacavir is expected to be taken up by the aquatic plants because of its high solubility.

Efavirenz, generally known as Sustiva, is categorised as NNRTIs underclasses of ARVDs. Its chemical formula is  $C_{14}H_9ClF_3NO_2$  with the IUPAC name of (4S)-6-Chloro-4-(2-cyclopropylethynyl)-4-(trifluoromethyl)-2,4-dihydro-1H-3,1-benzoxazin-2-one. Efavirenz is basically insoluble in water (Mlunguza, 2019). Efavirenz has a low solubility in water which could lead to it low concentrations detected in water. However, due to the high excretion percentage of efavirenz, it is expected to be present in high concentrations in the environment (Abafe et al., 2018).

Nevirapine (Viramune) belongs to a class of ARVDs known as NNRTIs. It is chemically termed is 1-cyclopropyl-5,11-dihydro-4-methyl-6Hdipyrido[3,2-b:20,30-e][1,4] diazepin-6-one) with the molecular formula of  $C_{15}H_{14}N_4O$  (Adaramoye et al., 2012). Nevirapine is poorly water-soluble. Its formulation was approved from 1996 to 1998. It is normally administered at a dosage of 200 mg, and the intended consumer takes it two times a day. Increasing the dosage to 400 mg ensued in variable bioavailability outlines (Raju et al., 2014).

Table 2.1 shows the structures and the physicochemical properties of the ARVDs (Abacavir, efavirenz and nevirapine). The solubility of hydrophobic analytes like the target ARVDs is poor; however, some studies indicated that these compounds are available in trace amounts in water (Schoeman et al., 2017, Abafe et al., 2018, Mtolo et al., 2019). These ARVDs have LogKow greater than 2; hence they are likely to bind in the solid matrix (K'oreje et al., 2016). Due to the LogKow above 2.5 but less than 4 (abacavir, 2.5 and nevirapine, 3.9), these compounds are expected to have medium sorption potential in solids, whereas efavirenz (5.2) is expected to have high sorption potential since its LogKow is greater than 4 (Schoeman et al., 2017). Moreover, the target ARVDs have a molar mass of less than 1000 g/mol, which indicates their potential to be taken up by plants (Madikizela et al., 2018).

Table 2.1: Physicochemical properties of the ARVDs of interest

Compound	Structure	Molar mass g/mol	Solubility mg/mL	pKa	logKow	Excretion % via urine and feces	Bioavailability	References
Abacavir		286.33	77.0	5.77	2.5	18	-	(Abafe et al., 2018)
Efavirenz		315.68	0.00855	-1.5	5.4	62	83	(Sathigari et al., 2009)
Nevirapine		266.89	0.7046	2.5	3.89	2.7	>90	(Ngumba et al., 2016)

### **2.3. Sources of ARVDs in the environment**

The presence of pharmaceuticals in the environment has raised apprehension in water brokers (Obidike and Mulopo, 2018), as water is an essential source for all living organisms. About 71% of the earth's surface is covered by water; however, only 3% is earth's fresh water, and 2.5% of earth's fresh water is locked up in ice caps, glaciers, and permafrost or covered up deep in the ground making them to be unavailable for usage (Ntuli and Pakade, 2020). Therefore, the quality and quantity of water will always matter. In most African countries, there is a scarcity of freshwater as a result of poor infrastructure as the water suppliers are being polluted with noxious wastes containing organic compounds. Water pollution results from a lack of water replenishments, poor sanitation facilities, improper disposal of expired drugs, and underperforming wastewater treatment plants to completely remove micro pollutants (K'oreje et al., 2016), (Ncube et al., 2018, Mlunguza et al., 2020).

The loads of various pharmaceuticals, including ARVDs are introduced into the environment in many pathways. The manufacturing industries introduce pharmaceuticals into the environment through disposal in landfills and discharge of untreated effluent. In the landfill site, pharmaceuticals leach through the soil underground and pollute ground water (Ngumba et al., 2016, Lin and Tsai, 2009). Whereas the untreated effluent from the manufacturing industries is discharged into the environment and reaches surface water through surface runoff, and some are transported into WWTPs via waste pipes. A significant amount of human medical compounds are discharged with the effluent from hospitals and households through defecation of the consumed and not completely metabolized pharmaceuticals in the human body or disposal of unused or expired drugs into the sewage systems. The WWTPs receive the wastewater containing pharmaceuticals from the sewage pipe. After the treatment processes in WWTPs, the effluent containing pharmaceuticals that were not completely decomposed in WWTPs is discharged into surface water. In contrast, some domestic effluents are transported into septic tanks and transferred straight to surface water or groundwater. The veterinary compounds are used to treat various diseases in animals. During the application, some pharmaceuticals pollute non-target, seep into the soil and reach underground water, and some reach surface water through rainwater runoff. The veterinary compounds are consumed by animals, and the incompletely metabolised compounds in the animals' bodies are excreted through urinary or faecal waste into the soil together with the one from the aerial sources. The pharmaceuticals from urban emergence, like accidental leakage, also reach surface water (Mtolo et al., 2019, Madikizela and Chimuka, 2017b). The polluted surface water is used in

agricultural areas for irrigation purposes, which is one of the pathways on how pharmaceuticals are introduced in agricultural areas. Plants growing in the contaminated soil or water absorb contaminants from the soil or water and introduce pharmaceuticals into the edible parts of the plants (Akenga et al., 2021, Mlunguza et al., 2020, Madikizela et al., 2018). Furthermore, surface water and underground water are reclaimed and remediated then supplied back to the household and served as drinking water (Lin and Tsai, 2009). Figure 2.1 indicates some possible sources of pharmaceuticals and routes in significant areas of the water and food chain (Patel et al., 2019).

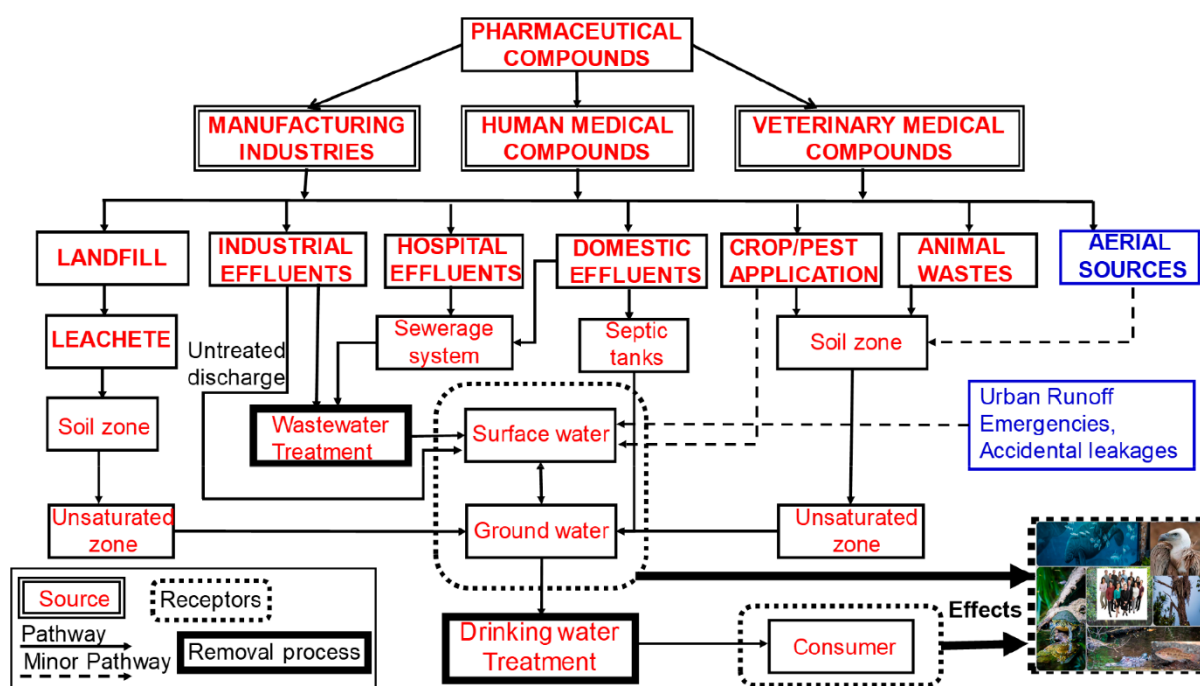


Figure 2.1: Pharmaceutical sources and routes in the water and food chain (Patel et al., 2019)

## 2.4. Effects of ARVDs

Regardless of preventing HIV transmission, reducing HIV-associated illness, and extending survival, ARVDs have been reported to have severe side effects on patients taking them as a daily treatment. The severe side effects include hepatotoxicity, rash, hypertriglyceridemia, central nervous system adverse effect, lipoatrophy, fatigue, appetite loss, lipodystrophy, nausea, and vomiting. Abacavir antiretroviral drug can cause disturbances in the central nervous system, such as psychosis and mania, and efavirenz is also associated with the toxicity central nervous system, resulting in vivid dreams irritation, and sleeplessness (Abers et al., 2014). Moderate, severe liver problems are also efavirenz side effects (Rimayi et al., 2018). It has been reported that pharmaceuticals can have adverse effects on aquatic organisms, such as

stunted growth, mortality, and impaired reproduction (Brausch et al., 2012). Some studies have been done to examine the toxicity and bioaccumulation of pharmaceuticals on organisms that are non-target, such as snails, mussels, crustaceans, fish, between other animals, reporting bioaccumulation factors of span range 0.66 – 32 022 (Ebele et al., 2017). Fish exposed to ARVDs contaminated water were observed to develop livers aberration (Rimayi et al., 2018). The environmental effects of ARVDs are not yet known regardless of their high consumption rates in the past three decades (Mosekiemang et al., 2019).

## **2.5. Occurrence of ARVDs in the environment**

Suppose the total number of patients on treatment is considered. In that case, it is sensible to suspect that, despite a few drugs lost due to their digestion system and transformation, ARVDs contribute significantly to the total ARDs stack in wastewater. Hence, the WWTPs have been recognized to distribute a significant amount of ARVDs into the environment (Madikizela et al., 2020, Ngumba et al., 2020, Ncube et al., 2018). In this regard, recent studies have reported the occurrence of ARVDs in aquatic and other environmental samples. Some studies were conducted in South Africa (Mlunguza et al., 2020, Mosekiemang et al., 2019, Mtolo et al., 2019, Afafe et al., 2018, Rimayi et al., 2018, Schoeman et al., 2017, Wooding et al., 2017, Schoeman et al., 2015). High concentrations of ARVDs ranging from ng/L to µg/L have been reported in aquatic environmental samples. Efavirenz is the ARVD that has been quantified at high concentrations in KwaZulu-Natal WWTPs than in other SA provinces and African countries. The highest concentration obtained in KwaZulu-Natal wastewater was 140.4 µg/L and 93.1 µg/L in influent and effluent wastewater, respectively (Mtolo et al., 2019). Whereas in Gauteng, the maximum concentration reported was 17.4 µg/L and 7.1 µg/L in influent and effluent wastewater, respectively (Schoeman et al., 2015). In Western Cape it was 15.4 µg/L and 18.1 µg/L in influent, and effluent wastewater, respectively. In a study conducted in Nigeria, efavirenz was found at a maximum of 1.02 µg/L in influent and 0.11 µg/L (K'oreje et al., 2016).

In a study conducted in KZN the highest concentration of nevirapine in wastewater was 2.8 µg/L in influent and 1.9 µg/L in effluent wastewater (Afafe et al., 2018). Other studies conducted in other SA provinces reported nevirapine's highest concentrations of 2.1 µg/L, influent (Schoeman et al., 2015), and 0.48 µg/L effluent wastewater (Schoeman et al., 2017) in Gauteng. In Western Cape, the maximum concentration of nevirapine reported was 0.00681 µg/L in influent and 0.000658 µg/L in effluent wastewater (Mosekiemang et al., 2019).

In other African countries, the presence of nevirapine has been reported with the maximum concentration in Kenya, 3.3 µg/L in influent (K'oreje et al., 2016) and 9.5 µg/L in the effluent (Kairigo et al., 2020). Nevirapine was found at a high concentration of 0.68 in influent and 1.728 in effluent wastewater in Zambia (Ngumba et al., 2020). The study conducted in Finland reported the highest concentration of 0.19 µg/L in influent and 0.1 µg/L in the effluent (Ngumba et al., 2016). Comparing the reported studies, nevirapine was found at high concentration in Kwa Zulu-Natal than other SA provinces, however, Kenya was found to be the most polluted than the other African countries and overseas countries.

There are few studies that monitored abacavir in wastewater. In the study conducted by Afafe and co-workers in KwaZulu-Natal, SA, the concentration of abacavir was found to be 14 µg/L in the influent wastewater and not quantified in effluent wastewater (Afafe et al., 2018). In a study conducted in Germany abacavir was found to be 0.225 µg/L in the influent wastewater and not detected in the effluent wastewater (Prasse et al., 2010). These findings indicate that WWTPs are amongst the main sources of ARVDs in the environmental water; therefore, the ARVDs have been monitored in the surface water.

Mlunguza and co-workers investigated the occurrence of ARVDs in KwaZulu-Natal, SA surface water, and high concentrations were reported, with the highest concentration of efavirenz up to 37.6 µg/L (Mlunguza et al., 2020). Another study that monitored efavirenz in KwaZulu-Natal, SA surface water reported an efavirenz maximum concentration of 2.5 µg/L (Mtolo et al., 2019). The maximum concentration reported in KwaZulu-Natal surface water was higher than the concentration reported in Gauteng, which was 0.354 µg/L (Rimayi et al., 2018) and 0.148 µg/L (Wooding et al., 2017). In Limpopo, efavirenz was not detected in the surface water (Wooding et al., 2017). The occurrence of nevirapine has been investigated in the surface water, and it was found at a maximum of 0.227 (Wooding et al., 2017), 0.057 µg/L (Rimayi et al., 2018) in Gauteng, and 0.044 µg/L (Wooding et al., 2017). Similar studies have been done in other African countries, and the maximum reported concentrations of nevirapine was 2.3 µg/L (Kairigo et al., 2020) in Kenya and in Zambia was 0.22 µg/L (Ngumba et al., 2020). The presence of efavirenz and nevirapine in wastewater influent have also been accompanied by the detection of their metabolites (Mosekiemang et al., 2019). Summarised results of the previously reported studies are shown in Table 2.2. Variance in the occurrence of ARVDs amongst different regions is generally reflective of the ARVDs consumption, the excretion rate, effectiveness and availability of wastewater collection and treatment facilities along with ecological and socio-economic conditions (Mtolo et al., 2019, Rimayi et al., 2018).



Table 2.2: ARVDs detected in South Africa, other African countries, and selected countries

Pharmaceutical Compound	Matrix	Concentration range (µg/L)	Extraction and quantification method	Country/ City	Reference
Efavirenz	Wastewater Influent	1.02 - 26.3	HF-LME and LC-MS <sup>2</sup>	SA/ Durban	(Mlunguza et al., 2020)
	Wastewater Effluent	3.27 – 37.3		SA/ Johannesburg	
	Surface water /Dam	nq - 37.3			
Efavirenz	Wastewater Influent	11.1 - 140.4	SPE/MIPs cartridge and LC-PDA	SA/Durban	(Mtolo et al., 2019)
	Wastewater Effluent	2.79 - 93.1			
	Surface water	nq - 2.45			
Abacavir, Efavirenz Nevirapine	Wastewater Influent	6.7 – 34	SPE/Oasis HLB cartridges and LC-MS <sup>2</sup>	SA/Durban	(Abafe et al., 2018)
	Wastewater Effluent	5.4 – 34			
Efavirenz	Surface water	0.02 – 0.354	SPE/Bond Elute Plexa cartridges and LC-MS <sup>2</sup>	SA/ Johannesburg	(Rimayi et al., 2018)

Efavirenz Nevirapine	Wastewater Influent Wastewater Effluent	0.05 - 1.4 0.5 - 2	SPE Oasis/HLB cartridges and GC- TOFMS  UE followed by a QuEChERs and GC- TOFMS	SA/ Johannesburg	(Schoeman et al., 2017)
Efavirenz Nevirapine	Surface water	0.00034-0.148 nd-0.0444	Direct sorption and GC×GCTOFMS	SA/ Johannesburg SA/ Louis Trichardt	(Wooding et al., 2017)
Efavirenz Nevirapine	Wastewater Influent Wastewater Effluent	2.1 – 17.4 0.1 - 7.1	SPE/Bond Elute cartridges, and GC- TOFMS	SA/ Johannesburg	(Schoeman et al., 2015)
Efavirenz Nevirapine	Wastewater Influent Wastewater Effluent	0.000681 – 0.0154 0.000658 – 0.00915	SPE/ Strata SDB-L Cartridges and LC- MS <sup>3</sup>	SA/ Western Cape	(Mosekiemang et al., 2019)
Nevirapine	Wastewater Effluent Surface water	9.5 0.9 – 2.3	SPE/ Oasis HLB and LC-MS <sup>2</sup>	Kenya/Nairobi	(Kairigo et al., 2020)

Nevirapine	Wastewater Influent	0.68	SPE/ Oasis HLB and LC-MS <sup>2</sup>	Zambia/ Lusaka	(Ngumba et al., 2020)
	Wastewater Effluent	1.720			
	Surface water	0.21 – 0.22			
	Underground water	nd – 0.0385			
Efavirenz Nevirapine	Wastewater Influent	0.85 – 3.3	SPE/ Oasis HLB and LC-MS	Kenya/Nairobi	(K'oreje et al., 2016)
	Wastewater Effluent	1.03 – 2.08			
	Surface water	1 – 2			
Nevirapine	Wastewater Influent	0.13 - 0.19	SPE/Oasis HLB cartridges and LC- MS <sup>2</sup>	Finland/Jyväskylä	(Ngumba et al., 2016)
	Wastewater Effluent	0.08 - 0.1			
Abacavir Nevirapine	Wastewater Influent	0.0048 – 0.0225	SPE/ Isolute ENV+ Cartridges and LC- MS	German/Frankfurt	(Prasse et al., 2010)
	Wastewater Effluent	0.0072 – 0.0321			

## 2.6. Occurrence of pharmaceuticals

Active ingredients of pharmaceutical compounds are absorbed by non-food and food crops growing in the polluted environment, either water or soil medium. Several studies have been conducted on the uptake of pharmaceuticals by plants. However, a straightforward mechanism to elaborate on the uptake of pharmaceuticals by plants and their translocation to the aerial part of the plant is not well understood. The crop's exposure can be either under agricultural land conditions on soil modified with sewage sludge or biosolids or irrigated with contaminated water (Bagheri et al., 2019, Carter et al., 2018, Mordechay et al., 2018, Paz et al., 2016, Prosser et al., 2014) or under controlled conditions such as a pot-trial method or hydroponic (Chuang et al., 2019, Kodešová et al., 2019, Tian et al., 2019, Al-Farsi et al., 2018, Azanu et al., 2016, Hurtado et al., 2016, Ahmed et al., 2015, Goldstein et al., 2014). In addition, plant uptake studies that have been conducted are mainly based on therapeutic treatments such as non-steroidal anti-inflammatory, antibiotics, anti-epileptics, and analgesics antidepressants hormones. These past studies are accompanied by reviews (Keerthanan et al., 2021, Madikizela et al., 2018, Al-Farsi et al., 2017).

A study conducted in Oman evaluated the uptake of pharmaceuticals by radish from the soil irrigated with treated wastewater. In this study, the radish showed the ability to take-up some of the target pharmaceuticals. Amoxicillin and sulfamethoxazole accumulated in the radish root of both high and low spiked concentrations treatments. Sulfamethoxazole was found at 1060  $\mu\text{g/kg}$  and 1890  $\mu\text{g/kg}$ , whereas amoxicillin was found to be 810  $\mu\text{g/kg}$ , and 910  $\mu\text{g/kg}$  for low and high spiked concentrations, respectively. It was also observed that radish could translocate amoxicillin and sulfamethoxazole when there is enough concentration. Hence only high spiked concentrations of radish managed to translocate amoxicillin, 1730  $\mu\text{g/kg}$ , and sulfamethoxazole, 6040  $\mu\text{g/kg}$ . The translocation factors obtained were 6.04  $\mu\text{g/kg}$  for sulfamethoxazole and 1.73  $\mu\text{g/kg}$  for amoxicillin (Al-Farsi et al., 2018).

Another study was conducted in Cyprus by Christstou and coworkers, where pharmaceutical uptake by tomatoes irrigated with wastewater for over a period of three years was investigated. Tomato fruit was analyzed, and the obtained highest concentration was 11.516  $\mu\text{g/kg}$ . The high bio-concentration factors were up to 132.28  $\mu\text{g/kg}$  (Christou et al., 2017). Azanu and coworkers conducted an experiment in Ghana to evaluate the uptake of pharmaceuticals by carrot and lettuce. The reported maximum concentrations of pharmaceuticals were 28.3  $\mu\text{g/kg}$ , and 136.8  $\mu\text{g/kg}$  in lettuce and carrots for tetracycline, 33.6  $\mu\text{g/kg}$  in lettuce, and 45.2  $\mu\text{g/kg}$  in a

carrot for amoxicillin, respectively. These results revealed that carrots absorb amoxicillin and tetracycline better than lettuce. Furthermore, tetracycline accumulates better in both lettuce and carrot than amoxicillin. The obtained BCF ranges were 0.3 - 0.4 in lettuce and 0.4 – 0.5 in carrots (Azanu et al., 2016).

The uptake of pharmaceuticals by sweet potato and carrot root vegetables irrigated with treated wastewater was investigated by Malchi et al. (2014) in Asia. The reported results showed the same trend of pharmaceuticals in carrot and sweet potato roots and leaves. Pharmaceuticals exhibited high concentrations in leaves, up to 65.81 µg/kg, then in roots at 10 µg/kg. High concentrations were found in carrots than in sweet potato, which was reported to be due to low lipid content in sweet potato. Also, the development of root structures is different. Sweet potatoes, after plantation, take 100 days to bulky the root, whereas carrots are gradual and dependent on the season (Malchi et al., 2014).

Another study was conducted in Spain to investigate the uptake of pharmaceuticals by lettuce, carrots, and green bean vegetables. The results showed that lettuce absorbed a high concentration of pharmaceuticals up to 113 µg/kg, whereas the carrot and green beans it was 60 µg/kg and 62.2 µg/kg, respectively. It has been reported that the hydroponic system assists in studying the pharmaceutical compound's uptake because a few factors need to be considered (Calderón-Preciado et al., 2013). García et al. (2018) investigated the uptake of carbamazepine and diclofenac by different species of lettuce in water. The obtained maximum concentration was 1400 µg/kg in leaves and 750 µg/kg in the root. Mini romaine showed a high concentration for both compounds in leaves, with diclofenac as the highest and a translocation factor greater than 1. In contrast, iceberg and oak leaves exhibited high concentrations of carbamazepine in roots. The reported bioconcentration factors in root and leaves were below 1, ranging from 0 to 0.83 µg/kg in leaf and 0.18 – 0.43 µg/kg in the root. (García et al., 2018). In consideration of the past studies and reviews, it has been revealed that there is little data on the pharmaceutical class ARVDs, which is equally essential as other pharmaceutical therapeutic treatments.

In this regard, a comprehensive insight on the occurrence of ARVDs (efavirenz, emtricitabine, disoproxil, and tenofovir) in hyacinth plants which are plants that naturally occur in the rivers or under wet conditions, has been done by Mlunguza et al. (2020). Different parts of the plant (roots, stems, and leaves) sampled from the surface of natural water were analysed, including the water where these plants grew. The concentrations of efavirenz detected in roots, stems, and leaves were 29.6 µg/kg, 11.42 µg/kg, and 9.98 µg/kg in Springfield samples and 17.2, 9.63,

and 8.91 µg/kg in Hartebeespoort dam samples. However, it is important to comprehensively elucidate the interactions of plant root-ARVDs by using a fully structured experimental approach. In this regard, a full structured hydroponic experimental approach was conducted by Akenga et al. (2021), monitoring the ARVDs (efavirenz, nevirapine, lamivudine, and oseltamivir phosphate) uptake by lettuce in water. The reported outcomes were positive, with high concentrations of efavirenz 3463 µg/kg. The study revealed that humans and other living organisms are at risk as lettuce is a common vegetable consumed almost every day by some individuals, and this could result in a daily unintentional consumption of ARVDs. It also showed that vegetables could accumulate ARVDs from the root to the aerial part of the plant, as the translocation factor of nevirapine was above 2. However, since Akenga and co-workers conducted a fully structured hydroponic approach, a full study providing the complexity of a natural agroecosystem environment is still needed. Furthermore, Akenga and co-workers' study evaluated only a leafy vegetable (lettuce). To close this gap, in this current work, a pot-plant study was conducted to investigate the uptake of three ARVDs (Abacavir, efavirenz, and nevirapine) into beetroot, spinach, and tomato. A summary of the results reported in previous studies done to assess the pharmaceutical uptake by vegetables is shown in Table 2.3. This brings a thought that vegetables have the potential to be used in the phytoremediation process for eradicating the ARVDs from the environment.

Table 2.3: Summarised studies of pharmaceutical uptake from soil and water by vegetables

Pharmaceutical group	Vegetable matrix	Growing medium	Extraction/analysis method	Concentration range (µg/kg)	Country/ City	Reference
Antiretroviral	Beetroot, spinach, and tomato	Soil	UE/LC-MS	6.77 – 40.21	South Africa /Pietermaritzburg	(Paper sent for possible publication)
Antiretroviral	Lettuce	Water	UE-SPE/ LC-MS	691 - 3463	England /Plymouth	(Akenga et al., 2021)
NSAIDs and antibiotics	Radish	Soil	UE-SPE/LC-MS <sup>2</sup>	1.06 - 1.89	Oman/Muscat	(Al-Farsi et al., 2018)
Anti-inflammatory and antiepileptics	Lettuce	Water	UE-SPE/UPLC and HR-QTOF-MS	10 - 1400	Spain/Murcia	(García et al., 2018)
NSAIDs and antibiotics	Tomato	Soil	UE/LC-MS <sup>2</sup>	0.155 - 11.615	Cyprus/Nicosia	(Christou et al., 2017)
Antibiotic	Carrot and lettuce	Soil	PLE/ SPE/LC-MS	4.4 – 45.2	Ghana/Kumasi	(Azanu et al., 2016)

NSAIDs and antiepileptics	carrots and sweet potatoes	Soil	Agitation/LC-MS	0.05 – 65.81	Asia/Jerusalem,	(Malchi et al., 2014)
Anti-inflammatory, NSAIDs, and antiepileptics	lettuce, carrots, and green beans	Soil	Pressurized fluid Extraction/ GC-MS	1 - 113	Spain/ Caldes de Montbui	(Calderón-Preciado et al., 2013)



## **2.7. Phytoremediation**

Phytoremediation of ARVDs is a process of removing the ARVDs from contaminated water, soil, and sludge through the diffusion of the dissolved compound and mass flow by the plant's root (Singh and Kumar, 2018). Phytoremediation involves four mechanisms to occur, which include i) absorption and accumulation of an organic substance, ii) translocation via stem to leaves after absorption, iii) metabolization of the organic substances in the rhizosphere or tissues of the plant through microbial activities, and iv) degradation of the organic substances by microorganisms and plants (Sasi, 2011). Researchers have reviewed and investigated the process of phytoremediation, and it has been said to fall under environmentally friendly cleaning methods (Jacklin et al., 2020, Arthur et al., 2005). The advantages of phytoremediation are that the cultivated plants in the remediation area look appealing in the eyes; a minor effort is needed to grow the plants, and the plants are easily monitored. It is cheaper than using other advanced cleaning methods such as membrane bioreactors, membrane techniques, activated carbon adsorption, electrochemical oxidation, and an advanced oxidation process (Singh and Kumar, 2018). These advanced technologies have been reported to be unsuccessful most of the time in the technological system, and they are pretty expensive (Wolecki et al., 2020). However, phytoremediation also has drawbacks, such as a larger area required for tree plantation, it is a slow process, and the pollutants should be within the roots zone for them to be reached by the roots (Sasi, 2011). There is little information on phytoremediation, and few plants have been investigated to remove organic pollutants submerged in the environment (Mahmoud and Hamza, 2017). It has been raised that the use of hydroponics can lead to a better solution in removing organic compounds in wastewater (Schröder et al., 2007). The investigation of pharmaceuticals and endocrine-disrupting compounds removal from biological WWTPs using hydroponic cultivation has been done. The three plants that have been explored are *Cyperus papyrus*, *Lysimachia nemorum*, and *Euonymus europaeus*. From the reported result, *Lysimachia nemorum* was found to be the best plant can as it takes high concentration up to 2.525 µg/kg (Wolecki et al., 2020).

### **2.7.1. Accumulation of ARVDs**

The accumulation of drugs in agricultural crops is a significant factor in human health risk assessment. The accumulation of ARVDs in vegetable plant tissues is expressed by a bio-concentration factor (BCF) which is calculated as the ratio of the ARVD concentration in the

plant tissue to the nominal concentration in the growth medium (Akenga et al., 2021). The accumulation of the target analyte concentration in roots is expressed by a root concentration factor (RCF), the ratio of the analyte concentration in roots to that in the exposure medium (soil or water) (Gurama and Usman, 2020). The movement of the target analyte from the root to the aerial part of the plant is expressed by the translocation factor (TF), signifying the uptake effectiveness of the available analytes from the system. It suggests whether the plant is able to accumulate the analyte or not. The TF expression is a ratio of the target analyte concentration in the aerial part of the plant to that in the roots (Al-Farsi et al., 2017). A vegetable plant with both translocation factor and bio-concentration factor greater than one has the potential to be used for phytoremediation. In addition, the vegetable plant with a translocation factor less than one and a bio-concentration factor greater than one has the potential for phytostabilization (Gurama and Usman, 2020).

A previous study has reported a weak relationship between  $\log$  RCF and  $\log$   $D_{ow}$  (octanol-water partitioning coefficient adjusted to the neutral fraction of ARVDs in water) and a negative relationship between  $\log$  TF and  $\log$   $D_{ow}$  (Akenga et al., 2021). However, it has been revealed that the different experimental approaches, plant species, target analyte dosage, and exposure period affect the results of the relationship between  $\log$  RCF or TF or BCF and  $\log$   $D_{ow}$  (Miller et al., 2016). Mostly, the uptake of neutral pharmaceuticals by the plant is higher than charged molecules because negatively charged species are repelled by cell walls with negative electrical potential. In contrast, positively charged species are attracted to the cell walls with negative electrical potential hence restraining their translocation into plants (Chuang et al., 2019). Some drug species could be changed in plant tissues and subsequently stuck in plant cells in reaction to pH variants in different tissues (Taiz et al., 2015, Goldstein et al., 2014).

## **2.8. Extraction Techniques**

Regardless of the advanced analysis methods, isolation of the target compounds from the intricate plant matrix, and removal of potential errors throughout the determination of the target analyte, is still challenging. Therefore, preparing a sample is an important step in the analytical procedure (Ötles and Kartal, 2016). In this study, ultrasonic extraction (UE), ultrasonic-assisted liquid-liquid microextraction (UADLLE), microwave-assisted extraction (MAE), and microwave-assisted extraction-solid phased extraction (MAE-SPE) were used for the extraction of ARVDs from the vegetable matrix.

### 2.8.1. Ultrasonic Extraction (UE)

Ultrasonic extraction is a well-known traditional method and a better method than other traditional refluxing methods (Kunene and Mahlambi, 2020). In the principle of ultrasonic extraction, the ultrasonic field allows the formation nearby of micro-cavitations in the liquid covering the sample matrix. The effects are dual: limited warming of the solvent, and cell wall disruption freeing its content, increasing diffusion of the extract. The kinetic energy is introduced in the mixture subsequent to the breakdown of cavitation effervesces closer to walls, improving the mass transfer from the solid to the liquid phase. The powered effects of ultrasonic induce a better penetration of solvent into the sample matrix, enabling the discharge of analytes and improving mass transfer (Keil, 2007). It is well-referred and recognized as fast, enhancement of extraction yield using a small quantity of solvent, it is a quite low-cost method, and faster kinetics (Annegowda et al., 2012, Oluseyi et al., 2011). A typical UE setup is shown in figure 2.2. This method has been used for the transportation of analytes from solid samples into the liquid phase and also to remove pharmaceuticals from vegetable matrices (Al-Farsi et al., 2018, Li et al., 2014). However, it has some disadvantages, which include a lack of selectivity requiring thorough sequential clean-up (Ros et al., 2016). In this regard, new methods have been developed whereby the ultrasonic extraction method is linked with various clean-up methods such as SPE (Akenga et al., 2021) and dispersive-SPE (Ros et al., 2016). In recent studies, the use of microextraction methods such as hollow fiber-liquid phase microextraction, dispersive liquid-liquid extraction, and others have drawn attention.

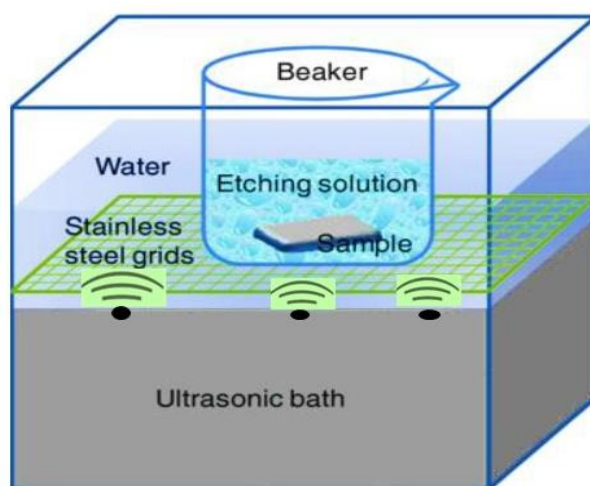


Figure 2.2: Typical setup of ultrasonic extraction (William AndrewToshiro K et al., 2012)

### **2.8.2. Ultrasonic assisted dispersive liquid-liquid microextraction (UADLLMAE)**

The method UADLLME consists of a basic UE procedure linked with the DLLME procedure. In this method, the analyte is extracted from the solid sample by means of an ultrasonic wave, and a DLLME method is utilised to clean up the extract attained from UE. The DLLME is a new rapid and simple extraction and preconcentration method developed by Rezaee et al (2016). In this technique, a suitable mixture of disperser solvent and extraction solvent are introduced into the aqueous sample by syringe quickly to achieve a cloudy mixture with dispersed extraction solvent small droplets in the aqueous solution. The mixture is vortexed and centrifuged. Subsequently, the extraction solvent float on top of the aqueous solution if it is a low-density extraction solvent or sediment in the bottom of the test tube if it's a high-density extraction solvent. The extraction solvent is then removed and transferred into a vial for analysis (Rezaee et al., 2006). A basic illustration of DLLME is shown in Figure 2.3 (Shiri et al., 2020).

The use of low-density extraction solvent in DLLME has recently gained attention to overcome DLLME drawbacks. Advantages of using low-density solvents are low toxicity, various choices of solvent, some methods do not involve centrifugation, and result in cleaner extract (Tan et al., 2018). Different parameters affect the efficiency of DLLME, such as extraction solvent, dispersive solvent, extraction solvent volume, a ratio of dispersive and extraction solvent, and extraction time (Rezaee et al., 2006). The advantages of DLLME include high efficiency, rapidity, requiring a small quantity of organic solvents, and easiness of operation (Gao et al., 2021). The DLLME also has drawbacks, such as that it often lacks to completely eliminate the interferences from matrix co-extractives, and that is the major reason why most DLLME applications reported have been focused on water samples which is a less complex matrix. Furthermore, it is not a selective extraction method (Khalilian and Rezaee, 2017). UADLLME has been used in the extraction of emerging pollutants from vegetables (Abril et al., 2018, Pirsaeheb et al., 2013, Bidari et al., 2011). Abril et, al (2018) reported high recoveries of pharmaceuticals at a span range of 85- 124 %.

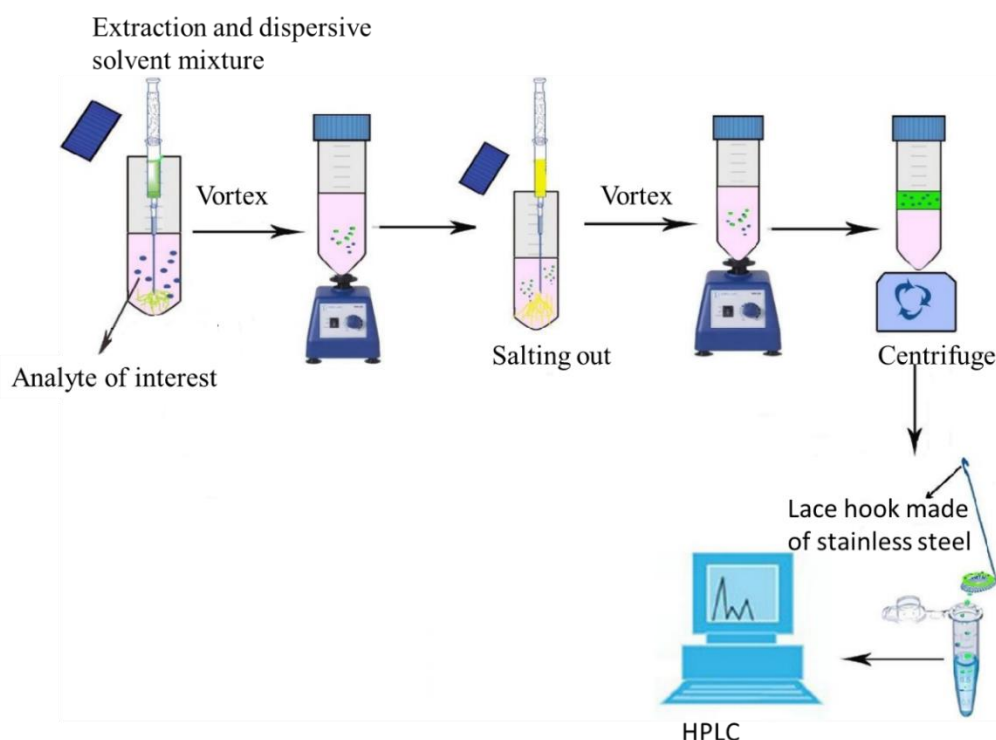


Figure 2.3: A schematic diagram illustrating a basic DLLME using light extraction solvent (Shiri et al., 2020)

### 2.8.3. Microwave-assisted extraction (MAE)

The MAE is a conventional method is used to extract soluble analytes into a solvent from various materials by means of microwave energy (Rehman et al., 2020). The MAE utilizes microwave radiation to introduce heat in the extraction solvent, therefore improving the diffusion of the extracting solvent into the sample and thus quickening the partitioning of the analyte from the solid sample to the solvent (Kataoka, 2019). A microwave device consists of four components, namely: 1) microwave generator, which is used to generate microwaves, 2) waveguide which is used to control the circulation of the microwave to the microwave cavity from the source, 3) applicator which is used to place the sample holder, and 4) circulator which is used to control the MAE movement (Tatke and Jaiswal, 2011). The MAE is considered to be a better method than the traditional methods. The principal improvement of MAE is its competence to rapidly heat the mixture of sample and solvent, ensuing in its broad applicability for the fast extraction of analytes, including thermally unstable substances. It accommodates water as an extraction solvent, which makes it an environmental friendly method and can also extract more medium to nonpolar compounds (Li et al., 2017). Furthermore, MAE also meets

the standards of other latest extraction techniques: ultrasound-assisted extraction, supercritical fluid extraction, and pressurized liquid extraction, in terms of equipment costs, uncomplicatedness, and performance (Ibrahim and Zaini, 2017). The information on dielectric properties is significant for every constituent and combination involved in microwave heating to be able to estimate the heating rates and describe the reaction of materials when exposed to microwave electric fields in dielectric heating uses. For example, a solvent used in the MAE should have a high dielectric loss that absorbs electromagnetic energy strongly. As a result, the dielectric properties of the solvent and material used are essential to be considered before MAE (Ibrahim and Zaini, 2017). A MAE image is shown in Figure 2.4. The MAE has been used to extract pollutants from vegetables (Moret et al., 2019, Singh et al., 2004). In the study conducted by Mlunguza et al. (2020), MAE was utilized to extract efavirenz from hyacinth plants. The recoveries up to 102% with LOD, 6.01  $\mu\text{g/kg}$  and LOQ, 10.29  $\mu\text{g/kg}$  were obtained indicating its good accuracy and sensitivity.



Figure 2.4: Typical image of microwave unit with a MAE sample holder

#### **2.8.4. Solid-phase extraction (SPE)**

The SPE is a sample preparation method developed in the 1980s by a combination of liquid chromatography and liquid-solid extraction. The enrichment, purification, and separation of the sample are primarily achieved by the selective process of desorption and adsorption of the

sample analytes by the solid phase sorbent. The SPE is mainly used to improve the sensitivity of detection and reduce the interference of the sample matrix (Mosekiemang et al., 2019). The SPE procedure involves the loading of a liquid sample containing analyte through the conditioned adsorbent bed. During the sample loading, the target analytes are retained in the adsorbent bed. Thereafter a solvent with a suitable strength is used to wash off the possible impurities without removing the target analytes. The adsorbent is then dried under a vacuum to remove traces of the washing solvent. Then, the target analyte is eluted with a small solvent quantity of a strong strength to completely remove the retained analyte in the adsorbent (Aries et al., 2011). It is significant to consider the SPE factors that may affect the efficiency of the SPE, such as the selection of the sorbent and the conditions of the extractions procedure to obtain the desirable multiresidues SPE recoveries (Ngumba et al., 2016).

There are a quite number of SPE sorbents widely used in the extraction of ARVDs in aqueous samples including hydrophilic-lipophilic balance (Oasis HLB), strong cation exchange (Oasis MCX), and strong anion exchange (Oasis MAX), Strata TM-X sorbent, ENVI-18, Strata C18, etc. It has been revealed that among the tailor-made sorbents the Oasis HLB is a better SPE sorbent for extraction of pharmaceuticals with a wide range of chemical properties and polarities. This sorbent is made of divinylbenzene and N-vinylpyrrolidine monomers which permit the retaining of lipophilic and hydrophilic compounds (Kafeenah et al., 2018, Ngumba et al., 2016). In the past studies conducted to evaluate the ARVDs present in water, desirable and consistent recoveries (80-120%) of efavirenz and nevirapine with other related drugs were reported (Abafe et al., 2018, Kafeenah et al., 2018, Schoeman et al., 2017, K'oreje et al., 2016, Ngumba et al., 2016). In this regard, SPE has been incorporated in extraction methods of pharmaceuticals from vegetables to preconcentrate and clean up the extract (Al-Farsi et al., 2018, García et al., 2018). Furthermore, high recoveries of ARVDs efavirenz (75%) and nevirapine (88%) have been reported where SPE was used as a clean-up method (Akenga et al., 2021). The general process of solid-phase extraction is illustrated in Figure 2.5. The SPE method has also been used to extract ARVDs in water (Mtolo et al., 2019).

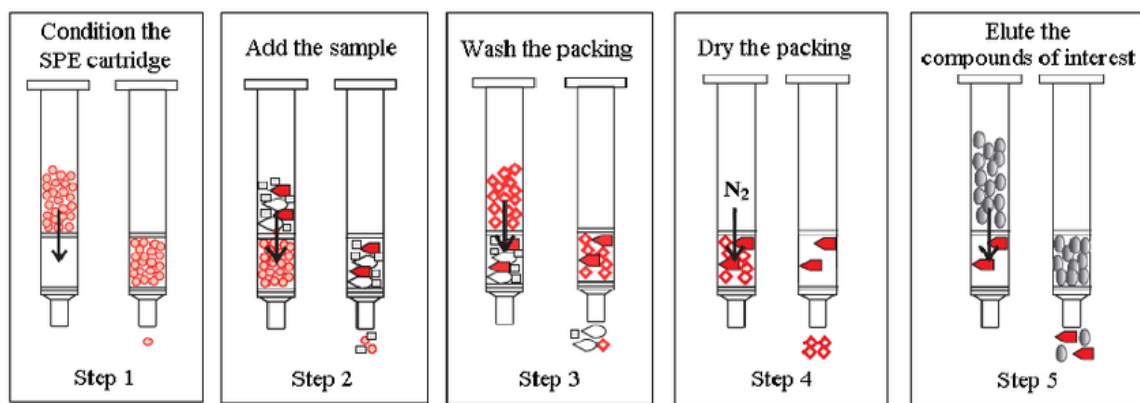


Figure 2.4: General process of Solid-phase extraction (Aries et al., 2019)

## 2.9. Removal of pharmaceuticals

### 2.9.1. Removal of ARVDs during treatment processes of wastewater in WWTPs

The incompetence of wastewater treatment plants in removing ARVDs during domestic wastewater treatment has been examined in a couple of wastewater treatment plants. Various efficient removal of ARVDs compounds varies across diverse WWTPs, which has been reported to be due to the degradation of the organic compounds in WWTPs relying on the efficiency of biological treatment and adsorption onto the sludge (Madikizela, 2017). The reported various efficient removals for efavirenz across WWTPs range from 34 to 98% (Mtolo et al., 2019). Elsewhere it has been reported that nevirapine and abacavir were found to be <0% and > 99 %, respectively (Prasse et al., 2010). In this regard, it is significant to investigate further the remediation measures that could be applied to improve wastewater treatment processes.

### 2.9.2. Strategies for removal of ARVDs and other related organic drugs in water

Many remediation methods have been explored for the removal of ARVDs and other related drugs in water, such as degradation, and photodegradation (Thakur et al., 2020, Hemmat et al., 2021), photo-Fenton, Fenton-like (Tang and Wang, 2020, Zhuan and Wang, 2020), adsorption (Kebede et al., 2019), photocatalysis (Hu et al., 2019), filtration (Liu et al., 2018), membrane bioreactors (Radjenovic et al., 2007), as well as coagulation (Xu et al., 2016). However, the investigation of adsorption procedures has recently gained attention for the remediation of water (Akpomie et al., 2019, Okoli and Ofomaja, 2018, Tella et al., 2018). Adsorption has been found to be a better and deliberated as a powerful alternative to conventional treatment methods for the removal of pollutants due to its versatility, low cost, reliability, simplicity, high capacity,



great efficiency, ease of operation, and consume less energy (Rosli et al., 2021). The attention drawn by adsorption methods has resulted in the development of various adsorbents, of which few have been explored to remove ARVDs in water. Nanofibers from *Mondia white* root extract have been investigated for the removal of ARVDs where up to 92% for efavirenz and 80% for nevirapine have been removed (Kebede et al., 2020). The adsorption of abacavir in the molecularly imprinted polymer sorbent was also investigated, and high removal percentage of up to 92% was reported (Qwane et al., 2020).

Graphite sorbents have also been investigated to remove organic compounds in water (Ivancev-Tumbas et al., 2020, Hoang et al., 2019). Exfoliated graphite (EG) has attracted incredible attention ever since it was discovered. It is a carbon-based compound characteristically hydrophobic and nonpolar and consists of two graphene layers joined by van der Waals forces. Classically, it is used in pencils and lubricants. The hydrophobic nature and high theoretical specific surface area of exfoliated graphite make it a very promising sorbent material for the adsorption of polar and nonpolar compounds (Wu et al., 2015). It consists of a broad spectrum of applications involving polymer reinforcement fillers, electromechanical resonators, sensors, and adsorbents. This is due to the extraordinary properties of graphite, which are hydrophobic nature, large-specific surface area, thermal and mechanical stability, multi-porosity, and low density (Hoang et al., 2019). Graphite has a thermal conductivity of  $5000 \text{ Wm}^{-1}\text{k}^{-1}$  and above  $1060 \text{ GPa}$  stiffness (Ion et al., 2011), and that makes it have the potential to act as a good adsorbent. The EG was previously characterized for the absorption of heavy metals in oil, where it was found to have the capacity to absorb heavy metals (Hristea and Budrugaec, 2008, Vieira et al., 2006). However, it has recently been investigated for utilization in removing organic dyes such as methylene blue and rhodamine (Mohanraj et al., 2020), methylene blue and congo red (Hoang et al., 2019), and methylene blue (Wu et al., 2021). Hence, this study aimed to utilize EG to study the absorptivity of ARVDs from water. To the best of our knowledge, it was used for the first time for removing ARVDs in water in the current study.

## **2.10. Characterization techniques**

The synthesized sorbents are normally characterized by techniques such as Fourier Transform Infrared spectroscopy (FTIR), scanning electron microscopy (SEM), Visible-Ultraviolet spectroscopy (UV-VIS), transmission electron microscopy (TEM), thermogravimetric analysis (TGA), Brunauer -Emmet Teller (BET), X-Ray diffraction (XRD), Raman spectroscopy and Energy-dispersive X-ray spectroscopy (EDX).

### **2.10.1. Fourier Transform Infrared Spectroscopy**

The FTIR spectrophotometer is an instrument that gives the IR spectrum faster than other traditional spectrophotometers (Mohamed et al., 2017). It allows one to study the vibration of the functional groups present in the complex, consequently characterizing its molecular structure. The FTIR comprises emission, reflection, absorption, or photoacoustic spectrum achieved by the Fourier transform of an optical interferogram (Doyle, 1992). A radiant blackbody source emits a beam of IR irradiation, which is then produced by the instrument. Therefore, the beam traverses into the interferometer where the programming occurs. The beam penetrates the sample matrix then the sample engrosses particular frequencies of energy that are differently characteristic of the sample from the interferogram. Then, the special interferogram signals for all frequencies are simultaneously measured by the detector in energy versus time. Meanwhile, a beam is overlaid to give a reference (background) for an instrument's operation. Lastly, the desired spectrum is attained when the interferogram mechanically takes off the spectrum of the background from the spectrum of the sample by Fourier transformation computer software (Petit and Madejova, 2013). The main components of FTIR are source, interferometer, and detector. The FTIR has been successfully used to characterize the various graphite-based sorbents. In the previous study the NG, GIC, and EG FTIR analysis has been reported. The result obtained for NG showed 3435 and 1569  $\text{cm}^{-1}$  peaks which were attributed to water absorbed. In the GIC spectrum,  $\text{SO}_2^{4-}$  was presented by the two peaks at 603 and 1080  $\text{cm}^{-1}$ , whereas the  $\text{NO}_3^-$  peak was observed at 1384  $\text{cm}^{-1}$ . Comparing GIC to EG, the observed absorption peaks at 973, 1233, and 1635  $\text{cm}^{-1}$  in EG were assigned to formic acid which was used in the second intervention prior to exfoliation (Shengtao et al., 2011).

### **2.10.2. Scanning Electron Microscopy**

The SEM is a robust and flexible technique for material characterization, which has become more prominent recently as the size of materials used in diverse applications has shrunk (Nanakoudis, 2019b). It is used to characterize the surface morphology (Ghodke et al., 2021). The SEM uses the electrons that are reflected to generate the image. As the wavelength of light is higher than that of electrons, the SEM resolution is greater than a light microscope resolution. In SEM, the sample is scanned by the electron beam in a scan configuration. The electron source primary produces electrons at the top of the column which are then released when their thermal energy disables the work purpose of the source material. They are then hastened and enticed by the positively-charged anode (Nanakoudis, 2019b). There are five key components

in an ordinary SEM: sample chamber, column, electron source, electron detector, and computer display. The experiment can be conducted by taking a probe of the electrons focused on the composite and scanned along with a pattern of corresponding lines to achieve the result. Due to the effect of the incident electrons, signals are formed and composed as images that permit one to study the sample's surface. It is highly recommended to characterize particle size and shape because the necessary image acquisition and sample preparation are comparatively rapid and simple (Vladár and Hodoroaba, 2020). The SEM has been used to characterize exfoliated graphite. The characterization result showed a smooth surface in the natural graphite while the intercalated graphite showed a cracked surface and curl edges with a distance in layers. After exfoliation of the intercalated graphite the worm-like structure was obtained as the final product (Chung, 2016, Yu et al., 2012).

### **2.10.3. Energy-dispersive X-ray spectroscopy**

The EDX is a well-known technique, and material scientists commonly utilize it. The EDX detector is used together with SEM to generate data about the sample. The SEM as an individual technique generates fewer data about the sample; however, when the EDX is incorporated, the data about the sample improves. The EDX can rapidly produce a sample of chemical composition information, including identifying elements existing, their concentration, and distribution (Nanakoudis, 2019a). In a conventional SEM, when the samples collide with the electron beam, they interact with the beam and produce identifiable X-rays. As a result of the principle that elements have different X-ray emission spectrums, they can be distinguished, and sample concentration can be measured. The initial beam of electron collision with the nucleus of the sample atom generates the X-ray. The electron in an atom's nucleus will be excited by a primary electron beam, which will emit it from the nucleus and produce an electron-hole. The missing emitted electron is replaced by an electron from the atom's outer shell, which discharges the extra X-ray. The ejected X-ray contains an X-ray continuum and characteristic X-ray (Abd Mutalib et al., 2017). The advantage of using EDX is that it can be used for quantitative and qualitative analysis. It does not destroy the sample, and not much sample preparation is required. As a result, it has become a necessary part of maintaining SEM (Nanakoudis, 2019a). This technique has been used to study exfoliated graphite. The EDX spectra for graphite have been previously reported by Ndlovu and co-workers. The EDX spectra for NG and EG both showed a carbon peak which is evidence that graphite is formed by  $sp^2$  hybridized carbon, however, the EG EDX spectra showed an extra peak of oxygen which is the result of intercalation (Ndlovu et al., 2011).

#### **2.10.4. Ultraviolet-Visible**

UV-Vis method is an essential technique for the optical study of compounds. It helps to identify the absorption bands of the target compound in the material. The unknown compound in the sample can also be identified with the help of UV-Visible spectroscopy. For this motive, the reference compound is compared to the spectrum of the essential compound; if the spectrums are matched for both compounds, the conclusion can be drawn about the unknown compound. It also helps measure the purity of the sample by comparing the absorption of the sample under consideration with the reference solution and also by absorption intensity relative calculation (Raja and Barron, 2021). UV-Visible measures the offsetting of light that passes through an under consideration sample. To detect the chromophore of the functional group in the material completely, it approves the absence and presence of the molecule, which should be a compound. Both ultraviolet and visible parts of light consist of adequate energy to excite electrons from the ground to higher energy levels. The beam of light with a specific wavelength passes the cuvette containing the sample. The sample absorbs the visible emission or the ultraviolet. Then the UV-Visible spectrometry chart recorder provides the spectrum, which indicates the wavelength whereby the sample is absorbed (Sobarwiki, 2013).

#### **2.10.5. Transmission electron microscopy**

TEM is the most potent microscope at a maximum potential magnification of 1 nanometer. TEM utilizes energetic electrons to provide crystallographic, compositional, and morphologic information on the sample. High resolutions, black and white images from the interaction that occurs between energetic electrons in the vacuum chamber and the prepared sample are produced in the TEM. The air is needed to create a space where electrons can move pumped out of the vacuum. Thereafter, the electrons pass through the lenses of electromagnetic. The beam passes through the solenoids down the column, make interaction with the screen where electrons are rehabilitated to light, and forms images (Williams and Carter, 1996).

#### **2.10.6. Thermogravimetric analysis**

The TGA is an analytical instrument used to study the thermal stability of the material (Sibiya and Moloto, 2017). In this method, the changes in the material weight are measured as the temperature increases, which helps to study the moisture and volatility content of the material. The components of TGA consist of a programmable furnace to control the sample heat and a

very sensitive measuring scale used to measure the changes in the sample weight. The thermally isolated measuring scale is positioned on top of the furnace, and the suspended wire hanging down from the scale is holding a sample pan into the furnace, and this wire is highly precise. The scale ensures that it has no thermal effect to ensure accuracy and precision and maximize the sensitivity of weighing (Ebnesajjad, 2010). The TGA has been used to study the thermal stability of exfoliated graphite. The obtained results for the NG TGA curve, between 700 and 1000°C showed a loss of weight reaching 23.88 wt.% whereas the TGA curve for EG showed two steps of weight lost between 230 and 1000 °C. In EG the thermal event occurred at a temperature between 230–530°C reaching 73.53 wt.% (Shengtao et al., 2011).

#### **2.10.7. Brunauer -Emmet Teller**

The BET theory was developed in 1938 by Brunauer Stephen. Its development was extended from the Langmuir theory, which was developed by Irving Longmuir in 1916 to encounter its shortcomings. The analysis in BET is based on the adsorption of the gas atom onto a surface of a sample; hence the BET provides the data on the surface area of the sample. Liquid N<sub>2</sub> is used to cool the sample surface prior to its analysis. During the surface cooling, nitrogen gas distributes over the surface of the sample, and the gas atoms get absorbed by the sample surface. Thereafter, the layers of adsorption are formed, and the sample is then removed from the nitrogen atmosphere and heated up. During heating, the adsorbed nitrogen gas is released and quantified. The data collected is represented as a BET isotherm, which plots the adsorbed gas volume as a relative pressure function. Some of the BET shortcomings include measuring only the surface area of the dry powdered sample, too much time required for manual preparation, and too much time needed for the gas molecules adsorption to occur (Raja and Barron, 2020, Naderi, 2015). The obtain BET result in the previous study showed a high surface area and total pore volume for EG compared to NG. The EG surface area and total pore volume were 30 m<sup>2</sup>/g and 46.10–3 cm<sup>3</sup>/g, whereas NG were 3 m<sup>2</sup>/g and 7.10–3 cm<sup>3</sup>/g, respectively (Hoang et al., 2019). Another study reported a surface area range of 33.15 to 52.78 m<sup>2</sup>/g and a total pore volume of 0.04052 to 0.06010 cm<sup>3</sup>/g (Sykam and Kar, 2014).

#### **2.10.8. X-Ray diffraction**

X-Ray Diffraction is a rapid analytical instrument used to provide data on unit cell dimensions and used for the identification of phases, structure, preferred crystal orientations, and other structural parameters, such as crystal defects, strain, crystallinity, and average grain size. The

XRD is based on the crystalline sample and constructive interference of monochromatic x-rays. The peak of XRD results from the constructive interference of a monochromatic beam of scattered x-rays at specific angles from a set of lattice planes in a sample. The atomic positions determined the intensities of the peaks within the lattice planes. In a given material, the XRD pattern is the figure print of periodic atomic arrangements. The analyzed sample in the fine particles ground, homogenized, and standard amount composition is determined (Kohli and Mittal, 2018). XRD has been used to analyse exfoliated graphite base material. The reported result of XRD for NG showed the spectrum with two broad NG characteristic diffraction peaks at  $28.6^\circ$  and  $54.68^\circ$  in line with the (0 0 2) and (0 0 4) planes. Whereas the EG showed a shift of  $28.6$  to a lower angle of  $26.6^\circ$  which signals the raise in the interlayer distance at (0 0 2). This diffraction peak was narrow and weak (Hoang et al., 2019). Another study reported comparable results with the diffraction peak at  $2\theta = 26.6$  obtained in NG and EG spectrums indicating that the c-c bond is not destabilized by the intercalation and oxidation. However, the peak intensity for EG was weak (Shengtao et al., 2011).

#### **2.10.9. Raman Spectroscopy**

Raman spectroscopy is a highly powerful technique used to study the vibrational and other low-frequency modes, including the rotational in the sample. It helps in investigating the uniqueness of the liquid or solid sample (Adya and Canetta, 2014). This technique is good for qualitative analysis and discrimination of inorganic/inorganic compounds in a mixture and only a small quantity of a sample is required to obtain the Raman spectrum. The material or compound's functional groups are usually represented by sharp bands in the Raman spectrum, which can be fined as a plot of Raman intensity versus the frequency shift of the Raman. This data can simply be interpreted to identify the presence of the compound and to determine the chemical structure of the compound. In Raman spectroscopy, to analyze the effect of Raman, the laser is used as a source of light because Raman effects are so light. The incident light strikes a sample, and two scatterings are obtained: Rayleigh and Raman scattering. To vibrate or rotate the molecule requires energy. The energy required to vibrate or rotate the molecule is equal to the energy difference between the Raman scattered light and the incident light (Ebnesajjad, 2010). The Raman spectroscopy for graphite has been reported where the G, D, D', and G' bands were shown at about 1358, 1578, 2445, 2445, and  $2724\text{ cm}^{-1}$  respectively. The D band for GIC had a high intensity (Ndlovu, 2012). In another study, the obtained Raman spectroscopy results for graphite showed the G and D bands which appeared at around 1360

and 1560 cm<sup>-1</sup> respectively. The intercalated graphite showed an increase in the D-band (Song et al., 2010).

## **2.11. Quantification Techniques**

Chromatographic techniques such as gas chromatography (GC) and high-performance liquid chromatography (HPLC) coupled with different detectors are commonly used for the determination of pharmaceuticals, including ARVDs.

### **2.11.1. High-performance liquid chromatography**

The HPLC is a well-known analytical separation technique used to separate molecules in a sample mixture (Harvey, 2019). In principle, a small sample volume (microliters) is introduced in a stream of the mobile phase, and high pressure from the pump moves the mobile phase containing the analytes throughout the column holding the stationary phase (Malviya et al., 2010). The analytes interact with the stationary phase and are separated based on their relative affinity for the stationary and mobile phases, resulting in their elution at different retention times. The elution of analytes can be operated under gradient or isocratic mode. The gradient elution involves the change of mobile phase composition during the separation of analytes, while isocratic elution consists of mobile phase composition used throughout the entire run (Patil, 2019). The separation can be conducted under the normal or reverse phase. The normal phase is rarely used for the separation of the analytes because it consists of a polar stationary phase, and most of the organic compounds are polar. Therefore, polar analytes are retained and absorbed in the stationary, hence they take long to be eluted. However, nonpolar analytes are eluted fast because they have a weak affinity for the stationary phase. The mobile phase is polar in a reverse phase, and the stationary phase is nonpolar. The mobile phase solvent system used is a liquid mixture of organic solvent with water. In a reversed-phase the nonpolar analytes have a strong affinity for a stationary phase; therefore, they result in a long retention time than the polar analytes as the stationary phase is nonpolar (Murugan et al., 2014). The HPLC is mostly used for the separation of components which are soluble in the liquid phase. It is widely used due to its accuracy and efficiency, and it is fast. However, it is expensive, and its sensitivity is low; hence, it requires the sensitive detector to be coupled to improve its performance (Malviya et al., 2010). The HPLC has been used as a reliable analytical tool for separating and quantifying ARVDs in most studies because they are nonvolatile compound (Azanu et al., 2016, Li et al., 2014). The ARVDs are often found in low levels in the

environmental samples, hence HPLC coupled with the mass spectrometry detector is often used because it is sensitive, and the results are approved using the built-in library (Harvey, 2019).

A mass spectrometry (MS) detector is an analytical tool used to identify the type of chemicals and the amount present in the sample. The identification is done by measuring the abundance of gas-phase ion and mass to charge ratio ( $m/z$ ), where the beam of energetic electrons is used to bombard the molecules in the sample and convert them into fast-moving positive ions. The molecules are broken and ionized into fragments of positive ions, and each type of ion has a specific  $m/z$  ratio. They are then separated according to their masses (Aryal, 2018b). The MS detector has been used to detect the target ARVDs (Akenga et al., 2021, Mlunguza et al., 2020). Other detectors that has also been used for the analysis of ARVDs linked with HPLC are ultraviolet-Visible (UV) detector and photodiode array detector. UV-VIS detector is a commonly used detector in HPLC, which works by passing ultraviolet and visible light through a flow cell containing the sample. The detector is then measuring the absorption of the diverse wavelengths that go through the cell. The properties inform of the target analyte in the sample is provided by the amount of light absorbed. The UV detector has been reported to have some drawbacks of low sensitivity and selectivity; however, using different sample preparation techniques helps eliminate interferences and enriches the analyte of interest, hence improving the selectivity and sensitivity (Madikizela, 2017).

Photodiode array (PDA) detector is utilized in the detection unit to detect the absorption from ultraviolet to visible region. It consist of many photodiode arrays to acquire data over a comprehensive range of wavelengths simultaneously, which is one of the advantages of PDA detector. The PDA detector disadvantages include great noise since there is a small amount of light; the PDA is also prone to several deviations, such as lamp fluctuations, as the reference light cannot be received. However, it has lately been enhanced to reduce its difference in performance from UV-VIS detectors (Mtolo et al., 2019)

### **2.11.2. Gas Chromatography**

It is used to analyse and separate components, help to study the purity of a particular compound, and also identify a compound. GC can be automated, it can analyse small samples, and it is very sensitive; however, it is limited to volatile compounds. This chromatography uses a carrier gas (such as argon, hydrogen, and nitrogen) as a mobile phase. The typically used carrier gas is helium because it is inert and has a small molecular mass. The separation is based on the partitioning of the analyte between the mobile phase and the stationary phase. Compounds with



greater affinity for the mobile phase get eluted first and result in a short retention time. Those with a greater affinity to the stationary phase are retained in the stationary phase for some time and get eluted later, hence having a long retention time (Piantanida and Barron, 2018). After the components emerge, the analytes pass the column detected by the detector which then sends the signal to the chart recorder, resulting in chromatogram peaks (Aryal, 2018a). The GC has been used for the analysis of ARVDs in wastewater, sludge, and surface water. In the previously reported studies where GC was used for analysis, it was usually linked with the MS detector, which proves the high sensitivity of MS that cannot be ignored (Schoeman et al., 2017, Wooding et al., 2017).

## 2.12. References

- Abafe, O. A., Späth, J., Fick, J., Jansson, S., Buckley, C., Stark, A., Pietruschka, B. & Martincigh, B. S. 2018. LC-MS/MS determination of antiretroviral drugs in influents and effluents from wastewater treatment plants in KwaZulu-Natal, South Africa. *Chemosphere*, 200, 660-670. doi:<https://doi.org/10.1016/j.chemosphere.2018.02.105>
- Abd Mutalib, M., Rahman, M., Othman, M., Ismail, A. & Jaafar, J. 2017. Scanning electron microscopy (SEM) and energy-dispersive X-ray (EDX) spectroscopy. *Membrane characterization*. Elsevier.
- Abers, M. S., Shandera, W. X. & Kass, J. S. 2014. Neurological and psychiatric adverse effects of antiretroviral drugs. *CNS drugs*, 28, 131-145. doi:<https://doi.org/10.1007/s40263-013-0132-4>
- Abril, C., Martín, J., Malvar, J. L., Santos, J. L., Aparicio, I. & Alonso, E. 2018. Dispersive liquid–liquid microextraction as a new clean-up procedure for the determination of parabens, perfluorinated compounds, UV filters, biocides, surfactants, and plasticizers in root vegetables. *Analytical and bioanalytical chemistry*, 410, 5155-5163. doi:<https://doi.org/10.1007/s00216-018-1165-9>
- Adaramoye, O. A., Adesanoye, O., Adewumi, O. & Akanni, O. 2012. Studies on the toxicological effect of nevirapine, an antiretroviral drug, on the liver, kidney and testis of male Wistar rats. *Human and experimental toxicology*, 31, 676-685. doi:<https://doi.org/10.1177/0960327111424304>
- Adeola, A. O., de Lange, J. & Forbes, P. B. 2021. Adsorption of antiretroviral drugs, efavirenz and nevirapine from aqueous solution by graphene wool: Kinetic, equilibrium,

- thermodynamic and computational studies. *Applied Surface Science Advances*, 6, 100157. doi:<https://doi.org/10.1016/j.apsadv.2021.100157>
- Adeola, A. O. & Forbes, P. B. 2021. Antiretroviral Drugs in African Surface Waters: Prevalence, Analysis, and Potential Remediation. *Environmental Toxicology and Chemistry*. doi: <https://doi.org/10.1002/etc.5127>
- Adya, A. K. & Canetta, E. 2014. Nanotechnology and its applications to animal biotechnology. *Animal Biotechnology*. Elsevier.
- Ahmed, M. B. M., Rajapaksha, A. U., Lim, J. E., Vu, N. T., Kim, I. S., Kang, H. M., Lee, S. S. & Ok, Y. S. 2015. Distribution and accumulative pattern of tetracyclines and sulfonamides in edible vegetables of cucumber, tomato, and lettuce. *Journal of Agricultural and Food Chemistry*, 63, 398-405. doi:<https://doi.org/10.1021/jf5034637>
- Akenga, P., Gachanja, A., Fitzsimons, M. F., Tappin, A. & Comber, S. 2021. Uptake, accumulation and impact of antiretroviral and antiviral pharmaceutical compounds in lettuce. *Science of The Total Environment*, 766, 144499. doi:<https://doi.org/10.1016/j.scitotenv.2020.144499>
- Akpomie, K. G., Fayomi, O. M., Ezeofor, C. C., Sha'Ato, R. & Van Zyl, W. E. 2019. Insights into the use of metal complexes of thiourea derivatives as highly efficient adsorbents for ciprofloxacin from contaminated water. *Transactions of the Royal Society of South Africa*, 74, 180-188. doi:<https://doi.org/10.1080/0035919X.2019.1614695>
- Al-Farsi, R., Ahmed, M., Al-Busaidi, A. & Choudri, B. 2018. Assessing the presence of pharmaceuticals in soil and plants irrigated with treated wastewater in Oman. *International Journal of Recycling of Organic Waste in Agriculture*, 7, 165-172. doi:<https://doi.org/10.1007/s40093-017-0176-4>
- Al-Farsi, R. S., Ahmed, M., Al-Busaidi, A. & Choudri, B. S. 2017. Translocation of pharmaceuticals and personal care products (PPCPs) into plant tissues: A review. *Emerging Contaminants*, 3, 132-137. doi:<https://doi.org/10.1016/j.emcon.2018.02.001>
- Amdany, R., Chimuka, L. & Cukrowska, E. 2014. Determination of naproxen, ibuprofen and triclosan in wastewater using the polar organic chemical integrative sampler (POCIS): A laboratory calibration and field application. *Water Sa*, 40, 407-414. doi:<https://doi.org/10.4314/wsa.v40i3.3>
- Annegowda, H., Bhat, R., Min-Tze, L., Karim, A. & Mansor, S. 2012. Influence of sonication treatments and extraction solvents on the phenolics and antioxidants in star fruits. *Journal of food science and technology*, 49, 510-514. doi:<https://doi.org/10.1007/s13197-011-0435-8>

- Aries, E., Chen, J., Collins, P., Hodges, J. & Pearson, S. 2011. Characterization of priority hazardous substances and priority substances in cokemaking and steelmaking effluents from UK integrated steelworks. *2nd International Conference and Exhibition Clean Technologies in the Steel Industry 26-28 September 2011 – Budapest*.
- Arthur, E. L., Rice, P. J., Rice, P. J., Anderson, T. A., Baladi, S. M., Henderson, K. L. & Coats, J. R. 2005. Phytoremediation—an overview. *Critical Reviews in Plant Sciences*, 24, 109-122. doi:<https://doi.org/10.1080/07352680590952496>
- Aryal, S. 2018a. *Gas chromatography- definition, principle, working, uses* [Online]. Available: <https://microbenotes.com/gas-chromatography/> [Accessed May 26 2020].
- Aryal, S. 2018b. *Mass Spectrometry (MS)- Principle, Working, Instrumentation, Steps, Applications* [Online]. [Accessed May 24 2020].
- Azanu, D., Mortey, C., Darko, G., Weisser, J. J., Styriahave, B. & Abaidoo, R. C. 2016. Uptake of antibiotics from irrigation water by plants. *Chemosphere*, 157, 107-114. doi:<http://dx.doi.org/10.1016/j.chemosphere.2016.05.035>
- Bagheri, M., Al-Jabery, K., Wunsch, D. C. & Burken, J. G. 2019. A deeper look at plant uptake of environmental contaminants using intelligent approaches. *Science of the total environment*, 651, 561-569. doi:<https://doi.org/10.1016/j.scitotenv.2018.09.048>
- Bartha, B., Huber, C., Harpaintner, R. & Schröder, P. 2010. Effects of acetaminophen in *Brassica juncea* L. Czern.: investigation of uptake, translocation, detoxification, and the induced defense pathways. *Environmental Science Pollution Research*, 17, 1553-1562. doi:<https://doi.org/10.1007/s11356-010-0342-y>
- Bernardino, J. I. & Arribas, J. R. 2017. Antiviral therapy. *Infectious Diseases*. Elsevier.
- Bidari, A., Ganjali, M. R., Norouzi, P., Hosseini, M. R. M. & Assadi, Y. 2011. Sample preparation method for the analysis of some organophosphorus pesticides residues in tomato by ultrasound-assisted solvent extraction followed by dispersive liquid–liquid microextraction. *Food Chemistry*, 126, 1840-1844. doi:<https://doi.org/10.1016/j.foodchem.2010.11.142>
- Brausch, J. M., Connors, K. A., Brooks, B. W. & Rand, G. M. 2012. Human pharmaceuticals in the aquatic environment: a review of recent toxicological studies and considerations for toxicity testing. *Reviews of Environmental Contamination Toxicology*, 218, 1-99. doi:[https://doi.org/10.1007/978-1-4614-3137-4\\_1](https://doi.org/10.1007/978-1-4614-3137-4_1)
- Calderón-Preciado, D., Matamoros, V., Savé, R., Muñoz, P., Biel, C. & Bayona, J. 2013. Uptake of microcontaminants by crops irrigated with reclaimed water and groundwater

- under real field greenhouse conditions. *Environmental Science and Pollution Research*, 20, 3629-3638. doi:<https://doi.org/10.1007/s11356-013-1509-0>
- Carter, L. J., Williams, M., Martin, S., Kamaludeen, S. P. & Kookana, R. S. 2018. Sorption, plant uptake and metabolism of benzodiazepines. *Science of the Total Environment*, 628, 18-25. doi:<https://doi.org/10.1016/j.scitotenv.2018.01.337>
- Christou, A., Karolia, P., Hapeshi, E. & Michael, C. 2017. Long-term wastewater irrigation of vegetables in real agricultural systems: Concentration of pharmaceuticals in soil, uptake and bioaccumulation in tomato fruits and human health risk assessment. *Water Research*, 109, 24-34. doi:<https://doi.org/10.1016/j.watres.2016.11.033>
- Chuang, Y.-H., Liu, C.-H., Sallach, J. B., Hammerschmidt, R., Zhang, W., Boyd, S. A. & Li, H. 2019. Mechanistic study on uptake and transport of pharmaceuticals in lettuce from water. *Environment international*, 131, 104976. doi:<https://doi.org/10.1016/j.envint.2019.104976>
- Chung, D. 2016. A review of exfoliated graphite. *Journal of materials science*, 51, 554-568. doi:<https://doi.org/10.1007/s10853-015-9284-6>
- Cihlar, T. & Fordyce, M. J. C. o. i. v. 2016. Current status and prospects of HIV treatment. 18, 50-56.
- Doyle, W. M. J. P. C. Q. 1992. Principles and applications of Fourier transform infrared (FTIR) process analysis. 2, 11-41.
- Ebele, A. J., Abdallah, M. A.-E. & Harrad, S. 2017. Pharmaceuticals and personal care products (PPCPs) in the freshwater aquatic environment. *Emerging contaminants*, 3, 1-16. doi:<https://doi.org/10.1016/j.emcon.2016.12.004>
- Ebnesajjad, S. 2010. *Handbook of adhesives and surface preparation: technology, applications and manufacturing*, William Andrew.
- Gao, X., Si, X., Yuan, Y., Chen, K. & Qin, K. 2021. Ultra-trace Extraction of Two Bactericides Via Ultrasound-Assisted Dispersive Liquid-Liquid Microextraction. *Journal of Chromatographic Science*, 59, 182-190. doi:<https://doi.org/10.1093/chromsci/bmaa083>
- García, M. G., Fernández-López, C., Pedrero-Salcedo, F. & Alarcón, J. J. 2018. Absorption of carbamazepine and diclofenac in hydroponically cultivated lettuces and human health risk assessment. *Agricultural Water Management*, 206, 42-47. doi:<https://doi.org/10.1016/j.agwat.2018.04.018>

- Ghodke, S. A., Maheshwari, U., Gupta, S., Sonawane, S. H. & Bhanvase, B. A. 2021. Nanomaterials for adsorption of pollutants and heavy metals: Introduction, mechanism, and challenges. *Handbook of Nanomaterials for Wastewater Treatment*. Elsevier.
- Goldstein, M., Shenker, M. & Chefetz, B. 2014. Insights into the uptake processes of wastewater-borne pharmaceuticals by vegetables. *Environmental Science and Technology*, 48, 5593-5600. doi:<https://doi.org/10.1021/es5008615>
- Gurama, H. M. & Usman, M. T. 2020. Phytoremediation potentials of some selected vegetables on polluted soils in Kano state. *Algerian Journal of Materials Chemistry*, 3, 39-47.
- Harvey, D. 2019. 12.5: High-Performance Liquid Chromatography [Online]. Available: [https://chem.libretexts.org/Courses/Northeastern\\_University/12%3A\\_Chromatographic\\_and\\_Electrophoretic\\_Methods/12.5%3A\\_High-Performance\\_Liquid\\_Chromatography](https://chem.libretexts.org/Courses/Northeastern_University/12%3A_Chromatographic_and_Electrophoretic_Methods/12.5%3A_High-Performance_Liquid_Chromatography) [Accessed May 14 2020].
- Hemmat, K., Khodabakhshi, M. R. & Zeraatkar Moghaddam, A. 2021. Synthesis of nanoscale zero-valent iron modified graphene oxide nanosheets and its application for removing tetracycline antibiotic: Response surface methodology. *Applied Organometallic Chemistry*, 35, e6059. doi: <https://doi.org/10.1002/aoc.6059>
- Hoang, N. B., Nguyen, T. T., Nguyen, T. S., Bui, T. P. Q. & Bach, L. G. 2019. The application of expanded graphite fabricated by microwave method to eliminate organic dyes in aqueous solution. *Cogent Engineering*, 6, 1584939.
- Hristea, G. & Budruga, P. 2008. Characterization of exfoliated graphite for heavy oil sorption. *Journal of thermal analysis calorimetry*, 91, 817-823.
- Hu, L., Zhang, Y., Lu, W., Lu, Y. & Hu, H. 2019. Easily recyclable photocatalyst Bi<sub>2</sub>WO<sub>6</sub>/MOF/PVDF composite film for efficient degradation of aqueous refractory organic pollutants under visible-light irradiation. *Journal of Materials Science*, 54, 6238-6257. doi:<https://doi.org/10.1007/s10853-018-03302-w>
- Hurtado, C., Domínguez, C., Pérez-Babace, L., Cañameras, N., Comas, J. & Bayona, J. M. 2016. Estimate of uptake and translocation of emerging organic contaminants from irrigation water concentration in lettuce grown under controlled conditions. *Journal of Hazardous Materials*, 305, 139-148. doi:<https://doi.org/10.1016/j.jhazmat.2015.11.039>
- Ibrahim, N. & Zaini, M. A. A. 2017. Solvent selection in microwave assisted extraction of castor oil. *Chemical Engineering Transactions*, 56, 865-870. doi:<http://doi.org/10.3303/CET1756145>
- Ion, A. C., Alpatova, A., Ion, I., Culetu, A. J. M. S. & B, E. 2011. Study on phenol adsorption from aqueous solutions on exfoliated graphitic nanoplatelets. 176, 588-595.

- Iori, V., Pietrini, F. & Zacchini, M. 2012. Assessment of ibuprofen tolerance and removal capability in *Populus nigra* L. by in vitro culture. *Journal of hazardous materials*, 229, 217-223. doi:<https://doi.org/10.1016/j.jhazmat.2012.05.097>
- Ivancev-Tumbas, I., Landwehrkamp, L., Hobby, R., Vernillo, M. & Panglisch, S. 2020. Adsorption of organic pollutants from the aqueous phase using graphite as a model adsorbent. *Adsorption Science and Technology*, 38, 286-303. doi:<https://doi.org/10.1177/0263617420945847>
- Jacklin, D., Brink, I. & de Waal, J. 2020. The potential use of plant species within a Renosterveld landscape for the phytoremediation of glyphosate and fertiliser. *Water South Africa*, 46, 94-103. doi:<https://doi.org/10.17159/wsa/2020.v46.i1.7889>
- K'oreje, K., Vergeynst, L., Ombaka, D., De Wispelaere, P., Okoth, M., Van Langenhove, H. & Demeestere, K. 2016. Occurrence patterns of pharmaceutical residues in wastewater, surface water and groundwater of Nairobi and Kisumu city, Kenya. *Chemosphere*, 149, 238-244. doi:<https://doi.org/10.1016/j.chemosphere.2016.01.095>
- Kafeenah, H. I., Osman, R. & Bakar, N. K. A. 2018. Disk solid-phase extraction of multi-class pharmaceutical residues in tap water and hospital wastewater, prior to ultra-performance liquid chromatographic-tandem mass spectrometry (UPLC-MS/MS) analyses. *Royal Society of Chemistry Advances*, 8, 40358-40368. doi:<https://doi.org/10.1039/C8RA06885B>
- Kairigo, P., Ngumba, E., Sundberg, L.-R., Gachanja, A. & Tuhkanen, T. 2020. Contamination of surface water and river sediments by antibiotic and antiretroviral drug cocktails in low and middle-income countries: occurrence, risk and mitigation strategies. *Water*, 12, 1376.
- Kanters, S., Vitoria, M., Doherty, M., Socias, M. E., Ford, N., Forrest, J. I., Popoff, E., Bansback, N., Nsanzimana, S. & Thorlund, K. 2016. Comparative efficacy and safety of first-line antiretroviral therapy for the treatment of HIV infection: a systematic review and network meta-analysis. *The lancet HIV*, 3, e510-e520. doi:[https://doi.org/10.1016/S2352-3018\(16\)30091-1](https://doi.org/10.1016/S2352-3018(16)30091-1)
- Kataoka, H. 2019. *Pharmaceutical analysis/ Sample preparation*, Japan, Elsevier Inc.
- Kebede, T., Seroto, M., Chokwe, R., Dube, S. & Nindi, M. 2020. Adsorption of antiretroviral (ARVs) and related drugs from environmental wastewaters using nanofibers. *Journal of Environmental Chemical Engineering*, 8, 104049. doi:<https://doi.org/10.1016/j.jece.2020.104049>

- Kebede, T. G., Dube, S. & Nindi, M. M. 2019. Removal of multi-class antibiotic drugs from Wastewater using water-soluble protein of *Moringa stenopetala* seeds. *Water environment research*, 11, 595. doi:<https://doi.org/10.3390/w11030595>
- Keerthanan, S., Jayasinghe, C., Biswas, J. K. & Vithanage, M. 2021. Pharmaceutical and Personal Care Products (PPCPs) in the environment: Plant uptake, translocation, bioaccumulation, and human health risks. *Critical Reviews in Environmental Science and Technology*, 51, 1221-1258. doi:<https://doi.org/10.1080/10643389.2020.1753634>
- Keil, F. J. 2007. Modeling of process intensification—An introduction and overview. *Modeling of Process Intensification*, 1-7. doi: <https://doi.org/10.1002/9783527610600.ch8>
- Khalilian, F. & Rezaee, M. 2017. Ultrasound-assisted extraction followed by solid-phase extraction followed by dispersive liquid–liquid microextraction for the sensitive determination of diazinon and chlorpyrifos in rice. *Food Analytical Methods*, 10, 885-891. doi:<https://doi.org/10.1007/s12161-016-0653-9>
- Kodešová, R., Klement, A., Golovko, O., Fér, M., Nikodem, A., Kočárek, M. & Grabic, R. 2019. Root uptake of atenolol, sulfamethoxazole and carbamazepine, and their transformation in three soils and four plants. *Environmental Science Pollution Research*, 26, 9876-9891. doi:<https://doi.org/10.1007/s11356-019-04333-9>
- Kohli, R. & Mittal, K. 2018. *Developments in Surface Contamination and Cleaning: Applications of Cleaning Techniques: Volume 11*, Elsevier.
- Kunene, P. & Mahlambi, P. 2020. Optimization and application of ultrasonic extraction and Soxhlet extraction followed by solid phase extraction for the determination of triazine pesticides in soil and sdiment. *Environmental Chemical Engineering*, 8, 103665. doi:<https://doi.org/10.1016/j.jece.2020.103665>
- Li, X.-W., Xie, Y.-F., Li, C.-L., Zhao, H.-N., Zhao, H., Wang, N. & Wang, J.-F. 2014. Investigation of residual fluoroquinolones in a soil–vegetable system in an intensive vegetable cultivation area in Northern China. *Science of the Total Environment*, 468, 258-264. doi:<https://doi.org/10.1016/j.scitotenv.2013.08.057>
- Li, Y., Li, S., Lin, S.-J., Zhang, J.-J., Zhao, C.-N. & Li, H.-B. 2017. Microwave-assisted extraction of natural antioxidants from the exotic *Gordonia axillaris* fruit: Optimization and identification of phenolic compounds. *Molecules*, 22, 1481. doi: <https://doi.org/10.3390/molecules22091481>
- Lin, A. Y.-C. & Tsai, Y.-T. 2009. Occurrence of pharmaceuticals in Taiwan's surface waters: Impact of waste streams from hospitals and pharmaceutical production facilities.

- Science of the Total Environment*, 407, 3793-3802.  
doi:<https://doi.org/10.1016/j.scitotenv.2009.03.009>
- Liu, Q., Li, L., Jin, X., Wang, C. & Wang, T. 2018. Influence of graphene oxide sheets on the pore structure and filtration performance of a novel graphene oxide/silica/polyacrylonitrile mixed matrix membrane. *Journal of materials science*, 53, 6505-6518. doi:<https://doi.org/10.1007/s10853-018-1990-4>
- Madikizela, L. M. 2017. *Determination of selected acidic pharmaceutical compounds in wastewater treatment plants*.
- Madikizela, L. M. & Chimuka, L. 2017a. Occurrence of naproxen, ibuprofen, and diclofenac residues in wastewater and river water of KwaZulu-Natal Province in South Africa. *Environmental monitoring and assessment*, 189, 348. doi:<https://doi.org/10.1007/s10661-017-6069-1>
- Madikizela, L. M. & Chimuka, L. 2017b. Simultaneous determination of naproxen, ibuprofen and diclofenac in wastewater using solid-phase extraction with high performance liquid chromatography. *Water South Africa*, 43, 264-274.
- Madikizela, L. M., Ncube, S. & Chimuka, L. 2018. Uptake of pharmaceuticals by plants grown under hydroponic conditions and natural occurring plant species: a review. *Science of the Total Environment* 636, 477-486. doi:<https://doi.org/10.1016/j.scitotenv.2018.04.297>
- Madikizela, L. M., Ncube, S. & Chimuka, L. 2020. Analysis, occurrence and removal of pharmaceuticals in African water resources: A current status. *Journal of Environmental Management*, 253, 109741. doi:<https://doi.org/10.1016/j.jenvman.2019.109741>
- Madikizela, L. M., Tavengwa, N. T. & Chimuka, L. 2017. Status of pharmaceuticals in African water bodies: occurrence, removal and analytical methods. *Journal of environmental management*, 193, 211-220. doi:<http://dx.doi.org/10.1016/j.jenvman.2017.02.022>
- Mahmoud, R. H. & Hamza, A. H. M. 2017. Phytoremediation application: plants as biosorbent for metal removal in soil and water. *Phytoremediation*. Springer.
- Malchi, T., Maor, Y., Tadmor, G., Shenker, M. & Chefetz, B. 2014. Irrigation of root vegetables with treated wastewater: evaluating uptake of pharmaceuticals and the associated human health risks. *Environmental Science and Technology*, 48, 9325-9333. doi:<https://doi.org/10.1021/es5017894>
- Malviya, R., Bansal, V., Pal, O. P. & Sharma, P. K. 2010. High performance liquid chromatography: a short review. *Journal of global pharma technology*, 2, 22-26.



- Miller, E. L., Nason, S. L., Karthikeyan, K. & Pedersen, J. A. 2016. Root uptake of pharmaceuticals and personal care product ingredients. *Environmental science technology*, 50, 525-541. doi:<https://doi.org/10.1021/acs.est.5b01546>
- Mlunguza, N. Y. 2019. *Hollow fibre liquid phase microextraction of pharmaceuticals in water and Eichhornia crassipes*.
- Mlunguza, N. Y., Ncube, S., Mahlambi, P. N., Chimuka, L. & Madikizela, L. M. 2019. Adsorbents and removal strategies of non-steroidal anti-inflammatory drugs from contaminated water bodies. *Journal of Environmental Chemical Engineering*, 103142. doi:<https://doi.org/10.1016/j.jece.2019.103142>
- Mlunguza, N. Y., Ncube, S., Mahlambi, P. N., Chimuka, L. & Madikizela, L. M. 2020. Determination of selected antiretroviral drugs in wastewater, surface water and aquatic plants using hollow fibre liquid phase microextraction and liquid chromatography-tandem mass spectrometry. *Journal of hazardous materials*, 382, 121067. doi:<https://doi.org/10.1016/j.jhazmat.2019.121067>
- Mohamed, M. A., Jaafar, J., Ismail, A., Othman, M. & Rahman, M. 2017. Fourier transform infrared (FTIR) spectroscopy. *Membrane Characterization*. Elsevier.
- Mohanraj, J., Durgalakshmi, D., Balakumar, S., Aruna, P., Ganesan, S., Rajendran, S. & Naushad, M. 2020. Low cost and quick time absorption of organic dye pollutants under ambient condition using partially exfoliated graphite. *Journal of Water Process Engineering*, 34, 101078. doi:<https://doi.org/10.1016/j.jwpe.2019.101078>
- Mordechay, E. B., Tarchitzky, J., Chen, Y., Shenker, M. & Chefetz, B. 2018. Composted biosolids and treated wastewater as sources of pharmaceuticals and personal care products for plant uptake: A case study with carbamazepine. *Environmental Pollution*, 232, 164-172. doi:<https://doi.org/10.1016/j.envpol.2017.09.029>
- Moret, S., Conchione, C., Sribinowska, A. & Lucci, P. J. F. 2019. Microwave-based technique for fast and reliable extraction of organic contaminants from food, with a special focus on hydrocarbon contaminants. 8, 503. doi:<https://doi.org/10.3390/foods8100503>
- Mosekiemang, T. T., Stander, M. A. & de Villiers, A. 2019. Simultaneous quantification of commonly prescribed antiretroviral drugs and their selected metabolites in aqueous environmental samples by direct injection and solid phase extraction liquid chromatography-tandem mass spectrometry. *Chemosphere*, 220, 983-992. doi:<https://doi.org/10.1016/j.chemosphere.2018.12.205>
- Mtolo, S. P., Mahlambi, P. N. & Madikizela, L. M. 2019. Synthesis and application of a molecularly imprinted polymer in selective solid-phase extraction of efavirenz from

- water. *Water Science and Technology*, 79, 356-365.  
doi:<https://doi.org/10.2166/wst.2019.054>
- Murugan, S., Thejaswini, N., Zeenathaman, S., SyamVijayakar, P., Sai Swathi Varma, S. & Niranjana Babu, M. 2014. A overview on high performance liquid chromatography. *American Journal Of Biological And Pharmaceutical Research*, 4, 56-159.
- Naderi, M. 2015. Surface Area: Brunauer–Emmett–Teller (BET). *Progress in filtration and separation*. Elsevier.
- Nanakoudis, A. 2019a. EDX Analysis with SEM: How Does it Work. *ThermoFisher Scientific*.
- Nanakoudis, A. 2019b. What is SEM? Scanning Electron Microscopy Explained. *ThermoFisher Scientific*.
- Ncube, S., Madikizela, L. M., Chimuka, L. & Nindi, M. M. 2018. Environmental fate and ecotoxicological effects of antiretrovirals: A current global status and future perspectives. *Water research*, 145, 231-247.  
doi:<https://doi.org/10.1016/j.watres.2018.08.017>
- Ndlovu, T. 2012. *Electrochemical detection of organic and inorganic water pollutants using recompressed exfoliated graphite electrodes*, University of Johannesburg (South Africa).
- Ndlovu, T., Arotiba, O. A., Sampath, S., Krause, R. W. & Mamba, B. B. 2011. Electrochemical detection and removal of lead in water using poly (propylene imine) modified recompressed exfoliated graphite electrodes. *Journal of Applied Electrochemistry*, 41, 1389-1396. doi:<https://doi.org/10.1007/s10800-011-0360-6>
- Ngumba, E., Gachanja, A., Nyirenda, J., Maldonado, J. & Tuhkanen, T. 2020. Occurrence of antibiotics and antiretroviral drugs in source-separated urine, groundwater, surface water and wastewater in the peri-urban area of Chungu in Lusaka, Zambia. *Water SA*, 46, 278-284. doi:<https://doi.org/10.17159/wsa/2020.v46.i2.8243>
- Ngumba, E., Kosunen, P., Gachanja, A. & Tuhkanen, T. 2016. A multiresidue analytical method for trace level determination of antibiotics and antiretroviral drugs in wastewater and surface water using SPE-LC-MS/MS and matrix-matched standards. *Analytical Methods*, 8, 6720-6729. doi:<https://doi.org/10.1039/C6AY01695B>
- Ntuli, T. D. & Pakade, V. E. 2020. Hexavalent chromium removal by polyacrylic acid-grafted Macadamia nutshell powder through adsorption–reduction mechanism: Adsorption isotherms, kinetics and thermodynamics. *Chemical Engineering Communications*, 207, 279-294. doi:<https://doi.org/10.1080/00986445.2019.1581619>

- Obidike, L. & Mulopo, J. Effect of High Concentration of Nevirapine on the Growth of E. Coli in Wastewater Treatment. Proceedings of the World Congress on Engineering and Computer Science, 2018.
- Okoli, C. P. & Ofomaja, A. E. 2018. Degree of time dependency of kinetic coefficient as a function of adsorbate concentration; new insights from adsorption of tetracycline onto monodispersed starch-stabilized magnetic nanocomposite. *Journal of environmental management*, 218, 139-147. doi:<https://doi.org/10.1016/j.jenvman.2018.04.060>
- Oluseyi, T., Olayinka, K., Alo, B. & Smith, R. M. 2011. Comparison of extraction and clean-up techniques for the determination of polycyclic aromatic hydrocarbons in contaminated soil samples. *African Journal of Environmental Science and Technology*, 5, 482-493.
- Ötles, S. & Kartal, C. 2016. Solid-Phase Extraction (SPE): Principles and applications in food samples. *Acta Scientiarum Polonorum Technologia Alimentaria*, 15, 5-15. doi:<https://doi.org/10.17306/J.AFS.2016.1.1>
- Patel, M., Kumar, R., Kishor, K., Mlsna, T., Pittman Jr, C. U. & Mohan, D. 2019. Pharmaceuticals of emerging concern in aquatic systems: chemistry, occurrence, effects, and removal methods. *Chemical reviews*, 119, 3510-3673. doi:<https://doi.org/10.1021/acs.chemrev.8b00299>
- Patil, M. 2019. *Difference between isocratic and gradient HPLC system* [Online]. Available: <https://chrominfo.blogspot.com/2019/12/difference-between-isocratic-and.html> [Accessed May 23 2020].
- Paz, A., Tadmor, G., Malchi, T., Blotevogel, J., Borch, T., Polubesova, T. & Chefetz, B. 2016. Fate of carbamazepine, its metabolites, and lamotrigine in soils irrigated with reclaimed wastewater: Sorption, leaching and plant uptake. *Chemosphere*, 160, 22-29. doi:<https://doi.org/10.1016/j.chemosphere.2016.06.048>
- Petit, S. & Madejova, J. 2013. Chapter 2.7-Fourier Transform Infrared Spectroscopy, Editor (s): Faïza Bergaya, Gerhard Lagaly, Developments in Clay Science. Elsevier.
- Piantanida, A. G. & Barron, A. R. 2018. Principles of gas chromatography. *OpenStax CNX*.
- Pirsaheb, M., Fattahi, N. & Shamsipur, M. 2013. Determination of organophosphorous pesticides in summer crops using ultrasound-assisted solvent extraction followed by dispersive liquid-liquid microextraction based on the solidification of floating organic drop. *Food Control*, 34, 378-385. doi:<https://doi.org/10.1016/j.foodcont.2013.05.013>

- Prabakaran, K., Li, J., Anandkumar, A., Leng, Z., Zou, C. B. & Du, D. 2019. Managing environmental contamination through phytoremediation by invasive plants: A review. *Ecological Engineering*, 138, 28-37. doi:<https://doi.org/10.1016/j.ecoleng.2019.07.002>
- Prasse, C., Schlüsener, M. P., Schulz, R. & Ternes, T. A. 2010. Antiviral drugs in wastewater and surface waters: a new pharmaceutical class of environmental relevance? *Environmental science technology*, 44, 1728-1735. doi:<https://doi.org/10.1021/es903216p>
- Prosser, R. S., Lissemore, L., Topp, E. & Sibley, P. K. 2014. Bioaccumulation of triclosan and triclocarban in plants grown in soils amended with municipal dewatered biosolids. *Environmental toxicology chemistry Central Journal*, 33, 975-984. doi: <https://doi.org/10.1002/etc.2505>
- Qwane, S. N., Mdluli, P. S. & Madikizela, L. M. 2020. Synthesis, characterization and application of a molecularly imprinted polymer in selective adsorption of abacavir from polluted water. *South African Journal of Chemistry*, 73, 84-91. doi:<http://dx.doi.org/10.17159/0379-4350/2020/v73a13>
- Radjenovic, J., Petrovic, M. & Barceló, D. 2007. Analysis of pharmaceuticals in wastewater and removal using a membrane bioreactor. *Analytical bioanalytical chemistry*, 387, 1365-1377. doi:<https://doi.org/10.1007/s00216-006-0883-6>
- Raja, P. M. V. & Barron, A. R. 2020. 2.3: *BET Surface Area Analysis of Nanoparticles* [Online]. Available: [https://chem.libretexts.org/Bookshelves/Analytical\\_Chemistry/Book%3A\\_Physical\\_Methods\\_in\\_Chemistry\\_and\\_Nano\\_Science\\_\(Barron\)/02%3A\\_Physical\\_and\\_Thermal\\_Analysis/2.03%3A\\_BET\\_Surface\\_Area\\_Analysis\\_of\\_Nanoparticles](https://chem.libretexts.org/Bookshelves/Analytical_Chemistry/Book%3A_Physical_Methods_in_Chemistry_and_Nano_Science_(Barron)/02%3A_Physical_and_Thermal_Analysis/2.03%3A_BET_Surface_Area_Analysis_of_Nanoparticles) [Accessed 22 July 2020].
- Raja, P. M. V. & Barron, A. R. 2021. 4.4: *UV-Visible Spectroscopy* [Online]. Available: [https://chem.libretexts.org/Bookshelves/Analytical\\_Chemistry/Physical\\_Methods\\_in\\_Chemistry\\_and\\_Nano\\_Science\\_\(Barron\)/04%3A\\_Chemical\\_Speciation/4.04%3A\\_UV-Visible\\_Spectroscopy](https://chem.libretexts.org/Bookshelves/Analytical_Chemistry/Physical_Methods_in_Chemistry_and_Nano_Science_(Barron)/04%3A_Chemical_Speciation/4.04%3A_UV-Visible_Spectroscopy) [Accessed May 31 2022].
- Raju, A., Reddy, A. J., Satheesh, J. & Jithan, A. 2014. Preparation and characterisation of nevirapine oral nanosuspensions. *Indian journal of pharmaceutical sciences*, 76, 62.
- Rehman, M. U., Khan, F. & Niaz, K. 2020. Introduction to natural products analysis. *Recent advances in natural products analysis*. Elsevier.
- Rezaee, M., Assadi, Y., Hosseini, M.-R. M., Aghaee, E., Ahmadi, F. & Berijani, S. 2006. Determination of organic compounds in water using dispersive liquid-liquid

- microextraction. *Journal of Chromatography A*, 1116, 1-9.  
doi:<https://doi.org/10.1016/j.chroma.2006.03.007>
- Rimayi, C., Odusanya, D., Weiss, J. M., de Boer, J. & Chimuka, L. 2018. Contaminants of emerging concern in the Hartbeespoort Dam catchment and the uMngeni River estuary 2016 pollution incident, South Africa. *Science of the Total Environment*, 627, 1008-1017. doi:<https://doi.org/10.1016/j.scitotenv.2018.01.263>
- Ros, O., Vallejo, A., Olivares, M., Etxebarria, N. & Prieto, A. 2016. Determination of endocrine disrupting compounds in fish liver, brain, and muscle using focused ultrasound solid–liquid extraction and dispersive solid phase extraction as clean-up strategy. *Analytical and bioanalytical chemistry*, 408, 5689-5700. doi:<https://doi.org/10.1007/s00216-016-9697-3>
- Rosli, F. A., Ahmad, H., Jumbri, K., Abdullah, A. H., Kamaruzaman, S. & Fathihah Abdullah, N. A. 2021. Efficient removal of pharmaceuticals from water using graphene nanoplatelets as adsorbent. *Royal Society open science*, 8, 201076. doi:<https://doi.org/10.1098/rsos.201076>
- Sasi, K. 2011. *Phytoremediation-Applications, Advantages and Limitations* [Online]. Available: <https://www.biotecharticles.com/Applications-Article/Phytoremediation-Applications-Advantages-and-Limitations-785.html> [Accessed March 15 2019 ].
- Sathigari, S., Chadha, G., Lee, Y. P., Wright, N., Parsons, D. L., Rangari, V. K., Fasina, O. & Babu, R. J. J. A. P. 2009. Physicochemical characterization of efavirenz–cyclodextrin inclusion complexes. 10, 81-87.
- Schoeman, C., Dlamini, M. & Okonkwo, O. 2017. The impact of a wastewater treatment works in Southern Gauteng, South Africa on efavirenz and nevirapine discharges into the aquatic environment. *Emerging Contaminants*, 3, 95-106. doi:<https://doi.org/10.1016/j.emcon.2017.09.001>
- Schoeman, C., Mashiane, M., Dlamini, M. & Okonkwo, O. 2015. Quantification of selected antiretroviral drugs in a wastewater treatment works in South Africa using GC-TOFMS. *Journal of Chromatography Separation Techniques*, 6, 1-7. doi:<https://doi.org/10.4172/2157-7064.1000272>
- Schröder, P., Navarro-Aviñó, J., Azaizeh, H., Goldhirsh, A. G., DiGregorio, S., Komives, T., Langergraber, G., Lenz, A., Maestri, E., Memon, A. R. J. E. S. & Research-International, P. 2007. Using phytoremediation technologies to upgrade waste water treatment in Europe. 14, 490-497.

- Sharrow, D. J., Godwin, J., He, Y., Clark, S. J. & Raftery, A. E. 2018. Probabilistic population projections for countries with generalized HIV/AIDS epidemics. *Population studies*, 72, 1-15. doi:<https://doi.org/10.1080/00324728.2017.1401654>
- Shengtao, Z., Anyan, G., Huanfang, G. & Xiangqian, C. 2011. Characterization of exfoliated graphite prepared with the method of secondary intervening. *International Journal Of Industrial Chemistry*, 2.
- Shiri, S., Alizadeh, K. & Abbasi, N. 2020. Salting out and vortex-assisted dispersive liquid–liquid microextraction based on solidification of floating organic drop microextraction as a new approach for simultaneous determination of phenol and chlorophenols in water samples. *Quarterly Journal of Iranian Chemical Communication*, 8, 7-23. doi:<https://dx.doi.org/10.30473/icc.2019.6270>
- Sibiya, N. P. & Moloto, M. J. 2017. Shape control of silver selenide nanoparticles using green capping molecules. *Green Processing and Synthesis*, 6, 183-188. doi:<https://doi.org/10.1515/gps-2016-0057>
- Singh, A. & Kumar, Y. 2018. Phytoremediation: cleaning environment using plants. *Trends in Plant Science*, 13, 99-111.
- Singh, S. B., Foster, G. D. & Khan, S. U. 2004. Microwave-assisted extraction for the simultaneous determination of thiamethoxam, imidacloprid, and carbendazim residues in fresh and cooked vegetable samples. *Journal of Agricultural and Food Chemistry*, 52, 105-109. doi:<https://doi.org/10.1021/jf030358p>
- Sobarwiki. 2013. *Schematic diagram of UV-Visible Spectrophotometer* [Online]. Available: [https://commons.wikimedia.org/wiki/File:Schematic\\_of\\_UV-\\_visible\\_spectrophotometer.png](https://commons.wikimedia.org/wiki/File:Schematic_of_UV-_visible_spectrophotometer.png) [Accessed April 21 2020].
- Song, S., Jeong, H. & Kang, Y. 2010. Preparation and characterization of exfoliated graphite and its styrene butadiene rubber nanocomposites. *Journal of Industrial and Engineering Chemistry*, 16, 1059-1065. doi:<https://doi.org/10.1016/j.jiec.2010.07.004>
- Swanepoel, C., Bouwman, H., Pieters, R. & Bezuidenhout, C. 2015. Presence, concentrations and potential implications of HIV-anti-retrovirals in selected water resources in South Africa. *Water Research Commission*.
- Sykam, N. & Kar, K. K. 2014. Rapid synthesis of exfoliated graphite by microwave irradiation and oil sorption studies. *Materials Letters*, 117, 150-152. doi:<http://dx.doi.org/10.1016/j.matlet.2013.12.003>
- Taiz, L., Zeiger, E., Møller, I. M. & Murphy, A. 2015. *Plant physiology and development*, Sinauer Associates Incorporated.

- Tan, Y. H., Chai, M. K. & Wong, L. S. 2018. A review on extraction solvents in the dispersive liquidliquid microextraction. *Malaysian Journal of Analytical Sciences*, 22, 166-174. doi:<https://doi.org/10.17576/mjas-2018-2202-01>
- Tang, J. & Wang, J. 2020. Iron-copper bimetallic metal-organic frameworks for efficient Fenton-like degradation of sulfamethoxazole under mild conditions. *Chemosphere*, 241, 125002. doi:<https://doi.org/10.1016/j.chemosphere.2019.125002>
- Tatke, P. & Jaiswal, Y. 2011. An overview of microwave assisted extraction and its applications in herbal drug research. *Research Journal of Medicinal Plants*, 5, 21-31. doi:<http://doi.org/10.3923/rjmp.2011.21.31>
- Tella, A. C., Owalude, S. O., Olatunji, S. J., Adimula, V. O., Elaigwu, S. E., Alimi, L. O., Ajibade, P. A. & Oluwafemi, O. S. 2018. Synthesis of zinc-carboxylate metal-organic frameworks for the removal of emerging drug contaminant (amodiaquine) from aqueous solution. *Journal of Environmental Sciences*, 64, 264-275. doi:<https://doi.org/10.1016/j.jes.2017.06.015>
- Thakur, A., Kumar, P., Kaur, D., Devunuri, N., Sinha, R. & Devi, P. 2020. TiO<sub>2</sub> nanofibres decorated with green-synthesized P Au/Ag@ CQDs for the efficient photocatalytic degradation of organic dyes and pharmaceutical drugs. *Journal of RSC Advances*, 10, 8941-8948. doi:<https://doi.org/10.1039/C9RA10804A>
- Tian, R., Zhang, R., Uddin, M., Qiao, X., Chen, J. & Gu, G. 2019. Uptake and metabolism of clarithromycin and sulfadiazine in lettuce. *Environmental Pollution*, 247, 1134-1142. doi:<https://doi.org/10.1016/j.envpol.2019.02.009>
- Vieira, F., Cisneros, I., Rosa, N., Trindade, G. & Mohallem, N. J. C. 2006. Influence of the natural flake graphite particle size on the textural characteristic of exfoliated graphite used for heavy oil sorption. 44, 2590-2592.
- Vladár, A. E. & Hodoroaba, V.-D. 2020. Characterization of nanoparticles by scanning electron microscopy. *Characterization of Nanoparticles*. Elsevier.
- William AndrewToshiro K, D., Marinescu, I. D. & Kurokawa, S. 2012. The Current Situation inUltra-Precision TechnologySilicon Single Crystals as an Example. In: Prof. Toshiro Doi, Prof Ioan D. Marinescu & Kurokawa, P. S. (eds.) *Advances In Cmp/Polishing Technologies Forthe Manufacture of Electronic Devices*. Waltham, MA 02451, USA: William Andrew.
- Williams, D. B. & Carter, C. B. 1996. The transmission electron microscope. *Transmission electron microscopy*. Springer.

- Wolecki, D., Caban, M., Pazda, M., Stepnowski, P. & Kumirska, J. 2020. Evaluation of the Possibility of Using Hydroponic Cultivations for the Removal of Pharmaceuticals and Endocrine Disrupting Compounds in Municipal Sewage Treatment Plants. *Molecules*, 25, 162. doi: <https://doi.org/10.3390/molecules25010162>
- Wooding, M., Rohwer, E. R. & Naudé, Y. 2017. Determination of endocrine disrupting chemicals and antiretroviral compounds in surface water: a disposable sorptive sampler with comprehensive gas chromatography–time-of-flight mass spectrometry and large volume injection with ultra-high performance liquid chromatography–tandem mass spectrometry. *Journal of Chromatography A*, 1496, 122-132. doi:<https://doi.org/10.1016/j.chroma.2017.03.057>
- Wu, K.-H., Huang, W.-C., Hung, W.-C. & Tsai, C.-W. 2021. Modified expanded graphite/Fe<sub>3</sub>O<sub>4</sub> composite as an adsorbent of methylene blue: Adsorption kinetics and isotherms. *Materials Science Engineering: B*, 266, 115068. doi:<https://doi.org/10.1016/j.mseb.2021.115068>
- Wu, X. L., Meng, L., Wu, Y., Luk, Y.-Y., Ma, Y. & Du, Y. 2015. Evaluation of graphene for dispersive solid-phase extraction of triazine and neonicotine pesticides from environmental water. *Journal of the Brazilian Chemical Society*, 26, 131-139. doi:<https://doi.org/10.5935/0103-5053.20140227>
- Xu, J., Xu, W., Wang, D., Sang, G. & Yang, X. 2016. Evaluation of enhanced coagulation coupled with magnetic ion exchange (MIEX) in natural organic matter and sulfamethoxazole removals: the role of Al-based coagulant characteristic. *Separation and Purification Technology*, 167, 70-78. doi:<https://doi.org/10.1016/j.seppur.2016.05.007>
- Yu, X.-J., Wu, J., Zhao, Q. & Cheng, X.-W. 2012. Preparation and characterization of sulfur-free exfoliated graphite with large exfoliated volume. *Materials Letters*, 73, 11-13. doi:<https://doi.org/10.1016/j.matlet.2011.11.078>
- Zhuan, R. & Wang, J. 2020. Enhanced degradation and mineralization of sulfamethoxazole by integrating gamma radiation with Fenton-like processes. *Radiation Physics and Chemistry*, 166, 108457. doi:<https://doi.org/10.1016/j.radphyschem.2019.108457>



## Chapter three

---

It is worth noting that this work is submitted in a form of papers, therefore, the details of procedures used are given in each paper.

**Paper 1 is presented as Chapter 3:** Determination of selected antiretroviral drugs in vegetables: ultrasonic extraction and ultrasonic-assisted dispersive liquid-liquid microextraction methods comparison. *Submitted to Journal of Separation Science and Technology.*

**Paper 2 is presented as Chapter 4:** Assessment of antiretroviral drugs in vegetables: evaluation of microwave-assisted extraction performance with and without solid-phase extraction cleanup. *Submitted to Journal of Separation Science Plus*

**Paper 3 is presented as Chapter 5:** Case study on antiretroviral drugs uptake by plants planted in pots and irrigated by water spiked with three selected antiretroviral drugs: bio-accumulation and bio-translocation to roots, stem, leaves, and fruits. *Submitted to the Journal of Agriculture water management.*

**Paper 4 is presented as Chapter 6:** Adsorption of antiretroviral drugs, abacavir, nevirapine, and efavirenz from river water and wastewater using exfoliated graphite: isotherm and kinetic studies. *Submitted to Journal of Environmental Chemical Engineering.*

### **3. Determination of selected antiretroviral drugs in vegetables: ultrasonic extraction and ultrasonic-assisted dispersive liquid-liquid microextraction methods comparison**

#### **Abstract**

This work presents two robust, simple, and cheap techniques based on ultrasonic extraction and ultrasonic-assisted dispersive liquid-liquid microextraction for simultaneous isolation of antiretroviral drugs (abacavir, nevirapine, and efavirenz) from vegetables. The detection and quantification of antiretroviral drugs were conducted with a liquid chromatograph-photodiode array for detection. These methods were optimized, validated, and applied to vegetable samples to assess the selected antiretroviral drugs. The limit of detection and quantification obtained ranged between 0.0081 - 0.015  $\mu\text{g/kg}$  and 0.027 - 0.049  $\mu\text{g/kg}$  for ultrasonic extraction and 0.0028 - 0.0051  $\mu\text{g/kg}$  and 0.0094 - 0.017  $\mu\text{g/kg}$  for ultrasonic-assisted dispersive liquid-liquid microextraction respectively. High recoveries ranging from 93 to 113% in ultrasonic extraction and 85 to 103% in ultrasonic-assisted dispersive liquid-liquid extraction with less than 10% RSD were obtained. These results indicated that ultrasonic-assisted dispersive liquid-liquid microextraction is more sensitive than the ultrasonic extraction method, even though they both have good accuracy and precision. Therefore, ultrasonic extraction can be recommended for routine analysis as ultrasonic-assisted dispersive liquid-liquid extraction showed the inability to extract analytes from root vegetables. The three target antiretroviral drugs were quantified in most samples with concentrations up to 8.18  $\mu\text{g/kg}$ . Efavirenz was the most dominant drug, while the potato was the most contaminated vegetable.

#### **3.1. Introduction**

The analytes removal and recovery from a solid matrix can be considered as a five steps procedure. These include the analyte desorption from active sites of the solid matrix, dispersing into the medium itself; analyte solubilization into the extraction solvent; analyte distribution in the extraction solvent; and collection of the analytes extracted. To achieve quantifiable and reproducible recoveries, each of the five procedure steps requires careful control and optimization (Camel, 2001). More attention is usually paid to the extraction step, and the step of the analyte collection is frequently ignored while it needs to be carefully controlled. The step of analyte desorption from the matrix controls the analyte removal, and recovery process from the solid matrix as the analyte-matrix interaction is not easily predicted, which is different from other matrices. As a result, the matrix from which the analyte will be extracted determines the approach to be applied for optimization of the analyte removal and recovery process.

Various well-known traditional extraction methods are employed to remove compounds in solid matrices, including Soxhlet extraction, shaking extraction, etc. Although high extraction efficiency may be obtained when implementing these methods, they present significant shortcomings, such as a significant amount of solvent consumption, prolonged extraction time, and no agitation provided, particularly Soxhlet extraction (Kunene and Mahlambi, 2020). With these regards, commonly used sensitive and robust analytical methods are presented to extract pharmaceutical compounds from solid matrixes, including microwave-assisted extraction, ultrasonic extraction, etc.

The ultrasonic extraction (UE) technique has been recognized as a better traditional extraction method. It has overcome some drawbacks from the well-known traditional extraction techniques as it is simple, cheap, and has reduced extraction time and solvent consumption (Ntombela and Mahlambi, 2019). This technique has been used to extract pharmaceuticals from the solid environmental matrix (Al-Khazrajy and Boxall, 2017, Aznar et al., 2014, Hlengwa and Mahlambi, 2020). In addition, ultrasonic has also been used to extract pharmaceuticals in plant matrices (Wu et al., 2012b, Chitescu et al., 2012). The extracts from the solid matrix can be cleaned up using numerous methods, including microextraction methods that have been rapidly developed. These generic microextraction methods are reviewed as better alternative methods. They reduce the possible errors usually introduced by the multi-step approaches, require small solvent quantity in microliters, reduce equilibrium time, and minimize the health effect of analytical chemists' conducting laboratory work and negative environmental impact. A dispersive liquid-liquid microextraction method is a fast and simple method with many advantages over conventional methods, such as high enrichment factor, high surface between the aqueous sample and the extraction solvent (Dias et al., 2021, Sajedi-Amin et al., 2017).

Massive loads of pharmaceuticals have been found in the environmental water and aquatic plants. Most studies indicated that these compounds are poorly removed in wastewater treatment plants (WWTPs) as their major purpose is not to remove organic compounds (Madikizela et al., 2017). As a result, pharmaceuticals in discharged water from households, pharmaceutical industries, hospitals, and other sources are not completely removed during wastewater purification. Some pollutants partition with the sludge, and some dissolve in water due to their high polarity; thus, they are discharged with effluent (Mtolo et al., 2019). Both streams of sludge and effluent have a high potential to pollute agricultural fields as 70% of the effluent from WWTPs is used to irrigate crops due to the scarcity of freshwater globally. The sludge is also introduced into the horticulture field to serve as a fertilizer. In this regard, crops

grown in pharmaceuticals contaminated/fertilized soil could absorb these pollutants (Madikizela et al., 2018). The occurrence of pharmaceuticals in plants has sizeable studies conducted. However, it has been proven that pharmaceuticals are taken up by plants and vegetables (Wu et al., 2012b). Their presence in vegetables could deteriorate crops' quality and pose a human health risk upon consumption.

Antiretroviral drugs (ARVDs) are pharmaceutical compounds that are an evolving class of environmental pollutants (Abafe et al., 2018, K'oreje et al., 2016). However, their environmental effect is still relatively unknown regardless of their high consumption rate in the past two decades, which drastically increases every year. It has been reported that prolonged unintentional consumption could result in drug resistance (Andrade et al., 2011). Until recently, analytical data for ARVDs were largely limited to human emanations such as meconium, saliva, plasma, and others (Himes et al., 2013). Unlike the more common pharmaceuticals, information on ARVDs in vegetables and environmental samples is quite comparatively limited (Mlunguza et al., 2020). Hence, this emphasizes the necessity for a robust and sensitive analytical technique that simultaneously detects different ARVDs to investigate their uptake by vegetables. Therefore, this work presents ultrasonic extraction and ultrasonic-assistance dispersive liquid-liquid microextraction (UA-DLLME) linked with liquid chromatography to isolate and quantify particular ARVDs in vegetable samples. To the best of our knowledge, this is the first time ARVDs (abacavir, nevirapine, and efavirenz) are analyzed in vegetables using UE and UA-DLLE.

## **3.2. Experimental**

### **3.2.1 Materials and chemicals**

Organic solvent with  $\geq 99\%$  purity, acetonitrile, methanol, and acetone were purchased from Sigma Aldrich and supplied by Honeywell (Steinheim, Germany). Chloroform 1-Octanol and 1-hetanol for synthesis with a purity of  $\geq 99\%$  were purchased from Merck KGAE (Darmstadt, Germany). High purity ARVDs abacavir, nevirapine, and efavirenz were bought from J & H Chemical Co. LTD (Hangzhou Zhejiang, China). Sodium chloride salt was purchased from Merk (Gauteng, South Africa).

### **3.2.2 Instrumentation**

A liquid chromatography (LC) system bought from Shimadzu (Tokyo, Japan) coupled with LC 2030/2040 photo-diode array (PDA) detector purchased from Shimadzu (Tokyo, Japan) was

used for detection and quantification. The detector wavelengths were 225 nm and 274 nm. The column Shim-Pack GIST C18-HP (4.6 mm×150 mm, 3 m) purchased from Shimadzu (Tokyo, Japan) was used to separate the target compounds from the standard or extract, which was injected by the autosampler into the LC system, eluted by the gradient elution. A mobile phase was 0.1% formic acid in acetonitrile (CH<sub>3</sub>CN) (solvent A) and 0.1% formic acid in water (H<sub>2</sub>O) (solvent B). A gradient program started with 50% of solvent A for the initial 5 minutes and ramped up to 70% for the next 7 minutes. The flow rate was 0.4 mL/min. The complete run was 12 min.

Vegetable samples were blended with a Sunbeam blender that was purchased from Clicks (KwaZulu-Natal, South Africa). IEins sci-E-VM-A vortex purchased from science Tech (KwaZulu-Natal, South Africa) was used to vortex the mixture of dispersive, extraction solvents, and ultrasonic extract. A centrifuge used to separate a solvent mixture in the UADLLME method was purchased from Shalom Laboratory (Durban, South Africa). The ultrasonic bath used to extract target ARVDs compounds in the vegetable matrix was purchased from Science Tech (Durban, South Africa). The extraction extract for the UE method was reduced using a rotary evaporator bought from IKA® Buchi Rotavapor Fluka (Steinheim, Germany). 0.2µm filter used to filter the final extract was purchased from Pall (Puerto Rico, United States).

### **3.2.3 Preparation of stock solution**

A 100 mg/L stock solution was prepared in a 100 mL volumetric flask by dissolving in acetonitrile a measured 10 g of each salt abacavir, nevirapine, and efavirenz. Five working solutions of ARVDs with series concentrations (0.1 -1.0 mg/L) were prepared in acetonitrile by diluting the 100 mg/L stock solution. These working solutions were analyzed by LC- PDA under optimum conditions to calibrate the LC-PDA. The results were used to construct three calibration curves that represent each target compound under the study.

### **3.2.4 Sample collection and pre-treatment**

Vegetable samples were purchased from veggie and fruit supermarkets around Scottville, Pietermaritzburg (KZN South Africa). These included root vegetables (carrot, potato, and sweet potatoes), leaf vegetables (cabbage and lettuce), and fruit vegetables (green paper,

butternut, and tomato). All samples used were washed with distilled water prior to blending and analyzed immediately after blending.

### **3.3. Sample extraction and preconcentration methods**

#### **3.3.1 Ultrasonic extraction method**

The extraction method used was adapted from Mnyandu and Mahlambi (2021). It was then further modified to improve extraction efficiency. The investigated factors were extraction solvent, sample mass, sonication time, and spike concentration. A 2g of the blended vegetable sample was placed in a 50 mL conical flask, and 10 mL of acetonitrile was added, followed by adding 2.5 g of NaCl salt. The mixture was hand swirled for 10 seconds and placed in the ultrasonicated for 30 minutes using an ultrasonic bath, followed by centrifugation for 5 minutes at 3000 rpm. The supernatant liquid was reduced to dryness using a rotary evaporator. The analyte was then re-dissolved with 1mL of acetonitrile and filtered with a 0.2  $\mu\text{m}$  filter into a 2 mL LC vial for analysis.

#### **3.3.2 Ultrasonic-assisted dispersive liquid-liquid micro-extraction method**

A 2 g of the composite vegetable sample was transferred in a 50 mL conical flask, and 10 mL of distilled water was added to a flask and mixed. The mixture was ultrasonicated for 30 minutes in the ultrasonic bath and centrifuged for 5 minutes at 3000 rpm, and then the supernatant liquid was transferred to a 50 ml centrifuge tube. The 1000  $\mu\text{L}$  mixture of acetonitrile (disperser solvent) and 1-heptanol (extraction solvent) (1:1 v/v) was added to the extract. 0.9 g of NaCl salt was also added to reduce the solubility of the extracting solvent from the aqueous sample. The mixture was then vortexed at 2500 rpm for 2 minutes. A cloudy solution was achieved, and it was then centrifuged for 5 minutes at 4000 rpm. Two phases were achieved; the organic phase was transferred into a polytope and dried out with nitrogen gas. The extracted analytes were re-dissolved by 100  $\mu\text{L}$  of acetonitrile and filtered in a 1 mL vial prior to LC-PDA analysis. The optimized UADLLME factors were extraction solvent, dispersive solvent, and dispersive and extracting solvent ratio.

#### **3.3.3 Method validation**

The proposed analytical techniques, which involve ultrasonic extraction, ultrasonic-assisted dispersive liquid-liquid microextraction, and the liquid chromatographic analysis for three targets ARVDs was validated for linearity, sensitivity, accuracy, and precisions.

### **3.4 Results and discussion**

#### **3.4.1 Optimization of ultrasonic extraction**

##### **3.4.1.1 Effect of extraction solvent on the recoveries of UE**

A type of solvent used to extract the analyte from the vegetable was investigated. It is significant to determine an ideal solvent that can permit the migration of the target analytes from the solid to a liquid phase. The investigated solvents were water, methanol, and acetonitrile. The obtained result indicated that acetonitrile was the suitable solvent for extraction of the target compounds among the tested solvents, as high recoveries ranging from 72 % to 108 % were obtained (Table 3.1). The possible reasons for high recoveries could be that acetonitrile has a high elution strength and chemical stability with low viscosity (Mnyandu and Mahlambi, 2021). Therefore, it can easily penetrate the solid matrix to remove the analyte and permit a high amount of analyte to be transported from the solid to a liquid phase. The low recoveries of nevirapine and efavirenz obtained when water was used as the extraction solvent could be due to that they have a high octanol-water partition coefficient ( $K_{ow}$ ); hence, they have less affinity for water compared to the solid matrix (Schoeman et al., 2015). The t-test results displayed that the average recovery result was not statistically different for all solvents used, as their p-values were above 0.05 (Table S3.1). The obtained p-values were ( $p>0.4$ ) for acetonitrile versus methanol, ( $p>0.2$ ) for acetonitrile versus water, and ( $p>0.6$ ) for methanol versus water. However, acetonitrile was taken as an optimum and used for further optimization due to its high recoveries.

##### **3.4.1.2 Effect of sample mass on the recoveries of UE**

The sample mass effect on the recoveries of ARVDs was investigated to determine the optimal mass that will prohibit the percolation of the solvent into a vegetable matrix. This may result in saturation and cause the removal of ARVDs to be more challenging. The investigated sample masses were 1 g, 2 g, 5 g, and 10 g. The recoveries showed a slight increase from 1 g to 2 g, and from 5 g to 10 g, the recoveries decreased. High and comparable recoveries were obtained in 1 g and 2 g sample mass range from 86 to 117% and from 92 to 118%, respectively (Table 1). This indicated that the solvent volume to sample mass ratio was suitable for achieving the effective interaction between the solvent and the sample. The low recoveries obtained in 5 g and 10 g sample mass could be possible due to insufficient solvent; hence the transportation of analyte was inadequate as an equilibrium state could be reached. Due to solvent saturation,

some of the target analytes remain in the sample matrix; thus, low recoveries are obtained (Kunene and Mahlambi, 2020). The t-test results showed that the average recovery results for 1 g, 2 g, and 5 g are not statistically different from each other, with the p-values greater than 0.05, ( $p>0.8$ ) for 1 g versus 2 g, ( $p>0.4$ ) for 1 g versus 5 g and ( $p>0.3$ ) for 2 g versus 5 g. However, 1 g, 2 g, and 5 g were all significantly different from 10 g with  $p>0.02$  for 1 g versus 10 g, 2 g versus 10 g, and 5 g versus 10g (Table S3.2). The sample mass of 2 g was then selected as the ideal and used for further optimization as it gave recoveries above 90% for all compounds.

#### **3.4.1.3 Effect of sonication time on the recoveries of UE**

Sonication time was one of the important parameters to be optimized as sufficient time could permit the migration of the analyte from the vegetable sample matrix into a liquid phase. The extraction time was varied from 10 to 60 minutes, while the other parameters were kept constant. High extraction efficiency (92 to 118%) for the targeted ARVDs occurred at 30 minutes; hence, it was chosen as the optimal extraction time (Table 3.2). The longer sonication time has been reported in other studies to improve extraction efficiency; however, poor performance resulted as extraction time further increased (Kunene and Mahlambi, 2020, Ntombela and Mahlambi, 2019). The extraction time of 60 minutes permitted low recoveries, which could indicate possible decomposition of the analyte. Another reason could be that when sonication time is prolonged, the contact area is diminished on the inner cell walls due to increasing distance, resulting from a rapid and constant disruption of cell walls (Liao et al., 2016). In a short (10 minutes) sonication time, low recoveries could be due to insufficient extraction time to allow the transportation of analytes to the solvent; thus, the analytes were left in the solid phase (Kunene and Mahlambi, 2020). The t-test revealed that the mean recovery for 10, 20, and 30 minutes are not statistically different with p-values above 0.05, ( $p>0.1$ ) for 30 minutes versus 20 minutes, and ( $p>0.07$ ) for 30 minutes versus 10 minutes. Even though they were not statistically different, the recoveries obtained for 30 minutes were all above 80%. The obtained p-value for 10 minutes versus 60 minutes ( $p>0.03$ ), for 20 minutes versus 60 minutes ( $p>0.02$ ), for 30 minutes versus 60 minutes ( $p>0.003$ ) showed to be all significantly different (Table S3.3).

#### **3.4.1.4 Effect of spike concentration on the recoveries of UE**

It was significant to investigate the concentration amount of ARVDs used to spike samples during the optimization of the analytical method. This approves that the method can accurately



detect the concentration in real samples independent of the amount of analyte present in the sample. The concentrations varied from 300, 500, and 1000  $\mu\text{g/kg}$ , and other factors were kept constant. High recoveries were obtained in all concentration levels of spike amount and were comparable (Table 3.2). The t-test results also confirmed that they are not significantly different with p-value ( $p>0.25$ ) for 300  $\mu\text{g/kg}$  versus 500  $\mu\text{g/kg}$ , ( $p>0.5$ ) for 300  $\mu\text{g/kg}$  versus 1000  $\mu\text{g/kg}$  and ( $p>0.7$ ) for 500  $\mu\text{g/kg}$  versus 1000  $\mu\text{g/kg}$  (Table S3.4). It was then concluded that the performance of the extraction method was independent of the amount of ARVDs available in the sample, which designates the accurate sensitivity and applicability of the method developed.

Table 3.1: Effect of extraction solvent and sample mass on the recoveries (%) RSD% of ultrasonic extraction (n=3)

<i>Extraction solvent</i>	<i>Abacavir</i>			<i>Nevirapine</i>			<i>Efavirenz</i>		
	Potato	Lettuce	Green pepper	Potato	Lettuce	Green pepper	Potato	Lettuce	Green pepper
Acetonitrile	82 ± 2.1	87 ± 1.1	83 ± 1.9	106 ± 2.2	108 ± 1.3	92 ± 1.2	72 ± 1.2	78 ± 1.1	75 ± 1.5
Methanol	91 ± 1.2	92 ± 1.0	93 ± 2.4	69 ± 1.1	78 ± 1.3	71 ± 1.0	69 ± 1.0	74 ± 0.9	74 ± 2.1
Water	79 ± 1.3	80 ± 1.0	79 ± 1.4	62 ± 0.3	69 ± 2.2	68 ± 1.1	37 ± 1.7	44 ± 2.0	43 ± 1.3
<i>Sample mass</i>									
1 g	93 ± 1.1	100 ± 1.2	100 ± 0.6	117 ± 2.0	109 ± 2.1	110 ± 1.4	86 ± 1.2	90 ± 1.3	90 ± 1.2
2 g	95 ± 0.8	99 ± 1.3	99 ± 1.6	117 ± 1.0	117 ± 1.1	118 ± 1.4	92 ± 0.3	100 ± 1.0	100 ± 1.5
5 g	82 ± 2.1	87 ± 1.1	83 ± 1.9	106 ± 2.2	108 ± 1.3	92 ± 1.2	72 ± 1.2	78 ± 1.1	75 ± 1.5
10 g	15 ± 1.7	39 ± 0.8	40 ± 1.1	57 ± 0.5	64 ± 1.3	68 ± 1.8	11 ± 1.0	15 ± 1.2	17 ± 0.8

Table 3.2: Effect of sonication time and spike concentration on the ARVDs recoveries % and RSD% of ultrasonic extraction (n=3)

<i>Sonication time</i>	<i>Abacavir</i>			<i>Nevirapine</i>			<i>Efavirenz</i>		
	Potato	Lettuce	Green pepper	Potato	Lettuce	Green pepper	Potato	Lettuce	Green pepper
10 min	75 ± 0.1	73 ± 0.9	79 ± 0.1	72 ± 2.0	72 ± 0.5	73 ± 0.5	75 ± 1.3	79 ± 0.3	79 ± 0.2
20 min	79 ± 1.8	79 ± 0.2	77 ± 1.8	84 ± 0.8	84 ± 1.1	84 ± 0.3	79 ± 0.9	79 ± 2.2	80 ± 0.4
30 min	95 ± 0.8	99 ± 1.3	99 ± 1.6	117 ± 1.0	117 ± 1.1	118 ± 1.4	92 ± 0.3	100 ± 1.0	100 ± 1.5
60 min	34 ± 2.0	40 ± 0.6	34 ± 0.8	53 ± 2.8	69 ± 3.0	53 ± 2.1	42 ± 2.3	42 ± 1.4	47 ± 0.1
<i>Spike concentration</i>									
300 µg/kg	110 ± 1.8	110 ± 0.1	112 ± 0.8	105 ± 1.3	100 ± 0.1	103 ± 0.2	108 ± 2.4	113 ± 0.6	102 ± 0.8
500 µg/kg	108 ± 1.0	106 ± 1.3	109 ± 0.2	101 ± 1.1	102 ± 0.9	101 ± 2.1	104 ± 2.8	102 ± 2.0	100 ± 0.3
1000 µg/kg	95 ± 0.8	99 ± 1.3	99 ± 1.6	117 ± 1.0	117 ± 1.1	118 ± 1.4	92 ± 0.3	100 ± 1.0	100 ± 1.5

### **3.4.2 Optimization of ultrasonic-assisted dispersive liquid-liquid extraction UADLLME**

#### **3.4.2.1 Effect of extraction solvent**

The effect of extraction solvent on the recoveries of UADLLME was investigated using chloroform, 1-octanol, and 1-heptanol. All investigated solvents were mixed with acetonitrile as a dispersive solvent. The obtained results indicated the poor removal of ARVDs when chloroform and 1-octanol were used as an extraction solvent. The 1-heptanol permitted high recoveries within the desirable range from 95 to 103 % in fruit vegetables and 85 % to 97% in leaf vegetables (Table 3.3). This could be because 1-heptanol has a high solubility in water, meaning it is more polar; hence, it can extract the target analytes as they are polar compounds (Ntombela and Mahlambi, 2019). Root vegetables were also investigated; however, their extract was not resulting in a clear separation. Therefore, they were excluded. This could be due to the percolation of solvent in starch particles in starchy samples. Other root samples with bright colors could be due to the intense color produced by the sample during extraction. The t-test showed the average recovery for 1-heptanol to be statistically different from 1-octanol and chloroform with a p-value of ( $p > 0.005$ ) for 1-heptanol versus 1-octanol and ( $p > 0.004$ ) for 1-heptanol versus chloroform. Whereas the average recovery for 1-octanol is not statistically different from chloroform with the p-value ( $p > 0.8$ ) (Table S3.5). Therefore, 1-heptanol was taken as the best extraction solvent as it gave higher recoveries than all solvents used.

#### **3.4.2.2 Effect of dispersive solvent**

The dispersive solvent must be soluble in both the aqueous sample and the extracting solvent. The investigated dispersive were acetonitrile, the mixture of acetonitrile and methanol (1:1 v/v), and acetonitrile and acetone (1:1 v/v). Acetonitrile as a dispersive solvent provided high recoveries of ARVDs. The obtained results could be due to that acetonitrile is a less viscous solvent with a high elution strength than acetone and methanol (Mnyandu and Mahlambi, 2021). As a result, acetonitrile can promote the dispersion of 1-heptanol in the aqueous phase, increasing the interaction between ARVDs and 1-heptanol, facilitating the transfer of ARVDS from the aqueous sample to 1-heptanol (Luo et al., 2019). The t-test results indicated that the mean recovery for acetonitrile is not statistically different from acetonitrile: methanol mixture and acetonitrile: acetone mixture. The p-value obtained is ( $p > 0.07$ ) for acetonitrile versus acetonitrile: methanol mixture, ( $p > 0.2$ ) for acetonitrile versus acetonitrile: acetone mixture, and ( $p > 0.4$ ) for acetonitrile: methanol mixture and acetonitrile: acetone mixture (Table S3.6). Even though the test result confirmed that the average recoveries for all tested dispersive solvents

are equal, acetonitrile recoveries were high. Thus it was chosen as an ideal and used to optimize other parameters of the method further.

### **3.4.2.3 Selection of dispersive and extraction solvent volume**

The ratio affects the extraction efficiency, the degree of dispersal of the extraction solvent in the liquid phase, and the dispersive mixture's formation (Dias et al., 2021). The investigated 1-heptanol and acetonitrile solvent volumes were 250  $\mu$ L:750  $\mu$ L, 200  $\mu$ L:800  $\mu$ L, and 150  $\mu$ L:850  $\mu$ L. The ratio 250  $\mu$ L:750  $\mu$ L provided high recoveries range between 85 to 103%. The other investigated ratios resulted in low recoveries, and this could be due to the dissolution of 1-heptanol in an aqueous sample resulting from the excess amount of dispersant (Luo et al., 2019). The t-test showed the mean recovery for 250  $\mu$ L:750  $\mu$ L to be not statically different from 200  $\mu$ L:800  $\mu$ L, ( $p>0.08$ ) but statistically different from 150  $\mu$ L:850  $\mu$ L ( $p>0.004$ ). The average recovery for 200  $\mu$ L:800 is statistically different from 150  $\mu$ L:850  $\mu$ L with the p-value ( $p>0.004$ ) (Table S3.6). Even though high recoveries were obtained with an extracting and dispersive volume of 200  $\mu$ L:800  $\mu$ L but they were lower than the average recovery for 250  $\mu$ L:750  $\mu$ L. Therefore, 250  $\mu$ L:750  $\mu$ L was selected as an optimum ratio.

Table 3.3: Effect of extraction solvent, dispersive solvent, and their ratios in a UDALLE recoveries

<i>extracting solvents</i>	<i>Abacavir</i>		<i>Nevirapine</i>		<i>Efavirenz</i>	
	lettuce	Green pepper	Lettuce	Green pepper	Lettuce	Green pepper
1-heptanol	97 ± 2.0	95 ± 1.4	89 ± 1.0	100 ± 1.5	85 ± 1.1	103 ± 1.6
1- Octanol	73 ± 1.0	78 ± 0.9	69 ± 2.1	73 ± 0.2	67 ± 1.6	84 ± 1.0
Chloroform	74 ± 2.0	82 ± 1.2	71 ± 1.9	78 ± 0.7	70 ± 0.7	72 ± 0.9
<i>Dispersive solvents</i>						
Acetonitrile	97 ± 2.0	95 ± 1.4	89 ± 1.0	100 ± 1.5	85 ± 1.1	103 ± 1.6
Acetonitrile: Methanol	68 ± 1.6	80 ± 1.1	52 ± 2.1	93 ± 1.2	61 ± 1.6	72 ± 0.8
Acetonitrile: Acetone	79 ± 1.9	96 ± 1.5	61 ± 0.9	94 ± 1.1	85 ± 2.0	78 ± 2.4
<i>Extraction: Dispersive solvent volume</i>						
250 µL : 750 µL	97 ± 2.0	95 ± 1.4	89 ± 1.0	100 ± 1.5	85 ± 1.1	103 ± 0.9
200 µL : 800 µL	88 ± 1.6	89 ± 1.0	82 ± 0.4	92 ± 1.1	80 ± 0.7	96 ± 0.06
150 µL : 850 µL	79 ± 1.0	75 ± 0.9	72 ± 1.6	78 ± 1.5	68 ± 1.3	80 ± 1.1

### 3.4.3 Method validation

The proposed analytical techniques involving ultrasonic extraction, ultrasonic-assisted dispersive liquid-liquid extraction, and the liquid chromatographic analysis was validated for linearity, sensitivity, accuracy, and precision of the analytical methods. These were performed by spiking a plant sample at 300 µg/kg of each target analyte. The linearity was investigated by analysing the series concentrations ranging from 0.1 – 1.0 mg/L. The obtained results were used to construct the calibration curve. The  $r^2$  values obtained ranged from 0.98 to 0.99, representing the LC-PDA instrument's good accuracy and precision. The spiked sample's recoveries for UE and UADLLE ranged from 93 to 113% and 85 to 103%, respectively. The recoveries for all analysed samples are presented in Table S3.7. The t-test showed that the mean average recovery for UE is not statistically different from UADLLME with the obtained p-value ( $p>0.4$ ) above 0.05, Table S3.8. The sensitivity was measured by the limits of quantification (LOQ), and detection (LOD) was measured as the concentrations at 10 and 3 signal-to-noise ratios, respectively. The obtained LOD and LOQ results ranged between 0.0081 - 0.015 µg/kg and 0.027 - 0.049 µg/kg for ultrasonic extraction and 0.0028 - 0.0051 µg/kg and 0.0094 - 0.017 µg/kg for ultrasonic-assisted dispersive liquid-liquid extraction, respectively. The t-test results confirmed that the UE LOD is not statistically different from the UADLLME as the p-value ( $p>0.4$ ) obtained is above 0.05. Whereas the UE LOQ is statistically different from UADLLME with the p-value ( $p>0.03$ ), Table S3.9. Even though the t-tests showed that the average recovery and LOD for UE and UADLLME are statically not different, UE is considered a better method as it has high recoveries than UADLLME. Furthermore, less than 10% relative standard deviation was obtained by performing triplicate analysis, indicating good precision of both methods (Table 3.4). The optimum results obtained imply that the selected ARVDs can be extracted and isolated at low vegetable concentrations using UE and UADLLME.

Table 3.4: Performance of ultrasonic extraction and ultrasonic-assisted dispersive liquid-liquid extraction in vegetables (n=3)

Target compounds	linearity	UE		UADLLME	
		LOD (µg/kg)	LOQ (µg/kg)	LOD (µg/kg)	LOQ (µg/kg)

Abacavir	0.9883	0.012	0.039	0.0045	0.015
Nevirapine	0.9768	0.015	0.049	0.0051	0.017
Efavirenz	0.9947	0.0081	0.027	0.0028	0.0094

### 3.4.4 Application of the optimized method in vegetables

The optimized and validated analytical method was implemented to monitor the level of abacavir, nevirapine, and efavirenz present in vegetables. The investigated vegetables were root (carrot, potato, and sweet potatoes), leaf (cabbage and lettuce), and fruit (green paper, butternut, and tomato). All the target compounds analyzed were quantified in all analyzed vegetables except nevirapine which was not detected in a cabbage sample (Table 3.5). From the average concentrations, it was observed that efavirenz was the most abundant compound with high concentrations in all samples except in potato and cabbage. Efavirenz reached a maximum average concentration of 8.18 µg/kg in a carrot and 8.13 µg/kg in a sweet potato sample. The highest average concentrations obtained for abacavir and nevirapine were detected in a cabbage sample of 2.91 µg/kg and a potato sample of 2.35 µg/kg, respectively. A high concentration of efavirenz could be due to that efavirenz excretion (16-61% faecal) which is higher than those of nevirapine (<3% urinary) and abacavir (1.2% urinary) (Schoeman et al., 2017). This results in a high amount of efavirenz reaching the wastewater treatment plants, and thus higher traces can be present in effluent water (used for irrigation) and sludge (used as fertilizer) and thus end up in vegetables.

It was noticed that high concentrations were obtained in root vegetables, which could be due to that the uptake of ARVDs by the vegetable is through roots from the contaminated water or soil source via mass transfer and diffusion (Herklotz et al., 2010). Also, roots are the part of the plant that absorbs the target and non-target nutrients found within the plant; therefore, roots get polluted first than other areal parts of the plant (Bartrons and Peñuelas, 2017). The varied consumption rates of ARVDs could also have triggered these observations. For instance, epzicom is manufactured with 600 mg of abacavir/ 300 mg of lamivudine, whereas Trizivir contains 300 mg of abacavir/ 150 mg of lamivudine/ 300 mg of zidovudine (Mosekiemang et al., 2019). The results achieved in this study are similar to those reported by Mlunguza et al. (2020), which evaluated the occurrence of ARVDs in aquatic plants (leaf, stem, and root). A high concentration of ARVDs was observed in the root sample, with a maximum concentration of 29.6 µg/kg for efavirenz (Mlunguza et al., 2020).



The analysis conducted on the effluent water from the Northern wastewater treatment plant revealed that the usage of effluent water has an impact on the presence of efavirenz in agricultural areas. Moreover, numerous studies reported a high concentration of efavirenz in effluent from wastewater treatment plants in South African provinces, for instance, in Gauteng (7.1  $\mu\text{g/L}$ ) (Schoeman et al., 2015); Western Cape (1.93  $\mu\text{g/L}$ ), (Mosekiemang et al., 2019); KwaZulu-Natal (37.3  $\mu\text{g/L}$ ), (Mlunguza et al., 2020), 33  $\mu\text{g/L}$  (Abafe et al., 2018), 93.1  $\mu\text{g/L}$  (Mtolo et al., 2019). It has been reported that the sludge removed during wastewater treatment contains high concentrations of ARVDs, up to 43000  $\mu\text{g/L}$  (Schoeman et al., 2017). These prove that the sludge used for soil fertilization in the agricultural area also contributes to the pollution of vegetables. There are no similar studies that previously reported the occurrence of target ARVDs in vegetables under study. However, the obtained concentration results are comparable with other pharmaceuticals and personal care products detected in vegetables (Calderón-Preciado et al., 2013, Goldstein et al., 2014). In vegetables, pharmaceutical and personal care product concentrations ranging from 0.043 to 1.287  $\mu\text{g/kg}$  have been previously detected (Wu et al., 2012a).

The average concentrations obtained using UADLLME were all slightly higher than those obtained using UE. Also, nevirapine was detected but not quantified by UADLLME, whereas it was not detected by the UE, which could be due to the higher sensitivity of UADLLME. Therefore it is more effective than UE. The comparison between the extraction methods was done only in the average concentrations obtained in leafy and fruit vegetables. The root vegetables were excluded due to the difficulties faced when using UADLLME. The potato and sweet potato samples were not resulting in two phases after centrifuging the mixture. A one-phase solution with a residue at the bottom of the tube was achieved. The poor extraction could be due to excessive starch contained in these vegetables. It was concluded that the organic solvent percolated in the residue produced by the sample. Although high concentrations were obtained in the use of UADLLME, however, the UE can be recommended for routine analysis due to the fewer steps of the method and its ability to extract target ARVDs in colorful, starchy, as well as root matrices where the UADLLME showed to be ineffective.

Table 3.5. Average concentrations of selected ARVDs, RSD% traced in vegetables (n = 3)

List of vegetables	Average concentration (µg/kg) ± RSD%					
	Abacavir		Nevirapine		Efavirenz	
	UE	UADLLME	UE	UADLLME	UE	UADLLME
Carrot	$1.00 \times 10^{-1} \pm 2.0$	-	$2.43 \times 10^{-1} \pm 2.0$	-	$8.18 \pm 2.3$	-
Potato	$2.34 \pm 2.7$	-	$2.35 \pm 2.3$	-	$2.34 \pm 2.3$	-
Sweet potato	$6.01 \times 10^{-1} \pm 1.0$	-	$6.52 \times 10^{-1} \pm 1.9$	-	$8.13 \pm 1.4$	-
Cabbage	$2.91 \pm 0.1$	$3.13 \pm 0.9$	nd	nq	$1.74 \pm 0.9$	$2.99 \pm 1.3$
Lettuce	$1.34 \pm 2.2$	$1.74 \pm 0.6$	$1.34 \pm 2.0$	$1.78 \pm 0.8$	$1.49 \pm 0.7$	$1.03 \pm 2.0$
Green pepper	$1.60 \pm 0.8$	$1.92 \pm 1.9$	$8.01 \times 10^{-1} \pm 0.07$	$1.05 \pm 1.3$	$2.10 \pm 0.3$	$2.47 \pm 1.0$
Butternut	$8.02 \times 10^{-2} \pm 1.4$	$1.28 \times 10^{-1} \pm 0.09$	$3.11 \times 10^{-1} \pm 0.01$	$4.11 \times 10^{-1} \pm 1.0$	$2.04 \pm 1.0$	$3.11 \pm 0.9$
Tomato	$2.63 \times 10^{-1} \pm 2.9$	$7.69 \times 10^{-1} \pm 0.6$	$3.94 \times 10^{-1} \pm 2.0$	$8.86 \times 10^{-1} \pm 1.7$	$8.94 \times 10^{-1} \pm 0.5$	$1.09 \pm 1.1$

nd – not detected; nq - not quantified; - not analyzed

### 3.5. Conclusion

The convenient extraction methods (UE and UADLLME) for abacavir, nevirapine, and efavirenz from vegetables, followed by their detection and quantification using LC-PDA, have been successfully developed. The concentration obtained ranged between 0.100 to 8.18  $\mu\text{g/kg}$  in root vegetables, from nd to 3.13  $\mu\text{g/kg}$  in leaf vegetables, and from 0.0802 to 3.11  $\mu\text{g/kg}$  in fruity vegetables. Efavirenz was the dominant compound and quantified at high concentration in most samples. The potato was the most polluted vegetable even though efavirenz concentration was less than the concentration obtained in carrots and sweet potato. The result obtained indicate that ARVDs are taken up through roots in vegetables and translocated into areas above the ground as they were present in leafy and fruit vegetables. The comparison between the extraction methods showed that UADLLME is more sensitive though they both have comparable accuracy and precision. However, the UE method can be recommended for a routine analysis due to its effectiveness and simplicity. The occurrence of ARVDs in various vegetable samples analyzed is a threat to human health; therefore, their continuous monitoring, especially in South Africa and other developing countries with a high rate of HIV-infected patients, is of paramount importance.

### References

- Abafe, O. A., Späth, J., Fick, J., Jansson, S., Buckley, C., Stark, A., Pietruschka, B. & Martincigh, B. S. 2018. LC-MS/MS determination of antiretroviral drugs in influents and effluents from wastewater treatment plants in KwaZulu-Natal, South Africa. *Chemosphere*, 200, 660-670. doi:<https://doi.org/10.1016/j.chemosphere.2018.02.105>
- Al-Khazrajy, O. S. & Boxall, A. B. 2017. Determination of pharmaceuticals in freshwater sediments using ultrasonic-assisted extraction with SPE clean-up and HPLC-DAD or LC-ESI-MS/MS detection. *Analytical Methods*, 9, 4190-4200. doi:<https://doi.org/10.1039/C7AY00650K>
- Andrade, C. H., Freitas, L. M. d. & Oliveira, V. d. 2011. Twenty-six years of HIV science: an overview of anti-HIV drugs metabolism. *Brazilian Journal of Pharmaceutical Sciences*, 47, 209-230. doi:<https://doi.org/10.1590/S1984-82502011000200003>
- Aznar, R., Sánchez-Brunete, C., Alberro, B., Rodríguez, J. A. & Tadeo, J. L. 2014. Occurrence and analysis of selected pharmaceutical compounds in soil from Spanish agricultural fields. *Environmental Science and Pollution Research*, 21, 4772-4782. doi:[https://doi.org/10.1016/0041-624X\(82\)90032-4](https://doi.org/10.1016/0041-624X(82)90032-4)

- Bartrons, M. & Peñuelas, J. 2017. Pharmaceuticals and personal-care products in plants. *Trends in Plant Science*, 22, 194-203. doi:<https://doi.org/10.1016/j.tplants.2016.12.010>
- Calderón-Preciado, D., Matamoros, V., Savé, R., Muñoz, P., Biel, C. & Bayona, J. 2013. Uptake of microcontaminants by crops irrigated with reclaimed water and groundwater under real field greenhouse conditions. *Environmental Science and Pollution Research*, 20, 3629-3638. doi:<https://doi.org/10.1007/s11356-013-1509-0>
- Camel, V. J. A. 2001. Recent extraction techniques for solid matrices—supercritical fluid extraction, pressurized fluid extraction and microwave-assisted extraction: their potential and pitfalls. *The Royal Society of Chemistry*, 126, 1182-1193. doi:<https://doi.org/10.1039/B008243K>
- Chitescu, C. L., Oosterink, E., de Jong, J. & Stolker, A. A. M. L. 2012. Ultrasonic or accelerated solvent extraction followed by U-HPLC-high mass accuracy MS for screening of pharmaceuticals and fungicides in soil and plant samples. *Talanta*, 88, 653-662. doi:<https://doi.org/10.1016/j.talanta.2011.11.054>
- Dias, R. A., Sousa, E. R., Silva, G. S., Silva, L. K., Freitas, A. S., Lima, D. L. & Sousa, É. M. 2021. Ultrasound-assisted dispersive liquid-liquid microextraction for determination of enrofloxacin in surface waters. *Microchemical journal*, 160, 105633. doi:<https://doi.org/10.1016/j.microc.2020.105633>
- Goldstein, M., Shenker, M. & Chefetz, B. 2014. Insights into the uptake processes of wastewater-borne pharmaceuticals by vegetables. *Environmental Science and Technology*, 48, 5593-5600. doi:<https://doi.org/10.1021/es5008615>
- Herklotz, P. A., Gurung, P., Heuvel, B. V. & Kinney, C. A. 2010. Uptake of human pharmaceuticals by plants grown under hydroponic conditions. *Chemosphere*, 78, 1416-1421. doi:<https://doi.org/10.1016/j.chemosphere.2009.12.048>
- Himes, S. K., Scheidweiler, K. B., Tassiopoulos, K. & Kacanek, D. H., Rohan Rich, Kenneth Huestis, Marilyn A, Pediatric HIV/AIDS Cohort Study 2013. Development and validation of the first liquid chromatography-tandem mass spectrometry assay for simultaneous quantification of multiple antiretrovirals in meconium. *Analytical Chemistry*, 85, 1896-1904. doi:<https://doi.org/10.1021/ac303188j>
- Hlengwa, N. & Mahlambi, P. 2020. Ultrasonic Followed by Solid Phase Extraction and Liquid Chromatography-Photodiode Array for Determination of Pharmaceutical Compounds in Sediment and Soil. *Bulletin of environmental contamination and toxicology*, 1-7. doi:<https://doi.org/10.1007/s00128-020-02829-6>

- K'oreje, K., Vergeynst, L., Ombaka, D., De Wispelaere, P., Okoth, M., Van Langenhove, H. & Demeestere, K. 2016. Occurrence patterns of pharmaceutical residues in wastewater, surface water and groundwater of Nairobi and Kisumu city, Kenya. *Chemosphere*, 149, 238-244. doi:<https://doi.org/10.1016/j.chemosphere.2016.01.095>
- Kunene, P. & Mahlambi, P. 2020. Optimization and application of ultrasonic extraction and Soxhlet extraction followed by solid phase extraction for the determination of triazine pesticides in soil and sediment. *Environmental Chemical Engineering*, 8, 103665. doi:<https://doi.org/10.1016/j.jece.2020.103665>
- Liao, J., Qu, B. & Zheng, N. 2016. Effects of process parameters on the extraction of quercetin and rutin from the stalks of *Euonymus Alatus* (Thumb.) Sieb and predictive model based on least squares support vector machine optimized by an improved fruit fly optimization algorithm. *Applied Sciences*, 6, 340. doi:<https://doi.org/10.3390/app6110340>
- Luo, Q., Wang, S., Adeel, M., Shan, Y., Wang, H. & Sun, L. N. 2019. Solvent demulsification-dispersive liquid-liquid microextraction based on solidification of floating organic drop coupled with ultra-high-performance liquid chromatography-tandem mass spectrometry for simultaneous determination of 13 organophosphate esters in aqueous samples. *Scientific Reports*, 9, 1-11. doi:<https://doi.org/10.1038/s41598-019-47828-8>
- Madikizela, L. M., Ncube, S. & Chimuka, L. 2018. Uptake of pharmaceuticals by plants grown under hydroponic conditions and natural occurring plant species: a review. *Science of the Total Environment* 636, 477-486. doi:<https://doi.org/10.1016/j.scitotenv.2018.04.297>
- Madikizela, L. M., Tavengwa, N. T. & Chimuka, L. 2017. Status of pharmaceuticals in African water bodies: occurrence, removal and analytical methods. *Journal of environmental management*, 193, 211-220. doi:<http://dx.doi.org/10.1016/j.jenvman.2017.02.022>
- Mlunguza, N. Y., Ncube, S., Mahlambi, P. N., Chimuka, L. & Madikizela, L. M. 2020. Determination of selected antiretroviral drugs in wastewater, surface water and aquatic plants using hollow fibre liquid phase microextraction and liquid chromatography-tandem mass spectrometry. *Journal of hazardous materials*, 382, 121067. doi:<https://doi.org/10.1016/j.jhazmat.2019.121067>
- Mnyandu, H. & Mahlambi, P. 2021. Optimization and application of QuEChERS and SPE methods followed by LC-PDA for the determination of triazines residues in fruits and vegetables from Pietermaritzburg local supermarkets. *Food Chemistry*, 129818. doi:<https://doi.org/10.1016/j.foodchem.2021.129818>

- Mosekiemang, T. T., Stander, M. A. & de Villiers, A. 2019. Simultaneous quantification of commonly prescribed antiretroviral drugs and their selected metabolites in aqueous environmental samples by direct injection and solid phase extraction liquid chromatography-tandem mass spectrometry. *Chemosphere*, 220, 983-992. doi:https://doi.org/10.1016/j.chemosphere.2018.12.205
- Mtolo, S. P., Mahlambi, P. N. & Madikizela, L. M. 2019. Synthesis and application of a molecularly imprinted polymer in selective solid-phase extraction of efavirenz from water. *Water Science and Technology*, 79, 356-365. doi:https://doi.org/10.2166/wst.2019.054
- Ntombela, S. & Mahlambi, P. 2019. Method development and application for triazine herbicides analysis in water, soil and sediment samples from KwaZulu-Natal. *Journal of Environmental Science and Health, Part B*, 1-11. doi:https://doi.org/10.1080/03601234.2019.1621113
- Sajedi-Amin, S., Asadpour-Zeynali, K., Khoubnasabjafari, M., Rashidi, F. & Jouyban, A. 2017. Development and Validation of Ultrasound Assisted and Dispersive Liquid-Liquid Microextractions Combined with HPLC-UV Method for Determination of Bosentan in Human Plasma and Urine. *Journal of the Brazilian Chemical Society*, 28, 868-877. doi:https://doi.org/10.21577/0103-5053.20160239
- Schoeman, C., Dlamini, M. & Okonkwo, O. 2017. The impact of a wastewater treatment works in Southern Gauteng, South Africa on efavirenz and nevirapine discharges into the aquatic environment. *Emerging Contaminants*, 3, 95-106. doi:https://doi.org/10.1016/j.emcon.2017.09.001
- Schoeman, C., Mashiane, M., Dlamini, M. & Okonkwo, O. 2015. Quantification of selected antiretroviral drugs in a wastewater treatment works in South Africa using GC-TOFMS. *Journal of Chromatography Separation Techniques*, 6, 1-7. doi:https://doi.org/10.4172/2157-7064.1000272
- Wu, C., Spongberg, A. L., Witter, J. D. & Sridhar, B. M. 2012a. Transfer of wastewater associated pharmaceuticals and personal care products to crop plants from biosolids treated soil. *Ecotoxicology and environmental safety*, 85, 104-109. doi:https://doi.org/10.1016/j.ecoenv.2012.08.007
- Wu, X., Conkle, J. L. & Gan, J. 2012b. Multi-residue determination of pharmaceutical and personal care products in vegetables. *Journal of chromatography A*, 1254, 78-86. doi:http://dx.doi.org/10.1016/j.chroma.2012.07.041

## Supplementary information

Table S3.1: t-Test result for the effect of extraction solvent on the recoveries (%)

t-Test: Two-Sample Assuming Unequal Variances			t-Test: Two-Sample Assuming Unequal Variances			t-Test: Two-Sample Assuming Unequal Variances		
	<i>Acetonitrile</i>	<i>Methanol</i>		<i>Acetonitrile</i>	<i>Water</i>		<i>Methanol</i>	<i>Water</i>
Mean	86,66666667	76,33333333	Mean	86,66666667	71,66666667	Mean	76,33333333	71,66666667
Variance	305,3333333	161,3333333	Variance	305,3333333	76,33333333	Variance	161,3333333	76,33333333
Observations	3	3	Observations	3	3	Observations	3	3
Hypothesized Mean Difference	0		Hypothesized Mean Difference	0		Hypothesized Mean Difference	0	
df	4		df	3		df	4	
t Stat	0,82850985		t Stat	1,32987178		t Stat	0,52430412	
P(T<=t) one-tail	0,226977219		P(T<=t) one-tail	0,137815096		P(T<=t) one-tail	0,3138892	
t Critical one-tail	2,131846786		t Critical one-tail	2,353363435		t Critical one-tail	2,131846786	
P(T<=t) two-tail	0,453954437		P(T<=t) two-tail	0,275630192		P(T<=t) two-tail	0,6277784	
t Critical two-tail	2,776445105		t Critical two-tail	3,182446305		t Critical two-tail	2,776445105	

Table S3.2: The t-test results for the effect of sample mass on the recoveries (%)

t-Test: Two-Sample Assuming Unequal Variances			t-Test: Two-Sample Assuming Unequal Variances			t-Test: Two-Sample Assuming Unequal Variances		
	1g	2g		1g	5g		1g	10g
Mean	98,66666667	101,3333333	Mean	98,66666667	86,66666667	Mean	98,66666667	27,66667
Variance	264,3333333	186,3333333	Variance	264,3333333	305,3333333	Variance	264,3333333	649,3333
Observations	3	3	Observations	3	3	Observations	3	3
Hypothesized Mean Difference	0		Hypothesized Mean Difference	0		Hypothesized Mean Difference	0	
df	4		df	4		df	3	
t Stat	-0,217571317		t Stat	0,870826165		t Stat	4,06841349	
P(T<=t) one-tail	0,419205511		P(T<=t) one-tail	0,216496494		P(T<=t) one-tail	0,01339498	
t Critical one-tail	2,131846786		t Critical one-tail	2,131846786		t Critical one-tail	2,353363435	
P(T<=t) two-tail	0,838411021		P(T<=t) two-tail	0,432992988		P(T<=t) two-tail	0,026789959	
t Critical two-tail	2,776445105		t Critical two-tail	2,776445105		t Critical two-tail	3,182446305	
t-Test: Two-Sample Assuming Unequal Variances			t-Test: Two-Sample Assuming Unequal Variances			t-Test: Two-Sample Assuming Unequal Variances		
	2g	5g		2g	10g		5g	10g
Mean	101,3333333	86,66666667	Mean	101,3333333	27,66666667	Mean	86,66666667	27,66667
Variance	186,3333333	305,3333333	Variance	186,3333333	649,3333333	Variance	305,3333333	649,3333
Observations	3	3	Observations	3	3	Observations	3	3
Hypothesized Mean Difference	0		Hypothesized Mean Difference	0		Hypothesized Mean Difference	0	
df	4		df	3		df	4	
t Stat	1,145662417		t Stat	4,413824965		t Stat	3,307400285	
P(T<=t) one-tail	0,157909152		P(T<=t) one-tail	0,010790632		P(T<=t) one-tail	0,014863335	
t Critical one-tail	2,131846786		t Critical one-tail	2,353363435		t Critical one-tail	2,131846786	
P(T<=t) two-tail	0,315818304		P(T<=t) two-tail	0,021581263		P(T<=t) two-tail	0,029726671	
t Critical two-tail	2,776445105		t Critical two-tail	3,182446305		t Critical two-tail	2,776445105	



Table S3. 3: The t-test results for the effect of extraction time on the recoveries (%)

t-Test: Two-Sample Assuming Unequal Variances			t-Test: Two-Sample Assuming Unequal Variances			t-Test: Two-Sample Assuming Unequal Variances		
	10 min	20 min		10 min	30 min		10 min	60 min
Mean	74	80,66666667	Mean	74	101,3333333	Mean	74	43
Variance	3	8,333333333	Variance	3	186,3333333	Variance	3	91
Observations	3	3	Observations	3	3	Observations	3	3
Hypothesized Mean Difference	0		Hypothesized Mean Difference	0		Hypothesized Mean Difference	0	
df	3		df	2		df	2	
t Stat	-3,429971703		t Stat	-3,440643569		t Stat	5,538069408	
P(T<=t) one-tail	0,020769455		P(T<=t) one-tail	0,037541694		P(T<=t) one-tail	0,015546144	
t Critical one-tail	2,353363435		t Critical one-tail	2,91998558		t Critical one-tail	2,91998558	
P(T<=t) two-tail	0,041538909		P(T<=t) two-tail	0,075083389		P(T<=t) two-tail	0,031092287	
t Critical two-tail	3,182446305		t Critical two-tail	4,30265273		t Critical two-tail	4,30265273	
t-Test: Two-Sample Assuming Unequal Variances			t-Test: Two-Sample Assuming Unequal Variances			t-Test: Two-Sample Assuming Unequal Variances		
	20 min	30 min		20 min	60 min		30 min	60 min
Mean	80,66666667	101,3333333	Mean	80,66666667	43	Mean	101,3333333	43
Variance	8,333333333	186,3333333	Variance	8,333333333	91	Variance	186,3333333	91
Observations	3	3	Observations	3	3	Observations	3	3
Hypothesized Mean Difference	0		Hypothesized Mean Difference	0		Hypothesized Mean Difference	0	
df	2		df	2		df	4	
t Stat	-2,565578255		t Stat	6,545914244		t Stat	6,067033396	
P(T<=t) one-tail	0,062118938		P(T<=t) one-tail	0,011275663		P(T<=t) one-tail	0,001863736	
t Critical one-tail	2,91998558		t Critical one-tail	2,91998558		t Critical one-tail	2,131846786	
P(T<=t) two-tail	0,124237876		P(T<=t) two-tail	0,022551326		P(T<=t) two-tail	0,003727472	
t Critical two-tail	4,30265273		t Critical two-tail	4,30265273		t Critical two-tail	2,776445105	

Table S3.4: The t-test results for the effect of spike concentration on the recoveries (%)

t-Test: Two-Sample Assuming Unequal Variances			t-Test: Two-Sample Assuming Unequal Variances			t-Test: Two-Sample Assuming Unequal Variances		
	300 µg/kg	500 µg/kg		300 µg/kg	1000 µg/kg		500 µg/kg	1000 µg/kg
Mean	107,6666667	104,3333333	Mean	107,6666667	101,3333333	Mean	104,3333333	101,3333333
Variance	6,333333333	12,33333333	Variance	6,333333333	186,3333333	Variance	12,33333333	186,3333333
Observations	3	3	Observations	3	3	Observations	3	3
Hypothesized Mean Difference	0		Hypothesized Mean Difference	0		Hypothesized Mean Difference	0	
df	4		df	2		df	2	
t Stat	1,33630621		t Stat	0,790295814		t Stat	0,368654364	
P(T<=t) one-tail	0,126200274		P(T<=t) one-tail	0,256089321		P(T<=t) one-tail	0,373875833	
t Critical one-tail	2,131846786		t Critical one-tail	2,91998558		t Critical one-tail	2,91998558	
P(T<=t) two-tail	0,252400549		P(T<=t) two-tail	0,512178642		P(T<=t) two-tail	0,747751665	
t Critical two-tail	2,776445105		t Critical two-tail	4,30265273		t Critical two-tail	4,30265273	

Table S3.5: The t-test results for the effect of extracting solvent on the recoveries (%)

t-Test: Two-Sample Assuming Unequal Variances			t-Test: Two-Sample Assuming Unequal Variances			t-Test: Two-Sample Assuming Unequal Variances		
	1-Heptanol	1-Octanol		1-Heptanol	Chloroform		1-Octanol	Chloroform
Mean	99,33333333	78,33333333	Mean	99,33333333	77,33333333	Mean	78,33333333	77,33333333
Variance	16,33333333	30,33333333	Variance	16,33333333	25,33333333	Variance	30,33333333	25,33333333
Observations	3	3	Observations	3	3	Observations	3	3
Hypothesized Mean Difference	0		Hypothesized Mean Difference	0		Hypothesized Mean Difference	0	
df	4		df	4		df	4	
t Stat	5,324471805		t Stat	5,903219461		t Stat	0,23214697	
P(T<=t) one-tail	0,00299375		P(T<=t) one-tail	0,002060323		P(T<=t) one-tail	0,413908671	
t Critical one-tail	2,131846786		t Critical one-tail	2,131846786		t Critical one-tail	2,131846786	
P(T<=t) two-tail	0,005987501		P(T<=t) two-tail	0,004120646		P(T<=t) two-tail	0,827817342	
t Critical two-tail	2,776445105		t Critical two-tail	2,776445105		t Critical two-tail	2,776445105	

Table S3.6: The t-test results for the effect of dispersive solvent and dispersive and extracting solvent volume on the recoveries (%)

t-Test: Two-Sample Assuming Unequal Variances			t-Test: Two-Sample Assuming Unequal Variances			t-Test: Two-Sample Assuming Unequal Variances		
	ACN	ACN: MEOH		ACN	ACN:ACT		ACN: MEOH	ACN:ACT
Mean	99,33333333	81,66666667	Mean	99,33333333	89,333333	Mean	81,66666667	89,33333333
Variance	16,33333333	112,3333333	Variance	16,33333333	97,333333	Variance	112,3333333	97,33333333
Observations	3	3	Observations	3	3	Observations	3	3
Hypothesized Mean Difference	0		Hypothesized Mean Difference	0		Hypothesized Mean Difference	0	
df	3		df	3		df	4	
t Stat	2,697628972		t Stat	1,624591083		t Stat	-0,917070056	
P(T<=t) one-tail	0,036967186		P(T<=t) one-tail	0,10135787		P(T<=t) one-tail	0,205498005	
t Critical one-tail	2,353363435		t Critical one-tail	2,353363435		t Critical one-tail	2,131846786	
P(T<=t) two-tail	0,073934371		P(T<=t) two-tail	0,20271574		P(T<=t) two-tail	0,41099601	
t Critical two-tail	3,182446305		t Critical two-tail	3,182446305		t Critical two-tail	2,776445105	
t-Test: Two-Sample Assuming Unequal Variances			t-Test: Two-Sample Assuming Unequal Variances			t-Test: Two-Sample Assuming Unequal Variances		
	250 $\mu$ L: 750 $\mu$ L	200 $\mu$ L:800 $\mu$ L		250 $\mu$ L: 750 $\mu$ L	50 $\mu$ L:850 $\mu$ L		200 $\mu$ L:800 $\mu$ L	150 $\mu$ L:850 $\mu$ L
Mean	99,33333333	92,33333333	Mean	99,33333333	77,666667	Mean	92,33333333	77,66666667
Variance	16,33333333	12,33333333	Variance	16,33333333	6,333333	Variance	12,33333333	6,33333333
Observations	3	3	Observations	3	3	Observations	3	3
Hypothesized Mean Difference	0		Hypothesized Mean Difference	0		Hypothesized Mean Difference	0	
df	4		df	3		df	4	
t Stat	2,264488237		t Stat	7,882407814		t Stat	5,879747322	
P(T<=t) one-tail	0,043125676		P(T<=t) one-tail	0,002127434		P(T<=t) one-tail	0,002090536	
t Critical one-tail	2,131846786		t Critical one-tail	2,353363435		t Critical one-tail	2,131846786	
P(T<=t) two-tail	0,086251352		P(T<=t) two-tail	0,004254868		P(T<=t) two-tail	0,004181072	
t Critical two-tail	2,776445105		t Critical two-tail	3,182446305		t Critical two-tail	2,776445105	

Table S3.7: Average recoveries % obtained for selected ARVDs in different matrices

Vegetables	Abacavir		Nevirapine		Efavirenz	
	UE	UADLLME	UE	UADLLME	UE	UADLLME
Carrot	100	-	93	-	112	-
Potato	110	-	105	-	108	-
Sweet potato	108	-	113	-	106	-
Cabbage	95	89	111	85	108	101
lettuce	110	94	100	90	113	91
Green pepper	112	95	103	100	102	103
Butternut	102	85	102	94	103	102
Tomato	106	92	99	89	91	102

Table S3.8: The t-test results for the average LOD and LOQ for UE and UADLLME

t-Test: Two-Sample Assuming Unequal Variances		
	<i>UE recovery %</i>	<i>UDLLME recovery %</i>
Mean	105,6666667	99,33333333
Variance	114,3333333	16,33333333
Observations	3	3
Hypothesized Mean Difference	0	
df	3	
t Stat	0,959644917	
P(T<=t) one-tail	0,204013901	
t Critical one-tail	2,353363435	
P(T<=t) two-tail	0,408027802	
t Critical two-tail	3,182446305	

Table S3.9: The t-test results for the average LOD and LOQ for UE and UADLLME

t-Test: Two-Sample Assuming Unequal Variances			t-Test: Two-Sample Assuming Unequal Variances		
	UE LOD ( $\mu\text{g/kg}$ )	DLLE LOD ( $\mu\text{g/kg}$ )		UADLLE LOQ ( $\mu\text{g/kg}$ )	UADLLE LOQ ( $\mu\text{g/kg}$ )
Mean	0,0081	0,004133333	Mean	0,038333333	0,0138
Variance	0,00004761	1,42333E-06	Variance	0,000121333	0,00001552
Observations	3	3	Observations	3	3
Hypothesized Mean Difference	0		Hypothesized Mean Difference	0	
df	2		df	3	
t Stat	0,981161786		t Stat	3,632365123	
P(T<=t) one-tail	0,214984571		P(T<=t) one-tail	0,017966857	
t Critical one-tail	2,91998558		t Critical one-tail	2,353363435	
P(T<=t) two-tail	0,429969143		P(T<=t) two-tail	0,035933713	
t Critical two-tail	4,30265273		t Critical two-tail	3,182446305	

## Chapter four

---

### 4. Assessment of antiretroviral drugs in vegetables: evaluation of microwave-assisted extraction performance with and without solid-phase extraction cleanup

#### Abstract

This study presents unique data on concentrations of antiretroviral drugs (abacavir, nevirapine, and efavirenz) in the root, leaf, and fruit vegetables. The microwave-assisted extraction, solid-phase extraction (SPE), and liquid chromatography (LC) coupled with a photodiode array detector were applied to assess antiretroviral drugs in vegetable samples. The analytical method showed high precision with linearity ( $R^2$ ) greater than 0.99, with acceptable recoveries ranging from 85 to 103% for microwave-assisted extraction and 82 to 98% for microwave-assisted extraction with SPE. The limit of detection and quantification ranged from 0.020 to 0.032  $\mu\text{g/kg}$  and 0.068 to 0.109  $\mu\text{g/kg}$  for microwave-assisted extraction and 0.019 to 0.066  $\mu\text{g/L}$ , and 0.065 to 0.22  $\mu\text{g/L}$  for microwave-assisted with SPE, respectively and the relative standard deviation less than 6%. The antiretroviral drugs concentration range obtained in vegetable samples is nd-1.48 for abacavir, nd – 27.9  $\mu\text{g/kg}$  for nevirapine, and nd – 13.14  $\mu\text{g/kg}$  for efavirenz. The microwave-assisted extraction method with SPE cleanup resulted in low concentration compared to microwave-assisted extraction without cleanup which could be due to its high limits of detection and quantification making it to be less sensitive. However, the concentration difference was not significant. Root vegetable (beetroot) exhibited high concentrations of antiretroviral drugs, while nevirapine was found to have high concentrations and as a dominant compound.

#### 4.1. Introduction

Antiretroviral drugs (ARVDs) are pharmaceutical compounds employed to treat human immunodeficiency virus. Like other pharmaceuticals, ARVDs are incompletely digested in the digestive system resulting in their excretion in pure or metabolized form through the feces and urine to the sewer system and thus reaching wastewater treatment plants (WWTPs) (Ncube et al., 2018). In WWTPs, ARVDs are partially removed and frequently released into the environment with the effluent (Ying et al., 2009). Even though ARVDs are detected at low concentrations in the environment, they are regarded as ‘pseudo-persistent’ as a consequence of their continuous discharge into the environment (Daouk et al., 2015). Due to the scarcity of fresh water, wastewater effluent is commonly used for irrigation in agricultural fields, where

ARVDs may be absorbed by crops and unintentionally consumed by humans, leading to drug resistance upon prolonged consumption. Moreover, using sewage sludge in agricultural lands as manure introduces ARVDs in agricultural fields (Azzouz and Ballesteros, 2012). Studies conducted in South Africa have confirmed that ARVDs are present in wastewater effluent (Mtolo et al., 2019, Ngumba et al., 2020).

Several studies that were previously conducted confirmed that irrigating with reclaimed wastewater introduces pharmaceuticals to receiving soils and the bulk plant parts (Christou et al., 2017, Kibuye et al., 2019, Tadić et al., 2021). Though not much work has been reported on the absorption of ARVDs by plants, a previous study showed that hyacinth plants in South African water could absorb the ARVDs (Mlunguza et al., 2020). A maximum concentration of 29.6 µg/kg and 17.2 µg/kg was observed in the roots of the hyacinth plant from Gauteng Province and KwaZulu-Natal Province, respectively. A study conducted in the United Kingdom on the uptake of ARVDs by lettuce plants from contaminated water displayed that they can accumulate in the plant roots and be translocated to the bulk of the plant. These results showed that root plants potentially absorb ARVDs from contaminated water (Akenga et al., 2021).

Various analytical techniques are used to extract pharmaceuticals in solid matrices. The commonly used methods are well-known traditional methods, which require long extraction times and large solvent volumes resulting in a time-consuming and environmentally unfriendly process. Due to that, they not only serve as an extraction method for phytoconstituents and as a reference to contrast new extraction methods. These drawbacks were overcome by introducing microwave-assisted extraction (MAE). The MAE utilizes microwave radiation to introduce heat in the extraction solvent, therefore improving the diffusion of the extracting solvent into the sample while quickening the partitioning of the analyte from the solid or liquid sample to the solvent. This resulted in it being widely used to quickly remove target compounds and thermally unstable substances. It also requires a small solvent volume and permits simultaneous analysis of multi-samples (Kaufmann and Christen, 2002, Moret et al., 2019). The MAE is generally followed by the cleanup method. SPE is a widely used analytical technique for sample enrichment, separation, and purification. SPE is based on the selective process of the sample analytes adsorption and desorption by the solid phase sorbent. The advantages of SPE include the usage of a small solvent, enhanced reproducibility and selectivity, elimination of emulsions, easier use and possible mechanization, and high recoveries (Ntombela and Mahlambi, 2019). Liquid chromatography photodiode array (LC-

PDA) is a widely used method for the detection and quantification of many compounds soluble in the aqueous phase. In addition, it is accurate, fast, and efficient (Mtolo et al., 2019). This study, therefore, aimed to optimize and apply an MAE method for ARVDs removal in vegetables that are based on the root (potatoes, onions, and beetroot), leaf (lettuce, and spinach), and fruit (green paper, cucumber, and eggplant). These vegetables were selected to represent different edible organs (root, leaf, and fruit) as they are commonly consumed in Africa. The SPE was then used to pre-concentrate and clean up the MAE extracts. The quantification and detection were done by liquid chromatography linked with the photodiode detector (LC-PDA) as it is most suitable due to the low volatility of ARVDs.

## **4.2. Experimental**

### **4.2.1. Standards and chemicals**

HPLC-grade hexane was purchased from Merck (Darmstadt, Germany). Acetone and methanol with purity  $\geq 99.5\%$  and  $\geq 99.7\%$  HPLC grade acetonitrile and sodium chloride was purchased from Sigma-Aldrich (Steinheim, Germany). The ARVDs salts with high purity above 95% (efavirenz, nevirapine, and abacavir) were purchased from J & H Chemical Co. LTD (Hangzhou Zhejiang, China).

### **4.2.2. Sample collection and pretreatment**

Vegetable samples including potato, beetroot, onion, lettuce, green pepper, spinach, cucumber, and eggplant, were purchased from Scottsville supermarket Pietermaritzburg (KwaZulu-Natal, South Africa). The vegetables were washed with distilled water, chopped, and blended using a blender. The composite sample was then stored in a less than 4 °C refrigerator for further analysis.

### **4.2.3. Instrumentation**

The analysis was performed using a Shimadzu LC system (Tokyo, Japan), with Shim-Pack GIST C18-HP the C18 column (3.5  $\mu\text{m}$  4.6 mm $\times$ 150 mm ID) from Shimadzu (Tokyo, Japan) kept at 30 °C. The mobile phase solvent system was acetonitrile: water and 0.1 % formic acid in water. The flow rate was 0.4 mL/min. The LC gradient program was 0–5 minutes (50–50 %, acetonitrile: water) and 6 – 12 minutes (70–30 %, acetonitrile: water). The detector used was LC 2030/2040 photo-diode array from Shimadzu (Tokyo, Japan). The detection wavelength was set at the optimum wavelengths of 225 and 274 nm. A Sunbeam blender purchased from



Clicks (KwaZulu-Natal, South Africa) was used to blend vegetables. A rotator16 multi-wave 500 microwave model purchased from Anton Paar GmbH (Johannesburg, South Africa) was used to extract compounds from the solid matrix. The IKA® Buchi Rotavapor R114 bought from Labotec (Flawil, Switzerland) was used to reduce the sample extract. The extract cleanup was performed by an SPE vacuum manifold purchased from Sigma Aldrich (Steinheim, Germany). The SPE sorbent used was Oasis HLB (60 mg, 3 mL) purchased from Biotage (Uppsala, Sweden). The 0.2 µm pore filters were purchased from Pall (Puerto Rico, United States).

#### **4.2.4. Microwave-assisted extraction procedure**

A blended sample (5 g) was transferred into a microwave vessel followed by adding 30 mL of acetone: hexane (1:1 v/v) and mixed. The vessel containing the mixture was sealed, and the microwave system performed the extraction. The microwave was set to the following conditions: extraction time was 10 minutes, the temperature rose from 0-150 °C at a pressure rate of 0.5 bar/s and cooled down to 55 °C, power was 507 W, and pressure was 18 bar. The obtained extract was evaporated to dryness using a Rotavapor. The extracted analytes were then redissolved with acetonitrile and analysed with LC-PDA. This method was adopted from Mlunguza et al. (2020) and further optimised. The factors affecting the target analyte's recovery in MAE were evaluated, including extraction solvent, sample mass, radiation time, and spike concentration.

#### **4.2.5. SPE Cleanup method**

The other batch of extract from MAE was subjected to SPE for cleanup and pre-concentration to assess its effect. The extract of 1 mL from microwave was diluted to 50 mL with distilled water, passed through the SPE cartridge conditioned with 3 mL of acetonitrile, and equilibrated with 2 mL of 10 % methanol-water. The impurities were then washed with 2 mL of distilled water, and the cartridge was dried under vacuum for 5 min to remove traces of water. The adsorbed analytes were eluted with 2 mL of acetonitrile. The extract was reduced to 1 mL, filtered with a 0.2 µm pore filter, and analysed LC-PDA. The SPE procedure was adopted Mtollo and coworkers (2019) and further adjusted. The conditioning solvent was optimized to improve the recoveries of the additional compounds.

#### 4.2.6. Analytical method validation

The method was validated by linearity, the limit of detection (LOD), the limit of quantification (LOQ), and the method's precision and accuracy. A stock solution was prepared by dissolving 10 mg of each target ARVDs salt in 100 mL of acetonitrile to make a final concentration of 100 mg/L. A volume of 10-50  $\mu$ L was taken from the stock solution into 5 mL volumetric flasks and topped up with acetonitrile to prepare a series of concentrations ranging from 200 to 1000  $\mu$ g/L flask. These solutions were then analysed with LC-PDA to calibrate the instrument. The calibration curves were plotted using the peak areas versus concentration for each ARVD to assess the linearity ( $R^2$ ). The extraction methods' LOD and LOQ, described as the lowest compound concentration that can be precisely and accurately detected and quantified, were investigated using the signal-to-noise (S/N) ratio, computed as  $S/N = 3$  for LOD and  $S/N = 10$  for LOQ. The precision and accuracy of the methods were presented as percentage relative standard deviation (%RSD) and percentage recovery. The percentage recovery and %RSD were tested by performing the extraction of ARVDs from the 1 mg/kg spiked and unspiked vegetable samples. The obtained peak areas were used with the corresponding gradients to calculate the recoveries, and the triplicate analysis was performed to estimate the RSD%.

#### 4.3. Result and discussion

##### 4.3.1. Optimization of Liquid Chromatograph-Photodiode array (LC-PDA)

The LC-PDA was optimized (mobile phase composition and detector wavelength) to obtain the instrument conditions that permit good separation of the target analytes (abacavir, nevirapine, and efavirenz) at reasonable retention times. The optimization was done by analyzing 1 mg/L of the prepared stock solution using the adopted method (Mtolo et al., 2019). Originally, isocratic elution was used, which consisted of the mobile composition of phase 70 % acetonitrile: 30 % water in formic acid (0.1 %) for 10 minutes, wavelength detection was 254 nm, the flow rate was 0.4 mL/min, and the column temperature was set at 30 °C. Under these conditions, the ARVDs were detected, but the separation of abacavir and nevirapine was incomplete, with efavirenz eluting at 10 minutes. The mobile phase composition was then changed to a gradient elution of 50 % acetonitrile: 50 % water in formic acid (0.1 %) from 0 minutes to 5 minutes and 70 % acetonitrile: 30 % water in formic acid (0.1 %) from 6 minutes to 12 minutes, and all other parameters were kept constant. The results showed improvement, and abacavir was eluted at 4.1 minutes, nevirapine at 5.1 minutes, and efavirenz eluted at 5.9 minutes (Figure S4.1). However, the peak intensities were low, indicating that the employed

wavelength was not optimum for abacavir and efavirenz. With this regard, the investigation of wavelength was done to determine their ideal absorption wavelength, where 225 nm and 274 nm were investigated. It was then found that nevirapine absorbed much better at 274 nm, whereas abacavir and efavirenz absorbed better at 225 nm (Figure S4.2 and S4.3). As a result, the optimum conditions for the LC PDA instrument which were used for further analysis were as follow: Flow rate 0.4 ml/min, wavelength 225 nm and 274 nm, column temperature 30°C, and mobile phase composition in a gradient mode of 50 % acetonitrile: 50 % water in formic acid (0.1 %) from 0-5 min and 70 % acetonitrile: 30 % water in formic acid (0.1 %) from 6-12 min.

### **4.3.2. Optimization of MAE**

#### **4.3.2.1. Effect of extraction solvent on the recoveries of MAE**

To allow effective microwave extraction, the extraction solvent must absorb microwave energy and have a higher dielectric constant as the microwaves penetrate the molecules proportionally to the dielectric constant (Costa, 2016, Singh et al., 2014). Therefore, the fulfillment of these requirements was investigated using hexane, methanol, acetone: hexane (1:1 v/v), and acetone: methanol (1:1 v/v). Low recoveries ranging between 20 to 50% in a root, 40 to 46% in a leaf, and 35 to 44% in a fruit vegetable were obtained when hexane was used as an extracting solvent (Figure 4.1). This could be because hexane has a low dielectric constant; therefore, it poorly absorbs microwave energy (Ibrahim and Zaini, 2017). Hexane was then mixed with acetone in a ratio of 1:1 v/v. The mixture of acetone: hexane 1:1 (v/v) permitted high recoveries of abacavir, nevirapine, and efavirenz ranging from 85 to 98 % in root vegetables, 92 to 103 % in leaf vegetables, and 96 to 103 % in fruit vegetables. This could be due to that acetone is a polar solvent with a high dielectric constant; hence it has the potential to absorb microwave energy. Also, this mixture resulted in a mixture of a polar and a non-polar solvent, thus permitting the extraction of all elements as they have different polarities. These observations agree with those of Ibrahim et al. (2017), where the extraction efficiency of the hexane in the microwave-assisted extraction was improved by the addition of a polar solvent like ethanol. Methanol and the mixture of methanol: acetone (1:1 v/v) gave low recoveries, which could be due to the fierce heat that could arise in the microwave. When a microwave energy solvent absorber is used, a rapid rise in temperature for a short period is anticipated. This may result in the target analytes decomposition as the extraction process continues (Ibrahim and Zaini, 2017). The t-test analysis was conducted to assess the statistical difference in the mean recoveries obtained.

The result (Table S1) showed that the average recoveries for hexane: acetone are statistically different from the average recoveries for methanol: acetone and hexane with a p-value less than 0.05. The obtained p values are  $p > 0.017$  and  $p > 0.010$  for hexane: acetone versus methanol: acetone and hexane: acetone versus hexane, respectively. In contrast, the recoveries for methanol are not statistically different from the average recoveries for methanol: acetone, hexane, and hexane: acetone. The obtained p-values are  $p > 0.44$  for methanol versus methanol:acetone,  $p > 0.20$  for methanol versus hexane, and  $p > 0.14$  for methanol versus hexane :acetone. On the other hand, it was revealed that the average recoveries for methanol: acetone are not statistically different from hexane as the  $p\text{-value} > 0.45$  was greater than 0.05. Even though, according to the t-test, average recoveries of methanol were not statically different from hexane: acetone but hexane: acetone had high recovery values and therefore was used for further analysis.

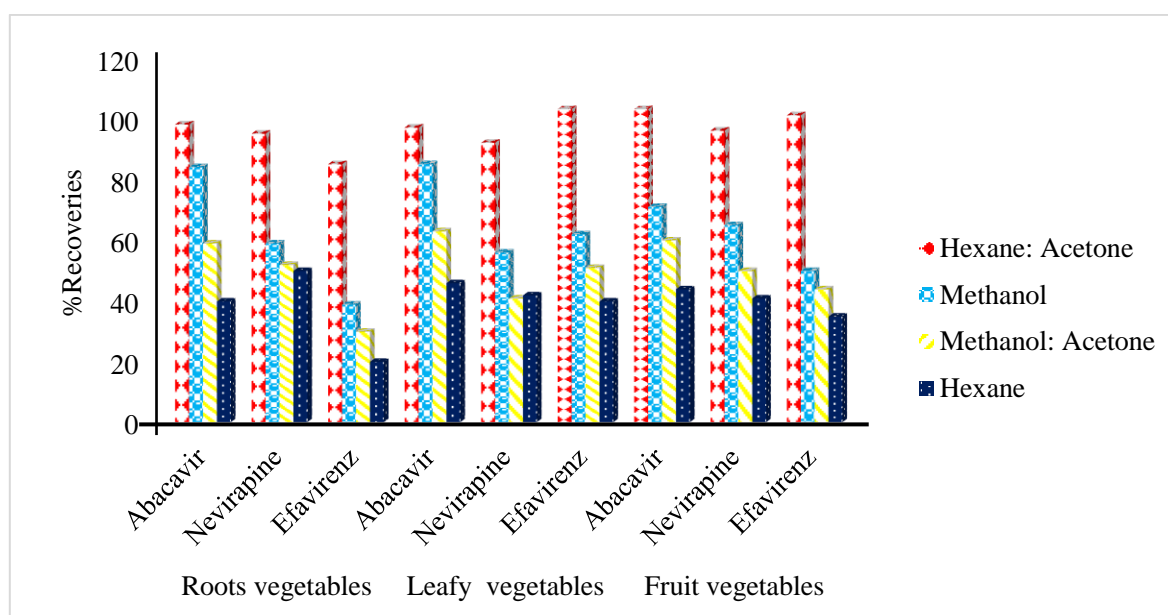


Figure 4.1: Effect of extraction solvent on the recoveries of antiretroviral drugs (n=3)

#### 4.3.2.2. Effect of spike concentration on the recoveries of MAE

This effect was evaluated by analysing vegetables spiked with ARVDs at 300, 500, and 1000  $\mu\text{g/kg}$  concentrations. The obtained results indicated that spike concentration has no much effect on the performance of the extraction method as the recoveries obtained were comparable (Figure 4.2). These results indicated acceptable accuracy of the developed method and assurance that it can be efficiently applied in real samples as it is independent of the

concentration of ARVDs present in the sample. Also, the statistical results approved that the average recoveries for all spike concentrations are not statistically different from each concentration as all the obtained p-values are greater than 0.05. The p-value is 0.18 for 1000  $\mu\text{g/kg}$  versus 500  $\mu\text{g/kg}$ ,  $p > 0.95$  for 1000  $\mu\text{g/kg}$  versus 300  $\mu\text{g/kg}$ , and 0.46 for 500  $\mu\text{g/kg}$  versus 300  $\mu\text{g/kg}$  (Table S2). However, 1000  $\mu\text{g/kg}$  spike concentration was used for further optimization.

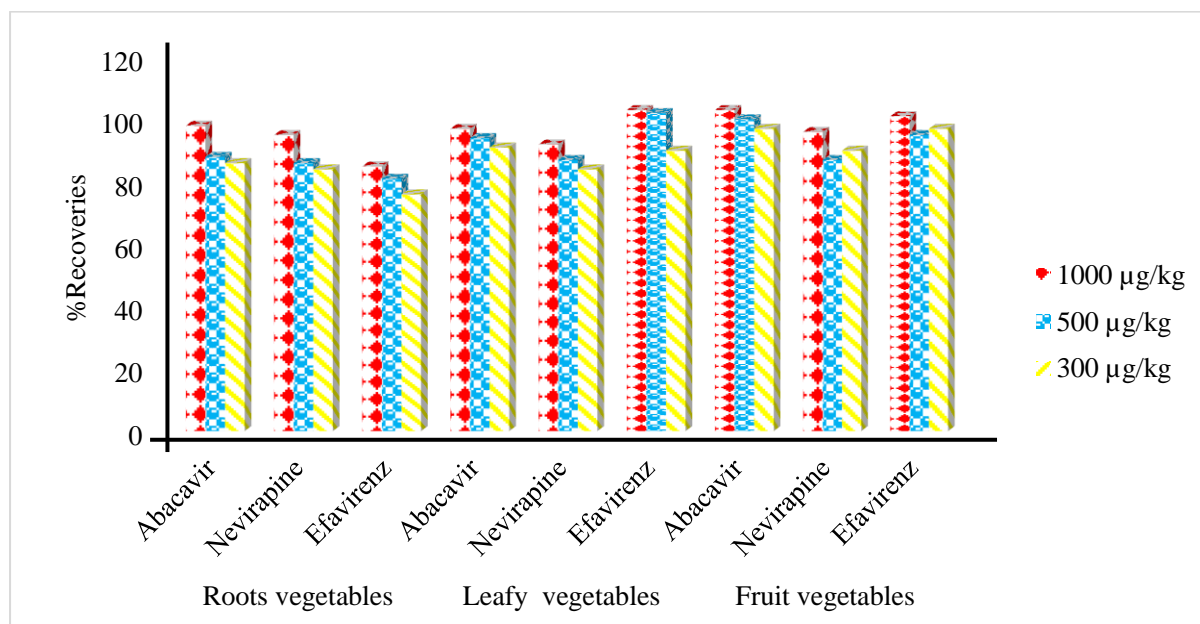


Figure 4.2: Effect of spike concentration on the recoveries of antiretroviral drugs (n=3)

#### 4.3.2.3. Effect of extraction time on the recoveries of antiretroviral drugs in microwave-assisted extraction

Time of irradiation is a significant factor in the MAE extraction process as the amount of extracted analytes can be improved when sufficient irradiation time has been applied. However, prolonged irradiation with microwave energy absorbing solvent may result in a risk associated with the degradation of thermolabile (Camel, 2001, Tatke and Jaiswal, 2011). The influence of irradiation time was examined using 5, 7, and 10 minutes. It was found that 10 minutes gave high recoveries ranging from 85 to 98 % in root vegetables, from 92 to 103 % in leaf vegetables, and from 96 to 103 % in fruit vegetables (Figure 4.3). The 5 and 7 minutes resulted in low recoveries, which could be due to insufficient time given for the interaction between the ARVDs and the extraction solvent. Thus, the lower amount of the ARVDs was transferred to the solvent. The t-test results (Table S2) displayed that the average recoveries for 5 minutes are

statistically different from 7 and 10 minutes as the p-values,  $p > 0.03$  for 5 minutes versus 7 minutes, and  $p > 0.021$  for 5 minutes versus 10 minutes obtained, are less than 0.05. Even though the average recoveries for 10 minutes versus 7 minutes are not statically different as the obtained p-value is 0.07 but 10 minutes, average recovery results are higher than 7 minutes. Therefore 10 minutes was taken as an optimum irradiation time and used in further analysis. In a study conducted by Mlunguza and co-workers on the extraction of ARVDs using MAE, the recoveries showed an increase with an increase in irradiation time. Their optimum radiation time was found to be 20 minutes for the extraction of efavirenz, as it gave the recovery range of 78 % to 87 % (Mlunguza et al., 2020).

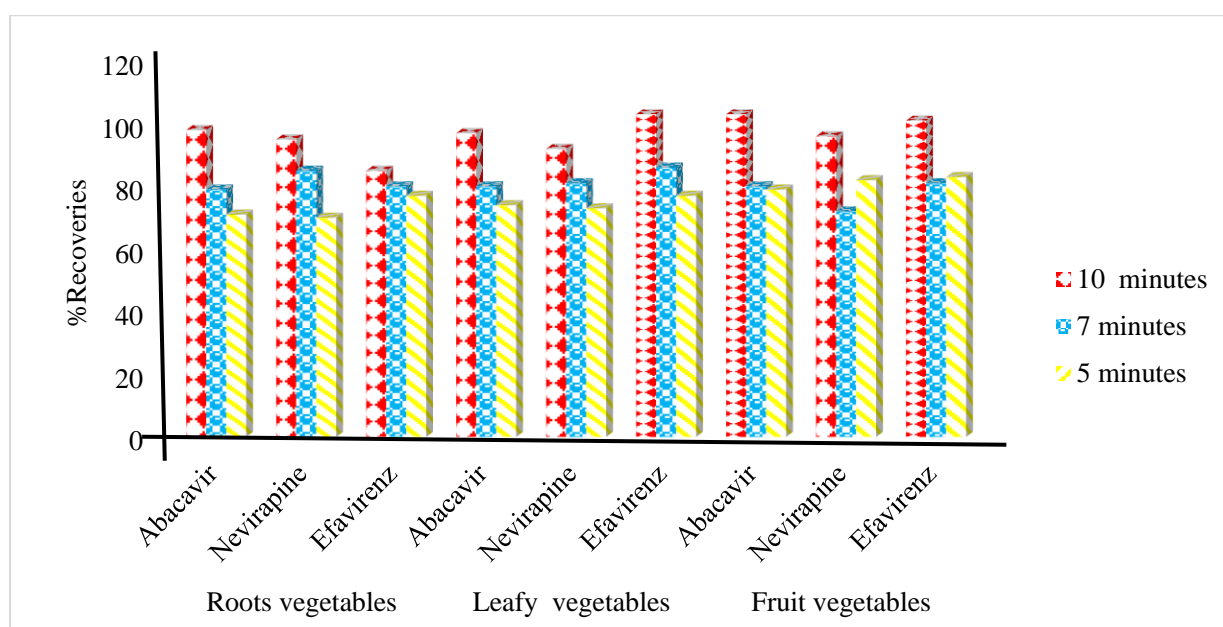


Figure 4.3: Effect of extraction time on the recoveries of antiretroviral drugs (n=3)

#### 4.3.2.4. Effect of solvent volume on the recoveries of microwave-assisted extraction

The hexane: acetone mixture volume was investigated using 10 mL, 20 mL, and 30 mL to discover its effect on the ARVDs recoveries from vegetables. The obtained results showed that increasing the solvent volume increased the recoveries of the ARVDs. Hence the solvent volume of 30 mL resulted in high recoveries ranging from 85 to 98 % in root vegetables, 92 to 103 % in leaf vegetables, and 96 to 103 % in fruit vegetables (Figure 4.4). This indicates that 30 mL was sufficient to dissolve a large amount of the analytes and eventually increased the analyte recovered in the solvent. Also, it signals that it was not too much to affect the microwaves' stirring efficiency, thus resulting in effective interaction between the solvent and

the sample (Madej, 2009). The low recoveries obtained when 10 mL solvent volume was used could be due to solvent saturation, meaning the equal amount of analyte present in the solid and liquid phase was reached. Therefore, the analytes transfer process reached a maximum; hence some analytes remained in the sample matrix (Li et al., 2017). The t-test result (Table S3) also showed that the average recoveries for 30 mL are statistically different from the average recoveries for 10 mL, with the p-value ( $p > 0.028$ ) less than 0.05. The 20 mL versus 10 mL solvent volume resulted in p values ( $p > 0.16$ ) greater than 0.05, meaning their average recoveries are not statistically different. The 30 mL gave higher recoveries of ARVDs than 20 mL even though they are not statistically different with the p-value ( $p > 8.085$ ); therefore, 30 mL was taken as optimum solvent volume.

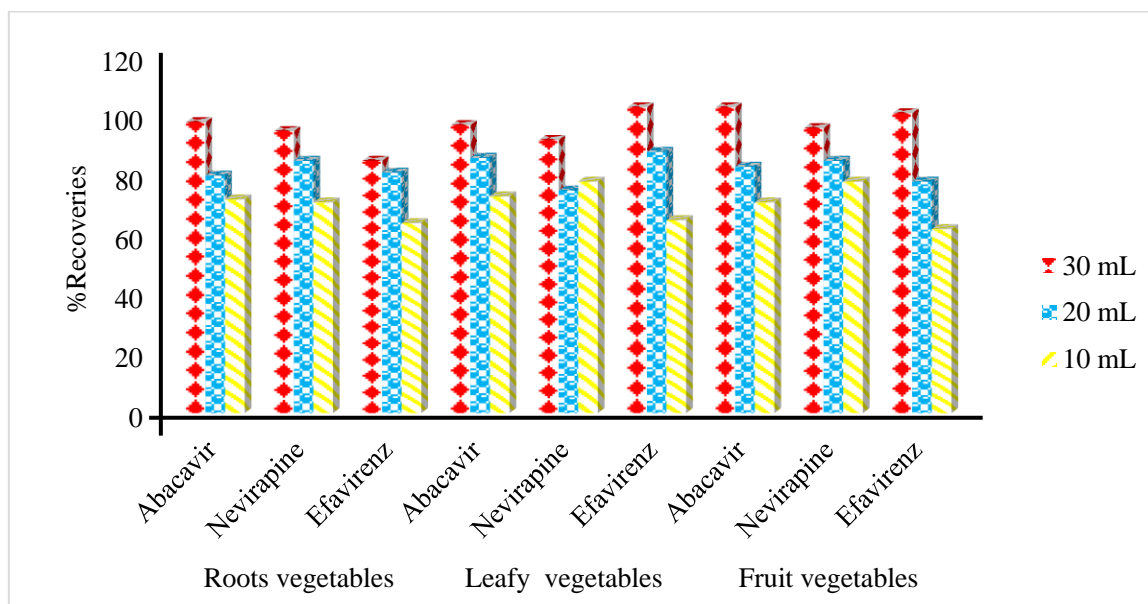


Figure 4.4: Effect of solvent volume on the recoveries of antiretroviral drugs (n=3)

### 4.3.3. Optimization of SPE

#### 4.3.3.1. Effect of conditioning solvent on the recoveries of SPE

The conditioning solvent was investigated using acetonitrile, acetonitrile: acetone (v/v 1:1), acetonitrile: methanol (v/v 1:1), and methanol: acetone (v/v 1:1). High recoveries ranged from 80 to 111% were obtained with all the selected solvents, which could be due to their related polarities (Figure 4.5). However, acetonitrile results were slightly higher; hence it was taken as an optimal solvent. This could be possibly due to that acetonitrile has a high elution strength, chemical stability, and low viscosity. The slightly lower recoveries obtained when a conditioning solvent, methanol, or acetone were involved could result from methanol's high

viscosity. The high viscous solvents may result in a slow penetration of the sorbent; therefore, high chances that these solvent mixtures were not completely interacting with all the functional groups present in a sorbent to activate the active sites for the analyte to bind in (Tankiewicz, 2019). While for acetone, it could be due to that it quickly evaporates, which could also affect the activation of the sorbent's functional groups. The recoveries obtained ranged from 98 to 104 % for acetonitrile, from 88 to 111 % for acetonitrile: methanol (v/v 1:1), from 80 to 87 % for acetonitrile: acetone (v/v 1:1) and from 83 to 96% for acetone: methanol (v/v 1:1) mixture. The t-test results displayed that the average recoveries of acetone: methanol are not statistically different from those of acetone: acetonitrile, acetonitrile: methanol, and acetonitrile as the p-values obtained are greater than 0.05. The obtained p-values are  $p > 0.18$  for acetone: methanol versus acetone: acetonitrile,  $p > 0.52$  for acetone: methanol versus acetonitrile: methanol, and  $p > 0.08$  for acetone: methanol versus acetonitrile (Table S4). The t-test results also showed that the average recoveries of acetonitrile versus acetonitrile: acetone are statistically different as the p-value  $p > 0.0026$  is less than 0.05. Acetonitrile: methanol versus acetonitrile: acetone resulted in a p-value of 0.21 above 0.05, which means they are not statistically different. Even though statistically, the average recoveries of acetonitrile are not statically different from acetonitrile: methanol and acetone: methanol, it gave a higher result.

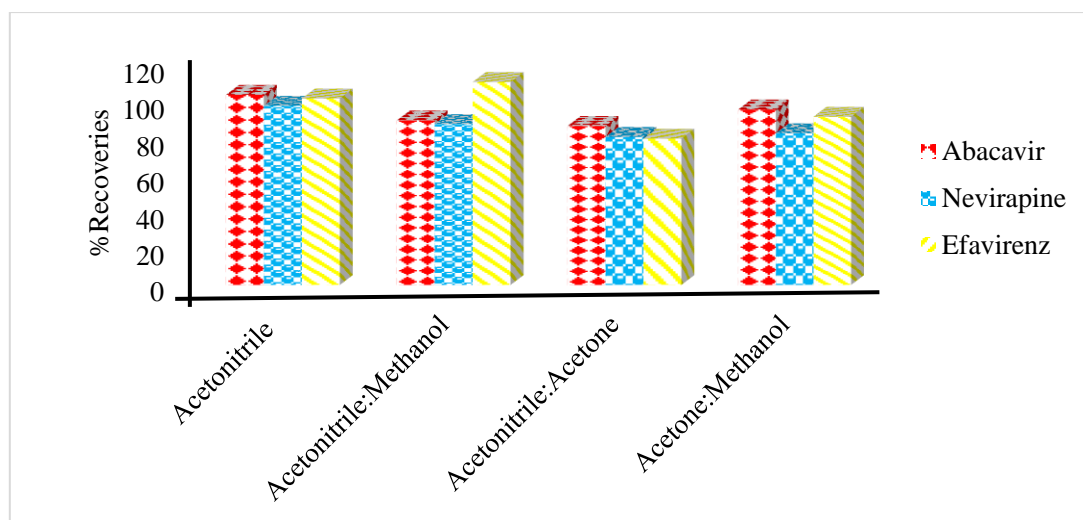


Figure 4.4: Effect of conditioning solvent on the recoveries of antiretroviral drugs (n=3)

#### 4.3.3.2. Effect of spike concentration on the recoveries of SPE

The effect of concentration was investigated by analysing distilled water spiked with ARVDs at 300, 500, and 1000  $\mu\text{g/L}$  concentrations. The findings showed that spike concentration has



no significant effect on the performance of the SPE method as similar recoveries were obtained ranging from 98-104 (Figure 4.6). These results showed that the developed method can be confidently applied to real samples as it is highly accurate and independent of the ARVDs concentration present in the sample. The statistical results confirmed that the average recoveries for all investigated spike concentrations are not statistically different from each concentration as all the obtained p-values are greater than 0.05. The p-value is 2.77 for 1000  $\mu\text{g/kg}$  versus 500  $\mu\text{g/kg}$ ,  $p>3.18$  for 1000  $\mu\text{g/kg}$  versus 300  $\mu\text{g/kg}$ , and 3.18 for 500  $\mu\text{g/kg}$  versus 300  $\mu\text{g/kg}$  (Table S5). However, 1000  $\mu\text{g/kg}$  spike concentration was used in further analysis. As all the recoveries were acceptable, no further optimization was done for the SPE method. The optimum SPE conditions were then applied to the clean-up step of the MAE extract.

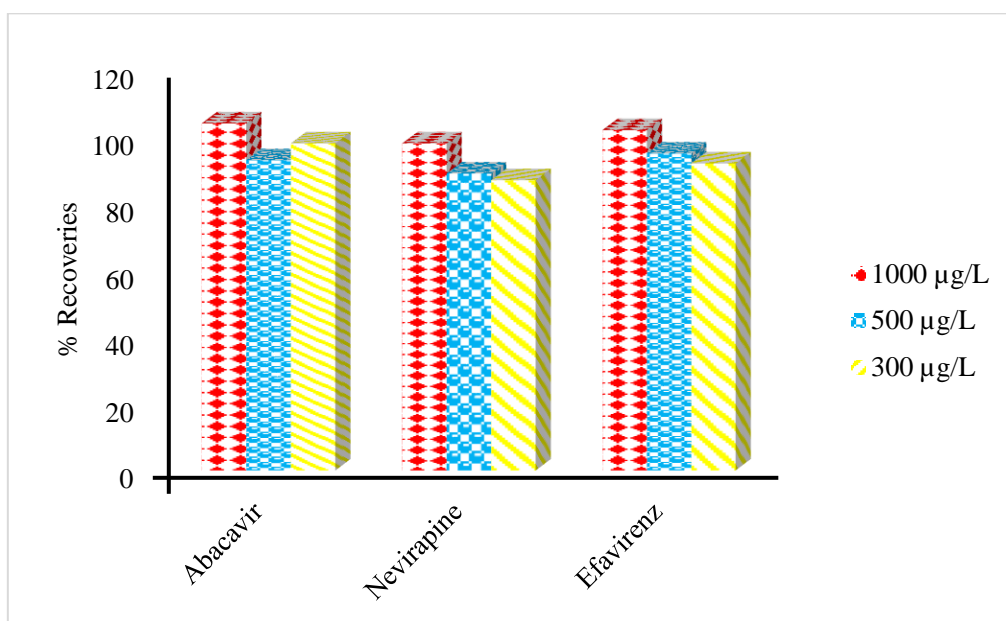


Figure 4.5: Effect of spike concentration on the recoveries of SPE (n=3)

#### 4.3.4. Method validation

The optimized methods were evaluated using the analytical parameters, including linearity, the limit of detection (LOD), limit of quantification (LOQ), recoveries, and repeatability. The calibration curves plotted (Figure S4.4) gave  $R^2$  values close to 1, which indicates the instrument's good precision (Table 4.1). The recoveries for all compounds were above 80% in the root, leaf, and fruit vegetables displaying high accuracy of the analytical methods. The LOD and LOQ ranged from 0.020 to 0.032  $\mu\text{g/kg}$  and from 0.068 to 0.109  $\mu\text{g/kg}$  for MAE and for

MAE-SPE they ranged from 0.019 to 0.066  $\mu\text{g/kg}$  and from 0.065 to 0.22  $\mu\text{g/kg}$  respectively. These results revealed good sensitivity of the method, indicating that it is adequate for trace analysis of the studied vegetable samples. In the comparison of MAE and MAE-SPE, the results suggested that MAE-SPE and MAE are both sensitive and comparable. Also the statistical result showed that they are not statistically different with the p-values ( $p>0.61$ ) (Table S6). The RSD % calculated were all found to be below 6%, signaling good precision of the methods. The recoveries obtained ranged from 85 to 103% for MAE, 87 to 104% for SPE, and 82 to 98 % for MAE-SPE indicating that MAE is slightly more accurate than MAE-SPE.

Table 4.1: Optimal performance of analytical techniques in vegetables (n=3)

Target compounds	Linearity	LOD (µg/kg)		LOQ (µg/kg)		MAE Recovery (%) ± RSD			MAE-SPE Recovery (%) ± RSD		
		MAE	MAE-SPE	MAE	MAE-SPE	Root	Leaf	Fruit	Root	Leaf	Fruit
Abacavir	0.9883	0.026	0.066	0.088	0.22	98 ± 2.7	97 ± 2.3	103 ± 1.5	92 ± 0.1	95 ± 1.2	98 ± 0.7
Nevirapine	0.9768	0.032	0.021	0.11	0.072	95 ± 2.0	92 ± 0.3	96 ± 2.4	88 ± 1.3	85 ± 1.0	89 ± 2.0
Efavirenz	0.9947	0.020	0.019	0.068	0.065	85 ± 2.1	103 ± 2.3	103 ± 0.7	82 ± 1.0	97 ± 0.8	98 ± 1.6

#### 4.3.5. Application of MAE and MAE-SPE

The optimized MAE and MAE-SPE methods were applied to root (potatoes, onions, and beetroot), leaf (lettuce, and spinach), and fruit (green paper, cucumber, and eggplant) vegetables. The SPE step was applied in the MAE extract to remove the background impurities and concentrate the target analytes in the extract. However, it was observed that it negatively impacted the concentrations of the detected analytes (Table 4.2) though the MAE results were statistically not different from MAE-SPE with  $p > 0.60$  (Table S6). On the other hand, some analytes were detected in MAE, whereas in MAE-SPE they were not detected. However, it was observed that the background noise was reduced in the MAE-SPE chromatograms, which indicates the removal of impurities during the SPE cleanup step (Figure S4.5). The results showed higher peak areas for MAE than MAE-SPE, possibly due to dilution. This negative impact could also be due to the multi-step extraction resulting from extraction methods combination, which might lead to loss of analytes; moreover, it lengthens the extraction process. Mnyandu and Mahlambi (2022) reported a similar finding on the extraction of herbicides using ultrasonic followed by SPE cleanup, where the concentrations were reduced by the cleanup step.

The obtained concentration ranges were nd – 27.9  $\mu\text{g/kg}$  and nd – 19.20  $\mu\text{g/kg}$  in MAE and MAE-SPE, respectively. The highest concentrations of abacavir, nevirapine, and efavirenz were  $1.48 \pm 0.5$ ,  $27.9 \pm 1.2$ , and  $13.0 \pm 1.4$   $\mu\text{g/kg}$ , respectively, which were detected in the beetroot root vegetable (Table 2). In a case study conducted by Akenga et al. (2021) on the absorption of efavirenz (3463  $\mu\text{g/kg}$ ) and nevirapine (2625  $\mu\text{g/kg}$ ) by lettuce plant, it was observed that both of these ARVDs highly accumulate in the plant roots. Also, Mlunguza et al. (2020) reported an efavirenz concentration of 29.9  $\mu\text{g/kg}$  in hyacinth plant roots which was higher than the other plant parts. The literature concentrations of efavirenz are above those obtained in this work.

Nevirapine was detected in all samples except in green pepper and lettuce samples. It has been reported that the concentration of compounds present in the plant is directly proportional to the concentration in the growing medium; hence this may indicate that there was a higher concentration of nevirapine in the medium where most of these vegetables were grown. Therefore, due to nevirapine's high photostability and poor biodegradability, it can accumulate in the growing medium. Also, due to its medium hydrophobicity ( $\log k_{ow}$  2-2.5), it can be absorbed from the growing medium or irrigation water and be highly transported to different parts of the vegetables (Vanková, 2010, K'oreje et al., 2016).

The detection of ARVDs in vegetables indicates a possible usage of wastewater effluent for their irrigation during the growing season and the sludge as fertilizer to prepare the soil for plantation, which might have been contaminated with ARVDs (Al-Farsi et al., 2017). The presence of nevirapine in WWTPs could be due to the high daily intake of ARVDs by HIV-infected people on HIV therapy treatment. It is also used as a medication to prevent HIV from a pregnant parent to an unborn baby. Hence, upon its excretion, its load is expected to reach the WWTPs where it is not entirely removed (Schoeman et al., 2015). A study conducted by (K'oreje et al., 2016) showed no removal of nevirapine in treated water, indicating its persistence within the treatment plant.

The lower concentrations obtained for abacavir could result from its high water solubility (77000 mg/L), making it to be poorly adsorbed and thus can leach down the soil pores and be unavailable for plant uptake. However, compound distribution within the plant tissues depends on the type of the plant, which could be the reason for different concentrations of the ARVDs obtained in different vegetables (Niu et al., 2022). No ARVDs were detected in potato, lettuce, and green pepper samples. This could be due to that the concentration levels are affected by different factors, including the molecular properties of the compounds, the concentration at which they are present in the irrigation water, as well as the properties of the plantation soil (Mordechay et al., 2021). Also, it may be due to that there was no source of pollution where they were planted, or they are present below the method's detection.

Table 4.2: Average concentrations of target ARVDs obtained in the selected vegetables (n=3)

List of vegetables	Average concentrations of ARVDs (µg/kg), RSD %					
	Abacavir		Nevirapine		Efavirenz	
	MAE	MAE-SPE	MAE	MAE-SPE	MAE	MAE-SPE
Potato	nq	nd	nq	nd	nq	nd
Beetroot	$1.48 \pm 0.5$	$0.991 \times 10^{-1} \pm 0.01$	$27.90 \pm 1.2$	$19.20 \pm 0.1$	$13.00 \pm 1.4$	$4.34 \pm 0.7$
Onion	$6.94 \times 10^{-2} \pm 1.0$	nq	$4.24 \pm 0.6$	$2.40 \times 10^{-1} \pm 0.01$	$1.77 \pm 0.9$	nq
Lettuce	nd	nd	nd	nd	nd	nd
Spinach	$9.41 \times 10^{-1} \pm 0.02$	nq	$1.11 \times 10^{-1} \pm 0.07$	nd	$1.81 \times 10^{-1} \pm 0.07$	nd
Green pepper	nd	nd	nd	nd	nd	nd
Cucumber	$4.00 \times 10^{-140} \pm 0.2$	$2.40 \times 10^{-1} \pm 0.2$	$9.37 \times 10^{-1} \pm 0.6$	$6.30 \times 10^{-1} \pm 0.01$	$1.83 \times 10^{-1} \pm 0.6$	$9.40 \times 10^{-2} \pm 0.01$
Eggplant	$1.00 \pm 0.1$	$3.53 \times 10^{-1} \pm 0.$	$1.47 \pm 0.7$	$7.71 \times 10^{-1} \pm 2.1$	$4.17 \pm 0.1$	$11.90 \pm 1.2$

Nd –not detected, Nq-not quantified

#### 4.4. Conclusion

The optimal conditions for the optimized analytical methods resulted in high recoveries with low LOD and LOQ values indicating high accuracy and sensitivity. The MAE without SPE cleanup showed better results and is recommended for a daily routine, and it reduces the extraction time required. High concentrations of ARVDs up to  $27.9 \pm 1.2 \mu\text{g/kg}$  were achieved. Root vegetable (beetroot) accumulated higher concentrations of selected ARVDs. Nevirapine was present at high concentration and was a dominant compound. The presence of ARVDs in vegetables indicates the significance of their unceasing monitoring for human and other life forms healthy purposes. Furthermore, the results found in this study will contribute to the insufficient reliable data on the occurrence of ARVDs in vegetables, especially in South African countries where the ARVDs are prevalent.

#### References

- Akenga, P., Gachanja, A., Fitzsimons, M. F., Tappin, A. & Comber, S. 2021. Uptake, accumulation and impact of antiretroviral and antiviral pharmaceutical compounds in lettuce. *Science of The Total Environment*, 766, 144499. doi:<https://doi.org/10.1016/j.scitotenv.2020.144499>
- Al-Farsi, R. S., Ahmed, M., Al-Busaidi, A. & Choudri, B. S. 2017. Translocation of pharmaceuticals and personal care products (PPCPs) into plant tissues: A review. *Emerging Contaminants*, 3, 132-137. doi:<https://doi.org/10.1016/j.emcon.2018.02.001>
- Azzouz, A. & Ballesteros, E. 2012. Combined microwave-assisted extraction and continuous solid-phase extraction prior to gas chromatography–mass spectrometry determination of pharmaceuticals, personal care products and hormones in soils, sediments and sludge. *Science of the Total Environment*, 419, 208-215. doi:<https://doi.org/10.1021/acs.est.9b06206>
- Camel, V. 2001. Recent extraction techniques for solid matrices—supercritical fluid extraction, pressurized fluid extraction and microwave-assisted extraction: their potential and pitfalls. *Analyst*, 126, 1182-1193. doi:<https://doi.org/10.1039/B008243K>
- Christou, A., Karolia, P., Hapeshi, E. & Michael, C. 2017. Long-term wastewater irrigation of vegetables in real agricultural systems: Concentration of pharmaceuticals in soil, uptake and bioaccumulation in tomato fruits and human health risk assessment. *Water Research*, 109, 24-34. doi:<https://doi.org/10.1016/j.watres.2016.11.033>

- Costa, R. 2016. The chemistry of mushrooms: A survey of novel extraction techniques targeted to chromatographic and spectroscopic screening. *Studies in Natural Products Chemistry*, 49, 279-306. doi:<https://doi.org/10.1016/B978-0-444-63601-0.00009-0>
- Daouk, S., Chevre, N., Vernaz, N., Bonnabry, P., Dayer, P., Daali, Y. & Fleury-Souverain, S. 2015. Prioritization methodology for the monitoring of active pharmaceutical ingredients in hospital effluents. *Journal of Environmental Management*, 160, 324-332. doi:<https://doi.org/10.1016/j.jenvman.2015.06.037>
- Ibrahim, N. & Zaini, M. A. A. 2017. Solvent selection in microwave assisted extraction of castor oil. *Chemical Engineering Transactions*, 56, 865-870. doi:<http://doi.org/10.3303/CET1756145>
- K'oreje, K., Vergeynst, L., Ombaka, D., De Wispelaere, P., Okoth, M., Van Langenhove, H. & Demeestere, K. 2016. Occurrence patterns of pharmaceutical residues in wastewater, surface water and groundwater of Nairobi and Kisumu city, Kenya. *Chemosphere*, 149, 238-244. doi:<https://doi.org/10.1016/j.chemosphere.2016.01.095>
- Kaufmann, B. & Christen, P. 2002. Recent extraction techniques for natural products: microwave-assisted extraction and pressurised solvent extraction. *Phytochemical Analysis: An International Journal of Plant Chemical and Biochemical Techniques*, 13, 105-113. doi:<https://doi.org/10.1002/pca.631>
- Kibuye, F. A., Gall, H. E., Elkin, K. R., Ayers, B., Veith, T. L., Miller, M., Jacob, S., Hayden, K. R., Watson, J. E. & Elliott, H. A. 2019. Fate of pharmaceuticals in a spray-irrigation system: From wastewater to groundwater. *Science of the Total Environment*, 654, 197-208. doi:<https://doi.org/10.1016/j.scitotenv.2018.10.442>
- Li, Y., Li, S., Lin, S.-J., Zhang, J.-J., Zhao, C.-N. & Li, H.-B. 2017. Microwave-assisted extraction of natural antioxidants from the exotic *Gordonia axillaris* fruit: Optimization and identification of phenolic compounds. *Molecules*, 22, 1481. doi:<https://doi.org/10.3390/molecules22091481>
- Madej, K. 2009. Microwave-assisted and cloud-point extraction in determination of drugs and other bioactive compounds. *TrAC Trends in Analytical Chemistry*, 28, 436-446. doi:<https://doi.org/10.1016/j.trac.2009.02.002>
- Mlunguza, N. Y., Ncube, S., Mahlambi, P. N., Chimuka, L. & Madikizela, L. M. 2020. Determination of selected antiretroviral drugs in wastewater, surface water and aquatic plants using hollow fibre liquid phase microextraction and liquid chromatography-tandem mass spectrometry. *Journal of Hazardous Materials*, 382, 121067. doi:<https://doi.org/10.1016/j.jhazmat.2019.121067>



- Mnyandu, H. & Mahlambi, P. 2022. Determination of triazines residues in fruits and vegetables: Methods comparison of ultrasonic solvent extraction with and without solid phase clean-up. *Separation Science and Technology*, 1-9. doi:<https://doi.org/10.1080/01496395.2022.2026391>
- Mordechay, E. B., Mordehay, V., Tarchitzky, J. & Chefetz, B. 2021. Pharmaceuticals in edible crops irrigated with reclaimed wastewater: Evidence from a large survey in Israel. *Journal of Hazardous Materials*, 416, 126184. doi:<https://doi.org/10.1016/j.jhazmat.2021.126184>
- Moret, S., Conchione, C., Srbinovska, A. & Lucci, P. J. F. 2019. Microwave-based technique for fast and reliable extraction of organic contaminants from food, with a special focus on hydrocarbon contaminants. *Food*, 8, 503. doi:<https://doi.org/10.3390/foods8100503>
- Mtolo, S. P., Mahlambi, P. N. & Madikizela, L. M. 2019. Synthesis and application of a molecularly imprinted polymer in selective solid-phase extraction of efavirenz from water. *Water Science and Technology*, 79, 356-365. doi:<https://doi.org/10.2166/wst.2019.054>
- Ncube, S., Madikizela, L. M., Chimuka, L. & Nindi, M. M. 2018. Environmental fate and ecotoxicological effects of antiretrovirals: A current global status and future perspectives. *Water Research*, 145, 231-247. doi:<https://doi.org/10.1016/j.watres.2018.08.017>
- Ngumba, E., Gachanja, A., Nyirenda, J., Maldonado, J. & Tuhkanen, T. 2020. Occurrence of antibiotics and antiretroviral drugs in source-separated urine, groundwater, surface water and wastewater in the peri-urban area of Chunga in Lusaka, Zambia. *Water SA*, 46, 278-284. doi:<https://doi.org/10.17159/wsa/2020.v46.i2.8243>
- Niu, Y., Wang, L., Wang, Z., Yu, S., Zheng, J. & Shi, Z. 2022. High-frequency monitoring of neonicotinoids dynamics in soil-water systems during hydrological processes. *Environmental Pollution*, 292, 118219. doi:<https://doi.org/10.1016/j.envpol.2021.118219>
- Ntombela, S. & Mahlambi, P. 2019. Method development and application for triazine herbicides analysis in water, soil and sediment samples from KwaZulu-Natal. *Journal of Environmental Science Health, Part B*, 54, 569-579. doi:<https://doi.org/10.1080/03601234.2019.1621113>
- Schoeman, C., Mashiane, M., Dlamini, M. & Okonkwo, O. 2015. Quantification of selected antiretroviral drugs in a wastewater treatment works in South Africa using GC-TOFMS.

- Journal of Chromatography Separation Techniques*, 6, 1-7.  
doi:<https://doi.org/10.4172/2157-7064.1000272>
- Singh, A., Nair, G. R., Liplap, P., Gariepy, Y., Orsat, V. & Raghavan, V. J. A. 2014. Effect of dielectric properties of a solvent-water mixture used in microwave-assisted extraction of antioxidants from potato peels. *Antioxidants*, 3, 99-113. doi:<https://doi.org/10.3390/antiox3010099>
- Tadić, Đ., Hernandez, M. J. B., Cerqueira, F., Matamoros, V., Piña, B. & Bayona, J. M. 2021. Occurrence and human health risk assessment of antibiotics and their metabolites in vegetables grown in field-scale agricultural systems. *Journal of Hazardous Materials*, 401, 123424. doi:<https://doi.org/10.1016/j.jhazmat.2020.123424>
- Tankiewicz, M. 2019. Determination of selected priority pesticides in high water fruits and vegetables by modified QuEChERS and GC-ECD with GC-MS/MS confirmation. *Molecules*, 24, 417. doi:<https://doi.org/10.3390/molecules24030417>
- Tatke, P. & Jaiswal, Y. 2011. An overview of microwave assisted extraction and its applications in herbal drug research. *Research Journal of Medicinal Plants*, 5, 21-31. doi:<http://doi.org/10.3923/rjmp.2011.21.31>
- Vanková, M. 2010. Biodegradability analysis of pharmaceuticals used in developing countries; screening with OxiTop C-110.
- Ying, G.-G., Kookana, R. S. & Kolpin, D. W. 2009. Occurrence and removal of pharmaceutically active compounds in sewage treatment plants with different technologies. *Journal of Environmental Monitoring*, 11, 1498-1505. doi:<https://doi.org/10.1039/b904548a>

## Supplementary information

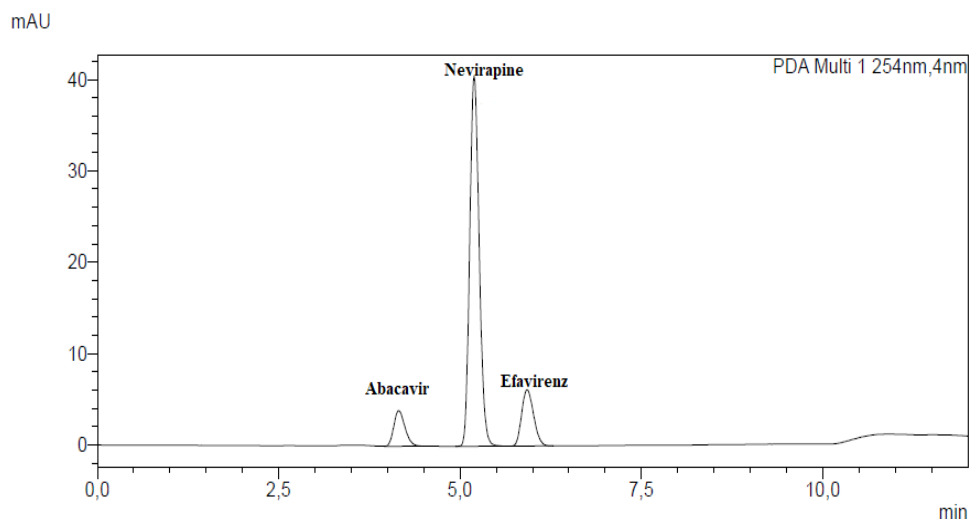


Figure S4. 1: A UV chromatogram of the selected ARVDs achieved at 254 nm, flow rate at 0.4 mL/min, column temperature 30 °C and gradient program of 50 % acetonitrile: 50 % water from 0-5 min and 70 % acetonitrile: 30 % water from 6-12 min.

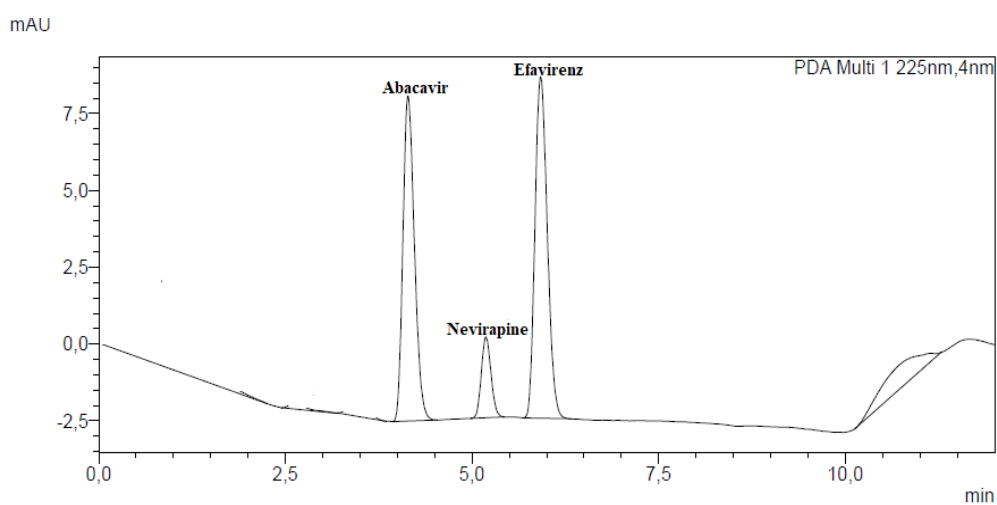


Figure S4. 2: A UV chromatogram of the selected ARVDs achieved at 225 nm, flow rate at 0.4 mL/min, column temperature 30 °C and gradient program of 50 % acetonitrile: 50 % water from 0-5 min and 70 % acetonitrile: 30 % water from 6-12 min.

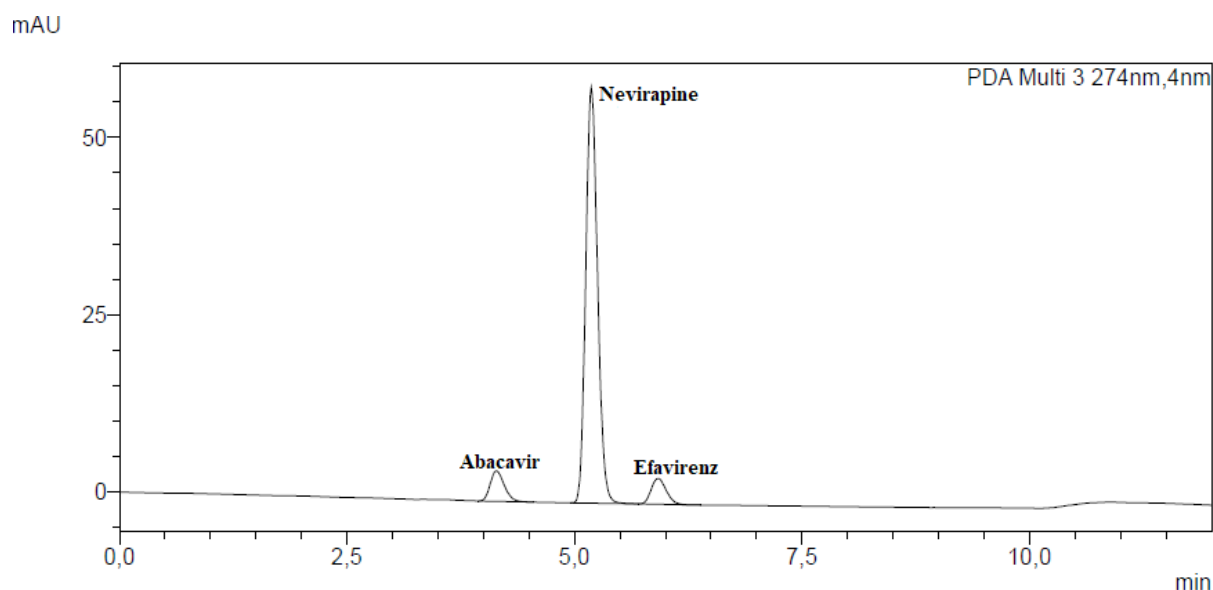


Figure S4.3: A UV chromatogram of the selected ARVDs achieved at 274 nm, flow rate at 0.4 mL/min, column temperature 30 °C and gradient program of 50 % acetonitrile: 50 % water from 0-5 min and 70 % acetonitrile: 30 % water from 6-12 min.

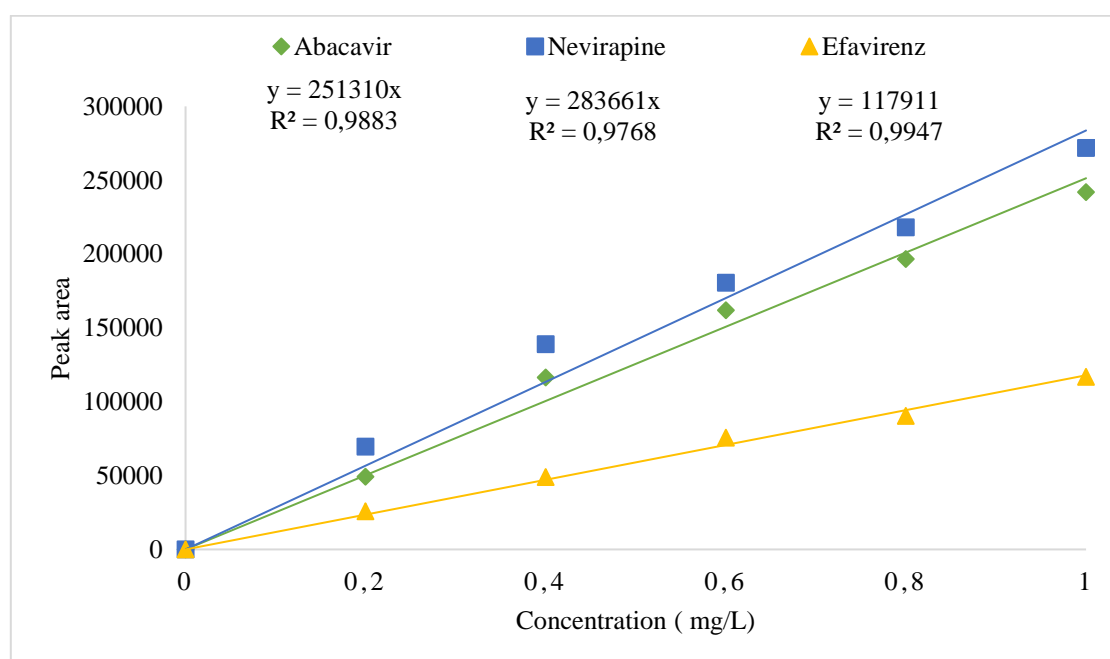


Figure S4. 4: Typical calibration curves for analytes obtained using LC-UV-PDA.

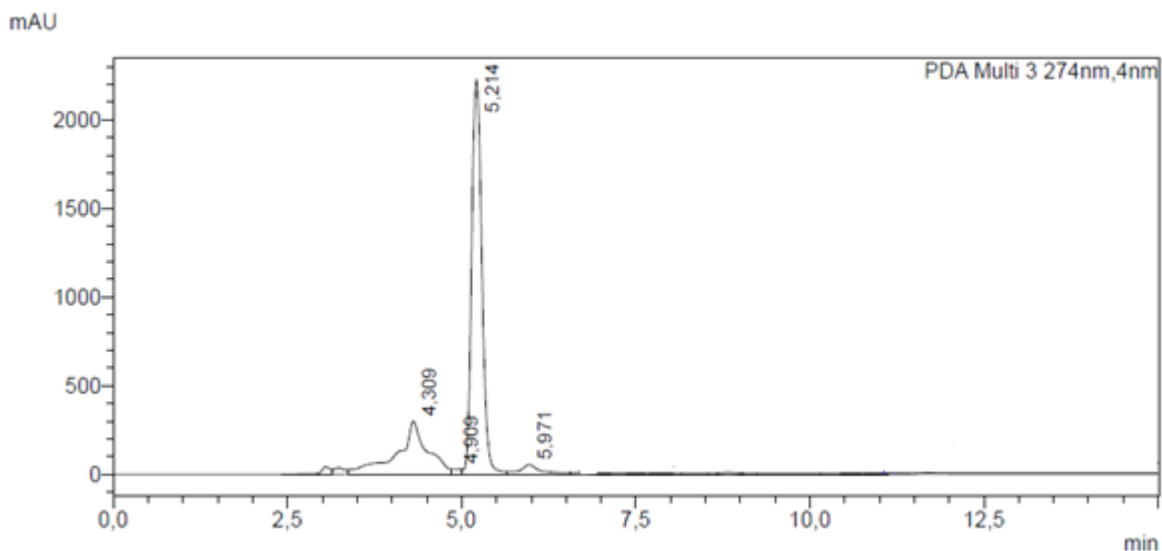


Figure S4. 5: A MAE chromatogram of the spiked green pepper sample obtained at 274 nm, the flow rate at 0.4 mL/min, column temperature 30 °C, and gradient program of 50 % acetonitrile: 50 % water from 0-5 min and 70 % acetonitrile: 30 % water from 6-12 min.

Table S4. 1: The t-Test result for the effect of extraction solvent on the recoveries of ARVDs in MAE

Hexane: Acetone			Methanol: Acetone			Hexane: Acetone		
Mean	92,66666667	60,66666667	Mean	92,66666667	47	Mean	92,66666667	36,66666667
Variance	46,33333333	508,3333333	Variance	46,33333333	229	Variance	46,33333333	233,3333
Observations	3	3	Observations	3	3	Observations	3	3
Hypothesized Mean Difference	0		Hypothesized Mean Difference	0		Hypothesized Mean Difference	0	
df	2		df	3		df	3	
t Stat	2,353393622		t Stat	4,766839654		t Stat	5,80000411	
P(T<=t) one-tail	0,071428571		P(T<=t) one-tail	0,008767823		P(T<=t) one-tail	0,005099501	
t Critical one-tail	2,91998558		t Critical one-tail	2,353363435		t Critical one-tail	2,353363435	
P(T<=t) two-tail	0,142857143		P(T<=t) two-tail	0,017535646		P(T<=t) two-tail	0,010199002	
t Critical two-tail	4,30265273		t Critical two-tail	3,182446305		t Critical two-tail	3,182446305	

Methanol: Methanol: Acetone			Methanol: Hexane			Methanol: Acetone		
Mean	60,66666667	47	Mean	60,66666667	36,66666667	Mean	47	36,66666667
Variance	508,3333333	229	Variance	508,3333333	233,3333333	Variance	229	233,3333
Observations	3	3	Observations	3	3	Observations	3	3
Hypothesized Mean Difference	0		Hypothesized Mean Difference	0		Hypothesized Mean Difference	0	
df	3		df	4		df	4	
t Stat	0,871748674		t Stat	1,526396947		t Stat	0,832383501	
P(T<=t) one-tail	0,223749679		P(T<=t) one-tail	0,100807259		P(T<=t) one-tail	0,226001212	
t Critical one-tail	2,353363435		t Critical one-tail	2,131846786		t Critical one-tail	2,131846786	
P(T<=t) two-tail	0,447499359		P(T<=t) two-tail	0,201614519		P(T<=t) two-tail	0,452002425	
t Critical two-tail	3,182446305		t Critical two-tail	2,776445105		t Critical two-tail	2,776445105	

Table S4. 2: The t-Test result for the effect of spike concentration and extraction time on the recoveries ARVDs in MAE

	1000 µg/kg	500 µg/kg		1 000 µg/kg	300 µg/kg		500 µg/kg	300 µg/kg
Mean	92,66666667	85	Mean	92,66666667	82	Mean	85	82
Variance	46,33333333	13	Variance	46,33333333	28	Variance	13	28
Observations	3	3	Observations	3	3	Observations	3	3
Hypothesized Mean Difference	0		Hypothesized Mean Difference	0		Hypothesized Mean Difference	0	
df	3		df	4		df	4	
t Stat	1,723922885		t Stat	2,142878497		t Stat	0,811502671	
P(T<=t) one-tail	0,091595432		P(T<=t) one-tail	0,049383989		P(T<=t) one-tail	0,23130197	
t Critical one-tail	2,353363435		t Critical one-tail	2,131846786		t Critical one-tail	2,131846786	
P(T<=t) two-tail	0,183190865		P(T<=t) two-tail	0,098767978		P(T<=t) two-tail	0,46260394	
t Critical two-tail	3,182446305		t Critical two-tail	2,776445105		t Critical two-tail	2,776445105	

	10 minutes	7 minutes		10 minutes	5 minutes		7 minutes	5 minutes
Mean	92,66666667	81,33333333	Mean	92,66666667	72,66666667	Mean	81,33333333	72,66666667
Variance	46,33333333	10,33333333	Variance	46,33333333	14,33333333	Variance	10,33333333	14,33333333
Observations	3	3	Observations	3	3	Observations	3	3
Hypothesized Mean Difference	0		Hypothesized Mean Difference	0		Hypothesized Mean Difference	0	
df	3		df	3		df	4	
t Stat	2,607680962		t Stat	4,4474959		t Stat	3,022438607	
P(T<=t) one-tail	0,039922266		P(T<=t) one-tail	0,010573144		P(T<=t) one-tail	0,019534755	
t Critical one-tail	2,353363435		t Critical one-tail	2,353363435		t Critical one-tail	2,131846786	
P(T<=t) two-tail	0,079844532		P(T<=t) two-tail	0,021146288		P(T<=t) two-tail	0,039069511	
t Critical two-tail	3,182446305		t Critical two-tail	3,182446305		t Critical two-tail	2,776445105	

Table S4. 3: The t-Test result for the effect of extraction solvent volume on the recoveries ARVDs in MAE

	30 mL	20 mL		30 mL	10 mL		20 mL	10 mL
Mean	92,66666667	82	Mean	92,66666667	75	Mean	82	75
Variance	46,33333333	7	Variance	46,33333333	37	Variance	7	37
Observations	3	3	Observations	3	3	Observations	3	3
Hypothesized Mean Difference	0		Hypothesized Mean Difference	0		Hypothesized Mean Difference	0	
df	3		df	4		df	3	
t Stat	2,529822128		t Stat	3,35201432		t Stat	1,827815388	
P(T<=t) one-tail	0,042718718		P(T<=t) one-tail	0,014257718		P(T<=t) one-tail	0,082514398	
t Critical one-tail	2,353363435		t Critical one-tail	2,131846786		t Critical one-tail	2,353363435	
P(T<=t) two-tail	0,085437436		P(T<=t) two-tail	0,028515435		P(T<=t) two-tail	0,165028795	
t Critical two-tail	3,182446305		t Critical two-tail	2,776445105		t Critical two-tail	3,182446305	

Table S4. 4: The t-Test result for the effect of conditioning solvent on the recoveries ARVDs in SPE

	ACN	ACN:MEOH		ACN	ACN:ACT		ACN	ACT:MEOH
Mean	101,3333333	96,3333333	Mean	101,3333333	82,6666667	Mean	101,3333333	90,3333333
Variance	9,33333333	162,333333	Variance	9,33333333	14,3333333	Variance	9,33333333	44,3333333
Observations	3	3	Observations	3	3	Observations	3	3
Hypothesized Mean Difference	0		Hypothesized Mean Difference	0		Hypothesized Mean Difference	0	
df	2		df	4		df	3	
t Stat	0,660978974		t Stat	6,645977286		t Stat	2,600764341	
P(T<=t) one-tail	0,288290961		P(T<=t) one-tail	0,001330522		P(T<=t) one-tail	0,040161379	
t Critical one-tail	2,91998558		t Critical one-tail	2,131846786		t Critical one-tail	2,353363435	
P(T<=t) two-tail	0,576581922		P(T<=t) two-tail	0,002661044		P(T<=t) two-tail	0,080322759	
t Critical two-tail	4,30265273		t Critical two-tail	2,776445105		t Critical two-tail	3,182446305	

	ACN:MEOH	ACN:ACT		ACN:MEOH	ACT:MEOH		ACN:ACT	ACT:MEOH
Mean	96,3333333	82,6666667	Mean	96,3333333	90,3333333	Mean	82,6666667	90,3333333
Variance	162,333333	14,3333333	Variance	162,333333	44,3333333	Variance	14,3333333	44,3333333
Observations	3	3	Observations	3	3	Observations	3	3
Hypothesized Mean Difference	0		Hypothesized Mean Difference	0		Hypothesized Mean Difference	0	
df	2		df	3		df	3	
t Stat	1,780926195		t Stat	0,722897396		t Stat	-1,733690231	
P(T<=t) one-tail	0,108439077		P(T<=t) one-tail	0,261002043		P(T<=t) one-tail	0,090694556	
t Critical one-tail	2,91998558		t Critical one-tail	2,353363435		t Critical one-tail	2,353363435	
P(T<=t) two-tail	0,216878155		P(T<=t) two-tail	0,522004086		P(T<=t) two-tail	0,181389112	
t Critical two-tail	4,30265273		t Critical two-tail	3,182446305		t Critical two-tail	3,182446305	

Table S4. 5: The t-Test result for the effect of concentration on the recoveries ARVDs in SPE

t-Test: Two-Sample Assuming Unequal Variances				t-Test: Two-Sample Assuming Unequal Variances				t-Test: Two-Sample Assuming Unequal Variances			
	1000 µg/L	500 µg/L			1000 µg/L	300 µg/L			500 µg/L	300 µg/L	
Mean	101,3333333	92,3333333	Mean		101,3333333	92,3333333	Mean		92,3333333	92,3333333	
Variance	9,33333333	9,33333333	Variance		9,33333333	30,3333333	Variance		9,33333333	30,3333333	
Observations	3	3	Observations		3	3	Observations		3	3	
Hypothesized Mean Difference	0		Hypothesized Mean Difference		0		Hypothesized Mean Difference		0		
df	4		df		3		df		3		
t Stat	3,608026766		t Stat		2,475085942		t Stat		0		
P(T<=t) one-tail	0,011298102		P(T<=t) one-tail		0,044829642		P(T<=t) one-tail		0,5		
t Critical one-tail	2,131846786		t Critical one-tail		2,353363435		t Critical one-tail		2,353363435		
P(T<=t) two-tail	0,022596205		P(T<=t) two-tail		0,089659285		P(T<=t) two-tail		1		
t Critical two-tail	2,776445105		t Critical two-tail		3,182446305		t Critical two-tail		3,182446305		

Table S4. 6: The t-Test result for MAE and MAE-SPE concentration limit and concentrations ( $\mu\text{g/kg}$ ) obtained in vegetables

	MAE LOD	MAE-SPE LOD		MAE LOQ	MAE-SPE LOQ
Mean	0,026	0,035333333	Mean	0,088666667	0,119
Variance	0,000036	0,000706333	Variance	0,000441333	0,007663
Observations	3	3	Observations	3	3
Hypothesized Mean Difference	0		Hypothesized Mean Difference	0	
df	2		df	2	
t Stat	-0,59333221		t Stat	-0,58360918	
P(T<=t) one-tail	0,30656044		P(T<=t) one-tail	0,309265809	
t Critical one-tail	2,91998558		t Critical one-tail	2,91998558	
P(T<=t) two-tail	0,61312089		P(T<=t) two-tail	0,618531619	
t Critical two-tail	4,30265273		t Critical two-tail	4,30265273	

	MAE concentrations	MAE-SPE concentrations
Mean	2,412183333	1,614958333
Variance	37,11539369	20,37884769
Observations	24	24
Hypothesized Mean Difference	0	
df	42	
t Stat	0,515079607	
P(T<=t) one-tail	0,304598917	
t Critical one-tail	1,681952357	
P(T<=t) two-tail	0,609197834	
t Critical two-tail	2,018081703	



## Chapter five

---

### **5. Case study on antiretroviral drugs uptake from soil irrigated with contaminated water: bio-accumulation and bio-translocation to roots, stem, leaves, and fruits**

#### **Abstract**

This study aimed to evaluate the potential of uptake of the commonly used antiretroviral drugs (ARVDs) in South Africa (abacavir, nevirapine, and efavirenz) by vegetable plants (beetroot, spinach, and tomato) from contaminated soil culture. The antiretroviral drugs were extracted from the soil and vegetables using ultrasonic extraction and quantified using a liquid chromatography photodiode array. The study results showed that all the studied vegetables have the potential to take up abacavir, nevirapine, and efavirenz from contaminated soil, be absorbed by the root, and translocate them to the aerial part of the plants. Abacavir was found at high concentrations to a maximum of 40.21  $\mu\text{g/kg}$  in the spinach root, 18.43  $\mu\text{g/kg}$  in the spinach stem, and 6.77  $\mu\text{g/kg}$  in the spinach soil, while efavirenz was the highest concentrations, up to 35.44  $\mu\text{g/kg}$  in tomato leaves and 8.86  $\mu\text{g/kg}$  in tomato fruits. Spinach root accumulated more ARVDs than beetroot and tomato. However, the accumulation of ARVDs in all studied plants showed that they could be used in phytoremediation. These results suggest that the quality of water used for crop irrigation needs to be assessed prior to irrigation to avoid vegetable plant pollution because irrigating with ARVDs contaminated water results in their uptake by plants and their traces might be transferred to the edible parts of crops and thus be indirectly consumed by humans.

#### **5.1. Introduction**

The traces of various pharmaceutical compounds such as antibiotics, analgesics, anti-epileptic, and antiretroviral drugs (ARDVs) have been found in several environmental compartments where wastewater treatment (WWTPs) have been reported to be their main source (Archer et al., 2017, Varga et al., 2010, Schoeman et al., 2015, Obidike and Mulopo, 2018, Mosekiemang et al., 2019, Mlunguza et al., 2020). On the other hand, the use of effluent water from wastewater treatment plants (WWTPs) for horticulture crop irrigation dominates nowadays due to freshwater scarcity. Therefore, this could lead to depreciation of food quality due to the potential risk of introducing traces of pharmaceuticals into the food chain. The application of biosolids, fertilizer contaminated animal manure, and soil amendment could also contribute to the concentration of pharmaceuticals in agricultural areas (García et al., 2018). The introduced pharmaceuticals, including ARDs in agricultural areas, accumulate in the soil, be absorbed by

vegetable plant's roots, and translocate to the aerial part of plant tissues via diffusion and transpiration. Consequently, they are unintentionally consumed by humans, posing a potential health risk (Madikizela et al., 2018). Also, drug resistance may result from prolonged accidental consumption. Moreover, the fish exposed to ARVDs were observed to have a liver abnormality; however, the effect of ARVDs on the environment is not yet known (Rimayi et al., 2018).

The plant uptake of organic compounds is subjected to various factors, including ionization propensities, molecular weight, hydrophobicity, and solubility. Table 5.1 shows the properties of the target ARVDs in the study. The root hairs' cell walls are negatively charged; therefore, the uptake of the anionic compounds is restricted by electron repulsion by the cell wall of the root hairs. Compounds of a molecular weight less than 1000 g/mol are susceptible to plant uptake. Therefore, the ARVDs of interest shown (Table 5.1) are expected to be highly absorbed by plant roots as their molecular weights are less than 400 g/mol (Zhang et al., 2017). Compounds with a high octanol-water coefficient (log Kow) hydrophobic nature allow the partition of the lipophilic structure of the plant, whereas those with a low hydrophobicity suggest an insignificant permeation into the lipophilic root cell membrane (Miller et al., 2016). The log Kow is attuned to log Dow for ionisable compounds to reflect the environmental pH. Compounds with log Dow greater than 4.5 tend not to be likely to undergo any significant translocation to aerial tissues of the plant (Kumar and Gupta, 2016). In the soil-to-plant system, the accumulation, fate, and behaviour of pharmaceuticals (including ARVDs) in plants may be affected in the growing system due to physical, chemical, and biological processes. The characteristics of soil, such as soil ion exchange capacity and organic carbon content, may affect the mobility of ARVDs and their availability in the medium (Eggen et al., 2011). The processes such as abiotic and biotic result in the elimination of organic compounds in the environment, reducing plant uptake of ARVDs. Also, the organic materials in the soil can change the properties of the soil surface and the availability of sorption sites. In contrast, high organic content can either promote or inhibit the sorption of organic compounds to soil (Miller et al., 2016) and thus controls the transfer of the compounds into the plant tissues.

The ARVDs are used to treat retrovirus infection, mainly the human deficiency virus (HIV). As the role of ARVDs is to treat and inhibit the replication of the virus, they do not destroy the viral load in the blood; hence the patients must take this medication for the rest of their lives to prevent replication (Ncube et al., 2018). This indicates that the WWTPs will keep receiving

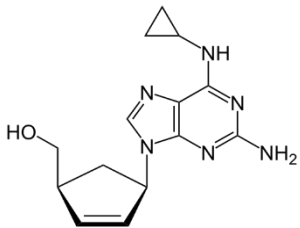
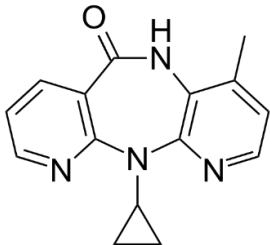
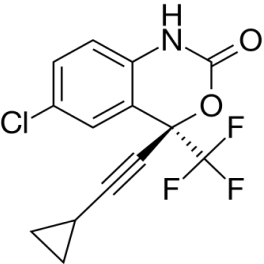
ARVDs through wastewater influents and will be continuously introduced into the environment. Consequently, sizeable studies have been done to monitor various classes of pharmaceuticals in vegetables worldwide which showed that vegetables and plants could accumulate and translocate pharmaceuticals (Wu et al., 2012). In a study conducted by Boxall and co-workers, the uptake of antibiotics in contaminated soil by lettuce leaves and carrots was assessed in the United Kingdom. The maximum concentrations of 170 and 23  $\mu\text{g/kg}$  were obtained in lettuce leaves and carrots, respectively, while 1373 and 1001  $\mu\text{g/kg}$  were reported in lettuce and carrots planted soils, respectively (Boxall et al., 2006). Another study was conducted in Israel (Goldstein et al., 2014) for the uptake of pharmaceuticals in cucumber and tomato plant leaves and fruits. The maximum concentration of 1.6  $\mu\text{g/kg}$  in tomato fruits, 380  $\mu\text{g/kg}$  in tomato plant leaves, 45  $\mu\text{g/kg}$  in cucumber fruits, and 410  $\mu\text{g/kg}$  in cucumber plant leaves were observed. In African countries, Amos and co-workers studied the uptake of non-steroidal anti-inflammatory drugs (naproxen, ibuprofen, and diclofenac) by water hyacinth in South African river water where the maximum concentration of 12  $\mu\text{g/kg}$  was observed for naproxen (Amos et al., 2019).

Even though some work has been done on the uptake of different classes of pharmaceuticals, there are very few studies that have been conducted on ARVDs. Mlunguza et al. (2020) reported on the uptake of ARVDs by water hyacinth (emtricitabine, tenofovir disoproxil, and efavirenz) in South African water. The results obtained showed that this aquatic plant has the ability to take up the studied ARVDs with the highest concentration of 29.6  $\mu\text{g/kg}$  of efavirenz accumulating in plant roots. It is worth noting that the ARVDs uptake analysis conducted by Mlunguza et al. (2020) did not involve a structured experimental approach to assess the uptake, while this approach is essential for the thorough assessment of the plant root-ARVD interactions (Akenga et al., 2021). In this regard, Akenga et al., 2021 applied a structured experimental approach by conducting hydroponic experiments to assess the ARVDs (nevirapine, lamivudine, and efavirenz) uptake by lettuce vegetable. The attained results revealed that the lettuce vegetable can take up the studied ARVDs with the highest concentration of 3463  $\mu\text{g/kg}$  of efavirenz bio-accumulating in lettuce vegetable roots. However, the hydroponic approach does not take into consideration the complex natural environment that includes the agroecosystem (Wu et al., 2015, Akenga et al., 2021).

Taking this into consideration, this current study aimed to conduct a phytoremediation approach to evaluate the potential uptake of the commonly used ARVDs in South Africa (abacavir, nevirapine, and efavirenz) by vegetable plants (beetroot, spinach, and tomato) in soil culture. According to Christou et al. (2019), leafy vegetables have been reviewed to accumulate organic pollutants better in association with fruit, cereals, and root vegetables. Moreover, the study by Akenga et al. (2021) revealed that ARVDs could be successfully taken up by the leafy vegetable (lettuce), where they highly accumulate in the roots of the lettuce plant. Hence, spinach was used in this study to represent leafy vegetables, while beetroot and tomato were added to represent the root and fruity vegetables, respectively. Even though numerous studies have been conducted on ARVDs in water (Mtolo et al., 2019), few studies report their occurrence in soil and plants (Akenga et al., 2021); this work, therefore, involved ARVDs accumulation in soil. The ultrasonic extraction method was used to extract the selected ARVDs, while a liquid chromatography photodiode array was employed to identify and quantify the extracted ARVDs.

To the best of our knowledge, this work presents, for the first time, a comprehensive study to evaluate the selected vegetables for uptake of the studied ARVDs from contaminated soil.

Table 5.1: Abacavir, nevirapine, and efavirenz structures, molecular masses, Log K<sub>ow</sub>, and pK<sub>a</sub> values (Akenga et al., 2021)

Name and molecular mass (g/mol)	Molecular structure	Log K <sub>ow</sub>	Solubility (mg/L)	pK <sub>a</sub>		Log D <sub>ow</sub>		
				Strong acid	Strong base	Beetroot pH (6.6 ± 0.03)	Spinach pH (5.7 ± 0.09)	Tomato pH (4.9 ± 0.07)
Abacavir (286.33)		1.2	77000	15.41	5.77	0.0192	-0.258	-0.845
Nevirapine (266.29)		2.5	191	10.37	-0.06	0.397	0.396	0.387
Efavirenz (315.68)		4.5	0.5	12.5	-1.5	-5.246	-6.146	-6.946

## **5.2. Experimental**

### **5.2.1. Materials and chemicals**

The ARVDs standards, abacavir, nevirapine, and efavirenz of a high purity >99.5%, were purchased from J & H Chemical Co. LTD (Hangzhou Zhejiang, China). Acetonitrile, methanol, acetone, and chloroform were obtained from Honeywell (Steinheim, Germany).

### **5.2.2. Liquid chromatography-photodiode array condition**

Detection and quantification were performed by a liquid chromatography (LC) system bought from Shimadzu (Tokyo, Japan) coupled with LC 2030/2040 photodiode array (PDA) detector from (Europe, Germany). The ARVDs were acquired at detector wavelengths of 225 nm and 274 nm. The autosampler injected 10  $\mu$ L of each standard extract into the LC system, separated by the column Shim-Pack GIST C18-HP (4.6 mm $\times$ 150 mm, 3  $\mu$ m) from Shimadzu (Tokyo, Japan). The mobile phase used was 0.1% formic acid in acetonitrile (CH<sub>3</sub>CN) (solvent A) and 0.1% formic acid in water (H<sub>2</sub>O) (solvent B) flowing at a rate of 0.4 mL/min. The gradient program started with 50% of solvent A for the initial 5 minutes and ramped up to 70% for the next 7 minutes, and the entire run time was 12 minutes.

### **5.2.3. Stock solution preparation**

A standard stock solution containing efavirenz, nevirapine, and abacavir antiretroviral drugs was prepared in a 100 mL volumetric flask by weighing 10 mg of the individual compound dissolved in acetonitrile to make a final concentration of 100 mg/L. The working solutions were prepared by diluting a stock solution into a series of concentrations ranging from 200 to 1000  $\mu$ g/L. The working solutions were injected into the LC-PDA to be identified, and the results were used to construct the calibration curves.

### **5.2.4. Field experiment**

Laboratory analysis and field experiments were conducted to assess the accumulation of ARVDs in soil, their absorption by plant roots, and translocation to stem, leaves and fruit. The field experiment was conducted outside the Chemistry Department Building at the University of KwaZulu-Natal (Pietermaritzburg). Beetroot, spinach, and tomato were selected as test crops because they are common vegetables and can be consumed with or without cooking. Beetroot, spinach, and tomato represent root, leaf, and fruity vegetables, respectively. The two-week-old

seedlings were bought from Bloom's nursery in Pietermaritzburg in September 2021, and their transplantation was performed immediately from the nursery. The plants were grown under a shelter that could only protect them from the rain to avoid ARVDs spiked concentration dilutions. The plants were grown in plastic pots which have drain holes underneath. A compost mixed with loam soil was used as a planting media. The soil used for the experiment had conductivity of  $1.40 \pm 0.01$  dS/m, a pH of  $6.9 \pm 0.02$ , and an organic matter of 14.91%. During the harvesting season, the pH of the soil samples was tested, which was found to be slightly acidic ( $4.9 \pm 0.07$  -  $6.6 \pm 0.03$ ), while the EC values were found to be the same ( $1.31 \pm 0.09$  -  $1.40 \pm 0.01$  dS/m) as before the plantation process (Table S5.1). The ARVDs were introduced into the soil by irrigating with tap water spiked with the target ARVDs mixture at 2000 and 5000  $\mu\text{g/L}$ . These high concentrations of ARVDs were selected to ensure that the selected ARVDs are available in the soil for plant uptake even if they leach but are high enough to allow the study of the uptake. Another reason was due to the soil media used, which may minimize the availability of ARVDs for plant uptake due to the abiotic and biotic processes in the soil to plant system. The tap water used had an electric conductivity of  $0.82 \pm 0.04$  dS/m and a pH of  $7.9 \pm 0.08$ . The volume of water used for irrigation was consistent for each plant/replicate set. The solutions were labeled based on the concentration of ARVDs in the solution. A pot-plant system was used in this project where 24 plantation pots of 17 cm diameter and 16 cm height were filled with 2.5 g of soil. The 12 plantation pots were used for a high spike experiment batch, and the other 12 pots were used for a low spike experiment batch. Each plant had one unspiked (control) and three spiked replicates for both high and low spike concentration experiments. Spiked tap water was prepared every 7<sup>th</sup> day for three months, made a 2400 mL (to reach the maturity stage of the individual plant prior to harvesting), and used immediately to minimize errors that may result from the decomposition of ARVDs in water. A 500 mg/L stock solution was prepared in a 100 mL volumetric flask by dissolving 50 mg of the individual compound in 20 mL of acetonitrile and topped with tap water. It was then used to spike tap water to a final concentration of 5000  $\mu\text{g/L}$  and 2000  $\mu\text{g/L}$ , and each plant was irrigated with 200 mL of these solutions, according to their experimental batches.

#### **5.2.5. Sample collection and pre-treatment**

Vegetables were harvested from the mini garden using a spatula. They were then washed with distilled water and cut/separated according to root, stem, leaf, and fruit before blending with the blender bought from Clicks (Pietermaritzburg, South Africa). Soil samples were air dried

at a room temperature for 24 hours, homogenized, mashed and sieved in a 2 mm sieve. Vegetable samples were analyzed on the same day of the harvest.

#### **5.2.6. Extraction and preconcentration of the selected compounds**

The ultrasonic extraction method was adopted from Mnyandu et al. (2022) and further optimized in our previous work to improve recoveries of all the analytes. The extraction method involved adding 2 g of a wet blended vegetable or grounded soil sample in a 50 mL conical flask containing 10 mL acetonitrile. Then 2.5 g of NaCl salt was added, and the mixture was ultrasonicated for 30 minutes using the ultrasonic bath purchased from Science Tech (Durban, South Africa). The extract was separated from the solid matrix using centrifugation at 3000 rpm for 5 minutes using a centrifuge bought from Shalom Laboratory (Durban, South Africa). The supernatant liquid was then reduced to dryness using a rotary evaporator and re-dissolved in 1 mL of acetonitrile. This was followed by filtration with a 0.2  $\mu$ m filter from Pall (Puerto Rico, United States) into a 2 mL LC vial prior to LC-PDA analysis (Mnyandu and Mahlambi, 2022).

#### **5.2.7. Method validation**

Ultrasonic and LC-PDA methods were validated using linearity, precision, accuracy, method limit of detection (LOD), and quantification (LOQ). Linearity was assessed by analyzing the prepared working solutions of a series of concentrations ranging from 200 to 1000  $\mu$ g/kg and drawing the calibration curves. The obtained  $R^2$  values obtained were above 0.98, indicating the good precision of the LC-PDA (Table 5.2). The limit of detection and quantification were measured using a signal-to-noise ratio of 3 and 10, respectively. The obtained LOD and LOQ range from 0.008-0.015  $\mu$ g/kg and 0.027-0.049  $\mu$ g/kg, respectively. The limits values were acceptable and showed that the methods were sensitive. The recovery test was done to investigate the accuracy of the method. A 1 mg/kg spiked fresh vegetable plants taken from the garden with the absence of ARVDs was analysed. The obtained recoveries were within the acceptable ranged, from 88-91%, 89-95%, 92-100%, and 91-106% for the soil, root, stem, and fruit part of the plant, respectively. Triplicate analysis were performed in the same day and the obtained results were used to calculate the %RSD. The obtained %RSD were less than 6% which indicate that the method was precise. These results showed that the methods are accurate and precise and thus can be effectively applied to determine the selected ARVDs in soil and plant samples.



Table 5.2: The linearity, LOD ( $\mu\text{g/kg}$ ), LOQ ( $\mu\text{g/kg}$ ), % recoveries of the analytical method, (n=3)

ARVD	Equation	Linearity	LOD	LOQ	Recoveries (%)			
					Soil	Root	Stem	Fruit
Abacavir	$y = 251310x + 6510$	0.9883	0.012	0.039	$88 \pm 1.0$	$90 \pm 0.5$	$100 \pm 2.0$	$106 \pm 2.4$
Nevirapine	$y = 28366x + 14679$	0.9768	0.015	0.049	$90 \pm 1.1$	$95 \pm 0.1$	$97 \pm 1.0$	$99 \pm 1.1$
Efavirenz	$y = 117911x + 2168$	0.9947	0.0081	0.027	$91 \pm 1.1$	$89 \pm 0.91$	$92 \pm 0.70$	$91 \pm 0.98$

### **5.3. Results and discussion**

#### **5.3.1. Phytoremediation of ARVDs by vegetables from the contaminated soil**

##### **5.3.1.1. The accumulation ARVDs in soil**

The harvesting of the vegetables was done in December 2021, which was three months from the plantation time. The obtained soil pH values during the harvesting season were slightly acidic; this implies that the accumulation of the ARVDs during the growing season was favored as the basic conditions do not promote soil accumulation (Zheng et al., 2013). Also, the soil organic matter content did not change throughout the plantation period (14.5% to 14.9%). The possible reason for high organic matter content in soil media used could be due to compose medium used containing organic manure, which contributed to an increase in organic matter and other minerals and nutrients in the soil. The control soil samples were analysed, and no ARVDs were detected. Low concentrations of ARVDs were observed in soil samples (Table 5.3); It was believed that the main reason could be due to that the ARVDs leached beyond the sampling depth as the extraction method has proven to be effective since the recovery obtained in the same matrix were within the desirable range; however, the experiment was not designed to collect leachates. Another possible reason could be the high organic matter, which may adjust soil properties and lead to the unavailability of the sorption sites. This results in a decrease in the sorption of ARVDs to soil particles, making them accessible for plant uptake or leaching deep in the soil layer (Miller et al., 2016). The low concentrations could also be due to the acceleration of ARVDs metabolism due to their short biological half-life; ARVDs degradation by a non-biotic and biotic process in soil; or ARVDs uptake by plant part (Al-Farsi et al., 2018). In beetroot and spinach soil samples irrigated with low spiked tap water, the concentrations were obtained in a span range of 0.08 - 2.75 µg/kg and 2.27 – 3.82 µg/kg, respectively. Whereas in soil samples irrigated with a high spike concentration of tape water, the range was 2.25 – 6.77 µg/kg; 4.91 – 6.77 µg/kg; and 1.96 – 6.58 µg/kg in beetroot, spinach, and tomato soil samples, respectively. The obtained results suggest that abacavir, nevirapine, and efavirenz have the ability to bind to soil particles. This indicates that as much as the organic matter content was high, the sorption of ARVDs took place even though no compounds were detected in low concentration spiked soil for tomatoes. This could result from the low octanol-water coefficient of the target ARVDs which enhances their binding ability to the matrix with high organic matter (Abafe et al., 2018). This study agrees with the previously reported studies

on the uptake of carbamazepine and ibuprofen from the soil with urine as fertilizer (Winker et al., 2010, Malchi et al., 2014)

#### **5.3.1.2. Absorption of ARVDs by root and transfer to stem, leaves, and fruits**

All the vegetable plants (beetroot, spinach, and tomato) were healthy in high and low spike concentrations, with the leaves developing normally during the growth period. However, after the maturation stage (3 months), the growth of the spinach from high spiked concentration plants declined. As a result, some spinach plants lost mature leaves and turned yellow like a burn, indicating damaged or poor roots growth, which could be related to plant efficiency in taking up the ARVDs. This is because the ARVDs may hinder the transportation of essential nutrients for growth, resulting from plant stress and thus negatively impacting plant growth (Miller et al., 2016). A similar effect was observed in the cucumber plant exposed to 17 pharmaceuticals and personal care products at concentrations up to 50 µg/L (Sun et al., 2018). No average concentrations were reported under tomatoes irrigated with water spiked at 2000 mg/L because there was a shortage of tomato seedlings; hence, no tomato was planted and irrigated with water spiked at 2000 mg/L.

All the ARVDs of interest were detected in all tested plant tissues (Table 5.3). The concentrations of ARVDs obtained in roots were higher than those found in soil, indicating the ability of the studied vegetables to absorb ARVDs from contaminated soil. This could be due to the low molecular mass compounds that can penetrate the root through the epidermis into the bulk of the root. Also, the soil samples' pH was 4.7 - 6.6, which is higher than the Pka values, especially for nevirapine (3.28) in all vegetable soil samples and abacavir (5.77) in beetroot, indicating that they existed in anionic form leading to their poor accumulation in the soil. This resulted from the electrostatic repulsion as the soil surface is negatively charged, and thus ARVDs were adsorbed by the root (Hlengwa and Mahlambi, 2020). However, since efavirenz Pka of 12.5, which is higher than pH in all vegetable soil samples, and abacavir in tomatoes were also adsorbed by the root, the adsorption might have been highly influenced by the organic content, which altered the soil properties and thus allowed the availability of ARVDs for root plant uptake (Miller et al., 2016). Abacavir was found at a high concentration in all samples analyzed except in leaves and was observed to accumulate in the roots with the highest concentration in spinach plant roots (Table 5.3). Higher concentrations for efavirenz and nevirapine were found in the leaves with a maximum of 35.44 µg/kg, and 15.39 µg/kg,

respectively, where the highest concentration was observed in tomato plant leaves. This could be due to that efavirenz and nevirapine's hydrophobic nature with  $K_{OW}$  of 4.5 and 2.5, respectively, which allow their partition to the lipophilic structure of the plant cell. These findings agree with those reported by Goldstein et al. (2014), where carbamazepine (log  $K_{OW}$  of 2.45) and lamotrigine (log  $K_{OW}$  of 2.57) higher concentrations were taken up compared to sulfapyridine and caffeine with (log  $K_{OW}$  of 0.35 and  $-0.07$ , respectively).

All the studied ARVDs were present in the tomato fruit sample, which could be due to the compounds' route of transportation within the plant being mainly controlled by the physicochemical properties of the plant (Goldstein et al., 2014). The obtained result agrees with the study Akeng et al. (2021) conducted, reporting the ARVDs (lamivudine, nevirapine, efavirenz, and oseltamivir) uptake by lettuce exposed to contaminated water. The concentration ranging from less than LOQ to 3463  $\mu\text{g/kg}$  were obtained with the higher concentrations in the roots of the lettuce plant (Akenga et al., 2021). Mlunguza et al. (2020) reported the uptake of ARVDs (emtricitabine, tenofovir disoproxil, and efavirenz) by water hyacinth plants. The highest concentration was observed for efavirenz with a maximum of 29.6  $\mu\text{g/kg}$  accumulating in plant roots, even though the structured experimental to study the uptake was not conducted.

### **5.3.2. ARVDs bioaccumulation in roots and bio-translocation to stem, leaf and fruit**

The bioaccumulation and bio translocation of abacavir, nevirapine, and efavirenz in beetroot, spinach, and tomato plants were calculated to evaluate the extent of pollution ARVDs may have in these vegetables, which can also be eaten raw. Also, it was important to understand whether these flourishing vegetable plants could assist in the phytoremediation of these ARVDs from the soil. The root concentration factor (RCF) expressed the accumulation in roots, which displays the ratio of the concentration in roots over that in the exposure media:  $\text{RCF} = C_{\text{root}}/C_{\text{soil}}$ . The accumulation of ARVDs in vegetable plant tissues was expressed by a bio-concentration factor (BCF) which was calculated as the ratio of the ARVD concentration in the plant tissue to the nominal concentration in the growth medium:  $\text{BCF} = C_{\text{plant tissue}}/C_{\text{soil}}$ . Moreover, the translocation of ARVDs in the vegetable plant's tissue/tissues was presented by a translocation factor (TF) which is a ratio of concentration in the areal part of the plant over that in roots:  $\text{TF} = C_{\text{stem or leaf or fruit}}/C_{\text{root}}$  (Al-Farsi et al., 2017).

The BCF obtained indicate that the vegetable plants have the ability to accumulate ARVDs from contaminated soil sources effectively. The BCF ranged from 2.0-14  $\mu\text{g/kg}$  in beetroot, 3.6

- 15 µg/kg in spinach, and 6 – 10 µg/kg in tomato (Table 5.4). The RCF range was 0.047 – 17.6 µg/kg; 0.34-5.9 µg/kg, and 0.14-2.82 µg/kg in beetroot, spinach, and tomato, respectively. The combined average concentrations of ARVDs in each plant were 86.49, 129.92, and 113.79 µg/kg in beetroot, spinach, and tomato, respectively (Figure 5.1). These results were mainly attributed to abacavir which contributed 53, 48, and 39% in beetroot, spinach, and tomato, respectively, even though efavirenz (42%) was the main contributor in tomato (Figure 5.2). Therefore, the possible reason for a high percentage of efavirenz in the tomato plant could be that its pKa is higher than the sample pH; hence it was present in an ionized form. In this case, it was positively charged, making it more attracted to the negatively charged cell wall of the plant root hairs (Miller et al., 2016). The results showed that spinach has a high potential for phytoremediation as the sum of the average concentrations of ARVDs is higher than in beetroot and tomato. However, the statistical result showed that the average concentration obtained in spinach is not statically different from that of beetroot and spinach as the p-values were greater than 0.05. The values were beetroot versus spinach ( $p>0.36$ ), beetroot versus tomato ( $p>0.54$ ), and spinach versus tomato ( $p>0.69$ ) (Table S5.2).

The accumulation of all the studied ARVDs was higher in spinach root than in beetroot and tomato (Table 5.4), but statistically not different as the obtained p-values are  $p>0.72$ ,  $p>0.96$ , and  $p>0.54$  for beetroot versus spinach, beetroot versus tomato, and spinach versus tomato, respectively (Table S5.3). The beetroot showed high translocation from root to stem, root to leaf, and root to stem plus a leaf, while the tomato had high translocation from root to fruit and root to stem, plus leaf plus fruit (Table 5.4). The TF for efavirenz was above 1 in all tissues for all the studied vegetables, indicating its high ability to migrate from the root tissues (Akenga et al., 2021). These findings confirmed that these ARVDs accumulated in the bulk of the studied plants, and spinach has the ability to accumulate more of these ARVDs than beetroot and tomato. The obtained results are within the reported root accumulation factor values for various categories of pharmaceuticals span a range of numerous orders of magnitude, from ~0.01 to ~1000 (Redshaw et al., 2008, Sabourin et al., 2012, Goldstein et al., 2014). The accumulation levels of the ARVDs were found to be higher in the plants exposed to higher concentrations of the ARVDs growing medium which was expected as more ARVDs were available to be absorbed by plants from the medium. These findings are similar to those reported by Akenga et al. (2021) and Al-Farsi et al. (2017) in their hydroponic exposure experiments for ARVDs and pharmaceuticals, respectively. The ARVDs accumulated from root to stem, leaves, and fruits observed in this study proved that abacavir, nevirapine, and

efavirenz are taken up by vegetable plants and have a high potential to pose a human health risk. Moreover, these results suggest that these vegetables can be used in the phytoremediation of the studied ARVDs to remove or reduce their concentration levels from contaminated soil. However, further studies still need to be conducted.

The uptake of chemicals by the plant can be influenced by numerous factors, including ionization propensities, molecular weight, hydrophobicity, and solubility, where hydrophobicity is one of the significant factors of neutral compounds. It is presented as an octanol-water partition coefficient ( $\log K_{ow}$ ) (Al-Farsi et al., 2017). In order to reflect the environmental pH, the octanol-water partition coefficient is converted to pH - adjusted octanol-water partitioning coefficient ( $\log D_{ow}$ ). The used pH solution were 4.9 (tomato), 5.7 (spinach), and 6.6 (beetroot). The relationship between the uptake of the ARVDs and  $\log D_{ow}$  was obtained by drawing the linear plot of the BCF, RCF, and the TF of the ARVDs against  $\log D_{ow}$ . In this case, three points representing the target compounds were used in to plot the graphs. The results (Figure 5.3 and 5.4) showed a strong relationship between  $\log D_{ow}$  and a BCF in spinach (Figure 5.3) and tomato (Figure 5.4) with the  $r^2$  0.8809 and 0.9494, respectively, which indicated that the hydrophobicity could be the main effect on the linearity. Similar results were observed in the RCF of spinach and tomato ( $r^2 = 0.8715$  and  $0.7388$ ) and their TF ( $r^2 = 0.7434$  and  $1$ ), displaying that the accumulation of ARVDs to roots and their immigration to the bulky of the plant is dependent on the hydrophobicity. Different results (Figure 5.5) were obtained for beetroot samples, where there was no relationship between  $\log D_{ow}$  to BCF ( $r^2 = 0.0767$ ) and  $\log D_{ow}$  to RCF ( $r^2 = 0.024$ ), whereas the relationship between  $\log D_{ow}$  and TF ( $r^2 = 0.3426$ ) was weak which means that there were other factors influencing the uptake of ARVDs (Akenga et al., 2021).

Table 5.3: Summary of the detected average concentrations ( $\mu\text{g/kg}$ ) of selected ARVDs in vegetables and soil (n=3)

Matrix	Vegetables	2000 $\mu\text{g/L}$ spiked tap water irrigated			5000 $\mu\text{g/L}$ spike tap water irrigated		
		Abacavir	Nevirapine	Efavirenz	Abacavir	Nevirapine	Efavirenz
Soil	Beetroot	$2.75 \pm 0.3$	$2.28 \pm 0.1$	$0.08 \pm 0.4$	$5.30 \pm 1.9$	$4.71 \pm 1.0$	$2.25 \pm 0.9$
	Spinach	$3.82 \pm 1.9$	$2.27 \pm 0.7$	$3.40 \pm 0.9$	$6.77 \pm 2.0$	$4.91 \pm 1.8$	$6.70 \pm 1.9$
	Tomato	-	-	-	$6.58 \pm 1.1$	$1.96 \pm 0.05$	$6.15 \pm 1.3$
Root	Beetroot	$10.90 \pm 1.5$	$0.68 \pm 0.01$	$1.41 \pm 0.2$	$20.45 \pm 2.1$	$0.22 \pm 0.3$	$2.25 \pm 0.5$
	Spinach	$18.16 \pm 1.9$	$7.76 \pm 0.8$	$1.17 \pm 0.2$	$40.21 \pm 3.0$	$15.11 \pm 1.1$	$3.41 \pm 1.0$
	Tomato	-	-	-	$18.56 \pm 1.8$	$4.38 \pm 0.9$	$0.85 \pm 0.01$
Stem	Beetroot	$6.87 \pm 1.0$	$0.39 \pm 0.01$	$3.83 \pm 0.2$	$17.6 \pm 2.4$	$0.92 \pm 0.04$	$8.26 \pm 1.3$
	Spinach	$7.43 \pm 1.0$	$6.26 \pm 0.01$	$4.00 \pm 0.7$	$18.43 \pm 1.9$	$15.80 \pm 1.4$	$8.96 \pm 1.1$
	Tomato	-	-	-	$3.87 \pm 0.6$	$0.44 \pm 0.01$	$2.88 \pm 0.3$
Leaf	Beetroot	$4.99 \pm 0.09$	$4.22 \pm 0.7$	$11.90 \pm 0.9$	$8.18 \pm 0.9$	$8.16 \pm 1.0$	$20.45 \pm 3.0$
	Spinach	$1.99 \pm 0.01$	$1.66 \pm 0.02$	$7.13 \pm 1.0$	$3.10 \pm 0.2$	$3.60 \pm 0.7$	$14.60 \pm 2.1$
	Tomato	-	-	-	$14.89 \pm 1.7$	$15.39 \pm 1.9$	$35.44 \pm 4.2$

Fruit	Tomato	-	-	-	$7.61 \pm 0.2$	$0.62 \pm 0.07$	$8.86 \pm 0.5$
-------	--------	---	---	---	----------------	-----------------	----------------

- : not analysed



Table 5.4: Average bio-accumulation and bio-translocation factors of the antiretroviral drugs found in different segments of vegetable plants (n=3).

	ARVDs	Bio-accumulation				Bio-translocation									
		Bio-concentration factor		Root concentration Factor		Root to Stem		Root to Leaf		Root to Fruit		Root to Stem + Leaf		Root to Stem + Leaf + Fruit	
		2000 (µg/kg)	5000 (µg/kg)	2000 (µg/kg)	5000 (µg/kg)	2000 (µg/kg)	5000 (µg/kg)	2000 (µg/kg)	5000 (µg/kg)	2000 (µg/kg)	5000 (µg/kg)	2000 (µg/kg)	5000 (µg/kg)	2000 (µg/kg)	5000 (µg/kg)
Beetroot	Abacavir	8	9	4.0	3.9	0.63	0.86	0.46	0.40	-	-	7.3	18	-	-
	Nevirapine	2.3	2.0	0.30	0.047	0.57	4.2	6.2	37	-	-	6.6	38	-	-
	Efavirenz	3	14	0.30	1.0	2,7	3.7	8.4	9.1	-	-	12	17	-	-
Spinach	Abacavir	7	9	4.8	5.9	0.41	0.46	0.10	0.08	-	-	7.5	19	-	-
	Nevirapine	7	7	3.4	3.1	0.81	1.0	0.21	0.24	-	-	6.5	16	-	-
	Efavirenz	3.6	15	0.34	0.51	3.4	2.6	6.1	4.3	-	-	10	13	-	-
Tomato	Abacavir	-	6	-	2.82	-	0.21	-	0.80	-	0.41	-	4.7	-	19
	Nevirapine	-	10	-	2.2	-	0.10	-	3.5	-	0.14	-	4.0	-	16

	Efavirenz	-	7	-	0.14	-	3.4	-	42	-	10.4	-	45	-	49
--	-----------	---	---	---	------	---	-----	---	----	---	------	---	----	---	----

: no sample analysis was done

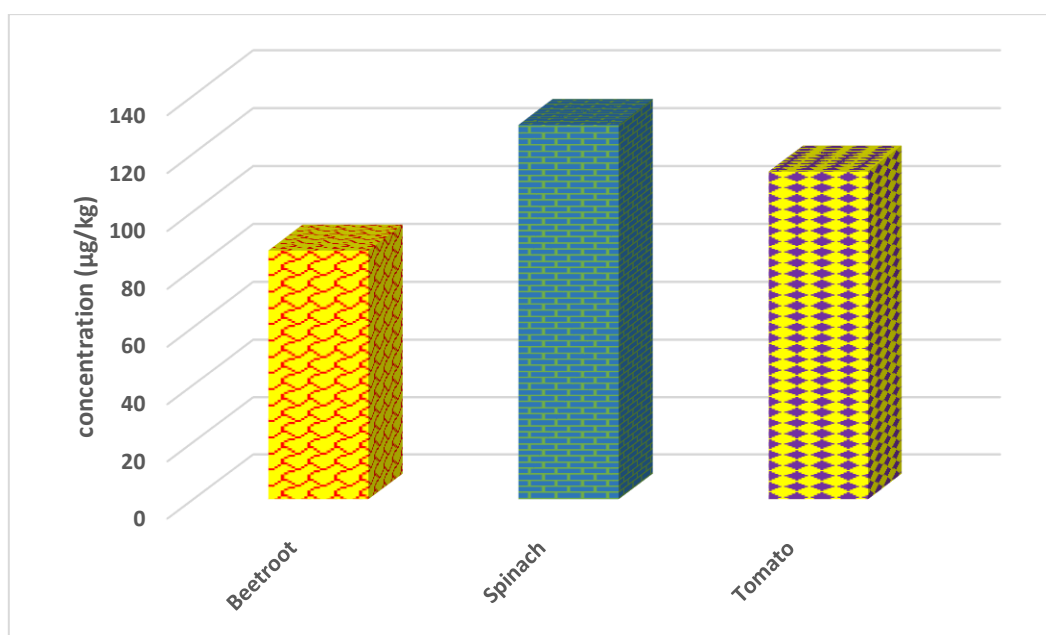


Figure 5.1: The concentrations of the combined ARVDs in each vegetable (beetroot, spinach, and tomato)

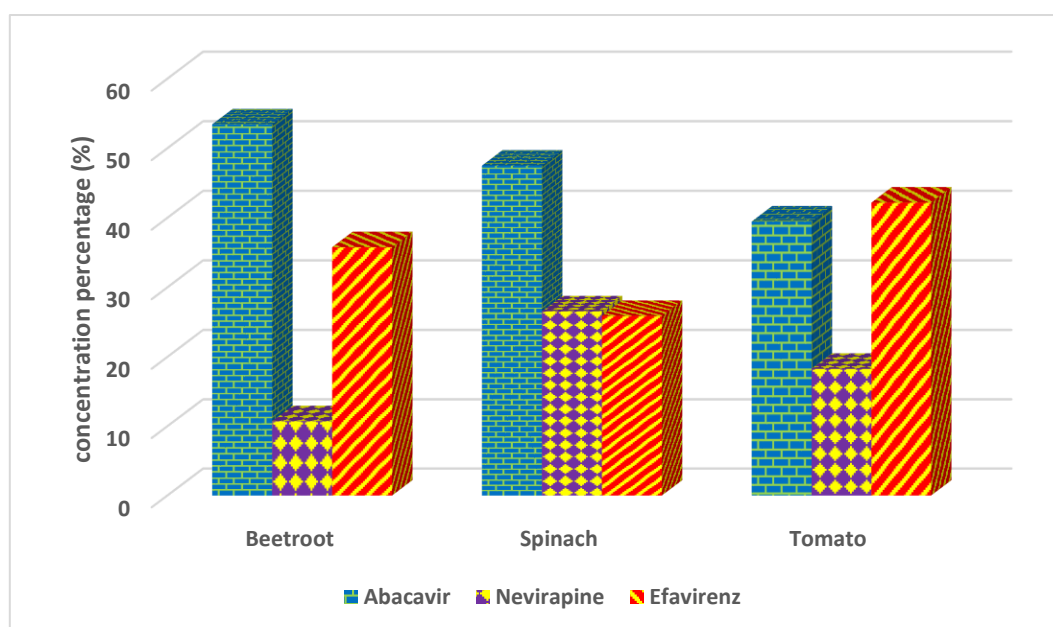


Figure 5.2: The individual ARVDs concentration percentage (%) in each vegetable (beetroot, spinach, and tomato)

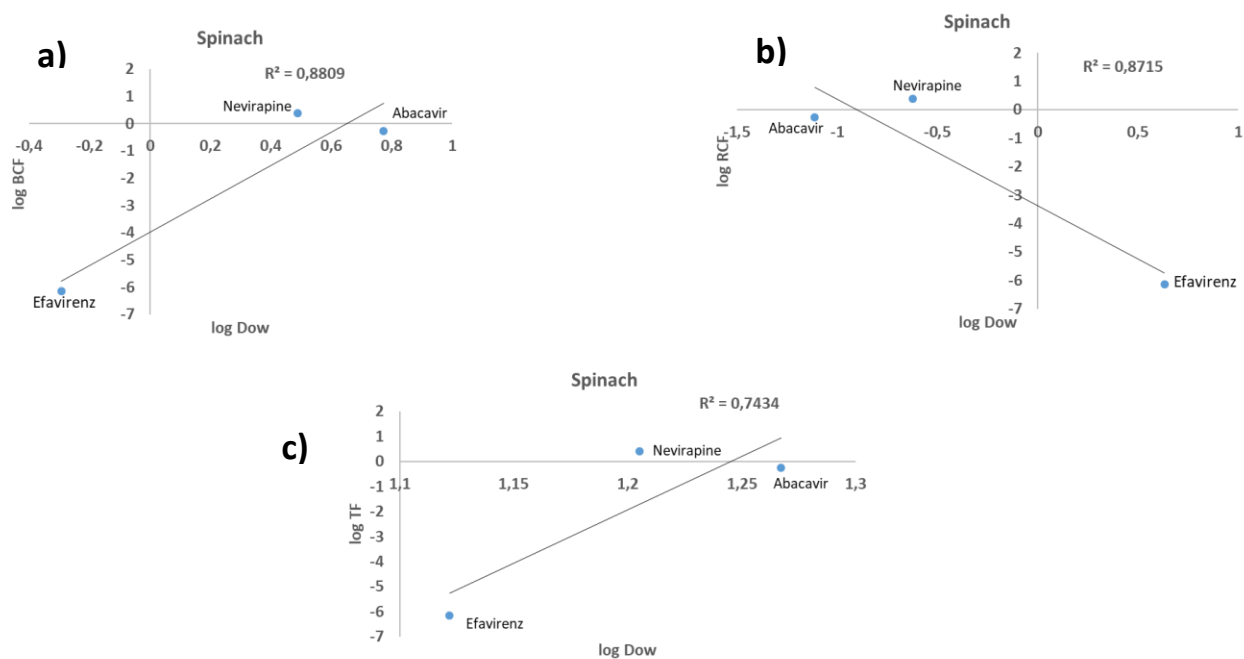


Figure 5.3: Assessment of a relationship between log Dow and BCF (a), RCF (b), and TF (c) in spinach.

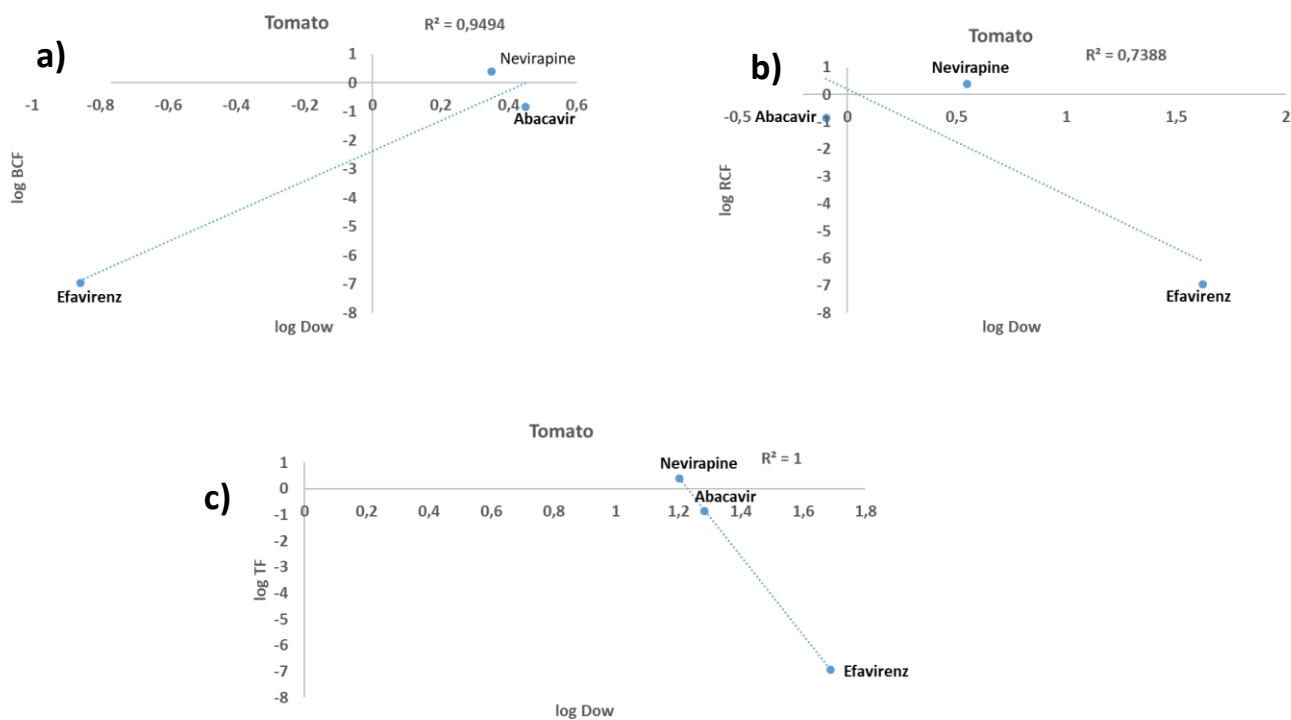


Figure 5.4: Assessment of a relationship between log Dow and BCF (a), RCF (b), and TF (c) in tomato.

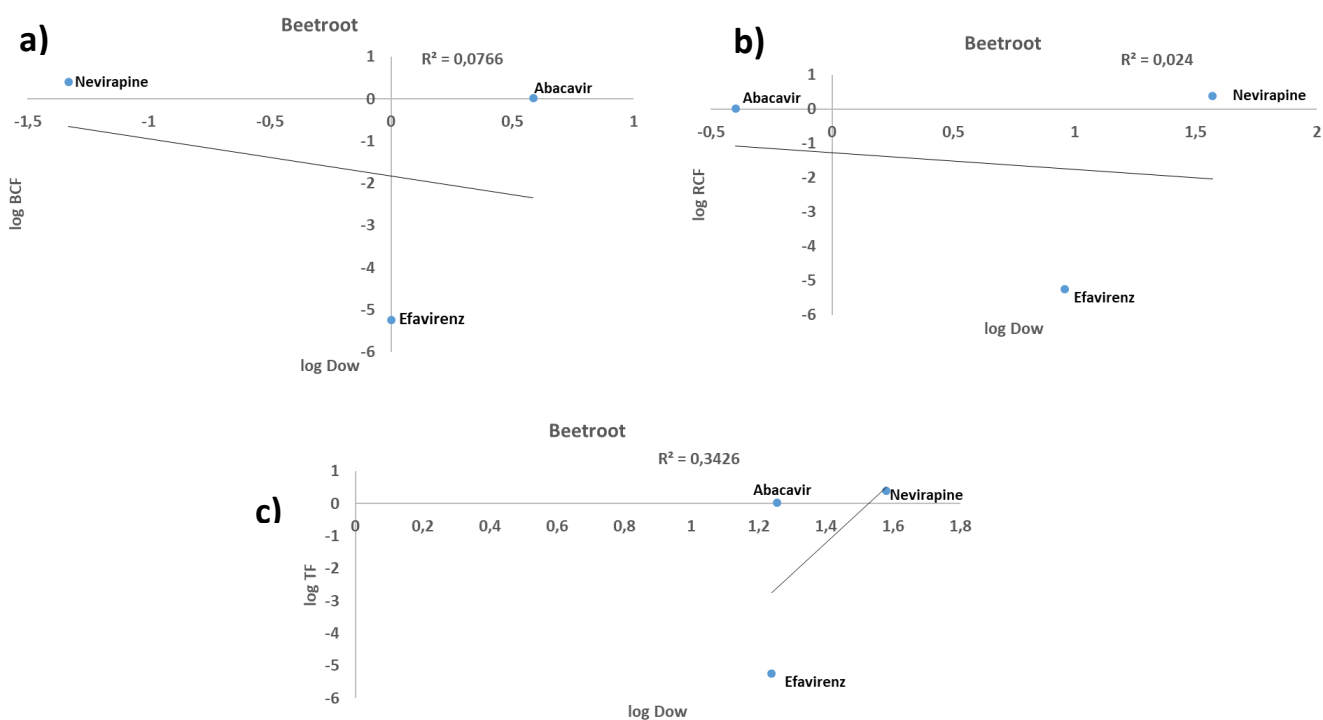


Figure 5.5: Assessment of a relationship between log Dow and BCF (a), RCF (b), and TF (c) in beetroot.

## 5.4. Conclusion

Beetroot, spinach, and tomato showed positive uptake of abacavir, nevirapine, and efavirenz from soil irrigated with antiretroviral drugs spiked tap water. They accumulated ARVDs into roots and translated them to the aerial part of the plant. The highest concentration obtained in soil, beetroot, spinach, and tomato is  $6.77 \pm 20 \mu\text{g/kg}$ ,  $20.45 \pm 30 \mu\text{g/kg}$ ,  $40.21 \pm 31 \mu\text{g/kg}$ , and  $18.56 \pm 18 \mu\text{g/kg}$ , respectively. The accumulation of all the studied ARVDs was higher in spinach roots. High translocation factor from root to stem and leaf was obtained in beetroot and spinach, whereas in tomato was obtained from root to stem, leaf and fruit. It can be concluded that irrigation with contaminated water can transfer ARVDs to the bulk of the plant. Abacavir, nevirapine, and efavirenz are taken up by vegetable plants and thus can pose human health risks upon continuous unplanned consumption. Furthermore, beetroot, spinach, and tomato plants can be employed in the phytoremediation of abacavir, nevirapine, and efavirenz to remove or reduce their concentration levels from contaminated soil.

## References

- Abafe, O. A., Späth, J., Fick, J., Jansson, S., Buckley, C., Stark, A., Pietruschka, B. & Martincigh, B. S. 2018. LC-MS/MS determination of antiretroviral drugs in influents and effluents from wastewater treatment plants in KwaZulu-Natal, South Africa. *Chemosphere*, 200, 660-670. doi:<https://doi.org/10.1016/j.chemosphere.2018.02.105>
- Akenga, P., Gachanja, A., Fitzsimons, M. F., Tappin, A. & Comber, S. 2021. Uptake, accumulation and impact of antiretroviral and antiviral pharmaceutical compounds in lettuce. *Science of The Total Environment*, 766, 144499. doi:<https://doi.org/10.1016/j.scitotenv.2020.144499>
- Al-Farsi, R., Ahmed, M., Al-Busaidi, A. & Choudri, B. 2018. Assessing the presence of pharmaceuticals in soil and plants irrigated with treated wastewater in Oman. *International Journal of Recycling of Organic Waste in Agriculture*, 7, 165-172. doi:<https://doi.org/10.1007/s40093-017-0176-4>
- Al-Farsi, R. S., Ahmed, M., Al-Busaidi, A. & Choudri, B. S. 2017. Translocation of pharmaceuticals and personal care products (PPCPs) into plant tissues: A review. *Emerging Contaminants*, 3, 132-137. doi:<https://doi.org/10.1016/j.emcon.2018.02.001>
- Amos S. P., Naicker, D., Mdluli, P. S. & Madikizela, L. M. 2019. Naproxen, ibuprofen, and diclofenac residues in river water, sediments and Eichhornia crassipes of Mbokodweni

- river in South Africa: an initial screening. *Environmental Forensics*, 20, 129-138.  
doi:<https://doi.org/10.1080/15275922.2019.1597780>
- Archer, E., Petrie, B., Kasprzyk-Hordern, B. & Wolfaardt, G. M. 2017. The fate of pharmaceuticals and personal care products (PPCPs), endocrine disrupting contaminants (EDCs), metabolites and illicit drugs in a WWTW and environmental waters. *Chemosphere*, 174, 437-446.  
doi:<https://doi.org/10.1016/j.chemosphere.2017.01.101>
- Boxall, A. B., Johnson, P., Smith, E. J., Sinclair, C. J., Stutt, E. & Levy, L. S. 2006. Uptake of veterinary medicines from soils into plants. *Journal of Agricultural Food Chemistry*, 54, 2288-2297. doi:<https://doi.org/10.1021/jf053041t>
- Eggen, T., Asp, T. N., Grave, K. & Hormazabal, V. 2011. Uptake and translocation of metformin, ciprofloxacin and narasin in forage-and crop plants. *Chemosphere*, 85, 26-33. doi:<https://doi.org/10.1016/j.chemosphere.2011.06.041>
- García, M. G., Fernández-López, C., Pedrero-Salcedo, F. & Alarcón, J. J. 2018. Absorption of carbamazepine and diclofenac in hydroponically cultivated lettuces and human health risk assessment. *Agricultural Water Management*, 206, 42-47.  
doi:<https://doi.org/10.1016/j.agwat.2018.04.018>
- Goldstein, M., Shenker, M. & Chefetz, B. 2014. Insights into the uptake processes of wastewater-borne pharmaceuticals by vegetables. *Environmental Science and Technology*, 48, 5593-5600. doi:<https://doi.org/10.1021/es5008615>
- Hlengwa, N. & Mahlambi, P. 2020. Ultrasonic Followed by Solid Phase Extraction and Liquid Chromatography-Photodiode Array for Determination of Pharmaceutical Compounds in Sediment and Soil. *Bulletin of Environmental Contamination and Toxicology*, 1-7.  
doi:<https://doi.org/10.1007/s00128-020-02829-6>
- Kumar, K. & Gupta, S. C. 2016. A framework to predict uptake of trace organic compounds by plants. *Journal of Environmental Quality*, 45, 555-564.  
doi:<https://doi.org/10.2134/jeq2015.06.0261>
- Madikizela, L. M., Ncube, S. & Chimuka, L. 2018. Uptake of pharmaceuticals by plants grown under hydroponic conditions and natural occurring plant species: a review. *Science of the Total Environment* 636, 477-486.  
doi:<https://doi.org/10.1016/j.scitotenv.2018.04.297>
- Malchi, T., Maor, Y., Tadmor, G., Shenker, M. & Chefetz, B. 2014. Irrigation of root vegetables with treated wastewater: evaluating uptake of pharmaceuticals and the

- associated human health risks. *Environmental Science and Technology*, 48, 9325-9333. doi:<https://doi.org/10.1021/es5017894>
- Miller, E. L., Nason, S. L., Karthikeyan, K. & Pedersen, J. A. 2016. Root uptake of pharmaceuticals and personal care product ingredients. *Environmental Science Technology*, 50, 525-541. doi:<https://doi.org/10.1021/acs.est.5b01546>
- Mlunguza, N. Y., Ncube, S., Mahlambi, P. N., Chimuka, L. & Madikizela, L. M. 2020. Determination of selected antiretroviral drugs in wastewater, surface water and aquatic plants using hollow fibre liquid phase microextraction and liquid chromatography-tandem mass spectrometry. *Journal of Hazardous Materials*, 382, 121067. doi:<https://doi.org/10.1016/j.jhazmat.2019.121067>
- Mnyandu, H. & Mahlambi, P. 2022. Determination of triazines residues in fruits and vegetables: Methods comparison of ultrasonic solvent extraction with and without solid phase clean-up. *Separation Science and Technology*, 1-9. doi:<https://doi.org/10.1080/01496395.2022.2026391>
- Mosekiemang, T. T., Stander, M. A. & de Villiers, A. 2019. Simultaneous quantification of commonly prescribed antiretroviral drugs and their selected metabolites in aqueous environmental samples by direct injection and solid phase extraction liquid chromatography-tandem mass spectrometry. *Chemosphere*, 220, 983-992. doi:<https://doi.org/10.1016/j.chemosphere.2018.12.205>
- Mtolo, S. P., Mahlambi, P. N. & Madikizela, L. M. 2019. Synthesis and application of a molecularly imprinted polymer in selective solid-phase extraction of efavirenz from water. *Water Science and Technology*, 79, 356-365. doi:<https://doi.org/10.2166/wst.2019.054>
- Ncube, S., Madikizela, L. M., Chimuka, L. & Nindi, M. M. 2018. Environmental fate and ecotoxicological effects of antiretrovirals: A current global status and future perspectives. *Water Research*, 145, 231-247. doi:<https://doi.org/10.1016/j.watres.2018.08.017>
- Obidike, L. & Mulopo, J. Effect of High Concentration of Nevirapine on the Growth of E. Coli in Wastewater Treatment. Proceedings of the World Congress on Engineering and Computer Science, 2018.
- Redshaw, C. H., Wootton, V. G. & Rowland, S. J. 2008. Uptake of the pharmaceutical fluoxetine hydrochloride from growth medium by Brassicaceae. *Phytochemistry*, 69, 2510-2516. doi:<https://doi.org/10.1016/j.phytochem.2008.06.018>



- Rimayi, C., Odusanya, D., Weiss, J. M., de Boer, J. & Chimuka, L. 2018. Contaminants of emerging concern in the Hartbeespoort Dam catchment and the uMngeni River estuary 2016 pollution incident, South Africa. *Science of the Total Environment*, 627, 1008-1017. doi:<https://doi.org/10.1016/j.scitotenv.2018.01.263>
- Sabourin, L., Duenk, P., Bonte-Gelok, S., Payne, M., Lapen, D. R. & Topp, E. 2012. Uptake of pharmaceuticals, hormones and parabens into vegetables grown in soil fertilized with municipal biosolids. *Science of the Total Environment*, 431, 233-236. doi:<https://doi.org/10.1016/j.scitotenv.2012.05.017>
- Schoeman, C., Mashiane, M., Dlamini, M. & Okonkwo, O. 2015. Quantification of selected antiretroviral drugs in a wastewater treatment works in South Africa using GC-TOFMS. *Journal of Chromatography Separation Techniques*, 6, 1-7. doi:<https://doi.org/10.4172/2157-7064.1000272>
- Sun, C., Dudley, S., Trumble, J. & Gan, J. 2018. Pharmaceutical and personal care products-induced stress symptoms and detoxification mechanisms in cucumber plants. *Environmental Pollution*, 234, 39-47. doi:<https://doi.org/10.1016/j.envpol.2017.11.041>
- Varga, M., Dobor, J., Helenkár, A., Jurecska, L., Yao, J. & Záray, G. 2010. Investigation of acidic pharmaceuticals in river water and sediment by microwave-assisted extraction and gas chromatography–mass spectrometry. *Microchemical Journal*, 95, 353-358. doi:<https://doi.org/10.1016/j.microc.2010.02.010>
- Winker, M., Clemens, J., Reich, M., Gulyas, H. & Otterpohl, R. 2010. Ryegrass uptake of carbamazepine and ibuprofen applied by urine fertilization. *Science of the Total Environment*, 408, 1902-1908. doi:<https://doi.org/10.1016/j.scitotenv.2010.01.028>
- Wu, C., Spongberg, A. L., Witter, J. D. & Sridhar, B. M. 2012. Transfer of wastewater associated pharmaceuticals and personal care products to crop plants from biosolids treated soil. *Ecotoxicology and Environmental Safety*, 85, 104-109. doi:<https://doi.org/10.1016/j.ecoenv.2012.08.007>
- Wu, X. L., Meng, L., Wu, Y., Luk, Y.-Y., Ma, Y. & Du, Y. 2015. Evaluation of graphene for dispersive solid-phase extraction of triazine and neonicotine pesticides from environmental water. *Journal of the Brazilian Chemical Society*, 26, 131-139. doi:<https://doi.org/10.5935/0103-5053.20140227>
- Zhang, C., Yao, F., Liu, Y.-w., Chang, H.-q., Li, Z.-j. & Xue, J.-m. 2017. Uptake and translocation of organic pollutants in plants: A review. *Journal of Integrative Agriculture*, 16, 1659-1668. doi:[https://doi.org/10.1016/S2095-3119\(16\)61590-3](https://doi.org/10.1016/S2095-3119(16)61590-3)

Zheng, H., Wang, Z., Zhao, J., Herbert, S. & Xing, B. 2013. Sorption of antibiotic sulfamethoxazole varies with biochars produced at different temperatures. *Environmental Pollution*, 181, 60-67. doi:<https://doi.org/10.1016/j.envpol.2013.05.056>

## Supporting documents

Table S5. 1: Soil parameters before plantation an after harvesting

Soil	Before planting			After harvesting		
	pH	EC (dS/m)	OM (%)	pH	EC (dS/m)	OM (%)
Beetroot	6.9 ± 0.02	1.40 ± 0.01	14.9 ± 0.1	6.6 ± 0.03	1.31 ± 0.01	14.8 ± 0.04
Spinach	6.9 ± 0.02	1.40 ± 0.01	14.9 ± 0.03	5.7 ± 0.09	1.40 ± 0.09	14.5 ± 0.1
Tomato	6.9 ± 0.02	1.40 ± 0.01	14.9 ± 0.04	4.9 ± 0.07	1.35 ± 0.01	14.9 ± 0.06

Table S5. 2: The t-test results for overall concentration of ARVDs in each vegetable plant.

<i>Beetroot</i> <i>Spinach</i>			<i>Beetroot</i> <i>Tomato</i>			<i>Spinac</i> <i>h</i> <i>Tomato</i>		
Mean	28,83	43,30667	Mean	28,83	37,93	Mean	43,31	37,93
Variance	344,3589	255,0172	Variance	344,3589	221,71	Variance	255	221,71
Observations	3	3	Observations	3	3	Observations	3	3
Hypothesized Mean Difference	0		Hypothesized Mean Difference	0		Hypothesized Mean Difference	0	
df	4		df	4		df	4	
t Stat	-1,024187519		t Stat	-0,6624718		t Stat	0,427	
P(T<=t) one-tail	0,181820914		P(T<=t) one-tail	0,27194558		P(T<=t) one-tail	0,346	
t Critical one-tail	2,131846786		t Critical one-tail	2,13184679		t Critical one-tail	2,132	
P(T<=t) two-tail	0,363641829		P(T<=t) two-tail	0,54389117		P(T<=t) two-tail	0,692	
t Critical two-tail	2,776445105		t Critical two-tail	2,77644511		t Critical two-tail	2,776	

Table S5. 3: The t-test result for accumulation of ARVDs in each vegetable plant.

<i>Beetroot</i> <i>Spinach</i>			<i>Beetroot</i> <i>Tomato</i>			<i>Spinach</i> <i>Tomato</i>		
Mean	8,15239	6,7245106	Mean	8,152388	7,994882	Mean	6,7245	7,994882
Variance	34,9683	6,5572159	Variance	34,96826	4,652734	Variance	6,5572	4,652734
Observations	3	3	Observations	3	3	Observations	3	3
Hypothesized Mean Difference	0		Hypothesized Mean Difference	0		Hypothesized Mean Difference	0	
df	3		df	3		df	4	
t Stat	0,38379		t Stat	0,043341		t Stat	-0,657	
P(T<=t) one-tail	0,36336		P(T<=t) one-tail	0,484077		P(T<=t) one-tail	0,2735	
t Critical one-tail	2,35336		t Critical one-tail	2,353363		t Critical one-tail	2,1318	
P(T<=t) two-tail	0,72672		P(T<=t) two-tail	0,968153		P(T<=t) two-tail	0,547	
t Critical two-tail	3,18245		t Critical two-tail	3,182446		t Critical two-tail	2,7764	

## Chapter six

---

### 6. Adsorption of abacavir, nevirapine, and efavirenz antiretroviral drugs from river water and wastewater using exfoliated graphite: isotherm and kinetic studies

#### Abstract

In this work, the exfoliated graphite was used to absorb antiretroviral drugs from river water and wastewater. The exfoliated graphite was prepared from natural graphite by intercalating it with the acids and exfoliating it at 800°C. The exfoliated graphite characterization using the Fourier Transform Infrared Spectroscopy showed functional groups such as phenolic, alcoholic, and carboxylic groups between 1000 cm<sup>-1</sup> and 1700 cm<sup>-1</sup>. This was further confirmed by Energy-dispersive X-ray spectroscopy results, which showed carbon as the main element and splashes of oxygen. The Scanning Electron Microscopy images showed increased c-axis distance between graphene layers after intercalation, which further increased after the exfoliation. The exfoliation at 800°C resulted in elongated absorbent, distorted cylinders, which were confirmed by the lower density of exfoliated graphite material compared to the natural graphite density. The X-ray diffraction pattern showed the characteristics of hexagonal phase graphitic structure by the diffraction plans (002) and (110). Raman spectroscopy results showed the natural graphite, graphite intercalated, and exfoliated graphite contained the D, G, D', and G' peaks at about 1350 cm<sup>-1</sup>, 1570 cm<sup>-1</sup>, 2440 cm<sup>-1</sup>, and 2720 cm<sup>-1</sup>, respectively indicating that the material's crystallinity was not affected by the modification. The parameters that affect the adsorption capacity and removal percentage (pH of a solution, adsorbent mass, and initial concentration and adsorption time) were investigated. The highest antiretroviral drugs removal from the water was achieved with a solution pH of 7, an adsorbent mass of 60 mg, and an adsorption time of 30 minutes. The kinetic model and adsorption isotherm studies showed that the experimental data fit well in pseudo-second-order kinetics and is well explained by Freundlich's adsorption isotherm. The maximum adsorption capacity of the exfoliated graphite for antiretroviral drugs ranges between 1.660-197.0, 1.660-232.5, and 1.650-237.7 mg/g for abacavir, nevirapine, and efavirenz, respectively.

#### 6.1. Introduction

Pharmaceuticals are natural or synthetic chemicals used in veterinary or human drugs as they consist of active ingredients designed to impact animals and human health positively. The pharmaceuticals in the human body could undergo metabolic reactions by enzymes resulting in metabolites. These metabolites and active compounds are excreted via faeces or urine, thus

introduced into the wastewater system, and eventually reach wastewater treatment plants (Madikizela and Chimuka, 2017). Pharmaceuticals in the environment could also arise from the discharging of expired drugs, households, hospital wastewater, and pharmaceutical industries (Elbalkiny et al., 2019). It has been reported that the presence of pharmaceuticals in river water is due to the wastewater treatment plants (WWTPs) discharges (Alvarez et al., 2005). These compounds are soluble in water and are highly polar, allowing them to easily outflow in wastewater treatment processes (Zunngu et al., 2017). The WWTPs are primarily designed to remove nutrients effectively, dissolved organic matter, and solids (Kebede et al., 2020); hence some pharmaceutical compounds are discharged with the effluent. In addition, it was reported that during wastewater treatment processes, de-conjugation occurs, and some metabolites return to their biologically active form resulting in their presence in the effluent and thus are discharged into the receiving rivers (Amdany et al., 2014).

Pharmaceuticals, such as antiretroviral drugs (ARVDs),  $\beta$ -blockers, contraceptives, non-steroidal anti-inflammatory drugs, sedatives, antidepressants, and antibiotics, are the most used compounds. This makes them emerging pollutants frequently detected in environmental water bodies (Luo et al., 2014, Wood et al., 2015, Mtolo et al., 2019). The ARVDs are amongst the regularly detected pharmaceuticals in countries and regions where HIV is prevalent (Ncube et al., 2018, Mlunguza et al., 2020). It has been reported that African countries have the highest number of people living with HIV, and in 2021 about 8.2 million people started antiretroviral treatment therapy (Adeola and Forbes, 2021). As a result, many research groups reported ARVDs occurrence in environmental samples. The presence of ARVDs in the environment raises concern due to their potentially deleterious impact on human health if unintentionally consumed from contaminated water and food and also in the aquatic organism if they are exposed to polluted water (Madikizela et al., 2017). Abacavir antiretroviral drug can cause disturbances in the central nervous system, such as psychosis and mania. Efavirenz is also associated with the toxicity central nervous system, resulting in vivid dreams, irritation, and sleeplessness (Abers et al., 2014). It has been reported that fish exposed to ARVDs contaminated water had livers aberration (Rimayi et al., 2018). The effect of ARVDs on the environment is not yet known; however, prolonged unintentional consumption of ARVDs could result in drug resistance (Mtolo et al., 2019). The effect associated with the ARVDs suggests the importance of the further search for their effective removal strategies from water sources.

The different methods that have been used for the removal of ARVDs and related drugs from water include adsorption (Kebede et al., 2020), coagulation (Xu et al., 2016), photo-Fenton, Fenton-like (Tang and Wang, 2020, Zhuan and Wang, 2020), photocatalysis (Hu et al., 2019), filtration (Liu et al., 2018), degradation, and photodegradation (Thakur et al., 2020, Hemmat et al., 2021), as well as membrane bioreactors (Radjenovic et al., 2007). Among the mentioned methods, adsorption is commonly used. This method is better and deliberated as a powerful alternative to conventional treatment methods for the removal of pollutants due to its versatility, low cost, reliability, simplicity, high capacity, great efficiency, ease of operation, and consume less energy (Rosli et al., 2021). They are environmentally friendly as there are low chances of generating secondary pollutants or unsolicited by-products (Adeola and Forbes, 2021).

It has been reported that the graphite-based sorbents have the ability to adsorb various contaminants such as halogenated organic dyes (Mohanraj et al., 2020), pharmaceuticals (Adeola and Forbes, 2021) due to their large surface area, delocalized  $\pi$ - $\pi$  electron system that can create a stable bonding with different contaminants (Al-Khateeb et al., 2014). Exfoliated graphite (EG) is a carbon-based material that displays a beehive-like structure, puffed-up with a low density and high thermal stability. The EG may result in a highly flexible and lubricate material when it is compressed, and in composite, it can be used as a filter (Chung, 1987). The EG's high potential surface area is achieved by disentangling the layers of graphite via intercalation prior to exfoliation. Furthermore, EG is manufactured at a minimal time and at a low cost, and its synthesis results in a high yield (Mohanraj et al., 2020).

In this study, a large surface area EG was employed for the first time to adsorb three ARVDs, (abacavir, nevirapine, and efavirenz). The studied ARVDs were selected based on their frequent detection in water as they are used as active ingredients or combined with other compounds to treat human immunodeficiency virus (HIV) type-1 and prevent the transfer of HIV from the mother to the unborn baby. Various parameters that affect the adsorption process, such as the pH of a solution, adsorbent mass, initial concentration, and adsorption time, were studied to obtain conditions that will allow high adsorption of the ARVDs from contaminated water. The adsorption equilibrium was analysed by using Freundlich and Langmuir isotherms. The mechanism and behaviour of adsorption were determined using the kinetic models' pseudo-first order and pseudo-second order.

## **6.2. Experimental**

### **6.2.1. Chemical and reagents**

Analytical grade reagents with a high purity  $\geq 95\%$  were used. Abacavir, nevirapine, and efavirenz were purchased from J & H Chemical Co. LTD (Hangzhou Zhejiang, China). Graphite was purchased from Sigma Aldrich (Johannesburg, South Africa). Nitric acid ( $\text{HNO}_3$ ) and sulphuric acid ( $\text{H}_2\text{SO}_4$ ) were purchased from Merck Chemicals (Johannesburg, South Africa). The solutions were prepared using distilled water from the distillation system.

### **6.2.2. Preparation of exfoliated graphite**

Natural graphite (NG) pieces of molecule estimated at  $300\ \mu\text{m}$  were intercalated with bisulfate anion for 24 hours by splashing in a blend of concentrated  $\text{H}_2\text{SO}_4$  and  $\text{HNO}_3$  (3:1, v/v) in surrounding conditions to produce graphite intercalated compound (GIC). The intercalated material was thoroughly washed to remove sulfate ions and to reach a pH of 7. The GIC was subjected to thermal shock at  $800\ ^\circ\text{C}$  for almost 30 seconds driving the intercalated material out of the graphite cross-section, in this manner breaking the layers as the intercalates were vaporized and ejected out of the graphite layers. The obtained material was alluded to as EG. This approach comes about within the puffed material termed exfoliated graphite (EG) (Ndlovu et al., 2011).

### **6.2.3. Stock solution preparation**

The stock solution was prepared in a 100 mL volumetric flask by weighing 10 mg of individual salt and dissolving in acetonitrile to make a final concentration of 100 mg/L solutions. The mixture was shaken for 1 minute and ultrasonicated for 2 minutes to permit a complete dissolution of salts. The working standards of series concentrations ranging from 0.2 to 1 mg/L were prepared by diluting the stock solution using acetonitrile as a diluent. They were then used to calibrate the high-performance liquid chromatography coupled with photodiode array detection (HPLC-PDA).

### **6.2.4. Instrumentation and liquid chromatography conditions**

The 2020 LC system and the 2030/2040 photo-diode array (PDA) detector used for detection and quantification were purchased from Shimadzu (Tokyo, Japan). The autosampler was employed to inject the standard solution of the ARVDs mixture and samples into the LC system. The column used to separate the ARVDs was a Shim-Pack GIST C18-HP (4.6

mm×150 mm, 3 m) purchased from Shimadzu (Tokyo, Japan). Gradient elution was applied to separate the compounds at a reasonable retention time. A gradient program started with 50% acetonitrile: 50% water from 0 to 5 minutes and 70% acetonitrile: 30% water from 6 minutes to 12 minutes. Compounds were detected at 225 nm and 274 nm wavelengths, and a flow rate of 0.4 mL/min was used.

The Fourier Transformed Infrared Spectroscopy (FTIR) was used to confirm the presence of functional groups in the material. The elemental composition and morphology of the EG were determined by utilizing energy dispersive x-ray spectroscopy (EDX), and scanning electron microscopy (SEM) from a JEO microscope (JSM840A) set off at 20 kV. The powder x-ray diffraction (XRD) was used to assess the graphitic structure of the graphite using the Rigaku MiniFlex600. The crystallinity of the exfoliated graphite was assessed using Renishaw inVia Raman microscope, and 600 grooves mm<sup>-1</sup> at an excitation wavelength of 514 nm. The FMH SHKO 20 orbital shaker purchased from DLD Scientific cc (Durban, South Africa) was used to shake the sample at 350 rpm.

#### **6.2.5. Batch adsorption**

The batch adsorption studies were conducted to measure adsorption equilibrium and kinetics of the exfoliated graphite in ARVDs solutions. This was conducted by separately adding measured quantities of EG 30 mg to each 10 mL of ARVDs in a polytome, followed by shaking for 30 minutes at room temperature. A 1 mL of each solution was filtered with a 2 µm syringe filter to a 2 mL LC vial, and the filtrate containing the remaining target analytes was analysed using the LC-PDA. The effect of adsorbent mass and adsorption time on the adsorption efficiency of exfoliated graphite was examined at 10 - 60 mg and 5 - 60 minutes, respectively.

#### **6.2.6. Sample collection**

Wastewater samples, effluent and influent were collected from wastewater treatment plants (WWTPs) located in Durban and Pietermaritzburg (KwaZulu-Natal, South Africa). The river water samples were collected from Pietermaritzburg along Umsunduzi River (College Road, and Bishop Store), a stream with an elevation of 47 meters and located in the North of Nteneshe and West of Buyingoma. Msunduzi passes through the households, agricultural areas, hospitals, and companies; hence there are possible discharges of pollutants including ARVDs into Umsunduzi River. Furthermore, Darville WWTPs is also a possible source of pollution as

it discharges effluent to Msunduzi River (Mtolo et al., 2019). Msunduzi receive the d Samples were collected into pre-cleaned 2.5 mL amber bottles. They were kept in the cooler box and transported into the laboratory, where they were filtered and kept in the refrigerator at 4°C until analysis time. The Global Positioning System (GPS) system was used to point the sampling points accurately, and the collected samples' physicochemical parameters were measured on sites. The coordination and parameter data are recorded in Table S6.1.

### **6.3. Result and discussion**

#### **6.3.1. Preparation of exfoliated graphite**

The EG materials was synthesized by intercalating the particles of NG with bisulphate anion and exfoliating at 800°C.

The volume of the material showed an increase during graphite exfoliation process as the bisulfate ions are vaporized and violent ejection at the extremely rapid temperature increases which resulted in graphite layers separation. The densities of the EG materials were determined by taking two different volumes measuring cylinders and adding the EG material without compacting it. The obtained weight and volume of EG were then used to calculate the densities of the EG materials. The obtained results were 0.0068, 0.144, and 0.54 g mL<sup>-1</sup> for EG, GIC, and NG, respectively, indicating that EG has a lower density. It was noticed that the density of EG is approximately eighty times less than the density of NG as a result of the largest c-axis distance observed after exfoliation. This result agrees with the study reported (Goudarzi and Motlagh, 2019), where the increase in temperatures up 800°C was proportional to increasing the exfoliation volume. In another reported study, a slightly high density of 0.019 mL<sup>-1</sup> was observed after exfoliated at 1000 °C (Bannov et al., 2021).

#### **6.3.2. Characterisation of exfoliated graphite**

The prepared exfoliated graphite was then characterized using low density, and analytical techniques such as SEM, EDX, FTIR, Raman spectroscopy, and XRD.

##### **6.3.2.1. SEM and EDX analysis**

The SEM results revealed that the NG particles had a smooth surfaced flake-like structure in morphology with a size range of 400-500 µm (Figure 6.1a). The SEM images showed an increase in the c-axis distance between graphene layers after the intercalation (Figure 6.1b). This was expected as the bisulfate ions were intercalated between these layers while exfoliation



expelled them, resulting in an accordion-like structure due to a further increase in the c-axis distance (Figure 6.1c) which is why EG has a lower density than the NG. The elongated, absorbent, distorted cylinders result were observed for exfoliated graphite where the length of particles was longer than the initial length with an unchanged diameter (Idris et al., 2022, Moosa and Abed, 2021).

The EDX spectrum showed that carbon was the main component in all the graphite materials. For the NG, only carbon peak was observed (Figure 6.1d), whereas, the GIC and EG material showed carbon and oxygen peaks (Figure 6.1e). The presence of oxygen in these materials was due to the oxygen containing functional groups added in NG in the intercalation stage. Similar observations were reported by Ndlovu (2012) for the exfoliated graphite material.

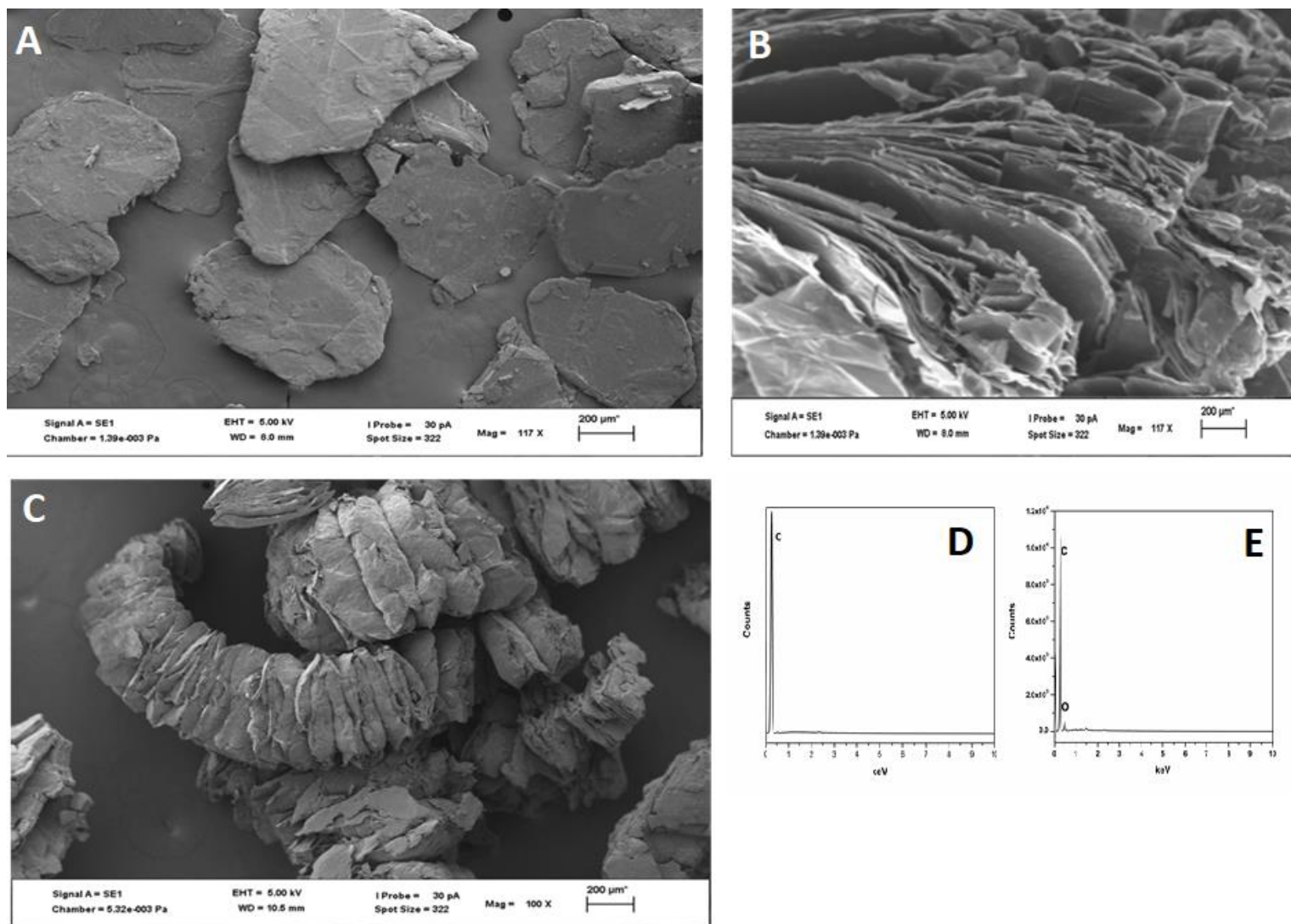


Figure 6.1: SEM images for NG (a), GIC (b), EG worm-like structure (c), EDX spectrum for NG (d) and EG (e).

### 6.3.2.2. Fourier-transform infrared spectroscopy

The FTIR results showed the C=C functional group with the peak at  $1635\text{ cm}^{-1}$  which was observed in the NG, GIC, and EG spectrums due to that C=C is the graphite base. The result also showed an increase in oxygen-containing group for GIC and EG compared to NG was observed (Figure 6.2). This is because NG is treated with a mixture of  $\text{HNO}_3$  and  $\text{H}_2\text{SO}_4$  to obtain GIC, which is eventually exfoliated at high temperature ( $800^\circ\text{C}$ ). The acid mixture introduces oxygen functional groups that consist of oxygen such as phenolic ( $1069\text{ cm}^{-1}$ ), alcoholic ( $1211\text{ cm}^{-1}$ ), and carboxylic groups ( $1651\text{ cm}^{-1}$ ) in the GIC and EG in dissimilar intensities. The GIC had peaks with high intensities than the EG and this can be considered a confirmation of a successful exfoliation process as it facilitate the decomposition or ejection of intercalates. This was also confirmed by EDX results which showed that NG was mainly carbon, while the EG had a visible oxygen peak due to oxidation by the acid mixture, as observed on the other reported study (Ndlovu et al., 2011). The NG and EG spectrums have similar shape of peaks due to that during exfoliation some acid ions are ejected from the GIC. These FTIR result also show a positive synthesis of EG.

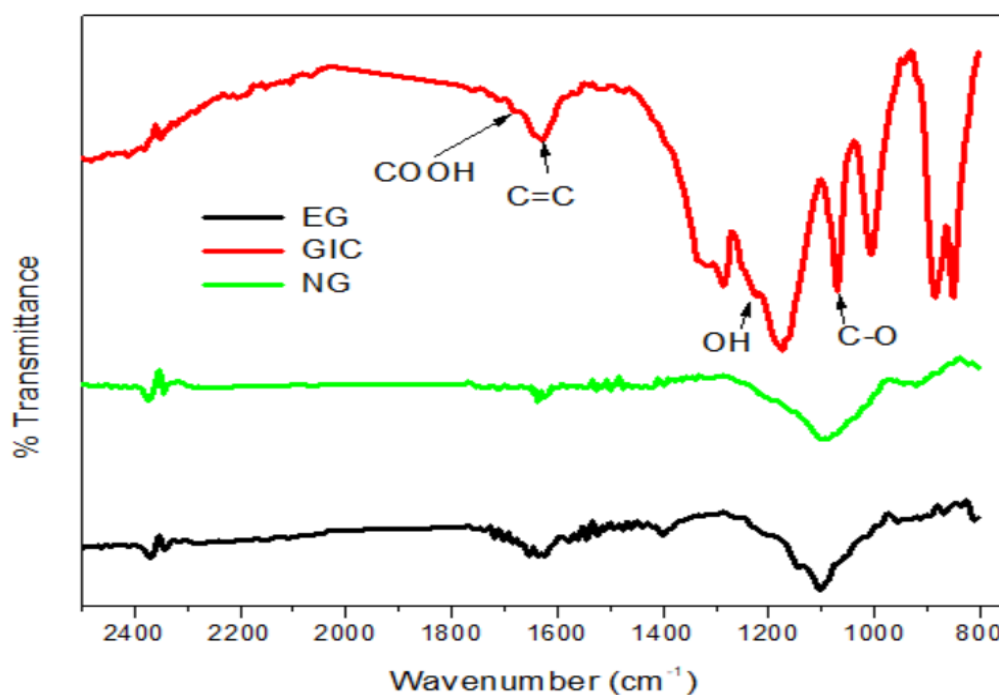


Figure 6.2: The FTIR spectrum of NG, GIC, and EG

### 6.3.2.3. Raman spectroscopy analysis

Raman spectroscopy result for graphite material normally show two intense bands which are the G and G' peaks at  $\approx 1580\text{ cm}^{-1}$  and  $2700\text{ cm}^{-1}$ . The G band indicate the  $\text{sp}^2$  carbon as a result of the doubly degenerate zone center  $\text{E}_{2g}$  mode. Whereas the G' band is the noticeable band detected in graphite materials which signals the second order of zone-boundary phonons (Dhakate et al., 2011). The defected graphite result in the peaks at  $\approx 1350\text{ cm}^{-1}$  and  $\approx 2400\text{ cm}^{-1}$  which are named D and D' bands. For the EG these peaks are normally observed due to defects or disorder that happen during intercalation and exfoliation (Wang et al., 2017). Raman spectroscopy results in this study showed that the crystallinity of the material was not affected by the intercalation and exfoliation processes as observed from the  $I_D/I_G$  ration which were found to be 0.107, 0.303, and 0.146 for NG, GIC, and EG respectively. The NG, GIC, and EG contained the D, G, D' and G' peaks at about  $1350\text{ cm}^{-1}$ ,  $1570\text{ cm}^{-1}$ ,  $2440\text{ cm}^{-1}$ , and  $2720\text{ cm}^{-1}$ , respectively (Figure 6.3). These results were consistent with other Raman Spectroscopy characterization of similar materials (Ndlovu, 2012).

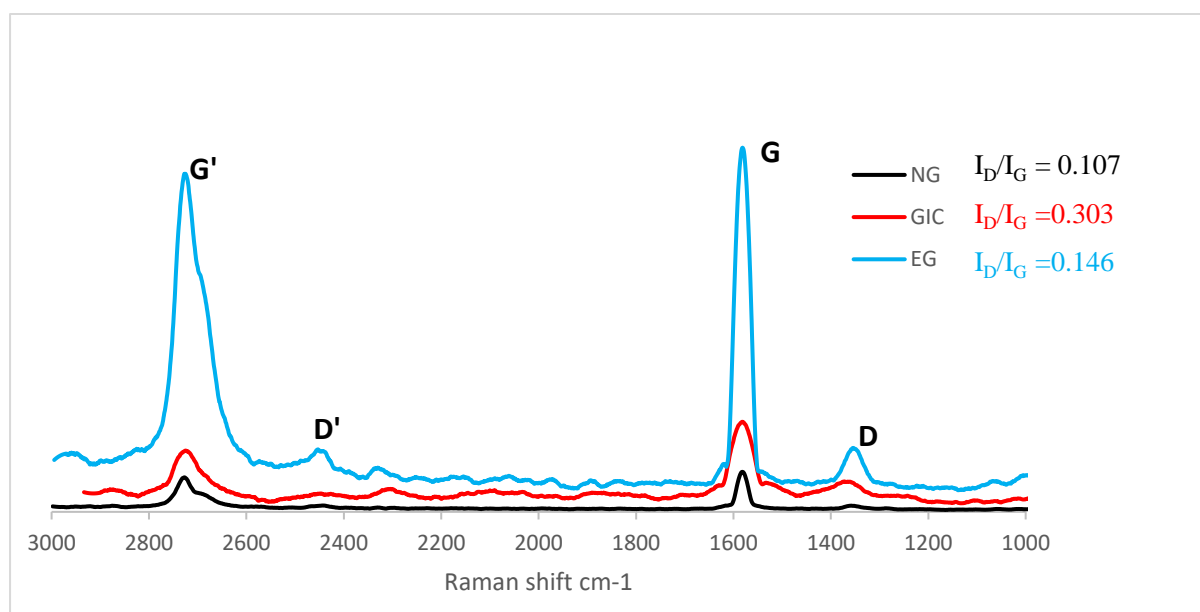


Figure 6.3: Raman spectrum of the different graphite material

### 6.3.2.4. X-ray diffraction analysis

The XRD patterns for NG, GIC, and EG material are exhibited in Figure 6.4. Two reflections were observed for the EG which are (002). The presence of these diffraction plans in the EG material indicates the presence of a hexagonal phase graphitic structure (Idris et al., 2022). In

the presented pattern, it was observed that all the graphite material showed the presence of one dominant peak at around  $26.74^\circ$ ,  $26.68^\circ$ , and  $26.02^\circ$  for NG, GIC, and EG, respectively. The XRD patterns of NG revealed that the peaks at  $26.74^\circ$  with inter planar distance of  $3.33 \text{ \AA}$  corresponds to the diffraction of (002) plane. Such results were reported by Bannov et al. (2021). The GIC showed a slightly broad peak at  $26.68^\circ$ . The broadening could be due to staking fault which is caused by the presence of acids. The similar observations were previously reported, where the staking faults were confirmed to be less at high than at a low exfoliation temperature (Ndlovu, 2012).

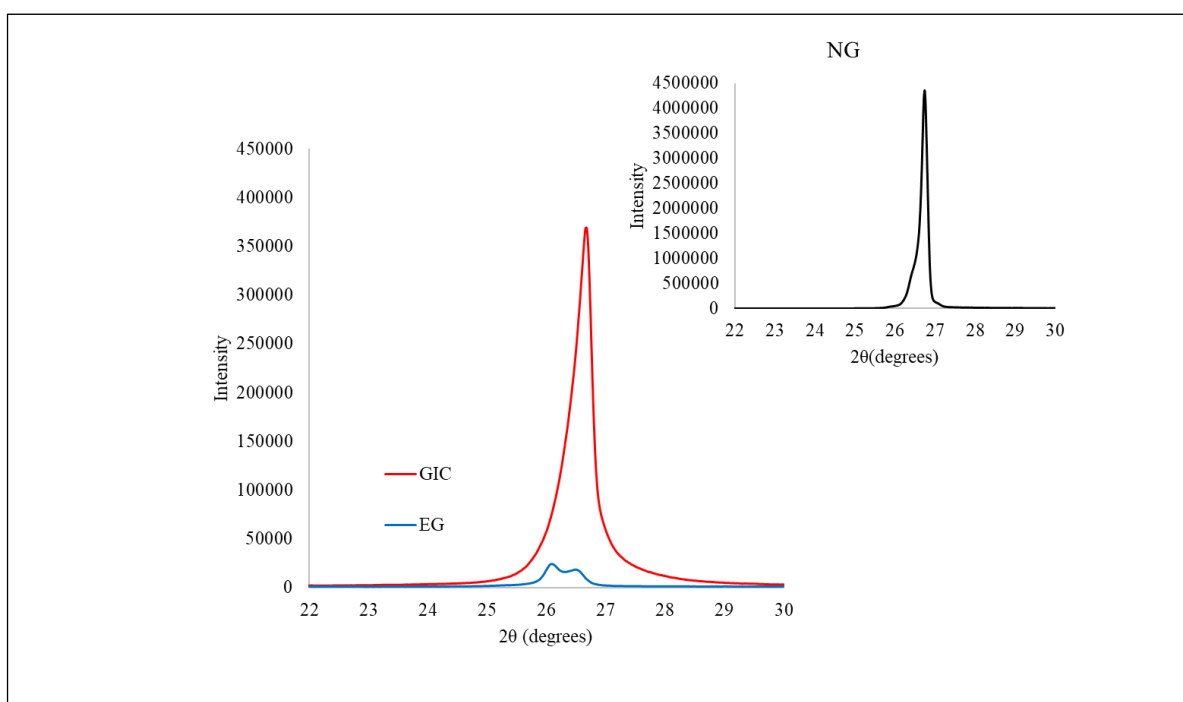


Figure 6.4: XRD pattern for NG, GIC, and EG

### 6.3.2.5. Point of Zero Charge ( $\text{pH}_{\text{PZC}}$ )

The pH where the net total particle charge is zero is called the point of zero charge ( $\text{pH}_{\text{PZC}}$ ) (Sharma, 2009). It is one of the significant parameters used to define variable-charge surfaces. If the pH of the material is above its  $\text{pH}_{\text{PZC}}$ , the surface will have a net negative charge and mainly show an ability to exchange cations. In contrast, if its pH is below its  $\text{pH}_{\text{PZC}}$ , the surface will have a net positive charge and mostly retain anions (electrostatically) (Zyoud et al., 2019). Hence, the functional groups present on the surface of any material are anticipated to partake in the charge-based repulsion of the analyte depending on the pH of the medium. The obtained  $\text{pH}_{\text{PZC}}$  for the different graphitic materials was 7.28, 3.25, and 6.31 for NG, GIC, and EG,

respectively (Figure 6.5). The plateau of the  $\Delta\text{pH}$  plot corresponds to the pH range where the buffering effect of the material takes place, where for all initial pH in that range, the final pH is almost the same and corresponds to  $\text{pH}_{\text{pzc}}$  (Ndlovu, 2012). For instance, the pH region where NG buffers the solution is from  $\sim 5$  to  $\sim 10$ . This implies that for all values of initial pH and the final pH are the same between pH 5 and 10, and equal to the  $\text{pH}_{\text{pzc}}$  (7.28). The near neutral  $\text{pH}_{\text{pzc}}$  for NG could be due to the absence of functional groups. The intercalation step introduces acidic and hydroxyl groups, shifting the  $\text{pH}_{\text{pzc}}$  to be acidic. This was observed for GIC, which had a  $\text{pH}_{\text{pzc}}$  of 3.25. The  $\text{pH}_{\text{pzc}}$  for EG was above pH 6. This indicates a decrease in the functional groups prompted by the acids on the surface of these materials, therefore increasing the  $\text{pH}_{\text{pzc}}$ .

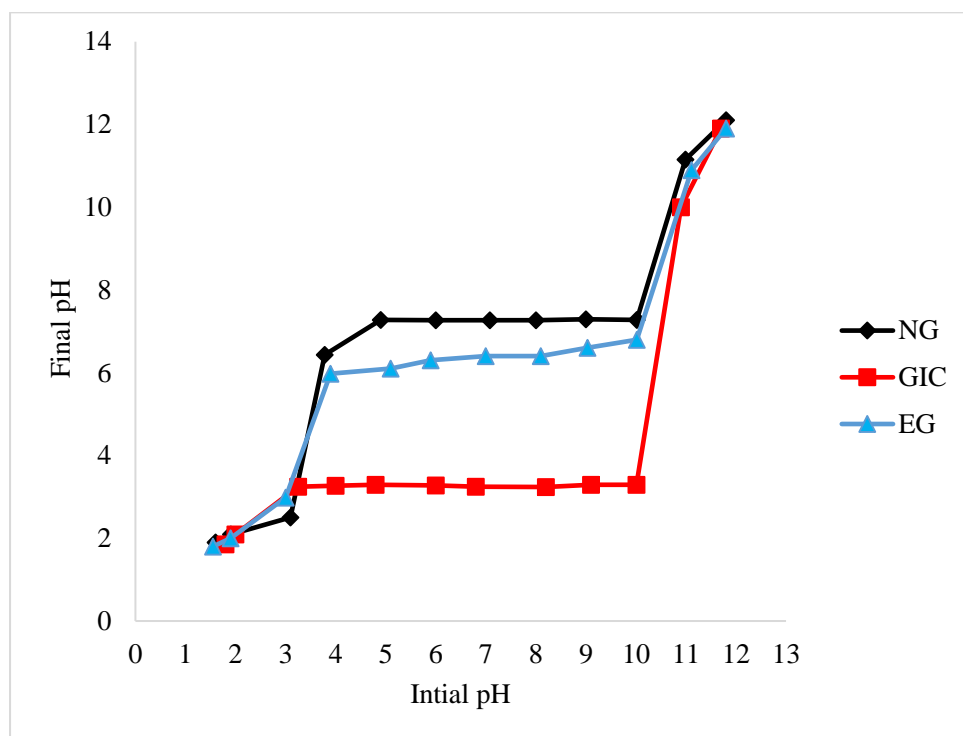


Figure 6.5: Point of Zero Charge graph for the different graphite material

### 6.3.3. Adsorption studies

The absorption capacity of graphite was investigated using the absorption method in order to determine the interaction rate and equilibrium. The absorption capacity of the target analytes was calculated using equation (1)

$$q_e = \frac{(C_o - C_f)V}{m} \quad (1)$$

Where  $q_e$  is the absorbed ARVDs per unit mass of EG (mg/g),  $m$  is the EG sorbent (g),  $V$  is the volume (L) of the absorption solution, and  $C_o$  and  $C_f$  are the initial and final concentration (mg/L) of ARVDs respectively.

The removal percentages (%R) of abacavir, nevirapine, and efavirenz were determined by using the following equation:

$$\% R = \frac{(C_o - C_t)}{C_o} \quad (2)$$

Where  $C_t$  is the concentration (mg/L) of the single drug at a given time (minutes)

#### **6.3.3.1. Effect of initial sorbate concentration**

The series of concentrations levels ranging from 0.01 to 2 mg/L were used to evaluate the absorption capacity. The amount of ARVDs absorbed per unit mass of EG adsorbent,  $q_e$  ( $\mu\text{g}/\text{mg}$ ), increased as the corresponding concentration increased from 0.01 to 2  $\mu\text{g}/\text{L}$ . The  $q_e$  values for the selected ARVDs increased at a maximum initial sorbate concentration (2mg/L), ranging from 1.660-197.0; 1.660-232.5, and 1.650-237.7 mg/g for abacavir, nevirapine, and efavirenz, respectively. This adsorption behaviour could be due to the high concentration ramp of analytes, which is the controlling force in mass transfer (Kebede et al., 2020). On the other hand, the removal percentage decreased as the concentration increases (Figure 6.5), resulting from the saturation of the active site in the sorbent. Similar behaviour was observed in a study conducted where Elbalkiny and co-workers where mesoporous silica nanoparticles were used to remove cephalosporins antibiotics in wastewater (Elbalkiny et al., 2019).

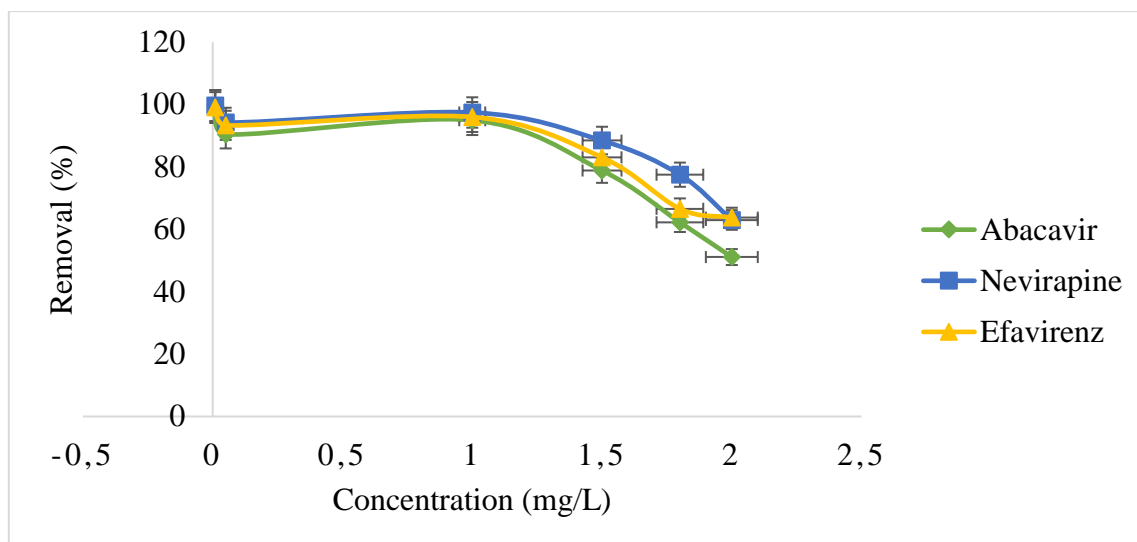


Figure 6.5: Initial adsorbate dosage effect on the removal percentage removal values of ARVDs onto EG

### 6.3.3.2. Effect of pH

The effect of pH on the efficiency of EG to remove ARVDs was investigated by mixing 30 mg of EG with 5 mL of 1 mg/L concentration of ARVDs solution. Varying the pH values in the absorption method may result in changing the adsorbent surface charges, degree of ionization, and adsorbent speciation (Yao et al., 2010). The pH was varied from 2 to pH 11. At a low pH below the pKa, the positive charges were predominant as the amine groups in the ARVDs were protonated, and the surface of the sorbent was positively charged. As a result, the low removal percentages were obtained due to electrostatic repulsion between the analyte and the sorbent (Kebede et al., 2020). The  $pH_{ZPC}$  of EG supports that as it was found at 6.31 which simple suggest that the sorbent surface has a net negative charge at pH greater than  $pH_{ZPC}$ , therefore, it mainly exchange positive charged compounds (Zyoud et al., 2019). The percentage removal increased with increasing pH from 2 to 7, abacavir (34 - 95%), nevirapine (34 – 97%), and efavirenz (50 - 98 %), (Figure 6.6). At pH 7 the compounds are in neutral form; they are expected to diffuse through sorbent surface or bond to the EG in positive charge via molecular interaction and hydrogen bonding, resulting in high removal percentages (Kebede et al., 2020). As the pH was further increased to pH 11. High removals of ARVDs were observed with a slight decrease in abacavir and nevirapine, which could be due to repulsion as the EG and the functional groups were negatively charged. The pH of efavirenz was below the pKa, therefore its functional group existed in the conjugate acid form. Efavirenz is highly soluble at alkaline



pH (pH 9), which could be the reason for a slight increase observed in its removal percentages (Panikumar et al., 2012). The pH 7 was then taken as the optimum pH.

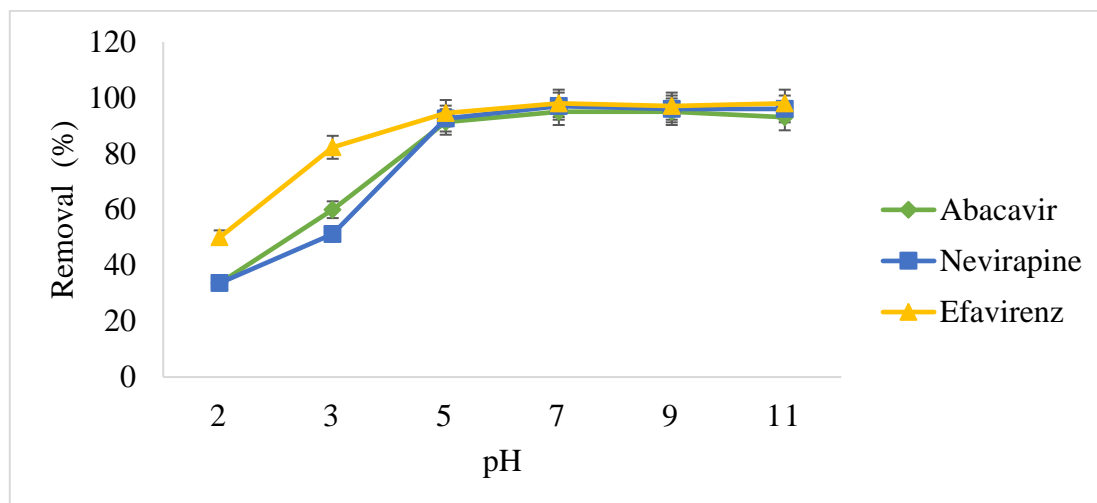


Figure 6.6: Effect of pH variation on ARVDs percentage removal onto EG

### 6.3.3.3. Effect of sorbent dosage

The sorbent mass was investigated as the higher the sorbent mass increases the active binding sites present in the surface of the sorbent and thus increases the ARVDs chelating (El-Araby et al., 2019). However, the removal percentages for ARVDs were comparable as the EG dosage gradually increased from 10 to 60 mg (Figure 6.7). This could be due to the overlapping of active sites, which hinder the chelation of ARVDs into the active site in the sorbent (Kebede et al., 2020). The obtained percentage removals and adsorption capacity ranged between 95-99 %.

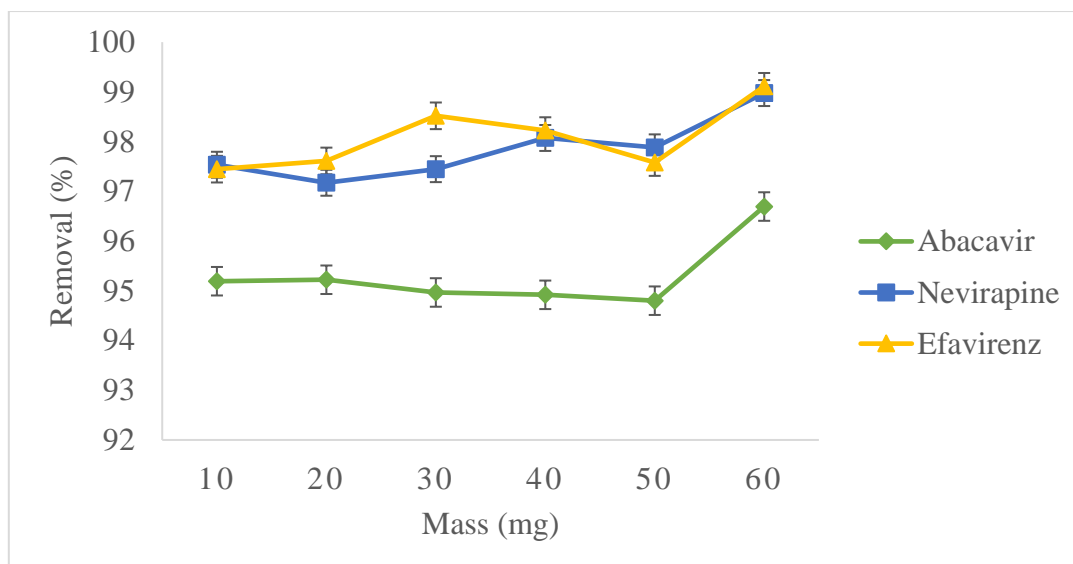


Figure 6.7: Effect of adsorbent mass variation on ARVDs removal percentage

#### 6.3.3.4. Effect of contact time

The investigated contact times were 5, 10, 15, 20, 25, and 30 minutes. The adsorption of the ARVDs occurred rapidly from 5 minutes to 20 minutes which could be due to numerous active binding sites available at the initial stage. The slowed adsorption was observed as the adsorption time increased, which could result from the reduction of the available active binding sites on the adsorbent surface. In addition, the unfilled active binding sites on the sorbent are challenging to be filled with ARVDs where repulsion is prompted between ARVDs that are already adsorbed on the EG surface, and the ARVDs residues in the solution have not yet been absorbed (El-Araby et al., 2019). As the time was further increased from 20 minutes to 30 minutes, the removals were comparable as it was observed that 25 minutes was enough to reach equilibrium, after which no significant change was observed. However, 30 minutes was used in future experiments performed. Abacavir, nevirapine, and efavirenz removal percentage reached 99, 99, and 98 %, respectively. The data is presented in the graph, Figure 6.8.

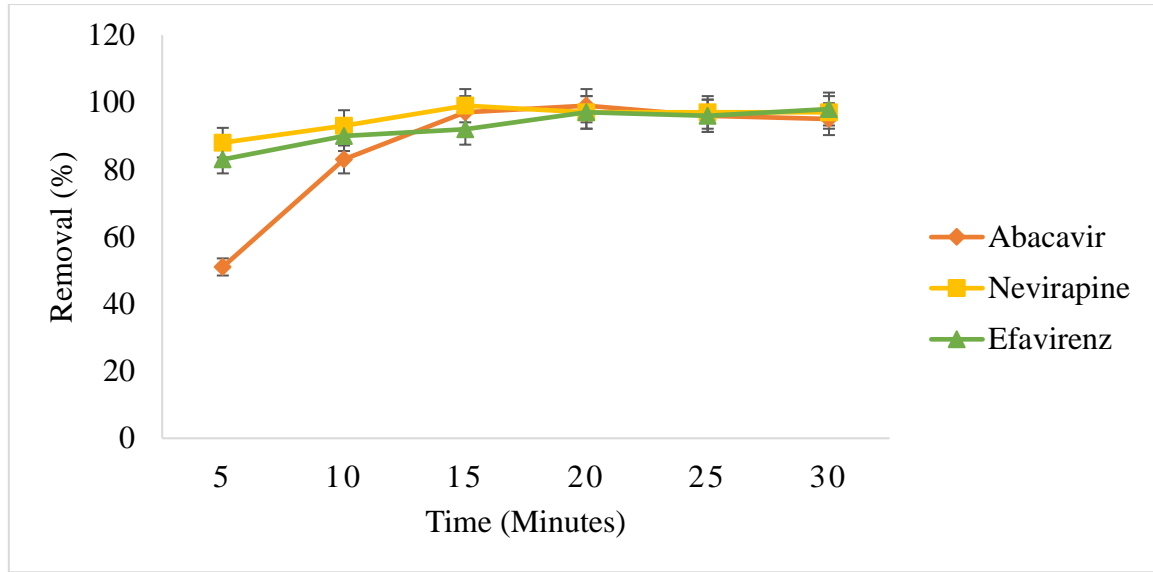


Figure 6.8: Effect of agitation time on the percentage removal of ARVDs onto EG

#### 6.3.4. Adsorption isotherms

The adsorption isotherms are mathematical models used to illustrate whether the ARVDs distribution between the solid and liquid phase at equilibrium is based on the homogeneity or heterogeneity of the sorbent (El-Araby et al., 2017). The adsorption system is determined by fitting the equilibrium data in well-known isotherm models such as Freundlich and Langmuir isotherms.

##### 6.3.4.1. Langmuir Isotherm

The Langmuir isotherm assumes that the adsorption only occurs when the adsorbent surface is totally homogenous (Yao et al., 2010). Additionally, the assumption is that on the surface of the adsorbent, the maximum adsorption corresponds to a saturated monolayer of the adsorbate molecules, and there is no important interaction among the species. Therefore, the adsorption energy is constant, and in the adsorbent surface plane, there is no transmigration of the adsorbate (El Haddad, 2016). The Langmuir is represented by equation 3,

$$\frac{C_e}{q_e} = \frac{1}{q_{max} \cdot b} + \frac{1}{q_{max}} C_e \quad (3)$$

Where  $q_e$  is the equilibrium capacity of ARVDs on the EG,  $C_e$  (mg/L) is the equilibrium ARVDs concentration in solution,  $q_{max}$  (mg/g) is the maximum capacity of the adsorbent, which represents monolayer coverage of adsorbent with adsorbate,  $b$  (L/mg) is the Langmuir

adsorption constant.  $q_{\max}$  and  $b$  are Langmuir constants related to adsorption efficiency and energy of adsorption, respectively. As displayed in Figure S6.1 a, c, and e, the linear plot of  $C_e/q_e$  versus  $C_e$  proposes the applicability of the Langmuir isotherm with a slope of  $1/q_{\max}$  and intercept of  $1/q_{\max} \cdot b$ . The Langmuir model described the adsorption data with an  $R^2$  value ranging between 0.5758 - 0.7349 for adsorption of abacavir, nevirapine, and efavirenz onto EG. The nature of the adsorption process was determined by the separation factor ( $R_L$ ), which was calculated using equation 4

$$R_L = \frac{1}{1 + bC_i} \quad (4)$$

Where  $C_i$  is initial concentration of ARVDs, The  $R_L$  value indicates whether the adsorption is favourable  $0 < R_L < 1$ , unfavourable  $R_L > 1$ , linear  $R_L = 1$ , irreversible  $R_L$  is  $= 0$ . The obtained  $R_L$  values shown in Table 6.1 were less than one and greater than zero, which indicates that the adsorption was favourable (El-Araby et al., 2019).

#### 6.3.4.2. Freundlich isotherm

The expression of Freundlich isotherm considers the ratio between the adsorbed solute on the solid phase (adsorbent surface) to the solute concentration in the solution, which varied when different concentrations are applied. Freundlich isotherm is used in the adsorption of the multilayer on the heterogeneous surface (Geçgel et al., 2015). The Freundlich logarithmic form is expressed using equation 5, (Freundlich, 1906).

$$\text{Log } (q_e) = \text{log } K_F + \frac{1}{n} \text{log } (C_e) \quad (5)$$

Where  $q_e$  and  $C_e$  are defined as above,  $K_F$  is the adsorption coefficient,  $n$  is the empirical factor linking the adsorption intensity of the solid adsorbent, which varies with the heterogeneity of the material. The greatness of  $n$  gives an indication if the adsorption process is favoured. The value of  $1/n$  ranging between one and zero shows that the adsorption easily occurs, the adsorbent surface is heterogeneous. As the value approaches zero, the adsorbent surface becomes more heterogeneous (Geçgel et al., 2015). The linear plot of  $\text{log } q_e$  versus  $\text{log } C_e$  with the intercept  $\text{log } K_F$  and slope  $1/n$  is obtained in Figure S6.1 b, d, and f. The  $R^2$  values obtained range from 0.9879 to 0.9949. The parameters related to both isotherm models tested are given in Table 6.1. The heterogeneity factor  $1/n$  shows that Freundlich isotherm is favourable as the values obtained were between zero and one. Based on the  $R^2$  values, the Freundlich model displayed a better correlation than the Langmuir model, confirming that the adsorption

occurred in a heterogeneous multilayer surface. The maximum absorption capacity of abacavir, nevirapine, and efavirenz were 400, 716, and 833  $\mu\text{g/kg}$ , respectively. The high  $K_F$  value obtained described the high affinity of the ARVDs towards EG (Elbalkiny et al., 2019).

Table 6.1: Parameters of Freundlich, and Langmuir isotherm for the adsorption of abacavir, nevirapine and efavirenz

ARVDs	Freundlich			Langmuir		
	$K_F$	$1/n$	$R^2$	$R_L$	$q_m$	$R^2$
Abacavir	122.74	0.9181	0.9879	0.4807	400	0.7349
Nevirapine	138.54	0.9502	0.9945	0.2538	716	0.6571
Efavirenz	140.08	0.9554	0.9949	0.2143	833	0.5758

### 6.3.5. Absorption kinetics

The adsorption kinetics describe the rate of adsorption and controlling mechanism to predict the reaction rate and reaction mechanisms and determine the required time for the adsorption process to reach equilibrium. The data obtained is significant for designing the adsorption system and process development (Sahoo and Prelot, 2020).

#### 6.3.5.1. Pseudo-first-order kinetic model

The pseudo first-order model is centered on the hypothesis that the rate of change of analyte uptake with time is directly proportional to the difference in saturation concentration and the amount of solid uptake with time, which is commonly appropriate over the initial phase of an adsorption process. It is ordinarily experiential that kinetics follow this pseudo first-order rate equation when adsorption occurs via diffusion through the interface (Sahoo and Prelot, 2020). The linearized formulas of pseudo-first order are expressed using equation 6.

$$\log(q_e - q_t) = \log q_e - \frac{K_1}{2.303} t \quad (6)$$

Where  $q_t$  (mg/g) and  $q_e$  (mg/g) are the absorbed amount of ARVDs per graphite unit mass at the time,  $t$  and equilibrium, respectively,  $k_1$  (1/minutes) is the absorption rate constant for the pseudo-first order kinetics models.

#### 6.3.5.2. Pseudo-second-order kinetic model

The pseudo-second order kinetic model is centered on the hypothesis that the rate-limiting step is chemisorption and forecasts the behaviour over the whole range of adsorption. Therefore, the adsorption rate is independent of the concentration of the analyte and dependent on adsorption capacity (Ho and McKay, 1999). The linearized formula of pseudo-second order is expressed using equation 7.

$$\frac{t}{q_t} = \frac{1}{k_2 q_e^2} \quad (7)$$

Where  $q_t$  (mg/g) and  $q_e$  (mg/g) are the absorbed amount of ARVDs per graphite unit mass at the time,  $t$  and equilibrium, respectively,  $k_2$  (1/minutes) are the absorption rate constant for the second order kinetics models.

#### 6.3.4.2. Weber-Morris intra-particle diffusion kinetic model

The Weber-Morris intra-particle diffusion adsorption process is identified by film diffusion (also well-known as external diffusion), pore diffusion, surface diffusion, or combination. A linear relationship is observed in the plot ARVDs adsorbed against the square root of the contact time if this model is involved in the process of adsorption and the line pass through the origin if it is the rate-limiting step (Ofomaja et al., 2020). The intra-particle kinetic model equation is expressed by equation 8 (Weber Jr and Morris, 1963).

$$q_t = K_{Diff} t^{\frac{1}{2}} + C \quad (8)$$

Where  $q_t$  (mg/g) is the absorbed amount of ARVDs per graphite unit mass at the time,  $K_{dif}$  is the intra-particle diffusion rate constant (mg/g min<sup>-1/2</sup>), and  $C$  (mg/g) is a constant that provides a signal of the thickness of the boundary layer.

The kinetic data resulted in higher linear regression coefficients values in a pseudo-second order kinetic model (Figure S6.2 a, c, and e) than in a pseudo-first order kinetic model (Figure S6.2 b, d, and f). Also, the experimental  $q_e$  values obtained were relatively closer to the  $q_e$  values obtained in the pseudo-second-order kinetic model than the  $q_e$  values obtained in a pseudo-first-order kinetic model. Therefore, the pseudo second-order kinetic model best describes the adsorption of abacavir, nevirapine, and efavirenz onto the EG adsorbent. This is due to the higher correlation coefficient and a good agreement between the calculated and the experimental  $q_e$  value. The pseudo-second-order kinetic model was then used to calculate the  $k$  value. The obtained  $k$  values for abacavir, nevirapine, and efavirenz were 0.0014, 0.0087,

and 0.0047, respectively (Table 6.2). The result obtained indicated that the interaction between the EG and the targeted ARVDs was through chemisorption (Khulu et al., 2021). Nevirapine was best described among other studied ARVDs. This signal that some chemical adsorption took place and significantly affected the mechanism and adsorption rate of nevirapine uptake. The difference in the experimental and theoretical amount of nevirapine absorbed ( $q_e$ ) into EG is more negligible, confirming that pseudo second order best described the interaction of EG and nevirapine. This behaviour agrees with the observation reported elsewhere in an adsorption study of nevirapine and efavirenz from an aqueous solution by graphene wool (Adeola and Forbes, 2021). Even though the pseudo-second order model described the data well, this model cannot describe the adsorption mechanism. Therefore, Weber-Morris intra-particle diffusion kinetic model was used to describe the adsorption mechanism. The linear plot of  $q_t$  versus  $t^{1/2}$  (Figure S 6.3), and the obtained data (Table 6.2) showed that the intra-particle diffusion was involved as the linear relationship was observed. The line in the graphs was not passing through the origin, meaning that intra-particle diffusion was not only the rate-limiting step but also other kinetic models. The obtained intercepts were larger which indicate that the boundary layer effect was greater especial for nevirapine and efavirenz. The EG has a high surface area and pore volume and shows that a boundary of the layer has some degree of control. The results showed that the percentage removal was higher, mostly at pH 7, confirming the potential interaction via hydrogen bonding, intra-particle diffusion, and electrostatic attraction interaction (Kebede et al., 2020).

Table 6.2: Kinetics constants for adsorption of ARVDs

ARVDs	Pseudo first order kinetics					Pseudo second order kinetic						Intra-particle diffusion model		
	Intercept	Slope	$q_e(\text{mg/g})$	$K_1(\text{min}^{-1})$	$R^2$	Intercept	Slope	$q_e(\text{mg/g})$	$q_e^2$	$K_2(\text{min}^{-1})$	$R^2$	$K_{\text{dif}}$ ( $\text{mgg}^{-1} \text{min}^{-1/2}$ )	C (mg/g)	R2
Abacavir	2.0062	-0.0733	101.43	-0.00122	0,7225	0,0189	0,0053	188.67	35599.85	0.0014	0,9917	17.97	76.79	0.7996
Nevirapine	2.1709	-0.0938	148.21	-0.00156	0,6962	0,0041	0,0060	166.66	27777.77	0.0087	0,9996	5.064	138.5	0.8355
Efavirenz	1.6866	-0.0547	48.59	-0.000911	0,8290	0,0074	0,0059	169.49	28727.37	0.0047	0,9992	7.948	122.8	0.9336



### **6.3.6. Application of the EG in River and wastewater samples**

This step aimed to demonstrate the applicability of the EG in the absorption of target ARVDs from the river water and wastewater samples. The quantification of the trace amounts of abacavir, nevirapine, and efavirenz in river water and wastewater indicated that the river water is less polluted than wastewater (Table 6.3). Bishopstowe and College Road river water samples were found to be polluted by the selected ARVDs. This could be because the Bishopstowe sampling point is located near the effluent discharging area of the Daville wastewater treatment plant (WWTP). The hospital and households located near the sampling point (College Road) could contribute to the pollution in College Road. High concentrations of the target ARVDs were obtained in wastewater samples, and Umbilo influent and effluent wastewater exhibited higher concentrations than the other WWTPs investigated. This could be because Umbilo is located closer to the residential areas; hence, the possible dumping of waste containing unused or expired ARVD could runoff to wastewater. The obtained concentrations in effluent water serve as proof that wastewater treatment plants have a potential impact on surface water pollution.

After assessing the presence of ARVDs in river water and wastewater, the EG was then used for adsorptive removal of ARVDs in the water samples. The obtained results showed that EG could be a potential sorbent with a high efficiency that can be used for the removal of abacavir, nevirapine, and efavirenz from wastewater and river water. The EG removed higher percentages up to 100% in other samples depending on the concentration that was present in the sample. The efficiency of EG on removing ARVDs showed comparable results in samples with similar concentrations, for instance, efavirenz in Amanzimtoti and Northern wastewater influent samples. In cases where the removals are not comparable, the possible reason could be the matrix effects as wastewater samples were from different WWTPs and have different background matrices. The matrix effect was reported elsewhere; the nanofiber was less effective in absorbing ARVDs and related drugs from wastewater than deionized water (Kebede et al., 2020).

Table 6.3: Average concentrations of ARVDs obtained in river water and wastewater

Sampling Area	Average concentration (µg/L) without EG			Average concentration (µg/L) (with EG )			Removal efficiency (%)		
	Abacavir	Nevirapine	Efavirenz	Abacavir	Nevirapine	Efavirenz	Abacavir	Nevirapine	Efavirenz
College Road	8.170	nq	13.99	nd	nd	nd	100	-	100
Bishopstowe	23.02	nq	16.99	nd	nd	nd	100	100	100
Amanzimtoti Influent	88.30	113,1	93.11	28.30	32.51	24.14	68	71	74
Amanzimtoti Effluent	63.77	92.11	71.21	10,45	10.44	13.12	84	89	82
Umhlathuzana Influent	102.0	83.51	103.1	28.27	18.71	29.77	72	78	71
Umhlathuzana Effluent	50.02	35.33	46.33	8.910	nd	3.881	82	100	92
Northern Influent	58.55	41.11	93.01	5.901	nq	22.11	89	100	76
Northern Effluent	nq	nq	10.03	nd	nd	nd	-	-	100
Umbilo Influent	118.4	83.71	113.0	43.36	20.63	32.27	63	75	71
Umbilo effluent	98.40	69.11	96.11	19.30	13.31	29.98	80	81	70

nq: not quantified; nd: not detected; -no analysis and, analysis of not quantified analytes

#### 6.4. Conclusion

The EG from the graphite sheet was successfully prepared, characterized, and effectively applied for the adsorption of ARVDs from river water and wastewater. The maximum adsorption capacity of the EG for ARVDs ranges between 1.660-197.0, 1.660-232.5, and 1.650-237.7 mg/g for abacavir, nevirapine, and efavirenz, respectively. The kinetic study displayed that the adsorption was well described by the pseudo-second order kinetic model, which confirmed that the interaction between the EG and the targeted ARVDs was through chemisorption. The intra-particle diffusion was involved in the adsorption process; however, it was not only the rate-limiting step but also other kinetic models that may control the rate of adsorption. From the isotherms, it was found that the obtained data was fitting well in the Freundlich isotherm, which proves that the adsorption process was occurring on the heterogeneous surface. The method was environmentally friendly, effortlessly modest, cost-effective, and has high removal efficiency for the assessed ARVDs from the environmental samples.

#### References

- Abers, M. S., Shandera, W. X. & Kass, J. S. 2014. Neurological and psychiatric adverse effects of antiretroviral drugs. *CNS drugs*, 28, 131-145. doi:<https://doi.org/10.1007/s40263-013-0132-4>
- Adeola, A. O. & Forbes, P. B. 2021. Antiretroviral Drugs in African Surface Waters: Prevalence, Analysis, and Potential Remediation. *Environmental Toxicology and Chemistry*. doi: <https://doi.org/10.1002/etc.5127>
- Al-Khateeb, L. A., Almotiry, S. & Salam, M. A. 2014. Adsorption of pharmaceutical pollutants onto graphene nanoplatelets. *Chemical Engineering Journal*, 248, 191-199. doi:<http://dx.doi.org/10.1016/j.cej.2014.03.023>
- Alvarez, D., Stackelberg, P., Petty, J., Huckins, J., Furlong, E., Zaugg, S. & Meyer, M. 2005. Comparison of a novel passive sampler to standard water-column sampling for organic contaminants associated with wastewater effluents entering a New Jersey stream. *Chemosphere*, 61, 610-622. doi:<https://doi.org/10.1016/j.chemosphere.2005.03.023>
- Amdany, R., Chimuka, L. & Cukrowska, E. 2014. Determination of naproxen, ibuprofen and triclosan in wastewater using the polar organic chemical integrative sampler (POCIS): A laboratory calibration and field application. *Water SA*, 40, 407-414. doi:<https://doi.org/10.4314/wsa.v40i3.3>

- Bannov, A. G., Ukhina, A. V., Maksimovskii, E. A., Prosanov, I. Y., Shestakov, A. A., Lapekin, N. I., Lazarenko, N. S., Kurmashov, P. B. & Popov, M. V. 2021. Highly Porous Expanded Graphite: Thermal Shock vs. Programmable Heating. *Materials*, 14, 7687. doi:<https://doi.org/10.3390/ma14247687>
- Chung, D. 1987. Exfoliation of graphite. *Journal of Material Science*, 22, 4190-4198. doi:<https://doi.org/10.1007/BF01132008>
- Dhakate, S., Chauhan, N., Sharma, S., Tawale, J., Singh, S., Sahare, P. & Mathur, R. 2011. An approach to produce single and double layer graphene from re-exfoliation of expanded graphite. *Carbon*, 49, 1946-1954. doi:<https://doi.org/10.1016/j.carbon.2010.12.068>
- El-Araby, H. A., Ibrahim, A. M. M. A. & Mangood, A. H. 2019. Removal of Copper(II) and Cadmium(II) Ions from Aqueous Solution by Adsorption on Modified Almond Shells. *International Journal of Engineering & Technology*, 19.
- El-Araby, H. A., Ibrahim, A. M. M. A., Mangood, A. H. & Adel, A.-H. 2017. Sesame husk as adsorbent for copper (II) ions removal from aqueous solution. *Journal of Geoscience and Environment Protection*, 5, 109. doi:<http://doi.org/10.4236/gep.2017.57011>
- Elbalkiny, H. T., Yehia, A. M., Safa'a, M. R. & Elsharty, Y. S. 2019. Removal and tracing of cephalosporins in industrial wastewater by SPE-HPLC: optimization of adsorption kinetics on mesoporous silica nanoparticles. *Journal of Analytical Science Technology*, 10, 1-12. doi:<https://doi.org/10.1186/s40543-019-0180-6>
- Freundlich, H. 1906. Over the adsorption in solution. *Journal of Physics and chemistry*, 57, 1100-1107.
- Geçgel, Ü., Kocabıyık, B. & Üner, O. 2015. Adsorptive Removal of Methylene Blue from Aqueous Solution by the Activated Carbon Obtained from the Fruit of *Catalpa bignonioides*. *Water, Air, & Soil Pollution*, 226, 238. doi:<https://doi.org/10.1007/s11270-015-2513-4>
- Goudarzi, R. & Motlagh, G. H. 2019. The effect of graphite intercalated compound particle size and exfoliation temperature on porosity and macromolecular diffusion in expanded graphite. *Heliyon*, 5, e02595. doi:<https://doi.org/10.1016/j.heliyon.2019.e02595>
- Hemmat, K., Khodabakhshi, M. R. & Zeraatkar Moghaddam, A. 2021. Synthesis of nanoscale zero-valent iron modified graphene oxide nanosheets and its application for removing tetracycline antibiotic: Response surface methodology. *Applied Organometallic Chemistry*, 35, e6059. doi: <https://doi.org/10.1002/aoc.6059>
- Ho, Y.-S. & McKay, G. 1999. Pseudo-second order model for sorption processes. *Process biochemistry*, 34, 451-465. doi:[https://doi.org/10.1016/S0032-9592\(98\)00112-5](https://doi.org/10.1016/S0032-9592(98)00112-5)

- Hu, L., Zhang, Y., Lu, W., Lu, Y. & Hu, H. 2019. Easily recyclable photocatalyst Bi<sub>2</sub>WO<sub>6</sub>/MOF/PVDF composite film for efficient degradation of aqueous refractory organic pollutants under visible-light irradiation. *Journal of Materials Science*, 54, 6238-6257. doi:<https://doi.org/10.1007/s10853-018-03302-w>
- Idris, A., Orimolade, B., Potlako, M., Feleni, U., Nkambule, T. T. & Mamba, P. B. B. 2022. Exfoliated Graphite: A surface Renewed Electrode for Environmental Applications. *Frontiers in Sensors*, 11. doi:<https://doi.org/10.3389/fsens.2022.861965>
- Kebede, T., Seroto, M., Chokwe, R., Dube, S. & Nindi, M. 2020. Adsorption of antiretroviral (ARVs) and related drugs from environmental wastewaters using nanofibers. *Journal of Environmental Chemical Engineering*, 8, 104049. doi:<https://doi.org/10.1016/j.jece.2020.104049>
- Khulu, S., Ncube, S., Kgame, T., Mavhunga, E. & Chimuka, L. 2021. Synthesis, characterization and application of a molecularly imprinted polymer as an adsorbent for solid-phase extraction of selected pharmaceuticals from water samples. *Polymer Bulletin*, 1-21. doi:<https://doi.org/10.1007/s00289-021-03553-9>
- Liu, Q., Li, L., Jin, X., Wang, C. & Wang, T. 2018. Influence of graphene oxide sheets on the pore structure and filtration performance of a novel graphene oxide/silica/polyacrylonitrile mixed matrix membrane. *Journal of Materials Science*, 53, 6505-6518. doi:<https://doi.org/10.1007/s10853-018-1990-4>
- Luo, Y., Guo, W., Ngo, H. H., Nghiem, L. D., Hai, F. I., Zhang, J., Liang, S. & Wang, X. C. 2014. A review on the occurrence of micropollutants in the aquatic environment and their fate and removal during wastewater treatment. *Science of the Total Environment*, 473, 619-641. doi:<https://doi.org/10.1016/j.scitotenv.2013.12.065>
- Madikizela, L. M. & Chimuka, L. 2017. Occurrence of naproxen, ibuprofen, and diclofenac residues in wastewater and river water of KwaZulu-Natal Province in South Africa. *Environmental Monitoring and Assessment*, 189, 348. doi:<https://doi.org/10.1007/s10661-017-6069-1>
- Madikizela, L. M., Tavengwa, N. T. & Chimuka, L. 2017. Status of pharmaceuticals in African water bodies: occurrence, removal and analytical methods. *Journal of Environmental Management*, 193, 211-220. doi:<http://dx.doi.org/10.1016/j.jenvman.2017.02.022>
- Mlunguza, N. Y., Ncube, S., Mahlambi, P. N., Chimuka, L. & Madikizela, L. M. 2020. Determination of selected antiretroviral drugs in wastewater, surface water and aquatic plants using hollow fibre liquid phase microextraction and liquid chromatography-

- tandem mass spectrometry. *Journal of Hazardous Materials*, 382, 121067. doi:<https://doi.org/10.1016/j.jhazmat.2019.121067>
- Mohanraj, J., Durgalakshmi, D., Balakumar, S., Aruna, P., Ganesan, S., Rajendran, S. & Naushad, M. 2020. Low cost and quick time absorption of organic dye pollutants under ambient condition using partially exfoliated graphite. *Journal of Water Process Engineering*, 34, 101078. doi:<https://doi.org/10.1016/j.jwpe.2019.101078>
- Moosa, A. & Abed, M. 2021. Graphene preparation and graphite exfoliation. *Turkish Journal of Chemistry*, 45, 493-519. doi:<https://doi.org/10.3906/che-2101-19>
- Mtolo, S. P., Mahlambi, P. N. & Madikizela, L. M. 2019. Synthesis and application of a molecularly imprinted polymer in selective solid-phase extraction of efavirenz from water. *Water Science and Technology*, 79, 356-365. doi:<https://doi.org/10.2166/wst.2019.054>
- Ncube, S., Madikizela, L. M., Chimuka, L. & Nindi, M. M. 2018. Environmental fate and ecotoxicological effects of antiretrovirals: A current global status and future perspectives. *Water research*, 145, 231-247. doi:<https://doi.org/10.1016/j.watres.2018.08.017>
- Ndlovu, T. 2012. *Electrochemical detection of organic and inorganic water pollutants using recompressed exfoliated graphite electrodes*. University of Johannesburg (South Africa).
- Ndlovu, T., Arotiba, O. A., Sampath, S., Krause, R. W. & Mamba, B. B. 2011. Electrochemical detection and removal of lead in water using poly (propylene imine) modified recompressed exfoliated graphite electrodes. *Journal of Applied Electrochemistry*, 41, 1389-1396. doi:<https://doi.org/10.1007/s10800-011-0360-6>
- Ofomaja, A. E., Naidoo, E. B. & Pholosi, A. 2020. Intraparticle diffusion of Cr (VI) through biomass and magnetite coated biomass: A comparative kinetic and diffusion study. *South African Journal of Chemical Engineering*, 32, 39-55. doi:<https://doi.org/10.1016/j.sajce.2020.01.005>
- Panikumar, A., Venkat, R., Sunitha, G., Babu, S. & Subrahmanyam, C. 2012. Development of biorelevant and discriminating method for dissolution of efavirenz and its formulations. *Asian Journal of Pharmaceutical and Clinical Research*, 5, 220-223. doi:<https://www.researchgate.net/publication/261107749>
- Radjenovic, J., Petrovic, M. & Barceló, D. 2007. Analysis of pharmaceuticals in wastewater and removal using a membrane bioreactor. *Analytical bioanalytical chemistry*, 387, 1365-1377. doi:<https://doi.org/10.1007/s00216-006-0883-6>

- Rimayi, C., Odusanya, D., Weiss, J. M., de Boer, J. & Chimuka, L. 2018. Contaminants of emerging concern in the Hartbeespoort Dam catchment and the uMngeni River estuary 2016 pollution incident, South Africa. *Science of the Total Environment*, 627, 1008-1017. doi:<https://doi.org/10.1016/j.scitotenv.2018.01.263>
- Rosli, F. A., Ahmad, H., Jumbri, K., Abdullah, A. H., Kamaruzaman, S. & Fathihah Abdullah, N. A. 2021. Efficient removal of pharmaceuticals from water using graphene nanoplatelets as adsorbent. *Royal Society Open Science*, 8, 201076. doi:<https://doi.org/10.1098/rsos.201076>
- Sahoo, T. R. & Prelot, B. 2020. Nanomaterials for the Detection and Removal of Wastewater Pollutants. *Micro and Nano Technologies*, 161-222. doi:<https://doi.org/10.1016/B978-0-12-818489-9.00007-4>
- Sharma, Y. 2009. Removal of a Cationic Dye from Wastewaters by Adsorption on Activated Carbon Developed from Coconut Coir. *Energy Fuels*, 23, 2983. doi:<https://doi.org/10.1021/ef9001132>
- Tang, J. & Wang, J. 2020. Iron-copper bimetallic metal-organic frameworks for efficient Fenton-like degradation of sulfamethoxazole under mild conditions. *Chemosphere*, 241, 125002. doi:<https://doi.org/10.1016/j.chemosphere.2019.125002>
- Thakur, A., Kumar, P., Kaur, D., Devunuri, N., Sinha, R. & Devi, P. 2020. TiO<sub>2</sub> nanofibres decorated with green-synthesized P Au/Ag@ CQDs for the efficient photocatalytic degradation of organic dyes and pharmaceutical drugs. *Journal of RSC Advances*, 10, 8941-8948. doi:<https://doi.org/10.1039/C9RA10804A>
- Wang, S., Wang, C. & Ji, X. 2017. Towards understanding the salt-intercalation exfoliation of graphite into graphene. *Royal Science of Chemistry Advances*, 7, 52252-52260. doi:<https://doi.org/10.1039/C7RA07489A>
- Weber Jr, W. J. & Morris, J. C. 1963. Kinetics of adsorption on carbon from solution. *Journal of the sanitary engineering division*, 89, 31-59.
- Wood, T. P., Duvenage, C. S. & Rohwer, E. 2015. The occurrence of anti-retroviral compounds used for HIV treatment in South African surface water. *Environmental Pollution*, 199, 235-243. doi:<https://doi.org/10.1016/j.envpol.2015.01.030>
- Xu, J., Xu, W., Wang, D., Sang, G. & Yang, X. 2016. Evaluation of enhanced coagulation coupled with magnetic ion exchange (MIEX) in natural organic matter and sulfamethoxazole removals: the role of Al-based coagulant characteristic. *Separation and Purification Technology*, 167, 70-78. doi:<https://doi.org/10.1016/j.seppur.2016.05.007>

- Yao, Z.-Y., Qi, J.-H. & Wang, L.-H. 2010. Equilibrium, kinetic and thermodynamic studies on the biosorption of Cu (II) onto chestnut shell. *Journal of Hazardous Materials*, 174, 137-143. doi:<https://doi.org/10.1016/j.jhazmat.2009.09.027>
- Zhuan, R. & Wang, J. 2020. Enhanced degradation and mineralization of sulfamethoxazole by integrating gamma radiation with Fenton-like processes. *Radiation Physics and Chemistry*, 166, 108457. doi:<https://doi.org/10.1016/j.radphyschem.2019.108457>
- Zunngu, S. S., Madikizela, L. M., Chimuka, L. & Mdluli, P. S. 2017. Synthesis and application of a molecularly imprinted polymer in the solid-phase extraction of ketoprofen from wastewater. *Comptes Rendus Chimie*, 20, 585-591. doi:<https://doi.org/10.1016/j.crci.2016.09.006>
- Zyoud, A. H., Zubi, A., Zyoud, S. H., Hilal, M. H., Zyoud, S., Qamhieh, N., Hajamohideen, A. & Hilal, H. S. 2019. Kaolin-supported ZnO nanoparticle catalysts in self-sensitized tetracycline photodegradation: zero-point charge and pH effects. *Applied Clay Science*, 182, 105294. doi:<https://doi.org/10.1016/j.clay.2019.105294>



## Supporting documents

Table S6. 1: Physicochemical parameter and sampling points coordinates

Sampling area	pH	DO	Temperature	Conductivity	Salinity	Total-Dissolved Solids	GPS Coordinates
Amanzimtoti Inf	7.014	3.83	23.61	1007	0.48	496	-30.007° - 30.917°
Amanzimtoti Eff	6.841	5.54	21.11	1247	0.61	620	
Mhlathuzane Inf	7.791	6.54	22.71	800	0.38	401	-29.876° - 30.881°
Mhlathuzane Eff	7.791	5.61	23.01	624	0.30	309	
Umbilo Inf	7.191	5.52	24.57	833	0.39	407	-29.845° - 30.891°
Umbilo Eff	7.058	5.87	24.81	538	0.26	272	
Northern Inf	7.153	5.38	22.73	778	0.38	388	-29.795° - 30.995°
Northern Eff	7.051	5.61	21.11	814	0.39	407	
Camp's drift	7.442	17.45	11.81	248	0.11	125	-29.630 ° - 30.365 °
College Road	8.001	16.76	14.60	235	0.11	118	-29.612 ° - 30.377 °
YMCA	6.500	15.93	13.33	241	0.11	120	-29.602 ° - 30.413 °
Wood House	7.743	12.04	18.61	220	0.10	110	-29.611 ° - 30.387 °
Bishopstowe	7.341	7.85	19.81	404	0.19	200	-29.618 ° - 30.447 °

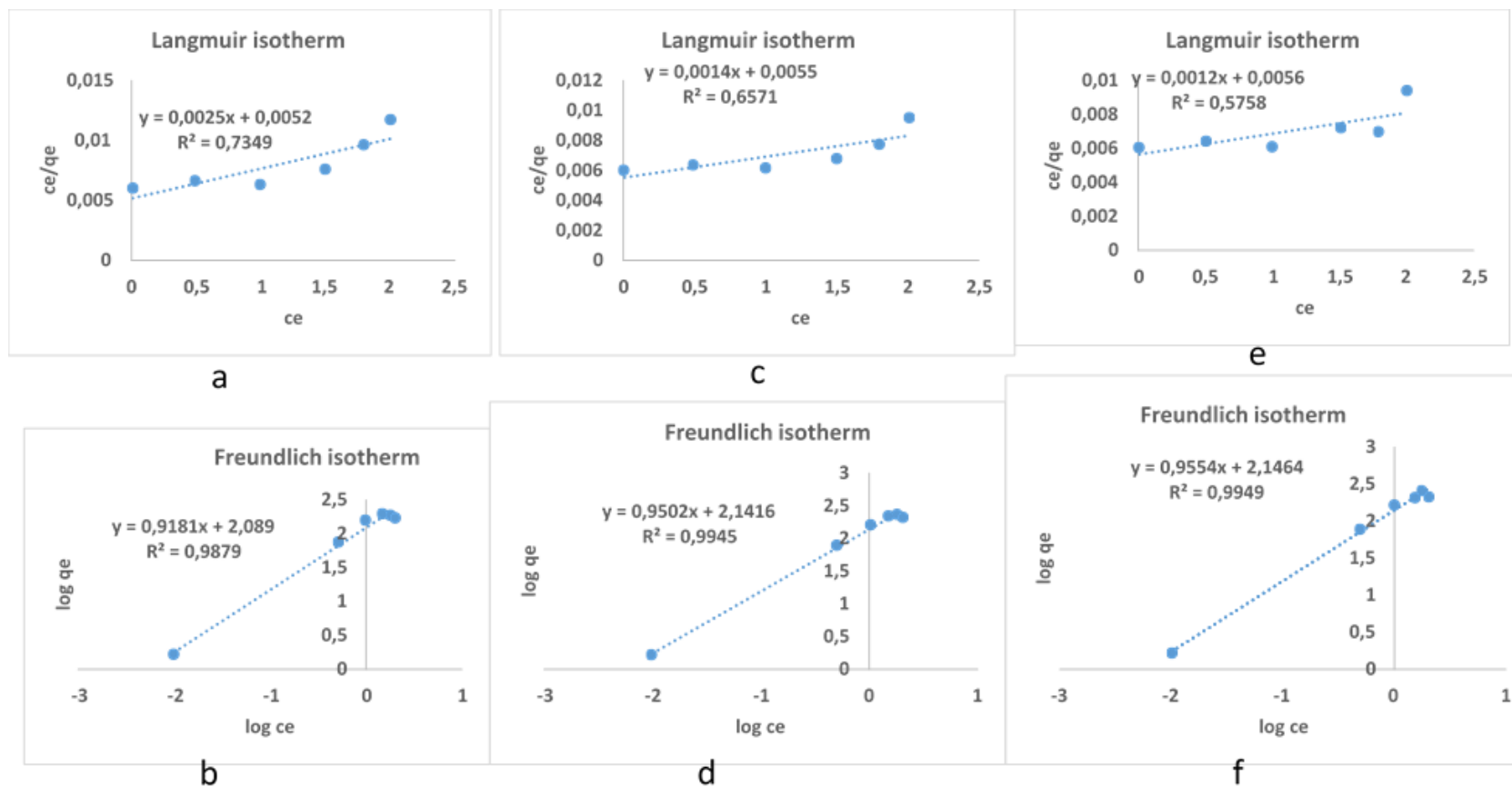


Figure S6.1: **a** Langmuir adsorption isotherm of abacavir, **b** Freundlich adsorption isotherm of abacavir, **c** Langmuir adsorption isotherm of nevirapine, **d** Freundlich adsorption isotherm of nevirapine, **e** Langmuir adsorption isotherm of efavirenz, and **f** Freundlich adsorption isotherm of efavirenz on EG at optimum conditions.

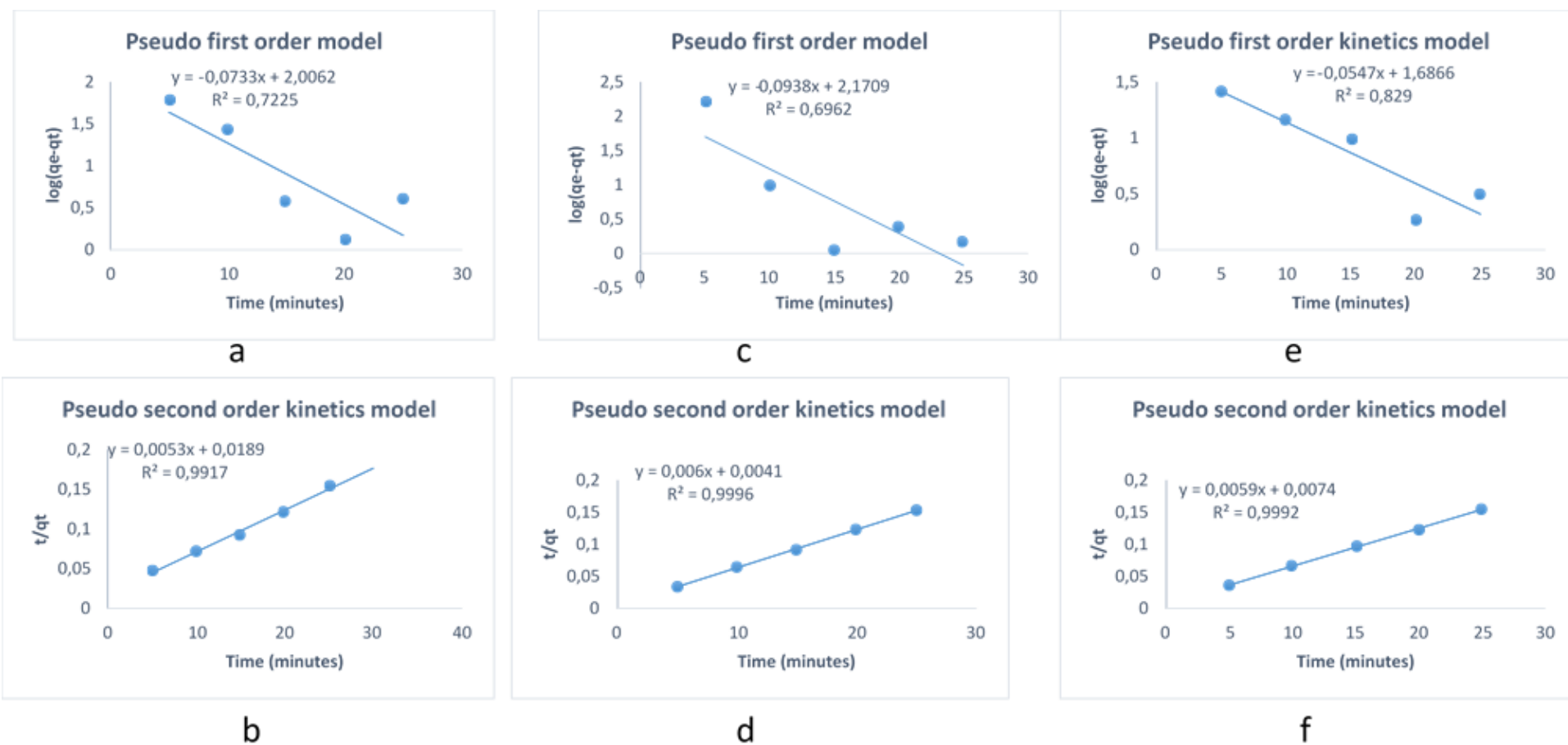


Figure S6.2: **a** pseudo-first-order adsorption kinetics of abacavir, **b** pseudo-second-order adsorption kinetics of abacavir, **c** pseudo-first-order adsorption kinetics of nevirapine, **d** pseudo-second-order adsorption kinetics of nevirapine, **e** pseudo-first-order adsorption kinetics of efavirenz, **f** pseudo-second-order adsorption kinetics of efavirenz on EG at optimum condition.

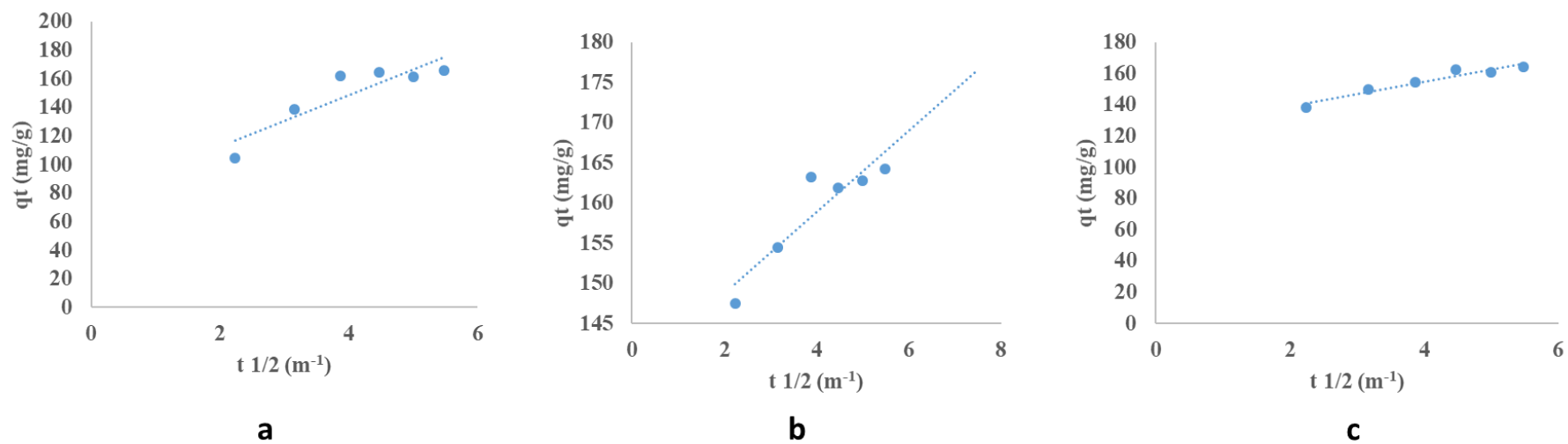


Figure S6.3: **a** Intra-particle diffusion model for the adsorption of abacavir, **b** Intra-particle diffusion model for the adsorption of nevirapine, **c** Intra-particle diffusion model for the adsorption of efavirenz on EG at optimum condition.

## Chapter seven

---

### 7.1. Conclusion

This research presented the analysis of ARVDs in vegetables, their uptake by vegetables from the soil irrigated with ARVDs spiked water, and their adsorption by exfoliated graphite in water. The appropriate extraction methods based on UE, UADLLME, MAE, and MAE-SPE of abacavir, nevirapine, and efavirenz from vegetables, followed by their quantitative analysis using LC-PDA were developed. The optimized methods were applied for trace quantification of the target ARVDs in different vegetables. The optimum conditions for extraction techniques that permitted the simultaneous extraction of the target ARVDs were found to be effective, with recoveries ranging from 93 to 113%, 85 to 103%, 85 to 103%, and 87 to 104 % for UE, UADLLME, MAE, and MAE-SPE, respectively. The detection and quantification limits found were as low as  $0.0081 \mu\text{g kg}^{-1}$  and  $0.027 \mu\text{g kg}^{-1}$ ,  $0.0028 \text{ kg}^{-1}$  and  $0.0094 \mu\text{gkg}^{-1}$ ,  $0.020 \mu\text{gkg}^{-1}$  and  $0.068 \mu\text{gkg}^{-1}$ ,  $0.019 \mu\text{gkg}^{-1}$  and  $0.065 \mu\text{gkg}^{-1}$  for UE, UADLLME, MAE, and MAE-SPE, respectively, with the RSD values less than 10%. The obtained results under optimum conditions showed that the developed extraction methods linked with the LC-PDA as a quantitative analysis technique could be practical substitutes for the removal and quantification of ARVDs in solid samples. The target ARDs investigated were detected in most vegetable samples, indicating that ARVDs are taken by plant roots and translocated to shoot parts of the vegetable plant. The highest concentration of abacavir, nevirapine, and efavirenz was  $3.13 \pm 0.9 \mu\text{gkg}^{-1}$ ,  $27.9 \pm 12 \mu\text{gkg}^{-1}$ , and  $13.0 \pm 14 \mu\text{gkg}^{-1}$ , respectively. It was found that potatoes and beetroot were the most polluted root vegetables. In comparing UE and UADLLME, high concentrations were obtained in UADLLME and found to be more sensitive than UE. However, UE can be recommended for daily analysis. In comparison of MAE and MAE-SPE, MAE was found to be more sensitive than MAE-SPE, and the obtained concentrations were higher in MAE than in MAE-SPE. This suggested that the MAE can be accurately used for routine analysis without the additional SPE clean-up step. The result showed that MAE and UE could effectively extract and quantify ARVDs without the preconcentration or clean-up methods.

The phytoremediation approach further confirmed the uptake of abacavir, nevirapine, and efavirenz by beetroot, spinach, and tomato plants irrigated with the ARVDs contaminated water. The studied ARVDs were present in all sample matrices harvested, confirming the uptake and translocation ability of the tested vegetables. The EG was successfully synthesised, characterized, and applied to remove ARVDs from water. The EG was able to remove abacavir, nevirapine, and efavirenz from river water and wastewater with the highest removal efficiency

of up to 100%. The kinetic model and adsorption isotherm studies showed that the experimental data fit pseudo-second-order kinetics and is well explained by Freundlich's adsorption isotherm.

## **7.2. Recommendations**

The occurrence of ARVDs in vegetables and water analysed in this work is a call for concern; therefore, the continuous monitoring of ARVDs in vegetables and water is necessary as the number of HIV-positive people and patients consuming ARVDs increases every day. The investigation of pharmaceutical class such as ARVDs needs extra attention to comprehend their occurrence in vegetables and other environmental samples, mainly in South Africa, as ARVDs are prevalent. It's confirmed that wastewater treatment plants are the primary source of ARVDs in ecological water. The quantification of ARVDs in wastewater effluent signals that ARVDs are released into the environment water. Therefore, a day-to-day test of these drugs in WWTPs might provide alertness and more relevant data on their occurrence and distribution; hence policymakers can conclude on their levels in different samples and document their maximum residue limits (MRLs). Exploring innovative, environmentally friendly, cost-effective, and simple strategies for WWTPs that could completely eradicate ARVDs in wastewater before discharge is necessary. The recent studies indicated the potential of the adsorption methods for adsorption of organic compounds; hence exploring various adsorbents for the adsorption of ARVDs should be considered. Detecting ARVDs in vegetables means that pollution also occurs in agricultural areas; therefore, continuous analysis of ARVDs in vegetables needs to be done to assess the occurrence of ARVDs in vegetables and the mechanism of their uptake by the plant. Furthermore, the investigation of the ability of different plant species to absorb ARVDs from contaminated soil is necessary. Places where people drink and irrigate crops with water from the rivers and use pit toilets, are more exposed to these drugs because river water might have high loads of pollutants from wastewater discharge as well as illegal dumping and run off. Hence environmental monitoring should be a standard to prevent human health risks as continuously unintentional consumption, and prolonged long exposure could result in drug resistance and other harmful effects.